Workshop IV

Stellar Variability

Chairman:

Dr. Borys Zhilyaev (MAO NASU, Ukraine)

Session 1–2. Flares in Late–Type Stars

Convener: Prof. Roald Gershberg (CrAO MESU, Ukraine)

SOME RESULTS OF INTERNATIONAL CAMPAIGNS INITIATED BY THE CRIMEAN ASTROPHYSICAL OBSERVATORY FOR INVESTIGATION OF FLARE STARS

R. E. Gershberg and N. I. Shakhovskaya

Crimean Astrophysical Observatory, Ministry of Ukraine for Education and Science
Naukove, 98409 Crimea, Ukraine
e-mail: gershberg@crao.crimea.ua, nish@crao.crimea.ua

In 1967–73 and in 1986–95, two sets of international cooperative programs were initiated by the Crimean Astrophysical Observatory for study of the UV Cet-type flare stars. The first set was dedicated to photometric observations, the second one was concerned the researches supported by the photometric patrol. We list the participants of the programs and the main scientific results both based on collected data and stimulated by them.

I

In 1967, on the Crimean Astrophysical Observatory's initiative, the XIII General Assembly of the IAU set up the Working Group on flare stars within the framework of the 27th Commission on variable stars. The aim of the Group was to organize an international cooperative monitoring of selected UV Cet-type stars to clarify a temporal distribution of flares in these objects. The schedules for 10–20 days sets of such observations have regularly published by IBVS. During 1967–1973 the 36 cooperative campaigns were carried out. Several dozens of observers from Abastumani Astrophysical Observatory (USSR, now Georgia), Armagh Observatory (Northern Ireland, UK), Belgrade Astronomical Observatory (Yugoslavia), Auckland Observatory (New Zealand), Boyden Observatory (Republic of South Africa), Byurakan Astrophysical Observatory (USSR, now Armenia), Catania Astrophysical Observatory (Italy), Crimean Astrophysical Observatory (USSR, now Ukraine), Department of Geodetic Astronomy, University of Thessaloniki (Greece), Konkoly Observatory (Hungary), Mt John Observatory (New Zealand), Mt Cuba Observatory, University of Delaware (USA), Observatorio Inter–Americano de Cerro Tololo (Chile), Steward Observatory, University of Arizona (USA), Tokyo Astronomical Observatory (Japan), Uttar Pradesh State Observatory (India), Vermilion River Observatory, University of Illinois (USA), Warsaw University Observatory (Poland) have participated in the campaigns. During all campaigns the eight program stars were monitored for more than 3000 hours and several hundreds of flares were registered.

The most detailed study of the temporal distributions of flares based on cooperative patrol for UV Cet and YZ CMi has been carried out by Oskanyan and Terebizh (1971a). They considered flare numbers within fixed time intervals and time durations between flares and showed that suggestion on a periodicity of flares proposed by some observers was not confirmed: in total the temporal distribution of flares corresponds to the Poisson's one with the highest probability, but numbers of very close flares exceed numbers expected for such a distribution. Oskanyan and Terebizh suggested that this excess was due to several bursts of the same flares. Similar results based on more homogeneous and larger data for more stars have been obtained later and the stellar analogs of the solar sympathetic flares as a cause of the excess of close flares was also considered.

The statistical features of the flare energy activity based on cooperative observations for the most active 4 observed stars – UV Cet, AD Leo, YZ CMi and EV Lac – were considered by Oskanyan and Terebizh (1971b)

Inauguration paper by Prof. Roald Gershberg, the UAA Laureate of 1997–2000 yrs "For the Outstanding Contribution for Advancement of Astronomy in Ukraine".

and Chugainov (1972) practically simultaneously and independently.

Byurakan researchers estimated an optical luminosity range of flares and their total energies that covered 4–5 orders of magnitude. They considered distributions of the flare amplitude and energy, and constructed their frequence functions. An essential difference of these statistical characteristics for the absolutely faintest UV Cet star from characteristics of brighter AD Leo, EV Lac and YZ CMi stars was noted because of fainter flares in UV Cet which were not possible to detect on the brighter stars. For the first time Oskanyan and Terebizh estimated a possible contribution of flares behind the detection threshold in total flare emission. They estimated that this total emission in the B band was about 1% of a quiet stellar luminosity and noted that rare but power flares give the main contribution into this total flare emission.

Chugainov (1972) proposed to use the accumulated frequencies for flare statistics and found the power law of the flare energy spectrum with a sharp break near a threshold of a certain flare detection (see Fig. 1). This circumstance has permitted to exclude certainly a region of faint flares, where flare statistics are affected with observational selection, to pick out a region of flare energy spectrum not affected with this distortion and to confront results of various observers. We converted observable magnitudes into absolute luminosities and construct flare energy spectra for several tens of flare stars within the range of M_V from 8^m to 17^m both for program stars of cooperative campaigns and for other ones (Gershberg, 1972; Gershberg and Shakhovskaya, 1983). Korotin and Krasnobabtsev (1985) have considered photographic observations of flare stars in the closest open stellar clusters and found there the power law of flare energy spectra as well. Then a general picture of the flare activity of stars within the range of 10 orders of magnitude was constructed (see Fig. 2); only physically significant regions of flare energy spectra are given in the plot for stars within the solar vicinity, for several flare star groups in Pleiades and in Orion cluster and for the solar flares. A systematical application of formalism of the detected general power spectrum turned out to be very fruitful and used by many investigators.

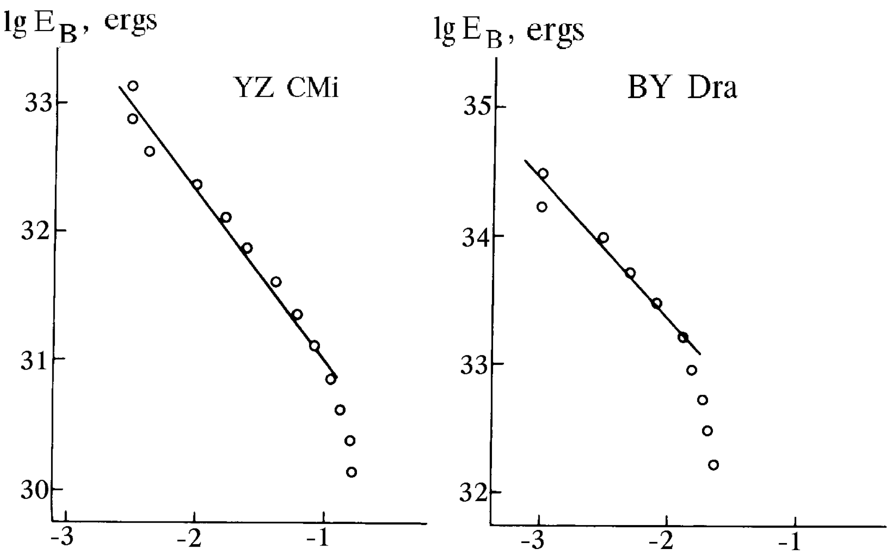

Figure 1: The energy spectra of YZ CMi and BY Dra flares in the B band (Gershberg and Shakhovskaya, 1983)

Thus, it was shown that the main flare energy release for observable spectral indices of flare energy spectra is connected strongly with rare but strong flares, and this flare energy is about several percents of the quiet luminosity of stars (Gershberg and Shakhovskaya, 1983). Then, the total flare energy release is close by an order of magnitude to chromospheric and coronal luminosities (Gershberg and Shakhovskaya, 1983; Shakhovskaya, 1989). When this result was confirmed by three independent research centers too (Whitehouse, 1985; Skumanich, 1985; Doyle and Butler, 1985), it became an initial point for the hypothesis about coronal heating by numerous microflares. Finally, a comparison of spectral indices of flare energy spectra of stars in stellar clusters of various ages gave a ground to suggest an evolution trend of the index (see Fig. 3). In any case, the spectral index of the solar flares at the solar maximum corresponds to young clusters while the index at the solar minimum corresponds to older clusters (Gershberg, 1989).

Referring to our results, Kurochka (1987) found the power energy spectrum of the solar optical flares (see Fig. 2), where such a spectrum was constructed with use of 15500 flares. Then Kasinsky and Sotnikova (1989) found the same character of the energy spectra for the solar flares at the soft X-ray. Moreover, these Irkutsk

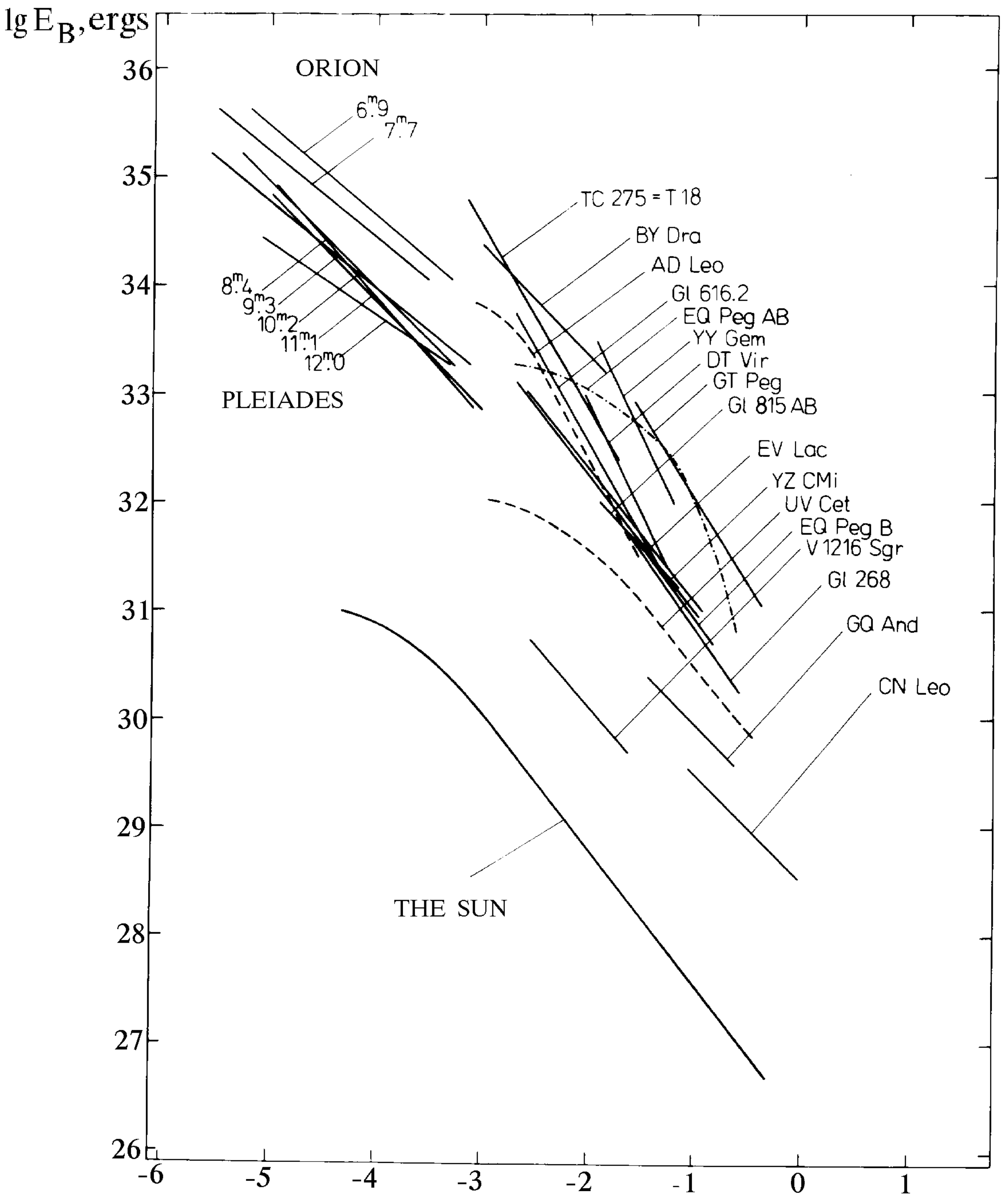

Figure 2: The energy spectra of stellar flares on flare stars in the solar vicinity and in Pleiades and Orion clusters and the energy spectra of the solar flares (Gershberg, Mogilevsky and Obridko, 1987)

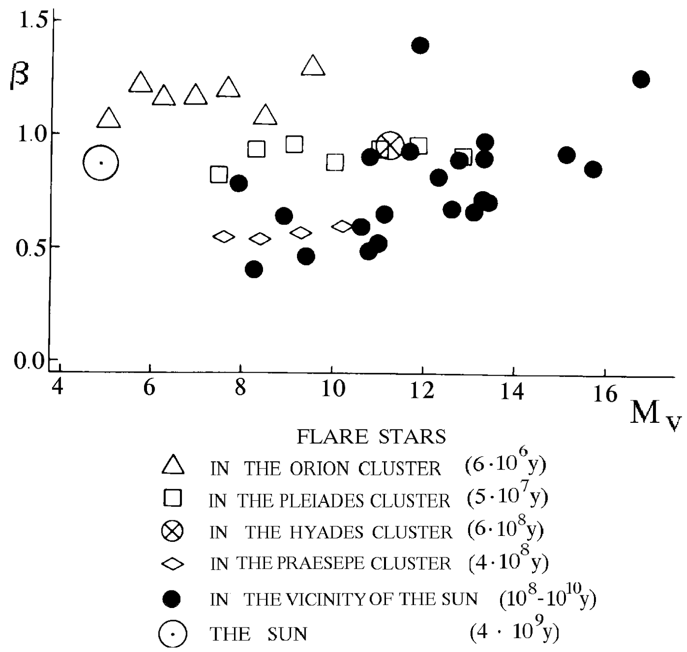

Figure 3: Spectral indices of energy spectra of stellar flares in the solar vicinity and in stellar clusters of different ages and of the solar flares (Gershberg, 1989)

researchers discovered a close correlation between the spectral index and the Wolf number, that is the systematic variations of the index over rather short time scale. Referring to this result, the 20 year series of the EV Lac monitoring were analyzed in the Crimean Astrophysical Observatory and the periodic variations of the stellar spectral index with $P \sim 7^{\mathrm{y}}\!.5$ were found (Alekseev and Gershberg, 1997).

Unfortunately, our hope to resolve the problem of a stellar flare energy source through consideration of spectral indices has been failed. It turned out that the power law of a flare energy spectrum fits to semi–qualitative concepts on dissipation in flares both magnetic (Pustil'nik, 1988) and kinetic (Kasinsky and Sotnikova, 1988) energy, to modern models of flares within the framework of the avalanche theory (Lu and Hamilton, 1991) as well as to the theory of the phase transitions in turbulent plasma (Pustil'nik, 1997).

II

In 1986–1995 the cooperative campaigns were dedicated to comprehensive investigations of EV Lac, one of the most active flare star in the Northern hemisphere. Having the declination about +44°, this star at the time of its opposition to the Sun in autumn nights can be uninterruptedly monitored for 8–9 hours. The ideology of these campaigns was to carry out a photometric patrol yearly for several nights allowing to fix the times of flares and time of quiet state of the star that is necessary for observations of other kinds. During these campaigns, the photometic patrol in the optical range was accompanied by the spectral, polarimetric, IR, UV observations and researches at the radio frequencies. Summary reports on the campaigns of 1986 and 1987 were published by R. E. Gershberg, V. P. Grinin, I. V. Ilyin, N. S. Nesterov, N. I. Shakhovskaya, R. G. Getov, M. S. Ivanova, K. P. Panov, M. K. Tsvetkov, A. G. Tsvetkova and G. Leto (Gershberg, Grinin *et al.*, 1991) and by R. E. Gershberg, I. V. Ilyin and N. I. Shakhovskaya (1991); on the campaign of 1989 – by A. V. Berdyugin, R. E. Gershberg, I. V. Ilyin, V. P. Malanushenko, N. I. Shakhovskaya, N. M. Shakhovskoy, I. Pagano, I. P. Panferova and L. A. Pustil'nik (Berdyugin, Gershberg *et al.*, 1995); on the campaign of 1990 – by R. E. Gershberg, I. V. Ilyin, A. N. Rostopchina, N. I. Shakhovskaya, G. A. Garbuzov, B. R. Pettersen, T. Korhonen, S. Avgoloupis, L. N. Mavridis, J. H. Seiradakis, R. K. Konstantinova–Antova, A. P. Antov, A. S. Melkonian, I. P. Panferova, L. A. Pustil'nik, P. M. Herouni and A. V. Oskanian; on the campaign of 1991 – by I. Yu. Alekseev, R. E. Gershberg, I. V. Ilyin, N. I. Shakhovskaya, N. M. Shakhovskoy, S. Avgoloupis, L. N. Mavridis, J. H. Seiradakis, M. R. Kidger, I. P. Panferova and L. A. Pustil'nik (Alekseev, Gershberg *et al.*, 1994); on the campaign of 1992 – by H. Abdul–Aziz, E. P. Abranin, I. Yu. Alekseev, S. Avgoloupis, L. L. Bazelyan, G. M. Beskin, A. I. Brazhenko, N. N. Chalenko, G. Cutispoto, J. J. Fuensalida, R. E. Gershberg, M. R. Kidger, G. Leto, Yu. F. Malkov, L. N. Mavridis, I. Pagano, I. P. Panferova, M. Rodonó, J. H. Seiradakis,

S. G. Sergeev, R. E. Spencer, N. I. Shakhovskaya and D. N. Shakhovskoy (Abdul–Aziz, Abranin *et al.*, 1995); on the campaign of 1993 – by E. P. Abranin, L. L. Bazelyan, I. Yu. Alekseev, R. E. Gershberg, S. Avgoloupis, J. H. Seiradakis, L. N. Mavridis, G. M. Beskin, S. N. Mitronova, I. P. Panferova and M. R. Kidger (Abranin, Bazelyan *et al.*, 1998); on the campaigns of 1994 and 1995 – by E. P. Abranin, I. Yu. Alekseev, S. Avgoloupis, L. L. Bazelyan, S. V. Berdyugina, G. Cutispoto, R. E. Gershberg, V. M. Larionov, G. Leto, V. N. Lisachenko, G. Marino, L. N. Mavridis, S. Messina, V. N. Mel'nik, I. Pagano, S. V. Pustil'nik, M. Rodonó, G. Sh. Roizman, J. H. Seiradakis, G. P. Sigal, N. I. Shakhovskaya, D. N. Shakhovskoy and V. A. Shcherbakov (Abranin, Alekseev *et al.*, 1998). The EV Lac monitorings were carried out at several observatories during some nights in vicinity of program dates, and results of these additional patrols were also included in the campaign reports.

The main results of these campaigns are following.

OPTICAL PHOTOMETRIC RESULTS

In 1986–95 the photometric patrol was carried out at the Crimean Astrophysical Observatory in the optical range in the UBVRI bands; in 1990–95 at the Stephanion Observatory of the University of Thessaloniki (Greece) in the B band; in 1987, 1989, 1992, 1994 and 1995 at the Astrophysical Observatory in Catania (Italy) in the UBV bands; in 1989–93 at the Special Astrophysical Observatory (Nizhny Arkhyz, USSR, now Russia) in the UB bands; in 1986–87 at the Rozhen Astronomical Observatory (Bulgaria) in the U band; in 1990 at the Byurakan Astrophysical Observatory (Armenia) in the U band; in 1990 at the Belogradchik Astronomical Observatory (Bulgaria) in the U band; in 1990 at the Instituto de Astrofisica de Canarias Nordic telescope (Spain) in the UBVRI bands; in 1995 at the Galilea Sea Astrophysical Observatory (Israel) in the BVR bands. In Crimea the 227 flares were detected for 307 hours of monitoring, at the Stephanion Observatory – 40 flares for 145 hours, in Catania, in Bulgaria and at the 6-m telescope in Russia – in of about 2 dozens of flares each for about 40, 50 and 20 hours, respectively, at the NORDIC telescope – 9 flares for 23 hours, in Armenia – 2 flare for more than 15 hours. It is important to emphasize that photometric investigations have been planned as auxiliary observations for other kinds of researches; however, the data gathered have presented an autonomous interest.

Rather large and homogeneous data obtained at the 1.25-m reflector AZT–11 of the Crimean Astrophysical Observatory with the UBVRI Piirola's photometer–polarimeter (1984) were used for different studies.

To clarify the nature of flare emission, the strongest of them were analyzed colourimetrically. For this task the colour indices U–B, B–V, V–R and V–I of a pure flare emission have been found at the ascending branches, at the brightness maxima and at the beginning of descending branches. On the other hand, such indices have been detected for different sources of radiation: for the black bodies of various temperatures, for synchrotron emissions with different indices of energy spectra of relativistic electrons, for radiation of hydrogen plasma of different temperatures, densities and optical thickness at the Balmer continuum (Chalenko, 1999). The confrontation of these calculations with observable characteristics of flares (see Figs. 4 and 5) permits to conclude that 1) none of considered radiation mechanisms can alone reproduce the flare radiation observed within the whole UBVRI range at any flare phase; 2) the UBV flare radiation is rather close to the black body ones for temperature from 10000 to 25000 K near brightness maxima of strong flares; 3) the hydrogen plasma of some optical thickness contribution increases in the longer wavelength regions from the brightness maxima and in the UBV bands as a flare decays. Mean parameters of the most powerful 9 flares from these data are following:

DU (mag)	colour indices of the pure flare radiation at brightness maxima (mag)				T_{bb} (K)	area (cm^2)
	U – B	B – V	V – R	V – I		
2.1	-0.87 ± 0.05	0.03 ± 0.02	0.47 ± 0.05	0.78 ± 0.18	14000	10^{19}

We have noted above the usage of the crimean patrol observations to detect periodicity in the spectral index of the EV Lac flare energy spectra.

Several flares that had been registered at the Special Astrophysical Observatory with the fast photometry mode have been analyzed for a search of an existence of high frequence components, but such components were not found within the range from 1 mcs to 10 s (Beskin *et al.*, 1995).

INFRARED STUDIES

In 1991–1993 the near IR monitoring was carried out in the K band by M. R. Kidger with a single channel chopping photometer mounted at the Cassegrain focus of the 1.5-m Carlos Sanchez telescope that operated on the island of Tenerife in the Spanish Observatorio del Teide of the Instituto de Astrofisica de Canarias.

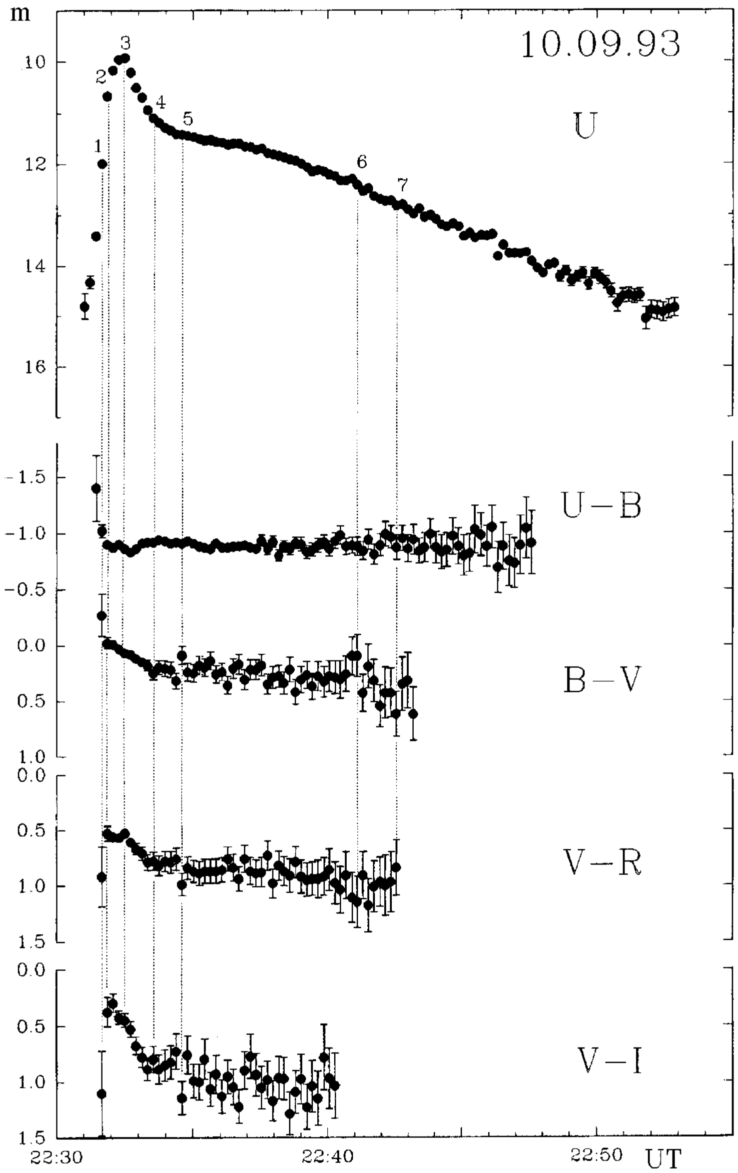

Figure 4: Light and colour indices' curves of the powerful EV Lac flare on September 10, 1993 at UT 23:32 (Abranin, Bazelyan *et al.*, 1998)

In 1994–1995 the IR patrol was carried out in the K band by G. Cutispoto, G. Leto, G. Marino, S. Messina, I. Pagano and M. Rodonó at the 91-cm reflector of the Astrophysical Observatory and Institute of Astronomy of Catania University, Catania, Italy.

In 1995 V. M. Larionov carried out the IR monitoring in the H band using the 70-cm telescope AZT-8 of the Crimean Astrophysical Observatory and the IR photometer of the Astronomical Institute of St. Petersburg University.

During all these campaigns the IR patrol covered one strong (September 10, 1993) and more than two dozens of faint flares detected in the U band. However, no synchronous variations of IR and of optical radiations were detected. It proves that IR brightness decrease found by Rodonó (1986) as well as its increases noted by Bruevich *et al.* (1980) are not general characteristics of the UV Cet-type flares. However, later, D. N. Shakhovskoy carried out the UBVRI monitoring for EV Lac within the framework of the B. E. Zhilyaev's program at the AZT-11. He found certainly two components of the flare on 5.10.96: the traditionally registerable emission component, which is the most visible in the U band, and the absorption component, which is more long, and is located

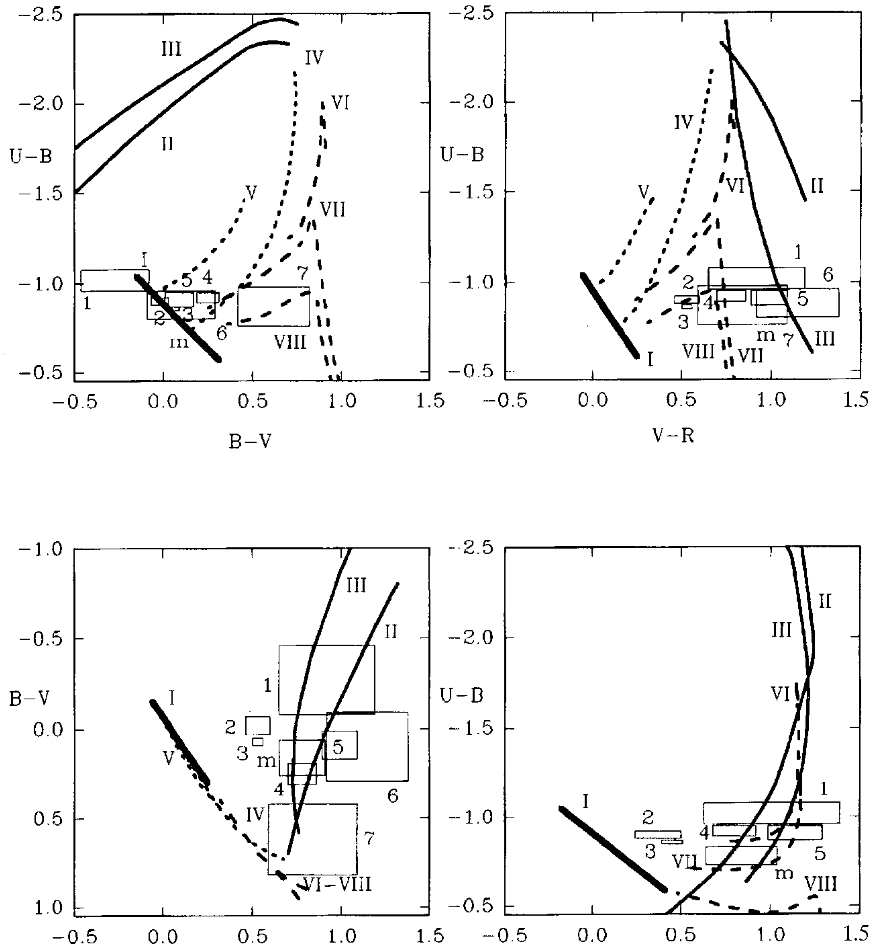

Figure 5: Colour–colour diagrams of the pure flare radiation of the EV Lac flare on September 10, 1993 at UT 23:32. I – black body radiation for the temperatures ranging from 6000 to 20000 K; II and III – emission of optically thin hydrogen plasmas in the Balmer continuum (Ba_C) with T = 10000 K and $n_e = 10^{12}$ and 10^{14} cm^{-3}, respectively; IV and V – emission of optically thick hydrogen plasmas in the Ba_C with T = 10000 and 15000 K, respectively; VI, VII, and VIII – radiation emitted by upper layers of dwarf stars heated with proton fluxes with energies higher than 1, 3 and 5 MeV, respectively. Numeration of rectangles corresponds to numbers of dotted vertical lines in Fig. 4 (Abranin, Bazelyan *et al.*, 1998)

symmetrically around emission component with amplitudes increasing toward longer wavelengths (Zhilyaev *et al.*, 1998). Then we revised previous IR records obtained in the cooperative monitorings during optical flares and found similar IR brightness decreases during faint flares (see Fig. 6). The physical meaning of these events remains unclear, but from the author's point of view the structure of appearance of "an emission peak in an absorption saucer" allows to present a lot of known colourimetric features that had no one–valued interpretation (Gershberg, 1998).

POLARIMETRY

Measurements of a linear polarization of EV Lac were carried out by N. M. Shakhovskoy, Crimean Astrophysical Observatory, at the Cassegrain focus of the 2.6-m Shajn reflector with a single channel polarimeter. During the 1989 and 1991 campaigns the polarimetry of 13 flares of EV Lac were obtained. The analysis of the U band flare polarimetry has shown that the polarization is less than 5% at 10 s time resolution and less than 2–3% at 50 s time resolution for all flares. The most powerful observed flare imposes more stringent constraints on the quoted values: 2% and 1%, respectively. Therefore, this the most clear result obtained in process of long observations suggests that the intrinsic optical radiation of flares is not polarized (see Fig. 7).

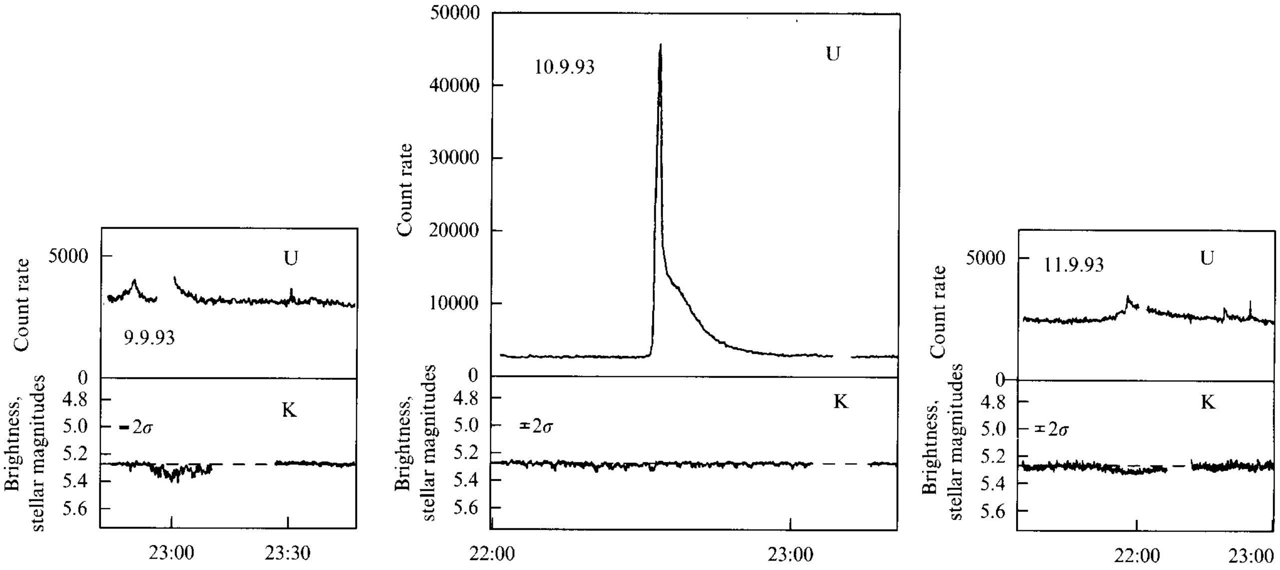

Figure 6: Segments of light curves of the EV Lac flares observed in the U band (Crimea) and K band (Canary) (Gershberg, 1998)

SPECTRAL INVESTIGATIONS

In 1986, 1987, 1990, 1992, 1994 and 1995 the spectral observations of EV Lac were carried out at the 2.6-m Shajn telescope in the Crimean Astrophysical Observatory. The CCD spectrographs with a low resolution in the Nasmyth focus and with a high resolution in the coude focus have been used. In 1989–1993 the spectral monitorings were fulfilled at the 6-m telescope of the Special Astrophysical Observatory, Nizhny Arkhyz, Russia. There the light beam from a star was splitted at the Nasmyth focus toward two devices: the spectrograph with a TV scanner covering the wavelength range from 3700 to 5200 ÅÅ and the fast photometer. In the 1994 campaign the spectral monitorings were carried out at the NORDIC telescope, Canary, with the echelle spectrograph SOFIN made in Crimea.

In 1986 and 1987 EV Lac was observed at the Shajn telescope in the H_α line region. In 1986 we found clear anticorrelation between the stellar brightness and the equivalent width of the line in the quiet state of the star. In 1987 the brightness of the star has decreased but an amplitude of rotational modulation also has decreased simultaneously, the H_α flux has increased slightly and the aforementioned anticorrelation has disappeared in such a state. These variations did not fit to a traditional scheme of stellar spottedness that is due to one or two compact starspots: if the spots are not too close to a pole in such a scheme that total brightness decrease should be accompanied with an increase of an amplitude of rotational modulation. In this connection the data obtained were interpreted as a result of an increase of the total spottedness with simultaneous more regular distribution of starspots along stellar longitudes. This conclusion initiated a development of a zonal model of red dwarf spottedness (Alekseev and Gershberg, 1996 ab, 1997b), in which a general picture of a stellar spottedness is determined instead of parameters of one or two compact starspots in traditional schemes. Up to date the UBVRI observations of 25 red dwarfs for more than 340 epochs are successfully processed within the framework of this spottedness model, some correlations between parameters of the models and global stellar characteristics are found, and the solar spottedness features fit to these correlations (Alekseev and Gershberg, 2000).

In 1989 the rotational modulation of emission features in the EV Lac spectrum were detected at the 6-m telescope while the constancy of absorption spectral features took place. In 1991 this result was confirmed.

In 1990 the H_α profiles were registered in Crimea during 3 strong flares: in two cases the red wing spread to +130 km/s and in the third case the blue wing spread to –100 km/s with undisturbed red wing. The decay of one of these flares was observed at the 6-m telescope, and a decay rate of H_δ line was found to be 1.5 faster as compared to the H_β decay rate. In 1992 emissions of Fe II, Fe I, Mg I in flare spectra, which were earlier rare detected or not detected, were registered at the Shajn telescope. The H_β profile analysis in moderate power flares has shown that the line broadening was negligible at the half maximum level, it became noticeable at the level of 20 maximum. The broadened profiles could be formally represented both by two Gaussians with different widths and by a set of 3–7 Gaussians of instrumental width with dispersion of maximum wavelengths

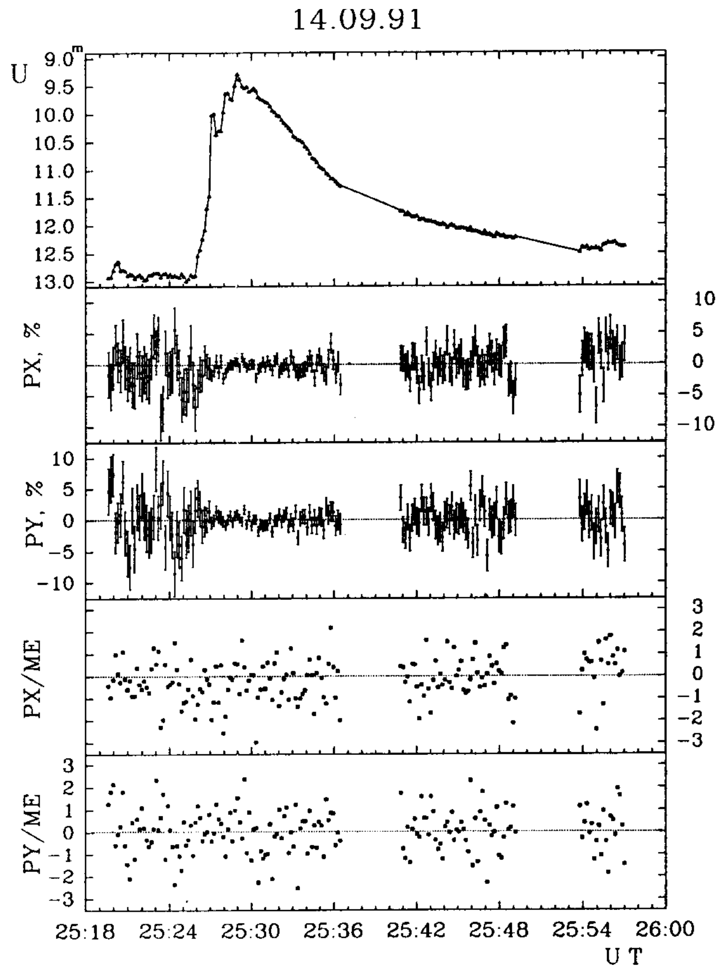

Figure 7: Photometric and polarimetric measurements of EV Lac during the most powerful flare on September 14, 1991 at 25:29 registered with 10 s time resolution: U band light curve (upper panel), normalized Stokes parameters PX and PY with their mean squared errors computed by quantum statistics (middle panel), and ratios of these parameters to their errors PX/ME and PY/ME (lower panel) (Alekseev, Gershberg *et al.*, 1994)

about 400–700 km/s in the velocity scale.

The very interesting data were obtained in Crimea during the night August 31/September 1, 1994, they are given in Fig. 8. The light curve of the star is shown in the top panel of the figure. A half of dozen of characteristic fast flares with different amplitudes and durations of several minutes are clearly visible. Also we see a long–lived glow that started at UT 20:46 and lasted at least until the strongest flare of the night at UT 23:24. The next panel demonstrates the equivalent widths of the H_β line. A close inspection of these two plots reveals the reaction of the line on separate flares. But the main feature of the temporal behavior of W_{H_β} is a dominating maximum connected with the enhanced stellar brightness over almost three hours. The equivalent widths of the Fe II + Mg I emission blend shown in the fifth panel of the figure shows the behavior similar to W_{H_β} with correlation coefficient 0.94. The third panel of the figure displays the equivalent width of the neutral helium line $\lambda\tilde{4}471$ Å. The comparison of this plot with the previous two ones shows that this line reacts more clearly to separate fast flares than H_β although these lines correlate mutually with the correlation coefficient 0.76.

The most interesting and unexpected results were obtained by patrolling the ionized helium λ 4686 Å emission (see the fourth panel in Fig. 8). Formally, this line does not correlate with the emissions considered above: its correlation coefficients lie within the range from 0.2 to 0.3. However, more close comparison of W_{HeII} with the stellar light curve reveals that almost all spectra with enhanced He II line were obtained during 15–30 minutes after the fast flares. The second intriguing feature of the He II emission is represented

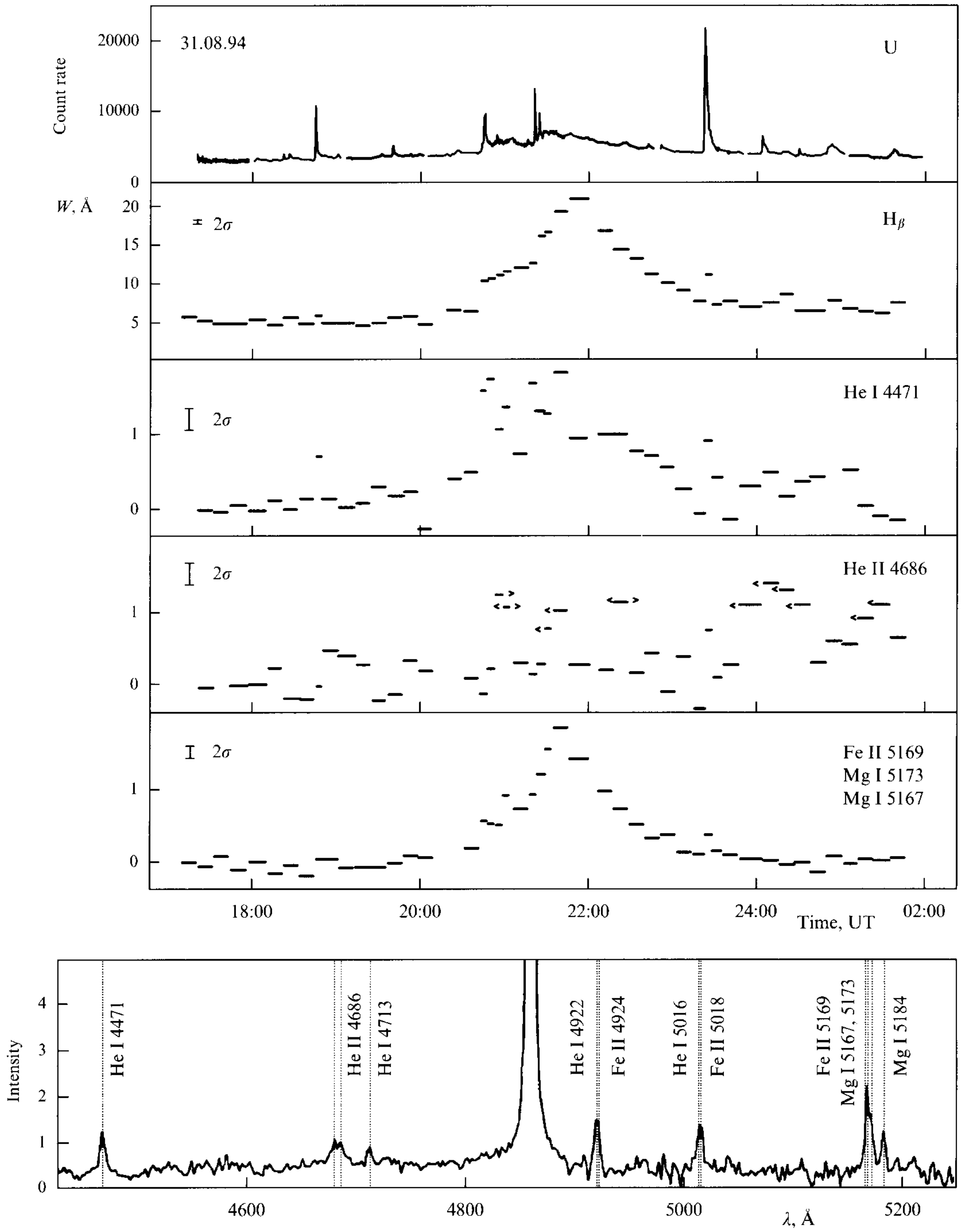

Figure 8: Results of photometrical and spectral monitorings of EV Lac obtained on the night of August 31/September 1, 1994, in Crimea. There are shown the count rate in the U band, the equivalent widths of the H_β, He I λ 4471 Å, He II λ 4686 Å emission lines and the blend of metallic lines; the spectrum of active states of the star is also presented (Gershberg, 1998)

in the bottom panel of the figure, where the added spectrum of all active states of the star registered during the 1994 campaign is shown. A sharp splitting of the He II emission is clearly seen in the plot: the long–wavelength component has a normal position while the short–wavelength one is shifted by -400 km/s. Among spectra obtained in the night considered, the eight spectra demonstrate only the short–wavelength component, two spectra show both components and one spectrum has only the long–wavelength component; these features are marked in the figure by $<$, $<>$ and $>$, respectively. The meaning of these observations is not clear yet. Apparently, the short–wavelength component of the line can emerge in a transition region between the stellar chromosphere and corona or inside the lower corona during the formation of moving structures, whose solar analogs produce transients in the interplanetary space.

In 1995 EV Lac was observed in Crimea in the H_α region. Results of this and previous campaigns were used by Baranovsky *et al.* (2000) to construct semi–empirical models of the quiet chromosphere of the star and its flares. The new qualitative results of this modelling are that a region with a significant spread along the height with a small vertical temperature gradient exists in the chromosphere of the cool dwarf – the similarly as in the solar chromosphere. This is the so-called a temperature plateau, where the most Balmer lines' fluxes are originated. Similar structure was also found in constructed flare models but in deeper layers.

RADIO MONITORING

During some campaigns, the EV Lac star has been monitored with several radio telescope to detect its radio emission. In 1986 and 1987 the star was observed at 8.2 mm with 22-m radio telescope of the Crimean Astrophysical Observatory; a stellar radio emission was not detected with a noise level of 30–50 mJy. In 1990 observations near 21 cm were fulfilled with the radio – optical telescope ROT 32/54/2.6 in Armenia; flare radio signals were not found with a noise level of 6–8 mJy. In 1992 the radio patrol for EV Lac was carried out at 6 cm with the broad–band Jodrell Bank interferometer, Great Britain. The patrol permitted to estimate a high limit of a stellar flux as 5 mJy.

In 1992 radio observations of EV Lac were begun at the decametric range with the radio telescope UTR–2 of the Institute of Radio Astronomy of the National Academy of Science of Ukraine.

The UTR–2 output is supplied by two two–channel radiometers at 25 and 20 MHz, the third similar radiometer was used to monitor an area shifted from EV Lac along the declination by 1°. During 30 hours of the EV Lac monitoring more than 30 bursts have been detected. About half of them were identified with terrestrial interference. The rest of them were individual bursts with durations of 3 s and often less than 1 s or compact groups of bursts with durations of about 10 s. The eight radio bursts were found to be coincident in time with optical flares and, therefore, were regarded as ones with the high probability of stellar origin. Groups of bursts were detected only during the one night when the optical activity level of the star was high. Only weak individual bursts were detected during the other nights with moderate and low optical activity; these two types of bursts exhibit different signal intensities as well. If one supposes that a radio source size is equal to the stellar disk, the fluxes detected correspond to the brightness temperature of 4×10^{17} to 1×10^{18} K. Thus, probability of detection of decametric emission from EV Lac seemed to be high, although some doubts should be kept.

During 20 hour monitoring in 1993 the 6 faint bursts were detected, but contrary to 1992 campaign, they could not be regarded as certain candidates for stellar sporadic decametric emission.

In 1994 campaign both the technical and analytical parts of decametric radio observations were essentially improved. During 33 hour monitoring the 18 radio bursts were detected and 4 criteria were applied to them to select bursts of non–terrestrial nature. As a result, the burst on August 26 at UT 22:08 was selected as one of probable stellar origin. Its duration is of about 10 s. It coincides with the optical flare with $\Delta U = 0^{m}\!.5$ and satisfies to the majority of criteria mentioned. This event with brightness temperature of about 10^{18} K, apparently, can be explained with plasma mechanism of radiation.

SPACE RESEARCH

The ASTRON space mission had the pointing and offset guiding system that did not permit to study EV Lac in a convenient autumn time. By this reason, we carried out such observations during 4 rather short sessions in Februaries of 1984, 1986 and 1987 with parallel photometric patrols from the Crimean Astrophysical Observatory. During two of these sessions we have registered flares.

During the session of February 24, 1984 a very short flare of a total duration of 2.4 s was registered as a strong burst in 4 successive telemetric records of 0.61 s each (Gershberg and Petrov, 1986). In that time a reality of such short flares was questionable, but later their existence was certainly confirmed by the fast photometry at the 6-m telescope (Beskin, Gershberg *et al.*, 1988).

During the session of February 6, 1986 the strong flare with $\Delta U \sim 3^m$ was registered in $\lambda\lambda$ 1536–1564 ÅÅ and $\lambda\lambda$ 2420–2448 ÅÅ regions and in the $\lambda\lambda$ 1700–6500 ÅÅ reference channel. The flare was registered in UV with the highest for that time temporal resolution less than 1 s. The analysis of this flare allowed to find two new qualitative features: the flaring of the CIV λ 1550 Å line begun 7 s before the beginning of the flare in continuum and the very fast and power burst of the line was registered at the beginning phase of the flare. This burst is similar to fast bursts of this line in the solar active regions but exceeded them by hundred times in respect areas, by several orders of magnitude in respect energy and it was an order of magnitude shorter (Burnasheva, Gershberg *et al.*, 1989).

In 1993 the ground–based observations of EV Lac were partly overlapped with monitorings by two space missions: IUE and EUVE. EUVE detected the EV Lac flare in the $\lambda\lambda$ 70–180 ÅÅ region. Up to date preliminary results were published only (Ambruster *et al.*, 1994).

Our deep thanks to all participants of the all cooperative programs for fruitful collaboration.

REFERENCES

[1] *Abdul–Aziz H., Abranin E. P., et al.* // Astron. and Astrophys. Suppl. Ser.–1995.–**114**.–P. 509.

[2] *Abranin E. P., Alekseev I. Yu., et al.* // Astron. and Astrophys. Transactions.–1998.–**17**.–P. 221.

[3] *Alekseev I. Yu., Gershberg R. E., et al.* // Astron. and Astrophys.–1994.–**288**.–P. 502.

[4] *Alekseev I. Yu. and Gershberg R. E.* // Astron. Rep.–1996a.–**73**, N 4.–P. 579–589.

[5] *Alekseev I. Yu. and Gershberg R. E.* // Astrofizika.–1996b.–**39**.–P. 67. (in Russian).

[6] *Alekseev I. Yu. and Gershberg R. E.* The Earth and the Universe / Eds G. Asteriadis, A. Bantelas, M. E. Contadakis, *et al.*–Thessaloniki: Ziti Editions, 1997a.–P. 43.

[7] *Alekseev I. Yu. and Gershberg R. E.* // Astron. Rep.–1997b.–**74**, N 2.–P. 240.

[8] *Alekseev I. Yu. and Gershberg R. E.* // 2000.–in preparation.

[9] *Ambruster C. W., Brown A., Pettersen B. R. and Gershberg R. E.* // Bull. Amer. Astron. Soc.–1994.–**26**.–P. 866.

[10] *Baranovsky E. A., Gershberg R. E. and Shakhovskoy D. N.* // Astron. Rep.–2000.–(in press).

[11] *Berdyugin A. V., Gershberg R. E., et al.* // Bull. Crimean Astrophys. Obs.–1995.–**89**.–P. 81.

[12] *Beskin G. M., Gershberg R. E., et al.* // Bull. Crimean Astrophys. Obs.–1988.–**79**.–P. 71.

[13] *Beskin G. M., Mitronova S. N. and Panferovo I. P.* Flares and Flashes / Eds J. Greiner, H. W. Duerbeck and R. E. Gershberg.–Lecture Notes in Physics.–**454**.–P. 85.

[14] *Bruevich V. V., Burnashev V. I., Grinin V. P., et al.* // Bull. Crimean Astrophys. Obs.–1980.–**61**.–P. 90.

[15] *Burnasheva B. A., Gershberg R. E., et al.* // Astron. Rep.–1989.–**66**.–P. 328.

[16] *Chalenko N. N.* // Astron. Rep.–1999.–**76**.–P. 529.

[17] *Chugainov P. F.* // Bull. Crimean Astrophys. Obs.–1972.–**46**.–P. 14.

[18] *Doyle J. G. and Butler C. J.* // Nature.–1985.–**313**.–P. 378.

[19] *Gershberg R. E.* // Astrophys. and Space Sci.–1972.–**19**.–P. 75.

[20] *Gershberg R. E.* // Mem. Soc. Astron. Ital.–1989.–**60**.–P. 263.

[21] *Gershberg R. E.* // Physics. Uspekhi.–1998.–**41**.–P. 807. (in Russian).

[22] *Gershberg R. E. and Shakhovskaya N. I.* // Astrophys. and Space Sci.–1983.–**95**.–P. 235.

[23] *Gershberg R. E. and Petrov P. P.* Flare stars and related objects / Ed. L. V. Mirzoyan.–Yerevan: Publ. House Armenian Acad. Sci., 1986.–P. 37.

[24] *Gershberg R. E., Mogilevsky E. I. and Obridko V. N.* // Kinematics and Physics of Celestial Bodies.–1987.–**5**.–P. 3.

[25] *Gershberg R. E., Grinin V. P., et al.* // Sov. Astron.–1991.–**68**.–P. 548. (in Russian).

[26] *Gershberg R. E., Ilyin I. V. and Shakhovskaya N. I.* // Sov. Astron.–1991.–**68**.–P. 959. (in Russian).

[27] *Gershberg R. E., Ilyin I. V., et al.* // Sov. Astron.–1993.–**70**.–P. 984. (in Russian).

[28] *Kasinsky V. V. and Sotnikova R. T.* // Issledovaniya po geomagnetismu, aeronomii i fizike Solntsa.–1988.–**83**.–P. 99. (in Russian).

[29] *Kasinsky V. V. and Sotnikova R. T.* // Solar and stellar flares: Proc. IAU Coll. N 104, Stanford, Aug. 15–18, 1989 / Eds B. M. Haisch and M. Rodonó.–Catania Astrophys. Obs. Special Publ., 1989.–P. 255.

[30] *Korotin S. A. and Krasnobabtsev V. I.* // Bull. Crimean Astrophys. Obs.– 1985.–**73**.–P. 131.

[31] *Kurochka L. N.* // Sov. Astron.–1987.–**64**.–P. 443. (in Russian).

[32] *Lu E. T. and Hamilton R. J.* // Astrophys. J.–1991.–**380**.–P. L89.

[33] *Oskanian V. S. and Terebizh V. Yu.* // Astrofizika.–1971a.–**7**.–P. 83. (in Russian).

[34] *Oskanian V. S. and Terebizh V. Yu.* // Astrofizika.–1971b.–**7**.–P. 281. (in Russian).

[35] *Pustil'nik L. A.* // Letters Sov. Astron.–1988.–**14**.–P. 940. (in Russian).

[36] *Pustil'nik L. A.* // Astrophys. and Space Sci.–1997.–**252**.–P. 325.

[37] *Rodonó M.* Flare stars and related objects / Ed. L. V. Mirzoyan.–Yerevan: Publ. House Armenian Acad. Sci., 1986.–P. 19.

[38] *Shakhovskaya N. I.* // Solar Phys.–1989.–**121**.–P. 375.

[39] *Skumanich A.* // Austral. J. Phys.–1985.–**38**.–P. 971.

[40] *Whitehouse D. R.* // Astron. and Astrophys.–1985.–**145**.–P. 449.

[41] *Zhilyaev B. E., Verlyuk I. A., et al.* // Astron. and Astrophys.–1998.–**334**.–P. 931.

STEPHANION OBSERVATORY. GREEK–UKRANIAN ASTROLINK

M. E. Contadakis[1], **S. Avgoloupis**[2], **L. N. Mavridis**[1]

[1] *University of Thessaloniki, Departement of Geodesy and Surveying*
54006 Thessaloniki, Greece
e-mail: kodadaki@vergina.eng.auth.gr

[2] *University of Thessaloniki, Departement of Physics, Section of Astronomy, Astrophysics and Mechanic*
54006 Thessaloniki, Greece

The Astronomical research developed during the 35 years of action of the Stephanion Observatory is reviewed in this report. During these years scientists from all the Astronomical Institutes of Greece as well as from many other countries conduct astronomical research programs realized in the Stephanion Observatory. The research on the red dwarfs is a dominant part of the scientific work done. The international cooperation of the Greek scientific teams was developed in the frame of this research. The Greek – Ukrainian scientific cooperation during the last decade in the frame of broader international cooperation as well as the bilateral ones were very prosperous and set the basis of a promising scientific cooperation in the future in the field of Astronomy.

INTRODUCTION

The moment of the twilight of a new century and, far much more, of a new millennium is a moment of the account for the achievements and the failures of the past, of the self potential resume and of the perspectives for the entire World, the particular Countries, the Institutes, the individuals and for the Scientific community as well. There is a specific reason that we refer ourselves to the Stephanion Observatory of Greece in a conference for the perspectives of the Ukrainian Astronomy in the new century. A tight scientific cooperation with scientists from the former eastern countries and from Ukraine as well was the started point for astronomers from the Stephanion Observatory working in the field of the variable stars. The best way to present this prosperous scientific cooperation is to refer ourselves to the research programs which has been developed at the Stephanion Observatory. In the following, after a brief presentation of the Stephanion Observatory a brief review of the research at the Stephanion Observatory will be presented. The long lasting prosperous scientific cooperation constitutes foundations of the best perspective for future scientific cooperation between Greek and Ukrainian astronomers.

THE STEPHANION OBSERVATORY

In spite of the famous blue Greek sky, Greece did not have, until the beginning of the 1960s, an observatory properly equipped for modern astrophysical observations. Two Balkan wars at the begining of the century, the social and economic integration of two million war refugees in 1922, two world wars and one civil war, leave no room for investments in basic research. Greek astronomers working in the field of modern astrophysics were inforced to work abroad. Nevertheless, in the 50s the Greek National Committee for Astronomy, under the Chairmanship of the late Professor Xanthakis, started a preparatory work for the selection of sites which could be suitable for the foundation of an astrophysical observatory, but no progress could be made because of the lack of the necessary funds. Among the best observational sites, the Stephanion of Corinth in Pelopones ($\delta = 22°49'44'', \alpha = 37°45'15''$) located at an altitude of 800 m was proposed. In 1966 the NATO Science Committee awarded a research grant to L. N. Mavridis and H. Neckel to install a 38-cm reflector (f/21) in Greece. This reflector has been belonged to the Hamburg Observatory and been involved in the variable star photoelectric observations program. Taking into account the Academy's research and the experience of a visit of a group of eminent astronomers in 1964, Mavridis and Neckel decided to install the 38-cm reflector in the outskirts of Stephanion. The photoelectric observations started in March 1967 and continued until September 1970, when the NATO project was terminated and the telescope was transported back to Hamburg. The following observations were carried out at the Stephanion Observatory with the Hamburg reflector: 1. Photoelectric observations of M-type stars in the B, V colours of the international U, B, V system by H. Neckel [26]. 2. Photoelectric observations of galactic cepheids in the U, B, V colours of the international U, B, V system by the team of the Aristotle University of Thessaloniki [4]. Meanwhile, the European scientific community had become aware of the great advantages of the site of the Stephanion Observatory. In October 1966 a satellite observing station belonging to CNES was installed in the grounds of the Stephanion Observatory. It included one Doppler tracking and one Laser ranging station. The station was in regular operation until the end of August 1967, when it was transferred to France [16]. In 1964, the 40-cm van Straaten Cassegrain reflector belonging to the Utrecht Observatory was installed in the grounds of the Stephanion Observatory. The operation of this telescope, which was used by the astronomers of all the astronomical institutes of the Netherlands, started in July 1967. The project which was known as the "Netherlands European Southern Observing Station" was terminated in the fall of 1973 and the telescope was transported again back to Utrecht [27]. In June 1971 a 30-inch Cassegrain reflector with asymmetric mount (focal ratio f/3 for the primary hyperbolic mirror and f/13.5 for the Cassegrain focus) constructed by the U. S. firm Astro Mechanics was installed in the grounds of the Stephanion Observatory. The new telescope was equipped with the following auxiliary equipment: (1) one Johnson dual channel photoelectric photometer with offset guider unit, constructed by Astro Mechanics, which is cooled with dry ice and is suitable for carrying out photoelectric observations in the U, B, V, R, I colours of the international U, B, V system and (2) one Meinel plane grating spectrograph with flat-field folded Schmidt camera f/2 focal ratio constructed also by Astro Mechanics. This telescope, which belongs to the Department of Geodetic Astronomy, Aristotle University of Thessaloniki and is of the light-collector type, turned out to be very suitable for the photoelectric observations of variable stars. The observations with the new telescope started in July 1971 and continue regularly until now. At that time it was the biggest telescope in the Balkan area.

SOME OF THE MAIN RESULTS OBTAINED WITH THE 30-inch REFLECTOR OF THE STEPHANION OBSERVATORY

The 30-inch reflector has been used since 1971 by the astronomers of the Aristotle University of Thessaloniki, the Democritus University of Thrace, the University of Ioannina and numerous astronomical institutions outside Greece for carrying out the photoelectric observations of variable stars. Three main types of variable stars are under investigation, namely: a) the flare stars of the solar neighborhood, b) the variables of the RS CVn type and c) the galactic cepheids. In the following the main research programs referring to the flare stars of the solar neighborhood and the RS CVn stars will be summarized [20]:

Monitoring of the Flare Activity and the Quiet-state Luminosity of Flare Stars

One of the main programs carried out with the 30-inch Cassegrain reflector is a systematic monitoring of the luminosity of selected flare stars of the solar neighborhood. This monitoring is being carried out mainly in the B color of the international U, B, V system. During most of the observing nights, however, additional observations are being made in the U, B, V colors of the same system. These observations allow us to study the behavior of the colors of the stars under investigation. The following flare stars of the solar neighborhood have been observed so far: EV Lac, BY Dra, AD Leo, UV Cet, YZ CMi, DT Vir, DO Cep, BD +160 2708, BD +550 1823 and Gl 182. The first result of these observations is the detection of stellar flares and the determination of the corresponding light curves. In this way many hundreds of flares of the stars under investigation could be detected and studied so far. In addition, to the flare patrol, it has been possible, through a proper arrangement of the observational procedure, to use the same observations for the determination of the quiet-state luminosity of the stars under observation during the monitoring period. The quiet-state luminosity being determined in such a manner refers to the B color or to the U, B, V colors of the international U, B, V system, depending on whether the monitoring is being carried out in the B or in the U, B, V colours. In this way very rich observational material concerning the flare activity and the quiet- state luminosity of the flare stars under investigation could be obtained so far [21]. This material is of special value for three reasons: (1) it covers a fairly long period of time (1971 until now), (2) it is of a high accuracy, and (3) it is homogeneous enough, because it has been obtained by the same team of observers, using the same methods for the execution and reduction of the observations and the same instruments. With the help of this observational material a number of investigations concerning the phenomenon of the flare activity could be carried out. In the following some of the main results of these investigations are being summarized.

Long- and Short-term Variations of the Flare Activity and the Quiet-state Luminosity

A great percentage of the observational material obtained at the Stephanion Observatory refers to EV Lac flare star. This star shows the well known BY Dra syndrome, *i.e.*, a short-term variation of the quiet-state luminosity with the period of 4.375 days and the amplitude $\Delta V = 0.08$ mag. This variation is being interpreted by most of the authors as indicating the existence of starspot(s) on the surface of the star, which are rotating with the same period. Evidence for rotational light modulation by transient starspot formation was found by analyzing the quiet state luminosity variations together with the flare frequency distribution over the phase for EV Lac, BY Dra and DO Cep flare stars [6, 7, 8]. With the help of the observational material obtained at the Stephanion Observatory it could be shown that, besides this short term variation of the quiet state luminosity, there is also a long-term fluctuation of the mean annual values B of the quiet-state luminosity of the star with the amplitude of about 0.3 mag and a period of about 5 years. Similar fluctuations show also the mean annual values of the flare frequency P(1) and the integrated flare intensity P(2) of the star. Moreover, very strong negative correlations exist between the values of B corresponding to a given year and the values of P(1) and P(2) corresponding to the previous year, in the sense that years with the enhanced flare activity are followed by years with the lower quiet-state luminosity [22]. This and other similar results could be interpreted as indicating that years with the enhanced flare activity are followed by years with the larger starspot coverage on the stellar surface. This conclusion, being confirmed by additional observations, could be of importance for a better understanding of the physical processes underlying the phenomenon of stellar activity [23].

Very Short-term Variations of the Quiet-state Luminosity

The existence of another type of variations of the quiet-state luminosity of EV Lac star the very short-term variations was established with the help of the observational material obtained at the Stephanion Observatory [25]. In fact, during most of the nights the luminosity of the star remains constant (standard deviation is less than 0.04 mag during 2 hours or more). In some other nights the luminosity of the star shows a fairly sinusoidal variation with a period between 0.5 and 2.0 hours and an amplitude between 0.1 and 0.2 mag. In some other nights, on the contrary, the stars luminosity shows very irregular variations with a duration of at least few hours and an amplitude of about 0.4 mag or even more.

Dependence of the Flare Activity on the Phase of the Short-term Periodic Light Variation of BY Dra

BY Dra is another flare star, besides EV Lac, for which numerous observations were carried out at the Stephanion Observatory. This observational material, together with additional material obtained at the Byurakan, Konkoly and Matra Observatories were used for a systematic study of the flare activity of this star during the period 1971–92 [24]. The following conclusions could be drawn: a) the flare activity of BY Dra shows also a long-term fluctuation with a very pronounced maximum during the years 1973–75 and a new enhancement of the activity from 1987 onwards, b) there is a clear tendency for the flares of BY Dra to appear during certain part of the period of the short-term periodic light variation of the star (P = 3.8285 days). This could be interpreted as indicating a pronounced tendency of the flares on BY Dra to be originated within the part of the stellar surface covered by the magnetic field (B = 2.800 Gauss, f = 60%).

Co-ordinated Simultaneous Multiwavelength Observations of Flare Stars

It is obviously that the physical processes connected with the phenomenon of flare activity, and more generally of stellar activity, would be better studied, if we could have at our disposal simultaneous observations of these stars in various spectral regions. For these reasons an effort is being made in recent years to organize co-ordinated multiwavelength observations of selected flare stars. In these campaigns, besides the optical observations, an effort is being made in order to secure also simultaneous observations in as many other spectral regions as possible, such as the X-rays and the ultraviolet spectral regions with the help of artificial Earth satellites, the region of radiowaves with the help of radio telescopes, *etc.* Because of the fairly great number of clear nights the Stephanion Observatory is a very welcome partner in most of these campaigns. In the following some of the programs of co-ordinated simultaneous multiwavelength observations of flare stars in which the Stephanion Observatory has been actively involved will be summarized:

1. Simultaneous optical and radio observations of UV Cet flare star in October 1972. In the framework of this joint program between the Stephanion Observatory and the Jodrell Bank Radioastronomy Observatory in the United Kingdom a very large flare was observed on October 11, 1972 on UV Cet flare star both in the optical region at the Stephanion Observatory (Δm greater than 4.5 mag) and in the radiowaves (408 MHz) at the Jodrell Bank. The maximum of the optical flare precedes that of the radio flux by approximately 8 minutes. These results have been of fundamental importance for a better understanding of the mechanism of the origin of radio flares [17].

2. Simultaneous optical, radio and X-ray (EXOSAT) observations of BY Dra flare star in September 1984 [9].

3. Simultaneous optical, radio and X-ray (EXOSAT) observations of UV Cet flare star in December 1985 [10].

4. Simultaneous optical, ultraviolet (IUE), and microwave (VLA) observations of Gl 182 flare star in October 1983 [18].

5. Co-operative optical and radio observations of EV Lac flare star in August 1990 [15].

6. Co-ordinated optical observations of EV Lac flare star in September 1991 [3].

7. Co-ordinated optical and radio observations of EV Lac flare star in September 1992 [1].

8. Co-ordinated observations of the red dwarf EV Lac flare star in 1993 [2].

9. Co-ordinated Multiwavelength Simultaneous high resolution photometry for observing rapid optical oscillation on red dwarfs. [28].

Co-ordinated Simultaneous Multiwavelength Observations of RS CVn Stars

The RS CVn stars are generally G- and K-type sub-giants in close binaries. They rotate with periods of, typically, a few days. At least one of the components of the system shows evidence of spots and other phenomena associated with flare activity. Until recently the flares on the RS CVn stars were detected mainly in the microwave region and less frequently in the ultraviolet and X-ray regions, while optical continuum flares were considered to be extremely rare. Observations of the RS CVn star II Peg carried out at the Stephanion Observatory in August 1989 and July-September 1990 tend to dispel that idea [19]. A number of co-ordinated simultaneous multiwavelength observations of RS CVn stars have been organized in recent years. The Stephanion Observatory participated actively again in some of these campaigns, such as the followings:

1. Simultaneous optical, ultraviolet (IUE), X-ray (GINGA) and radio (VLA) observations of RS CVn star II Peg in August 1989 [11].

2. Simultaneous optical and ultraviolet (IUE) observations of RS CVn star HR 1099 in December 1989 [14].

3. Simultaneous optical and ultraviolet (IUE) observations of RS CVn star II Peg in July/September 1990 [12].

4. Simultaneous optical observations of RS CVn star II Peg in August 1991 [5].

5. Simultaneous optical and ultraviolet (IUE) observations of RS CVn star SZ Psc in September 1991 [13].

CONCLUDING REMARKS

From the discussion above it becomes evidently that fairly important observational research programs in the field of stellar activity (flare stars, RS CVn stars) have been carried out so far at the Stephanion Observatory. These activities make the Stephanion Observatory one of the leading astrophysical observatories all over the world in the field of stellar activity. Furthermore, the research activities carried out at the Stephanion Observatory have contributed very considerably to the development of Optical Observational Astronomy in Greece, as manifested by the fact that 13 Greek astronomers have participated successfully in the observational research programs carried out at this observatory and published their results in leading astronomical journals. Another important point is that, due to the predominant field of the research (stellar activity) conducted at the Stephanion Observatory, Greek scientists came in early contact and cooperation, which is continued ever since, with Ukrainian scientists who traditionally occupy a leading place in the research on stellar activity all over the world. This is obviously from the mentioned above, a brief account of the scientific work was done in Stephanion. A great percentage of this work was done in cooperation with the Ukrainian Astronomical Institutes. Today most of the Greek astronomers which are interested in optical astrophysics have the possibility to work in Greece. Apart of the 30-inch reflector of the Stephanion Observatory, two 1.23-m reflectors (at Kryonerio, Pelopones and Skinaka, Crete) with a wealth of auxiliaries and much more smaller telescopes are in their disposal while a Robotic 2-meter, fully equipped with auxiliaries, will be in operation on 2001. Many of them have cooperation with the Ukrainian scientists too. In concluding we may say that Greek-Ukrainian cooperation will be continued in the new century with the best perspectives and that the Stephanion Observatory plays a key role in this cooperation.

REFERENCES

[1] *Abdud-Aziz H., et al.* // Astron. and Astrophys. Suppl. Ser.–1995.–**114**.–P. 509.

[2] *Abranin E. P., et al.* // Astrophys. and Space Sci.–1998.–**257**.–P. 131.

[3] *Alekseev I. Yu., et al.* // Astron. and Astrophys.–1994.–**288**.–P. 502.

[4] *Asteriadis G., Mavridis L. N., Tsioumis A.* // Proc. Academy of Athens.–1977.–**51**.–P. 540.

[5] *Byrne P. B., et al.* Physics of Solar and Stellar Coronae / Eds G. F. Linsky, S. Serio.–Kluwer Acad. Publ., 1993.–P. 439.

[6] *Contadakis M. E.* // Astron. and Astrophys.–1995.–**300**.–P. 819–822.

[7] *Contadakis M. E.* // Proc. 2nd Hellenic Astron. Conf., June 29–July 1, 1995 / Eds M. E. Contadakis, J. D. Hadjidemetriou, L. N. Mavridis, J. H. Seiradakis.–Thessaloniki, Greece: Ziti Publication, 1996.–P. 240–245.

[8] *Contadakis M. E.* // Cool Stars, Stellar Systems, and the Sun: Ninth Cambridge Workshop / Eds R. Pallavicini, A. K. Dupree.–ASP Conf. Ser.–1997.–**109**.–P. 595.

[9] *de Jager C., et al.* // Astron. and Astrophys.–1986.–**156**.–P. 95.

[10] *de Jager C., et al.* // Astron. and Astrophys.–1989.–**211**.–P. 157.

[11] *Doyl J. G., et al.* // Astron. and Astrophys. Suppl. Ser.–1992.–**96**.–P. 351.

[12] *Doyle J. G., Mathioudakis M., Murphy H. M., et al.* // Astron. and Astrophys.–1993.–**278**.–P. 499.

[13] *Doyle J. G., Mitrou C. K., Mathioudakis M., et al.* // Astron. and Astrophys.–1994.–**291**.–P. 135.

[14] *Foing B.H., et al.* // Astron. and Astrophys.–1994.–**292**–P. 543.

[15] *Gershberg R. E., et al.* // Astron. Rep.–1993.–**37**.–P. 4977.

[16] *Kovalevsky J.* // BSAF.–1967.–**81**.–P. 244.

[17] *Lovell B., Mavridis L. N., Contadakis M. E.* // Nature.–1972.–**250**.–P. 124.

[18] *Mathioudakis M., et al.* // Astron. and Astrophys.–1991.–**244**–P. 155.

[19] *Mathioudakis M., Doyle J. G., Avgoloupis S., et al.* // Mon. Notic. Roy. Astron. Soc.–1992.–**255**.–P. 48.

[20] *Mavridis L. N.* // Greek Prospects for the 21st century: Proc. Conf. Astronomy of 2000+, 12–13 November 1998, Athens, Greece / Eds E. Kontizas, R. Korakitis, J. Ventura.–1998.–P. 109.

[21] *Mavridis L. N., Asteriadis G., Mahmoud F. M.* Compendium in Astronomy / Eds E. G. Mariolopoulos, P. S. Theocaris, L. N. Mavridis.–Dordrecht: Reidel, 1982.–P. 253.

[22] *Mavridis L. N., Avgoloupis S.* // Astron. and Astrophys.–1986.–**154**.–P. 171.

[23] *Mavridis L. N., Avgoloupis S.* // Astron. and Astrophys.–1993.–**154**.–L. 5.

[24] *Mavridis L. N., Avgoloupis S., Seiradakis J., Varvoglis P. P.* // Astron. and Astrophys.–1995.–**296**.–P. 705.

[25] *Mavridis L. N., Varvoglis P. P.* // Proc. First Panhellenic Astron. Meeting, Athens, September 21–23, 1993 / Ed. P. Laskaridis.–1993.–P. 203.

[26] *Neckel H.* // Astron. and Astrophys. Suppl. Ser.–1974.–**18**.–P. 169.

[27] *Van der Wal P. B., Nagel C., Voordes H. R., de Boer K. S.* // Astron. and Astrophys. Suppl. Ser.–1972.–**6**.–P. 131.

[28] *Zhilyaev B., et al.* // Astron. and Astrophys.–2000.–accepted.

ROSAT X–RAY OBSERVATIONS OF STELLAR FLARES: UV CET TYPE STARS OF THE SOLAR VICINITY

V. Hambaryan[1,2], **R. Neuhäuser**[2], **B. Stelzer**[2], **and A. D. Schwope**[1]

[1] *Astrophysikalisches Institut Potsdam, An der Sternwarte 16, 14482 Potsdam, Germany*
e-mail: vhambaryan@aip.de

[2] *Max-Planck Institute für Extraterrestrische Physik, D-85740 Garching bei München, Germany*

We present the results of a comprehensive survey of X-ray observations of flare stars in the solar neighborhood carried out with the *ROSAT* satellite. The data sample comprises 525 PSPC and 149 HRI pointed as well as *ROSAT* All-Sky (RASS) survey observations pertaining 143, 69 and 463 stars, respectively, from the catalogue of UV Cet type stars and related objects of Gershberg *et al.* [1]. In total, the sample represents nearly 1350 hours monitoring of flare stars at X-ray wavelengths (0.1–2.4 KeV). The timing analysis of the data has been performed by Scargle's [2] change point detection method using Bayesian model comparison technique, directly applicable to the unbinned data. We present results of brightness variations corresponding to the 94 PSPC, 40 HRI and 26 RASS detections. Both quiescent and flare emission is estimated and hardness ratios for PSPC observations are presented. For 9 comparatively powerful flares observed by the PSPC, time resolved spectroscopy is presented clearly indicating an increase of coronal metallicity abundance at flare maximum.

INTRODUCTION

The discovery and study of red dwarf flare stars (FSs) in the solar vicinity and in star clusters and associations had a fundamental significance for the study of the physics and evolution of red dwarf stars.

Stellar flares represent one of the most challenging problems of contemporary astrophysics. Both solar and stellar observations have shown the flare phenomenon to be very complex, and in recent years important progress has been made from observations over wide wavelength ranges.

FSs were discovered in the late 1940s in the solar vicinity and named UV Cet type variables (classical FSs). According to a recent definition by Gershberg *et al.* [1], these stars are on the lower part of the main sequence and show phenomena inherent to solar activity (sporadic flares, dark spots, variable emission from chromospheres and coronae, radio, X-ray and UV bursts). At present, the total number of known UV Cet type stars is 463 (Gershberg *et al.* [1]).

Further, systematic investigations of stellar flares in nearby stellar clusters (*e.g.*, Pleiades) and associations (*e.g.*, Orion) have revealed a fundamental significance of this phenomenon for the physics and evolution of the young low-mass stars and protostars (see, *e.g.*, Mirzoyan [3], Montmerle [4]). At present, the observations of stellar flares at different wavelengths of the electromagnetic spectrum has become a scientifically productive area of astrophysics.

In the 1970s, the first X-ray studies of stellar flares were made, in particular with the *Einstein Observatory* (*EO*) (1978–1981) and the *EXOSAT* Observatory (1983–1985). Comprehensive reviews of the *EO* observations of stellar X-ray flares are presented by Haisch [5] and of the *EXOSAT* observations by Pallavicini, Stella & Tagliaferri [6]. X-ray observations of some stellar flares obtained during the *ROSAT* All-Sky Survey as well as in *ROSAT* pointings are discussed by Schmitt [7].

However, to date no systematic investigation of flare stars and stellar flares based on *ROSAT* observations has been done. X-ray observations by *ROSAT* are very well suited for statistical examination: Several physical quantities of individual X-ray photons are registered, namely the time of photon arrival, the direction of incidence, and the photon energy.

On the other hand, the wide spread timing analysis methods of datasets based on time binning technique give rise to certain difficulties: First of all, one has no a priori knowledge of the relevant timescales of a given flare to be detected, and, therefore, many different binnings of the data have to be considered; second, the bins must be large enough so that there will be enough photons to provide a good statistical sample, while larger bins will dilute short flares; moreover, the common practice of binning data overlooks a considerable amount of information and introduces a dependency of results on the sizes and locations of the bins. Meanwhile, it has been known for some time (Cash [8]) that fitting models to unbinned data is quite straightforward (see, for discussion, Scargle & Bapu [9]).

Hence, it is worthwhile to examine the available observational data of *ROSAT* in a straightforward and systematic way for variability testing, in particular, for UV Cet type flare stars.

For the flare event detection, we shall use the method described by Scargle [2] based on Bayesian statistics due to the nearly ideal Poisson nature of photon registration by the *ROSAT* detectors (Trümper [10], Pfeffermann *et al.* [11]).

In this article we will try to address various items relevant to detections and studies of flares with *ROSAT*.

1. DATA REDUCTION AND RESULTS

Details of our data reduction procedure have been described by Hambaryan *et al.* [12], (HNS) and briefly are as follows: from *ROSAT* PSPC and HRI pointed observations, as well as All-Sky Survey data in the direction of each optically known UV Cet type star we have extracted all photon events registered within a radius corresponding 0.95 quantile of the point spread function for the corresponding detector (Zimmermann *et al.* [13]). As a background for a given source the data from a nearby sector are used (HNS).

1.1 VARIABILITY TESTING

As mentioned in the introduction, for flare event detection we have used a method developed by Scargle [2] based on Bayesian statistics. The method is applicable to data that are known to be from a nearly ideal Poisson process, *i.e.*, a class of independent, identically distributed processes, having zero lengths of dead time.

The data gathered in *ROSAT* observations (telescope+detector) allow the measurement of arrival times of individual X-ray photons to the nearest $\approx 10^{-4}$ s (*i.e.*, an accuracy which is much smaller than the shortest time scales that are considered to be responsible for flare events on stars). Another departure from Poisson ideal distribution of counts is related to the detectors finite dead time (see, for discussion, Scargle & Bapu [9]).

Nevertheless, the arrival times of photons registered by *ROSAT* and presented in the so-called Photon Events Tables in this context can be considered as close to a Poisson process, *i.e.*, the arrival of a photon in any interval is independent on that in any other non-overlapping one.

Scargle's [2] method is designed for application to photon counting data and uses it for decomposition into a piecewise constant Poisson process. For example, let's assume that during a continuous observational interval of length T, consisting of m discrete moments in time, at which it was possible to make measurements (spacecraft's "clock ticks" $m = T/\delta t$), a set of photon arrival times D $(t_i, t_{i+1}, ..., t_{i+n})$ is registered. Suppose now that we want to use these data to compare two competing hypotheses. The first hypothesis is that the data are generated from constant rate Poisson process (model M_1) and the second one from two-rate Poisson process (model M_2). Evidently, model M_1 is described by parameter ν of one rate Poisson process while the model M_2 by parameters ν_1, ν_2 and τ describing two different parts of dataset D divided by any point τ from observational interval T (with lengths T_1 and T_2) at which the Poisson process switches from parameter (count rates) ν_1 to ν_2.

By taking as a background information (I) the proposition that one of the models under consideration is true and by using Bayes' theorem we can calculate the posterior probability (the probability that M_k $(k = 1, 2)$ is the correct model) of each model by (see, *e.g.*, Jaynes [16])

$$P(M_k|D, I) = \frac{P(D|M_k, I)}{P(D|I)} P(M_k|I) \tag{1}$$

where $P(D|M_k, I)$ is the (marginal) probability of the data given M_k, and $P(M_k|I)$ is the prior probability of model M_K $(k = 1, 2)$. The term in the denominator is a normalization constant, and we may eliminate it by calculating the ratio of the posterior probabilities instead of probabilities directly. Indeed, the extent to which the data support model M_2 over M_1 is measured by the ratio of their posterior probabilities and is called posterior odds ratio

$$O_{21} \equiv \frac{P(M_2|D, I)}{P(M_1|D, I)} = \left[\frac{P(D|M_2, I)}{P(D|M_1, I)}\right] \left[\frac{P(M_2|I)}{P(M_1|I)}\right]. \tag{2}$$

The first factor on the right-hand side of Eq. (2) is the ratio of the *integrated* or *global* likelihoods of the two models and is called the *Bayes factor* for M_2 against M_1, denoted by B_{21}. The global likelihood for each model can be evaluated by integrating over nuisance parameters and the final result for discrete Poisson events can be represented by (see, for details, Scargle [2])

$$B_{21} = \frac{1}{B(n+1, m-n+1)} \sum B(n_1+1, m_1-n_1+1) \times B(n_2+1, m_2-n_2+1) \Delta\tau \tag{3}$$

where B is the *beta function*, n_j and $m_j, (j = 1, 2)$, are the number of recorded photons and the number of "clock ticks" in the observational intervals of lengths T_1 and T_2, respectively, $\Delta\tau$ is the time interval between successive photons, and the sum is over the photons' index.

The second factor on the right-hand side of Eq. (2) is the prior odds ratio, which will often be equal to 1 (see below), representing the absence of a priori preference for either model.

It follows that the Bayes factor is equal to the posterior odds when the prior odds is equal to 1. When $B_{21} > 1$, the data favor M_2 over M_1, and when $B_{21} < 1$ the data favor M_1.

If we have calculated the odds ratio O_{21}, in favor of model M_2 over M_1, we can find probabilities for model M_2 by inverting Eq. (2), giving

$$P(M_2|D, I) = \frac{O_{21}}{1 + O_{21}} \, . \tag{4}$$

Applying this approach iteratively to the observational data set, the Scargle [2] method returns an array of rates, $(\lambda_1, \lambda_2, ..., \lambda_{cp})$, and a set of so-called "change points" $(\tau_1, \tau_2, ..., \tau_{cp-1})$, giving the times when an abrupt change in the rate is determined, *i.e.*, a significant variation. This is the most probable partitioning of the observational interval into segments during which the photon arrival rate was discernibly constant, *i.e.*, had no statistically significant variations. Unlike most, this method does not stipulate or predetermine time bins – instead the data themselves determine an effective, non-uniform binning in time. Therefore, this data analysis procedure does not itself impose a lower limit to the time scale on which variability can be detected. There are two free parameters in the method that are used to halt the segmentation process: The first is the minimum number of events that are allowed in a block (we have chosen two) and the second is a prior odds ratio that may be applied to disfavor segmentation. The prior odds ratio (second factor in the right-hand side of Eq. (2)) represents the relative likelihood assigned to the two models before the data is considered. Although this would appear to warrant a value of unity, in practice a larger value is used to prevent the method from making an incorrect decision to segment when two models are almost equally likely.

To have strong evidence in favor of segmenting, Scargle [2] suggests to use as a prior odds ratio a quantity which is equal to the ratio of the length of the observational interval and the desired time resolution of the data. For interpreting *Bayes factors* (B_{21}) considered above, there are some rules of thumb for evidence of model M_2 against M_1 (Jeffreys [17], Raftery [18]). Furthermore, it should be noted that this point is not crucial – we find very similar results independent on the choice of the prior odds ratio.

As it is well known, owing to the spacecraft orbits, *ROSAT* pointing observations contain data gaps. The integrated likelihoods that are used to decide between the above mentioned models M_1 and M_2 do not depend on the photon arrival times, only on the number of observing time resolution elements (number of *ROSAT* "clock ticks"), and the number of registered photons in the observational interval (see Eq. (3)). Therefore, in this context, the correct treatment of data gaps is to ensure that the gap length is not counted in the number of "clock ticks" (numbers m_j in Eq. (3)). In the case of *ROSAT* pointed observations by PSPC or HRI, we allowed to take into account this point with a special descriptor available in the Photon Events Tables (see Zimmermann *et al.* [13]).

Application of the above described procedure to the *ROSAT* archived data revealed in total 160 significant brightness variations corresponding to the 94 PSPC, 40 HRI and 26 RASS detections.

In order to estimate flare parameters we have converted the observed count rates to the fluxes and luminosities for each segment subtracting background and radiation of the star in the quiescent level.

The count rates of the flare in each energy band are expressed as

$$X_{Band}(t) = [X_{Flare}(t) + X_0]/X_0 - 1, \tag{5}$$

where X_0 is the quiescent star radiation count rates in the particular energy band, determined from data outside the flare event. This quantity can be used to determine the so-called equivalent duration of the flare

$$X_{ED} = \sum X_{Band}(t_k)\Delta t_k, \tag{6}$$

where $X_{Band}(t_k)$ is given by Eq. (5) for each kth segment. $X_{Band}(t_k)$ expresses the energy of the flare in terms of the quiescent star's energy.

An estimate of the luminosity of the quiescent star, in each band, can be made by multiplying count rates by an energy conversion factor and taking into account the distance of the star. Assuming that the spectrum of the star in the quiescent level is consistent with a one-temperature Raymond-Smith spectrum (Raymond & Smith [19]), a thermal spectrum from an hot, optically thin plasma of solar abundance, we use 1 KeV, *i.e.*, $\sim 10^7$ K, as temperature of the X-ray emitting plasma, which is typical for late-type stars (Neuhäuser *et*

Table 1: Distribution of detected flares in different energy bands for *ROSAT* PSPC pointed observations on the UV Cet type stars

ROSAT PSPC energy band	Number of flares
Broad-Soft-Medium-Hard	32
Broad-Soft-Medium	2
Broad-Soft-Hard	4
Broad-Medium-Hard	11
Broad-Hard	23
Only Broad	22
Total	94

al. [14]). Because foreground absorption is negligible for our objects, we use an energy conversion factor of 10^{-11} cts cm^2 erg^{-1} (Zimmermann *et al.* [13]) for the PSPC observation.

Furthermore, flare detection and parameter estimation procedures have been applied to different energy bands. Namely, the so-called hardness ratios (X-ray colors) which are defined as follows: if $X_{s,m,h}$ are the count rates in the soft (0.1 to 0.4 KeV), medium (0.5 to 0.9 KeV), and hard (0.9 to 2.0 KeV) bands, respectively, then

$$HR\,1 \;=\; \frac{X_h + X_m - X_s}{X_h + X_m + X_s} \quad \text{and} \quad HR\,2 \;=\; \frac{X_h - X_m}{X_h + X_m}$$

with this definition hardness ratios range from -1 to $+1$. If no counts are detected, *e.g.*, in the soft band, then HR1=1, but one can estimate a lower limit to HR1 by using the upper limit to the soft band count rate X_s in the formula above. These quantities have been computed for different observational phases, *i.e.*, for the star in the quiescent level as well as for flare radiation alone.

Many flares have been detected in different energy bands of the *ROSAT* PSPC observations. In Table 1 a summary of detected variations in different energy bands for *ROSAT* PSPC pointed observations are presented.

Mutual dependences between flare luminosities $\log L_X$ in different energy bands for *ROSAT* PSPC pointed observations are represented by simple proportionality relations:

$$\begin{array}{llll}
\log L_B = 0.994 \log L_S + 0.511, & \rho = 0.985 & \log L_B = 1.016 \log L_M + 0.377, & \rho = 0.963 \\
\log L_B = 1.056 \log L_H - 0.832, & \rho = 0.979 & \log L_H = 0.903 \log L_S + 2.431, & \rho = 0.969 \\
\log L_H = 1.025 \log L_M - 0.617, & \rho = 0.988 & \log L_M = 0.888 \log L_S + 2.738, & \rho = 0.952
\end{array} \qquad (7)$$

where index "B" corresponds to the broad, "S" – soft, "M" – medium, "H" – hard band as defined above and ρ is the coefficient of the correlation.

In Fig. 1 hardness ratios (HR2 versus HR1) of detected flares (filled circles) and corresponding stars (open circles) are shown. Note that flare radiation corresponds to the segment having maximum count rate.

1.2 SPECTRAL ANALYSIS

Since we do not have a sufficient number of counts for a detailed study of the evolution of the coronal temperature for most of the detected flares, we performed a spectral fit for the brightest of them (comparatively powerful ones) using a one temperature (1-T) Raymond-Smith (RS) model (Raymond & Smith [19]) including a photoelectric absorption term using the Morrison & McCammon [20] cross sections. Since the absorption for investigated objects is negligible (they are in the solar vicinity) we allow the parameter N_H to vary in the range $10^{18} - 10^{19}\,\mathrm{cm}^{-2}$. The abundance was left free. We fit the data for different time intervals: namely, for segments corresponding to Bayesian blocks (*i.e.*, in the time intervals within which data can be thought of being as generated from single rate Poisson process). These blocks were selected using the minimum number of photons for each segment equal to 500 as a halting rule (together with prior odds-ratio equal to 1) for further desegmentation (see Scargle [2], HNS).

Spectral fits have been performed using the XSPEC V10.0 package. Although abundances in stellar coronae in all cases show lower values than solar one, (an issue which is still debated; see, *e.g.*, Sciortino *et al.* [21]) these results are *not* to be interpreted as a measurement of abundances in the flare emission of these stars, since lower resolution X-ray measurements tend to have a bias toward lower abundances (*cf.* Schmitt *et al.* [22]). However, our results are consistent with an independent determination by Sciortino *et al.* [21] (*e.g.*, EV Lac) and may serve for comparative analysis of metal abundances during the evolution of a flare (the same initial values of the parameters of a model were used for different time intervals and different stars).

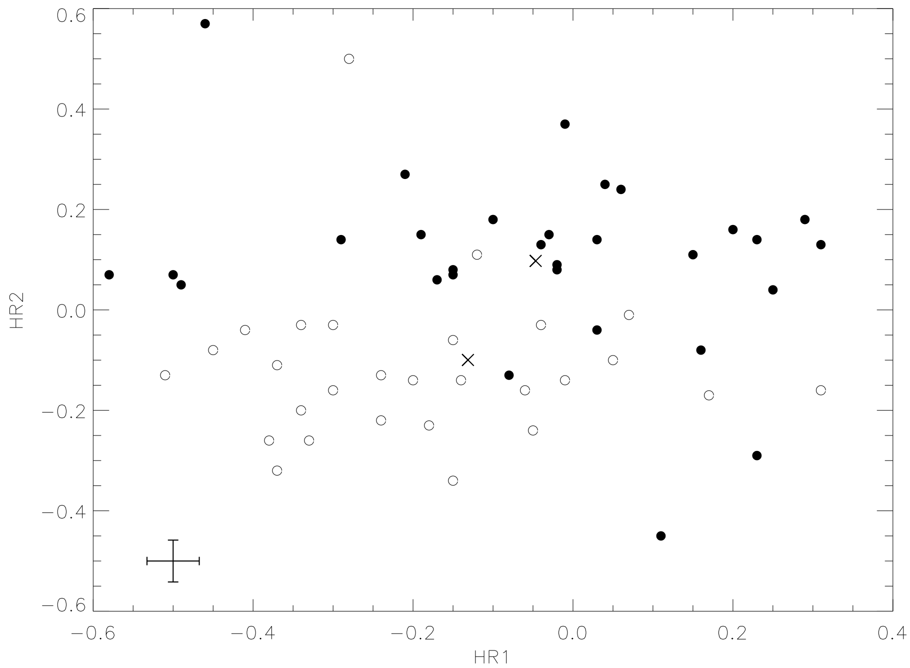

Figure 1: Hardness ratios (X-ray colors, $HR2$ versus $HR1$) for only flare radiation (filled circles) and corresponding stars in an inactive state (open circles) of the *ROSAT* PSPC observations of the UV Cet type stars. (x) – are corresponding to the mean values of each sample. Typical error bars are shown bottom left

In addition, all of the spectra mentioned above have been fitted also with a combination of absorbed thermal emission model using the MEKAL code as implemented in XSPEC, implementing the optically thin, collisional ionization equilibrium emissivity model described in Mewe *et al.* [23]. Everywhere, the presence of absorbing material has been accounted for using a WABS component in XSPEC and the global metal abundance has been left free, while abundance ratios were kept fixed in the fitting process. These abundance values are determined as relative to the "solar" case.

The results are clearly indicating, *in all cases*, an increase of coronal metal abundances at flare maximum (see Sciortino *et al.* [21], Favata & Schmitt [24]).

It should be noted that an acceptable fit also may be achieved with the two temperature (2-T) RS model holding metallicity abundance at the solar value.

2. CONCLUSIONS

We have analyzed *ROSAT* pointed (PSPC and HRI) as well as All Sky Survey data for flare detection on the UV Cet type flare stars of the solar vicinity. During the monitoring time of $\sim$ 1350 hours, the 160 flares or variations were detected using a Bayesian approach for change point detection.

It should be noted that all variations detected by the method have an high significant level (at least one of the detected change points has a posterior probability more than 0.9973).

Of course, all of these variations can not be connected with flares. X-ray brightness level in different Bayesian blocks sometimes could be associated with spots covered on the surface of a star.

Tight statistical correlations are observed between radiated flare luminosities in different X-ray bands.

On average, the radiation during flares is harder than in the quiescent state of a star.

Time resolved X-ray spectroscopy for some of the flares (under assumption of a 1T-model hot, optically thin plasma) clearly indicates an increase of coronal metallicity abundance at flare maximum.

Acknowledgments. VH wishes to acknowledge the warm hospitality of Professor J. Trümper and the Max-Planck-Institut für Extraterrestrische Physik during his stay as a Visiting Fellow. ROSAT is supported by the German government (BMBF/DLR) and the Max-Planck-Society. This project was supported by the Bundesministerium für Bildung und Forschung through the Deutsches Zentrum für Luft- und Raumfahrt E. V. (DLR) under grant number 50 OR 9706 8 and 50 OR 0003. The responsibility for the content of the publication lies with the authors.

REFERENCES

[1] *Gershberg R. E., Katsova M. M., Lovkaya M. N., et al.* Catalogue and bibliography of the UV Cet-type flare stars and related objects in the solar vicinity // Astron. and Astrophys.–1998.–**139**.–P. 555.

[2] *Scargle J.* // Astrophys. J.–1998.–**504**.–P. 405.

[3] *Mirzoyan L. V.* // Optical flares: Observations and Interpretation: Proc. IAU Coll. N 151 / Eds J. Greiner, H. W. Duerbeck and R. E. Gershberg.–Springer, 1995.–P. 47.

[4] *Montmerle T.* // Eds G. Micela, R. Pallavicini, S. Sciortino.–Mem. Soc. Astron. Ital.–**68**, N 4.–Soc. Astron. Ital., Firenze, 1997.–P. 1017.

[5] *Haisch B. M.* // Activity in Red Dwarf Stars / Eds P. B. Byrne, M. Rodonó.–Astrophys. and Speace Sci. Lib.–1983.–**102**.–P. 255.

[6] *Pallavicini R., Stella R., Tagliaferri G.* // Astron. and Astrophys.–1990.–**228**.–P. 443.

[7] *Schmitt J. H. M. M.* // Astrophys. J. Suppl. Ser.–1994.–**90**.–P. 735.

[8] *Cash W.* // Astrophys. J.–1979.–**228**.–P. 939.

[9] *Scargle J. D., Bapu G. J.* Point Processes in Astronomy: Exciting Events in the Universe // preprint, 1998, available at *http://ccf.arc.nasa.gov/~scargle/hand_www.ps*

[10] *Trümper J.* // Adv. Space Res.–1982.–**2**, N 4.–P. 241.

[11] *Pfeffermann E., et al.* // Proc. SPIE.–1986.–**733**.–P. 519.

[12] *Hambaryan V., Neuhäuser R., Stelzer B.* // Astron. and Astrophys.–1999.–**345**.–P. 121 (HNS).

[13] *Zimmermann H. U., Boese G., Becker W., et al.* // EXSAS Users Guide, MPE Report, *ROSAT* Scientific Data Center, Garching, 1998.

[14] *Neuhäuser R., Sterzik M. F., Schmitt J. H. M. M., et al.* // Astron. and Astrophys.–1995.–**297**.–P. 391.

[15] *Cruddace R. G., Hasinger G. R., Schmitt J. H. M. M.* // Astronomy from Large Databases: ESO Conf. and Workshop Proc. 28 / Eds F. Murtagh, A. Heck.–Garching, 1988.–P. 177.

[16] *Jaynes E. T.* // Probability Theory: The Logic of Science, 1997, available at *http://bayes.wustl.edu*

[17] *Jeffreys H.* Theory of Probability, (3rd ed.), Oxford University Press, 1961.

[18] *Raftery A. E.* // Bayesian Model Selection in Social Research, University of Washington, preprint, 1994, available at *http://www.stat.washington.edu/raftery/Research/Bayes/bayes_papers.html*

[19] *Raymond J. C., Smith B. S.* // Astrophys. J. Suppl. Ser.–1977.–**35**.–P. 419.

[20] *Morrison R., McCammon D.* // Astrophys. J.–1983.–**270**.–P. 119.

[21] *Sciortino S., Maggio A., Favata F., Orlando S.* // Astron. and Astrophys.–1999.–**342**.–P. 502.

[22] *Schmitt J. H. M. M., Stern R.A., Drake J.J., Kürster M.* // Astrophys. J.–1996.–**464**.–P. 898.

[23] *Mewe R., Gronenschild E. H. B. M., van den Oord, G. H. J.* // Astron. and Astrophys.–1985.–**62**.–P. 197.

[24] *Favata F., Schmitt J. H. M. M.* // Astron. and Astrophys.–1999.–**350**.–P. 900.

INTERNATIONAL COOPERATION ON TRANSIENT OBJECT OBSERVATIONS: IMPORTANCE AND RECENT RESULTS

D. Nogami[1], T. Kato[2], H. Yamaoka[3], and M. Uemura[2]

[1] *Universtäts-Sternwarte, Geismarlandstr. 11, D-37083 Göttingen, Germany*
e-mail: daisaku@uni-sw.gwdg.de/nogami@kusastro.kyoto-u.ac.jp

[2] *Department of Astronomy, Kyoto University, Sakyo-ku, Kyoto 606-8502, Japan*

[3] *Department of Physics, Kyushu University, Ropponmatsu, Fukuoka 810-8560, Japan*

We are living in a very exciting era when the nature of the universe is dramatically being revealed. Transient objects are a group, research of which will promisingly become more active in astronomy. We review some topics currently urged to be solved by international cooperations, concentrating gamma-ray bursts, dwarf novae, X-ray transients, and supernovae among such transient objects. We then argue importance of the telescope distribution for covering whole the sky and of the international network for exchanging information and opinions.

1. INTRODUCTION

A variety of transient objects with quite short timescales has recently been discovered, giving unprecedented insights of the Universe. The study of these objects has been rapidly progressing. Most of the observations carried out so far, however, are too fragmentary and insufficient to reveal the whole nature of such phenomena. Then, it is the time that we must consider to establish the system to smoothly organize a coordinated international observation soon after a burst detection by various methods and to continue the observation until deducing all the physics which appear only in the active state. Significance of these observations will increase in the future. Since the Ukraine is located in a quite important place, we would appeal to the Ukrainian astronomical society for positive contributions to observations of transient objects.

We put focus mainly on optical observations, unless otherwise stated. Spotting gamma-ray bursts (GRBs), dwarf novae, X-ray transients (XRTs), and supernovae (SNe), we will outline some points which are desired to be observationally clarified, in the next section. Note that discoveries other than what we mention here is, of course, expected, because we can not explain all in this short contribution and this paper is based on our *current* knowledge. Because the progress of the science in this field is currently quite rapid, the contents of this paper may be already a little obsolete when this proceedings are published. We will describe some respects on the coordinated observations in the section 3. Then, the concluding remark is placed at the end.

2. OBSERVATIONS OF TRANSIENT OBJECTS

Here we pick up some types of transient objects, for which international cooperative observations will yield great improvement on our understanding. They are gamma-ray bursts, dwarf novae, X-ray transients, and supernovae. The study of the transient object physics has been quite rapidly progressing recently. Readers should keep in mind that some topics reviewed in this contribution may be a little *obsolete*, especially in the GRB field, even when the proceedings are published.

2.1 Gamma-Ray Bursts

Gamma-ray bursts are one of the most catastrophic and energetic events in the Universe. The duration of GRBs is quite short, from 0.01 to 1000 seconds, but some of their total radiated energies are believed to reach the order of 10^{53} erg.

The first GRB was discovered in 1969 [21]. During 23 years since then, the nature of GRB had been mystery, although thousands of burst events had been caught during this interval. The GRB burst study, then, had two great turning points. The first one is the advent of BATSE in 1992 [12]. This detector revealed the isotropic distribution of GRB in the sky, suggesting GRBs to occur at the cosmological distance, *e.g.*, [11]. The second is the discovery of the X-ray and optical afterglow of GRB970402 in 1997 [39]. Following this discovery, afterglows of many GRBs have been found successively, which have made rapid progress of the GRB study in these 3 years.

In the gamma ray region, the event shows violent variability in many cases, while the afterglow in X-ray to radio shows rather smooth power-law decay, where the power-law index α is of about 1.0 (see Greiner's personal collection of light curves, URL: *http://www.aip.de/~jcg/grb.html*). The optical flux of afterglows does not seem to be scaled directly by the GRB strength, *e.g.*, [1]. These two facts suggest that different radiation mechanisms work for the GRB and for the afterglow. The current standard GRB model, namely, the fireball+blast wave model ([43] for a review) depicts an image: a certain mechanism drives an expansion of a fireball, then, the internal shock in the relativistic ejecta causes gamma-ray radiation. After the ejecta collides with the ambient matter, the afterglow from X-ray to radio is generated in the forward external shock by synchrotron radiation. The radiation due to the forward shock in the late stage does not clearly reflect what the central engine is. This is why the early observations are needed.

This model generally explains observations of GRBs well, but still have some problems. One of the most important is the optical flash and the radio bump of GRB990123. Observations of this GRB by the Robotic Optical Transient Search Experiment (ROTSE) caught an optical peak of $m_V = 8.95$ about 30 sec after the BeppoSAX trigger [22]. This flash seemed to decay with $\alpha \sim 2.0$ for ~ 15 min, followed by a usual power-law decay $\alpha \sim 1.1$. The radio bump was seen about 1 day after the GRB event [13]. Such an optical flash and a radio bump may be explained by a reverse external shock, *e.g.*, [48]. Akerlof *et al.* [1], however, reported that their ROTSE follow-up observations of six GRBs with localization errors of 1 deg^2 or better produced no detection of the optical flash. It is needed to carry out as many follow-up observations as possible, as soon after the GRB trigger as possible, in order to make constraints on the mechanism and on the criteria for emergence of such exceptional behavior.

What is the central engine of the fireball? This is also a big problem. The currently strong hypotheses are 1) mergers of neutron star-neutron star or neutron star-black hole binaries [30], 2) collapsars of massive rapidly rotating stars with strong magnetic fields, so-called hypernovae, *e.g.*, [40], and 3) collapsars of supermassive neutron stars in low mass X-ray binaries, so-called Supranovae [55].

The GRB distribution in the host galaxies is predicted in the neutron-star binary model [3]: $\sim 15\%$ of all burst progenitors may be able to escape from their parent galaxy, and $\sim 50\%$ will be located more than 8 kpc from their original site. Clarification of the GRB locations may be a key to the progenitor problem.

Vietri [54] showed that the delay time (t_d) of the afterglow onset after the end of the GRB is a good indicator of the ambient matter density, which corresponds to the interstellar matter if $t_d \sim 15$ sec, to galactic halo if $t_d \sim 5$ min, and to the intergalactic matter if $t_d \sim 4$ hr. The measurement of the delay time in many GRBs by the prompt follow-up multi-wave length observation will make constraints on the progenitor, for example, collapsars of massive stars should occur in a dense medium and cause an afterglow immediately after the GRB.

In the case of GRB980425, the type-Ic supernova 1998bw was almost simultaneously discovered in the error box of the GRB position [13]. This association of a supernova and a GRB is explainable by the hypernova model [18, 29]. The redshift of SN 1998bw was measured to be z ~ 0.0085, meaning that γ-ray energy is about an order of 5 smaller than those of usual GRBs. There is a possibility that many such supernovae has been missed in the γ-ray region.

Taking advantage of the brightness of GRBs, there has been proposed a movement to make use of GRBs for investigation of the high-z universe. Using 7 GRBs with well-determined redshifts, Fenimore & Ramirez-Ruiz [9] found a relationship between the temporal variability of GRBs and the absolute luminosity: smooth bursts are intrinsically less luminous (see also [44]). This relation and reasonable assumptions concerning the star formation rate and the GRB rate will bring us information on the star formation history in the high-z region (*cf.* [24]). Confirmation of this relation by determining z in many GRBs is needed.

The BATSE and BeppoSAX projects have achieved a great success, but the large error box of, for instance, a few degree, at the early phase of GRB observations is one of the reasons why it is difficult to carry out follow-up observations. However, the next generation missions of HETE-2 (High Energy Transient Explorer, see *http://space.mit.edu/HETE/*) and *Swift* (see *http://swift.sonoma.edu*) will amazingly improve the situation. The latter is planed to have an ability to yield the GRB position of a few arcmin accuracy within ~ 15 sec after the burst and a set of information of the $\sim$ arcsec position, a finding chart, and the redshift of the source within ~ 200 sec. Coordinated observations of GRB afterglows promptly after catching GRBs will continue to renew our view of GRBs and the Universe.

2.2 Dwarf Novae

Dwarf novae are a class of cataclysmic variable stars, which are binary stars of a white dwarf and a late-type main-sequence star, and they show many kinds of variability mostly due to the accretion disk around the white dwarf (for a thorough review, [57]). Among dwarf novae, SU UMa-type stars are characterized by the two types of outburst, namely, normal outburst and superoutburst. The former typically lasts 3–5 days and the amplitude is of about 3–4 magnitude. The superoutburst lasts about 3 times longer than the normal outburst and reaches of about by 0.5–1 magnitude brighter than the normal outburst. Superhumps only observed during superoutbursts are modulations with ~ 0.1–0.3 mag. The superhump period ($P_{\rm sh}$) is 1–3% longer than the orbital period ($P_{\rm orb}$), and very gradually decreases as the superoutburst proceeds. These characteristics are basically understood in the frame of the thermal-tidal disk instability theory (for a review, *e.g.*, [38]).

Some stars out of such a standard scheme, however, recently have been reported. Several extreme stars in SU UMa-type dwarf novae, called WZ Sge stars, *e.g.*, [37], have been proven to show peculiar evolution of the superhump (see N99). For instance, in AL Com, modulations with a period equal to its orbital period were observed within 2 days from the onset of the 1995 superoutburst, then gradually declined (see [33]). Usual superhumps with a period 1.0% longer than $P_{\rm orb}$ were seen 10 days after. Interestingly, this superhump period became longer as time went, which may suggest extension of the accretion disk. The $P_{\rm sh}$-elongation phenomenon was also observed in other WZ Sge-related stars, HV Vir [20], SW UMa [32, 49] and V1028 Cyg [2].

Another interesting, recent topic concerning superhumps is the transition from the 'negative' superhump to the usual superhump during a superoutburst. This was observed around a maximum of a superoutburst in ER UMa [15], the prototype of another group of extreme SU UMa stars (for a review, [19]), and possibly during the 2000 superoutburst in BC UMa [53].

These phenomena would challenge the standard disk instability model, but the observations are still not enough to construct a new detailed model. It is needed to clarify the evolution of superhumps by continuous observations from soon after the superoutburst detection in many SU UMa-type dwarf novae.

2.3 Soft X-ray Transients

Soft X-ray transients, also called X-ray novae, are low-mass X-ray binaries of a neutron star or a black hole and a main-sequence, or a subgiant secondary star of typically less than 1 $M_\odot$ (for a review of SXTs, [52]). The outburst shape of SXTs have been pointed out to be similar to that of dwarf novae, especially for the fast-rise-exponential-decay-type outburst, *e.g.*, [23], and the trial to explain the SXT outbursts using the disk instability theory has been carried out since 1982 [6]. This challenge is still continuing, taking into account X-ray irradiation of the accretion disk and the secondary star, evaporation, and so on, *e.g.*, [5, 7, 8], which requires observers to reveal the evolution of the accretion disk during the outburst by continuous multiwavelength monitoring.

The superhumps are also seen in SXTs in outburst, *e.g.*, [36]. It is, however, difficult to recognize superhumps in SXTs, because of contamination of orbital modulations due to irradiation of the secondary star and long orbital periods ($\geq$ several hours). How the superhump in SXTs evolve is an interesting subject to test whether the disk instability theory works in SXTs in the same way in dwarf novae. In addition, one can make constrains on the binary parameters including the primary mass from the superhump observations [28]. This method is quite useful to roughly judge if the primary star is a black hole or not, because most of SXTs are quite faint in quiescence and it is difficult to make the radial velocity study, or even to find its optical counterpart.

In March 2000, an outburst of the SXT, XTE J1118+480 was detected by the RXTE All Sky Monitor [45]. Soon after the detection report to VSNET (vsnet-alert 4501), a VSNET campaign of the international coordinated observation of this star started (before the IAU Circular was published!) (see *http://www.kusastro.kyoto-u.ac.jp/vsnet/Xray/xtej1118.html*). Then, this campaign was extended to a multiwavelength one with the X-ray satellite ASCA (see *http://www.kusastro.kyoto-u.ac.jp/vsnet/Xray/xtej1118-camp.html*).

Most recently, two curious X-ray transients has been discovered successively. They are CI Cam [27, 50] and V4641 Sgr [17, 26, 51]. The peculiarities of these stars are their quite short durations of the ourbutst (a few days), and their bright quiescent magnitudes, a little fainter than 13 mag. Because of the short timescale of the outburst, such X-ray transients may have been missed many times so far. Considering their brightness, which means that they are close to us, say within 1.0 kpc [16], there possibly exist much more black holes in our vicinity than our expectation. We can see how important quick operations in response to a discovery of a transient object are.

2.4 Supernovae

The greatest topic in the recent supernova research is the utility of type Ia supernovae (SNeIa) as cosmological standard candles. The most impressive result would be that Einstein's cosmological constant was proved to exist in 1998 from the comparison of the recession velocities and the maximum visual magnitude of supernovae detected in the deep images, whose images have galaxies at the redshift of ~ 0.3 to ~ 0.8 [46, 41].

The progenitor of SNeIa is considered as a white dwarf in a binary system which explodes when exceeding the Chandrasekhar mass, *e.g.*, [34]. This scheme suggests the maximum brightness to be constant for all SNeIa. However, this constancy has been recently doubted from the observations, for instance, the discoveries SN 1991T and SN 1991bg. The former was ≥ 0.6 mag brighter than the average SNIa (*e.g.*, [10]) and the latter was over 1.0 mag fainter than the average SNIa (*e.g.*, [25]).

A statistical analysis of light curves of many type Ia supernovae gave an empirical relation between the light curve and the decline rate in the sense that an SNIa more rapidly declining is less luminous [42]. There is a correlation between the spectrum and the maximum brightness [35]. It was also reported that the SNIa brightness may be depend on the color of the host galaxy [4]. The characteristics of SNIa seem to have a correlation with the distance from the galaxy core [56]. Then, it was reported that the light curve before the maximum is different in type Ia supernovae in nearby galaxies and in far galaxies, even after corrected with the decline-rate correlation [47]. There has not yet existed a theoretical model which can explain all these features well. It is urgent to discover many type Ia supernovae as at an early phase as possible and to clarify the nature by dense follow-up observations.

The observation of line γ-rays emitted by the decay of radioactive elements will give us precious information on the nature of SNeIa, especially the distribution of those elements which are the energy source of supernovae. In this observation, it is crucial to inform γ-ray observers of the discovery of a supernova and its type in a quite early phase, because the line γ-ray reaches its maximum intensity earlier than the optical light. It is only in SN 1987A in the Large Magellanic Cloud and in 1991T that the γ-ray lines have been detected so far.

The relationship between peculiar supernovae and GRBs is as we have already mentioned.

Conclusively, of importance are discovery of many SNe and reveal of its nature by 1) detection of supernovae in an early phase by systematic observations, 2) follow-up observations to confirm the existence, to carry out astrometry, and to clarify the type, and 3) long-term monitoring to draw a detailed light curve and chase the spectrum variation.

3. INTERNATIONAL COOPERATION

As we have reviewed so far, there are many topics about which we can deduce fruitful information only by international cooperative observations of transient objects from soon after onsets of *bursts*. Because of short timescales of the phenomena and need of continuous coverage as long as possible, we must consider two critical infrastructure to realize those observations. One is by the telescope network, and the other is by the method of information exchange.

3.1 Telescope Network

The ideal situation is that telescopes usable for those observations are distributed all over the world, and whole the sky is observable anytime by several, or more, telescopes (at least one is for photometry/imaging, at least one is for spectroscopy, one is for spectropolarimetry if possible) in each wavelength. The current situation is, unfortunately of course, far from it.

The GRB flashes, *i.e.*, simultaneous optical flashes with the γ-ray like as observed with GRB 990123, cannot be observed everywhere on the Earth. The maps of the Earth viewed from the direction of GRBs at the moment of GRB detections (*http://www.rc.kyushu-u.ac.jp/~yamaoka/GRB/grb.html*, cooperated with A. Nomura) show the "observable hemisphere" of the GRB flashes. Of course, the GRB flashes cannot be observed from the sunlit portion of this map even if they existed. The observable region is quite restricted. For example, Ukrainian people might be able to carry out the search of the GRB970828 afterglow from the evening. The early afterglow of GRB990506 could be caught only from the east area of Asia, Australia, and New Zealand. After the observation in these region, the results would have been relayed to following observers in the central Asia and Europe.

In making a plan of an international multi-longitudinal campaign at this time, it should be emphasized that Ukraine is located in a quite important point. In the north hemisphere, there are relatively many telescopes from Europe to North America. We can expect relatively dense coverage in this region. The region from North America to Europe, however, has fewer eyes to the sky. Especially, only a few large telescopes with an aperture > 2 m exist in this region (see *http://www.seds.org/billa/bigeyes.html*). If we consider only over-2.5-m telescope, the Crimean Astrophysical Observatory has the very *next* telescope to the large telescopes in Hawaii. It is, therefore, expected that the Crimean Observatory plays a quite important role in future international campaigns of transient object observations by spectroscopy. To fill the gap from Hawaii to Ukraine, it is also expected that 3-m, or larger, telescopes are constructed in Japan or in the Asian continent.

As for photometry, more observatories can join international campaigns. Recently, as the CCD camera has very rapidly become a popular device even for amateur observers, the chances of collaboration between professionals and amateurs has been increasing. It is, hence, easier to organize a photometric campaign than a spectroscopic one. Even in this case, the coverage in the hemisphere from North America to Europe is sparser than in the hemisphere from Europe to North America. Contributions from Ukraine does not decrease their importance even in this field.

It will become more important for observatories to accept Target-of-Opportunity observations more flexibly. The telescopes and detector systems to be constructed in future should be designed to be able to change the observation mode in a short time in response to a burst alert.

3.2 Method of Information Exchange

The information should be easily, rapidly, and smoothly exchanged between the discoverer(s) of a burst and other observers and between preceding observers to following observers. This leads to effective calls for observation from whole the world, sharing the current state of the target, and discussion of the observation strategy which will vary in time according to various factors, for instance, the target state and the status of other observers.

Such an information network is now being developed, such as The GRB Coordinates Network (GCN; *http://gcn.gsfc.nasa.gov/gcn/*), the Variable Star Network (VSNET; *http://www.kusastro.kyoto-u.ac.jp/vsnet/*), and so on. The VSNET is basically an aggregation of mailing lists concerning variable stars, especially transient objects described here. Subscribers live in over 100 countries and exceed 500 persons. An article posted to a sub-list of VSNET is distributed to all subscribers of the list within one hour. Making use of VSNET, many international coordinated campaigns have been organized, and yielded splendid results. One most recent example is the simultaneous multi-wavelength observations of the X-ray transient, XTE J1118+460 in outburst from X-ray by ASCA to near-IR (see *http://www.kusastro.kyoto-u.ac.jp/vsnet/Xray/xtej1118-camp.html*).

The GCN is a network specialized to GRB, as the name indicates. Although GCN has a mailing list for follow-up observers, the unique point is that the dedicated phone line (but currently only in US) and the internet socket connection are available. The latter two enable the GCN computer to distribute the coordinates and the time obtained by the BATSE and other detectors in space to the computers at observatories within a few second. The combination of this system and automated robotic telescopes, like ROTSE, surely bears fruitful results. If a new object is discovered by prompt comparison of the images given by the telescope with old images or plate archives and spectra of the new object can be obtained also by a robotic telescope within a short timescale, the study of transient objects will make a great progress[1].

Consolidation of the network is indispensable for further progress of the transient object observations, and we are on the way of the development. This should be a topic to be discussed by all astronomers in the related field.

REFERENCES

[1] *Akerlof C., Balsano R., Barthelmy S., et al.* // Astrophys. J. Lett.–2000.–**532**.–P. L25–L28.

[2] *Baba H., Kato T., Nogami D., et al.* // Publs Astron. Soc. Jap.–2000.–**52**.–P. 429–436.

[3] *Bloom J. S., Sigurdsson S., Pols O. R.* // Mon. Notic. Roy. Astron. Soc.–1999.–**305**.–P. 763–769.

[4] *Branch D., Romanishin W., Baron E.* // Astrophys. J.–1996.–**465**.–P. 73–78.

[5] *Cannizzo J. F.* // Astrophys. J.–2000.–**534**.–P. L35–L38.

[6] *Cannizzo J. F., Wheeler J. C., Ghosh P.* // Pulsations in Classical and Cataclysmic Variable Stars / Eds J. P. Cox, C. J. Hansen.–Univ. of Colorado Press, Boulder, 1982.–P. 13.

[7] *Esin A. A., Kuulkers E., McClintock J. E., et al.* // Astrophys. J.–2000.–**532**.–P. 1069–1077.

[8] *Esin A. A., Lasota J. -P., Hynes R. I.* // Astron. and Astrophys.–2000.–**354**.–P. 987–994.

[9] *Fenimore E. E., Ramirez-Ruiz E.* // Astrophys. J.–2000.–submitted (astro-ph/0004176).

[10] *Filippenko A. V., Richmond M. W., Matheson T. et al.* // Astrophys. J. Lett.–1992.–**384**.–P. L15–L18.

[11] *Fishman G. J., Meegan C. A.* // Annu. Rev. Astron. and Astrophys.–1995.–**33**.–P. 415–458.

[12] *Fishman G. J., Meegan C. A., Wilson R. B., et al.* // Astrophys. J. Suppl. Ser.–1994.–bf 92.–P. 229–283.

[13] *Galama T. J., Briggs M. S., Wijers R. A., et al.* // Nature.–1999.–**398**.–P. 394–399.

[14] *Galama T. J., Vreeswijk P. M., van Paradijs J., et al.* // Nature.–1998.–**395**.–P. 670–672.

[15] *Gao W., Li Z., Wu X., et al.* // Astrophys. J. Lett.–1999.–**52**.–P. L55–L58.

[16] *Hjellming R. M.* // Astrophys. J. Lett.–2000.–submitted.

[17] *in't Zand J., Heise J., Bazzano A., et al.* // IAU Circ.–1999.–N 7119.

[18] *Iwamoto K., Mazzali P. A., Nomoto K., et al.* // Nature.–1998.–**395**.–P. 672–674.

[19] *Kato T., Nogami D., Baba H., et al.* // Disk Instabilities in Close Binary Systems / Eds S. Mineshige, J. C. Wheeler.–Tokyo: Universal Academy Press, 1999.–P. 45–52.

[20] *Kato T., Nogami D., Baba H., et al.* // Wild Stars in the Old West: Proc. 13th North American Workshop on Cataclysmic Variables and Related Objects / Eds S. B. Howell, E. Kuulkers, C. Woodward.–San Francisco: ASP, 1998.–P. 9–17.

[1] This is very one of the aims of the *Swift* project.

[21] *Klebesadel R. W., Strong I. B., Olson R. A.* // Astrophys. J. Lett.–1973.–**182**.–P. L85–L88.

[22] *Kulkarni S. R., Djorgovski S. G., Odewahn S. C., et al.* // Nature.–1999.–**398**.–P. 389–394.

[23] *Kuulkers E.* // Disk Instabilities in Close Binary Systems / Eds S. Mineshige, J. C. Wheeler.–Tokyo: Universal Academy Press, 1999.–P. 169–176.

[24] *Lamb D. Q., Reichart D. E.* // Astrophys. J.–2000.–**536**.–P. 1–18.

[25] *Leibundgut B., Kirshner R. P., Phillips M. M., et al.* // Astron. J.–1993.–**105**.–P. 301–313.

[26] *Markwardt C. B., Swank J. H., Marshall F. E.* // IAU Circ.–1999.–N 7120.

[27] *Marshall F. E., Strohmayer T. E., Lewin W. H. G.* // IAU Circ.–1998.–N 6857.

[28] *Mineshige S., Hirose M., Osaki Y.* // Publs Astron. Soc. Jap.–1992.–**44**.–P. L15–L18.

[29] *Nakamura T., Mazzali P. A., Nomoto K., et al.* // Astron. Nachr.–1999.–**320**.–P. 363.

[30] *Narayan R., Paczyński B., Piran T.* // Astrophys. J. Lett.–1992.–**395**.–P. L83–L86.

[31] *Nogami D.* // Disk Instabilities in Close Binary Systems / Eds S. Mineshige, J. C. Wheeler.–Tokyo: Universal Academy Press, 1999.–P. 13–20.

[32] *Nogami D., Baba H., Kato T., et al.* // Publs Astron. Soc. Jap.–1998.–**50**.–P. 297–302.

[33] *Nogami D., Kato T., Baba H., et al.* // Astrophys. J.–2000.–**490**.–P. 840–846.

[34] *Nomoto K., Iwamoto K., Kishimoto N.* // Science.–1997.–**276**.–P. 1378–1382.

[35] *Nugent P., Phillips M., Baron E., et al.* // Astrophys. J. Lett.–1995.–**455**.–P. L147–L150.

[36] *O'Donoghue D., Charles P. A.* // Mon. Notic. Roy. Astron. Soc.–1996.–**282**.–P. 191–205.

[37] *O'Donoghue D., Chen A., Marang J. P., et al.* // Mon. Notic. Roy. Astron. Soc.–1991.–**250**.–P. 363–372.

[38] *Osaki Y.* // Publs Astron. Soc. Pacif.–1996.–**108**.–P. 39–60.

[39] *Paczyński B., Wijers R.* // Nature.–1997.–**386**.–P. 650–651.

[40] *Paczyński B.* // Astrophys. J.–1998.–**494**.–P. L45–L48.

[41] *Perlmutter S., Aldering G., Goldhaber G., et al.* // Astrophys. J.–1999.–**517**.–P. 565–586.

[42] *Phillips M. M.* // Astrophys. J. Lett.–1993.–**413**.–P. L105–L108.

[43] *Piran T.* // Phys. Rep.–1999.–**314**.–P. 575–667.

[44] *Reichart D. E., Lamb D. Q., Fenimore E. E., et al.* // Astrophys. J.–2000.–submitted (astro-ph/0004302).

[45] *Remillard R., Morgan E., Smith D., et al.* // IAU Circ.–2000.–N 7389.

[46] *Riess A. G., Filippenko A. V., Challis P., et al.* // Astron. J.–1998.–**116**.–P. 1009–1038.

[47] *Riess A. G., Filippenko A. V., Li W., et al.* // Astron. J.–1999.–**118**.–P. 2668–2674.

[48] *Sari R., Piran T.* // Astrophys. J.–1999.–**520**.–P. 641–649.

[49] *Semeniuk I., Olech A., Kwast T., et al.* // Acta Astron.–1997.–**47**.–P. 201–209.

[50] *Smith D., Remillard R., Swank J., et al.* // IAU Circ.–1998.–N 6855.

[51] *Stubbings R., Pearce A.* // IAU Circ.–1999.–N 7253.

[52] *Tanaka Y., Shibazaki N.* // Annu. Rev. Astron. and Astrophys.–1996.–**34**.–P. 607–644.

[53] *Uemura M., Kato T., Shugarov S. Y., et al.* // 2000, vsnet-alert 4586 (*http://www.kusastro.kyoto-u.ac.jp/vsnet/Mail/vsnet-alert/msg*04586.*html*)

[54] *Vietri M.* // Astroparticle Phys.–in press (astro-ph/0003036).

[55] *Vietri M., Stella L.* // Astrophys. J. Lett.–1999.–**527**.–P. L43–L46.

[56] *Wang L., Hoflich P., Wheeler J. C.* // Astrophys J. Lett.–1997.–**483**.–P. L29–L32.

[57] *Warner B.* Cataclysmic Variable Stars.–Cambridge Academy Press, Cambridge, 1995.

HIGH–FREQUENCY OPTICAL OSCILLATIONS ON THE FLARE STAR EV LACERTAE

B. E. Zhilyaev[1], Ya. O. Romanyuk[1], I. A. Verlyuk[1], O. A. Svyatogorov[1], V. R. Khalack[1], A. V. Sergeev[2], R. K. Konstantinova-Antova[3], A. P. Antov[3], R. S. Bachev[3], I. Yu. Alekseev[4], V. E. Chalenko[4], D. N. Shakhovskoy[4], M. E. Contadakis[5], and S. J. Avgoloupis[6]

[1] *Main Astronomical Observatory, NAS of Ukraine*
27 Akademika Zabolotnoho, 03680 Kyiv, Ukraine
e-mail: zhilyaev@mao.kiev.ua

[2] *International Center for Astronomical and Medico-Ecological Research*
27 Akademika Zabolotnoho, 03680 Kyiv, Ukraine

[3] *Institute of Astronomy, Bulgarian Academy of Sciences,*
72 Tsarigradsko shose, BG-1784 Sofia, Bulgaria

[4] *Crimean Astrophysical Observatory, Ministry of Ukraine for Education and Science*
Naukove, 98409 Crimea, Ukraine

[5] *Department of Geodesy and Surveying University of Thessaloniki*
GR-54006, Thessaloniki, Greece

[6] *Department of Physics Section of Astrophysics, Astronomy and Mechanics,*
University of Thessaloniki, GR-54006, Thessaloniki, Greece

Due to many-site multicolor synchronous monitoring of the flare star EV Lac and the careful treatment of the data obtained, we have confirmed the reality of rapid optical brightness oscillations during a significant part of a flare lifetime as was discovered by Rodonó in 1974 [3]. Our findings, based on three flare events in EV Lac, allow us to conclude that high frequency optical oscillations are coherent, with periods of 13 and 26 s and amplitudes of 0.025 mag in the B band and larger by a factor of 5 in the U band. As found, UBV color indices of the mean flare light curve differ significantly from those of the oscillations.

OBSERVATIONS, METHODS AND RESULTS

Amongst the vast variety of stellar flare light curves, a special place is occupied by the flare in the Hyades flare star HII 2411, which occured on November 20, 1972 and was detected by Rodonó [3]. During this rather intense flare, he registered highly oscillatory phenomena with the oscillation period varying from 13.7 to 12.4 s throughout the recording time of about 12 min; the oscillation amplitude appeared to be constant and was equal to about 25% of the mean intensity in the quiescent phase in white light. Here, for the first time, we describe similar optical brightness pulsations in the EV Lac flares which we detected with a more accurate technique including many-site multichannel monitoring and which we analyzed with much more sophisticated methods.

The observational data for the flare star EV Lac reported here were obtained from four separate sites over 19 nights in September– October 1998. The instruments which were used were the following: the 2-m Ritchey-Chretien and the 60-cm Cassegrain telescopes at Peak Terskol; the 30-inch telescope at the Stephanion Observatory in Greece; the 1.25-m reflector AZT-11 at the Crimean Observatory; the 60-cm Cassegrain telescope at the Belogradchik Observatory. The typical integration time was 0.1 s. The UBV data were converted to a relative intensity scale with respect to the mean values of quiescent fluxes.

To detect small oscillations, large intrinsic intensity variations must first be removed. To achieve this, we apply high-pass filtering. The near-ideal Kaiser filter was used [2]. The filter coefficients are

$$h(k) = h(-k) = \frac{\sin(\pi \nu_c k)}{\pi\ k} \cdot \frac{I_0(\eta\sqrt{1-(k/l)^2})}{I_0(\eta)}, \tag{1}$$

where $I(x)$ is the modified Bessel function of the zero order, η is the parameter that enters the filter model, l is the number of filter coefficient pairs. Three basic input parameters, *i.e.*, the filter passband ν_c given in units of the Nyquist frequency, the width of transition band and the stopband loss in the decibel scale, completely determine quantities η, l and the filter as a whole (for more details see [1]). In our cases the cutoff frequency value of 0.033 Hz was employed. This removes any variations in time scales greater than 30 s.

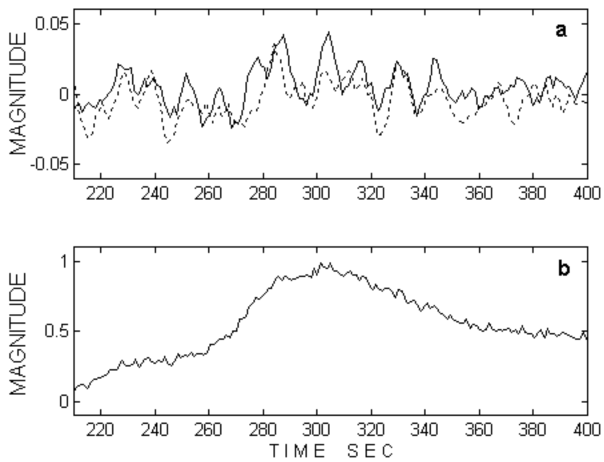

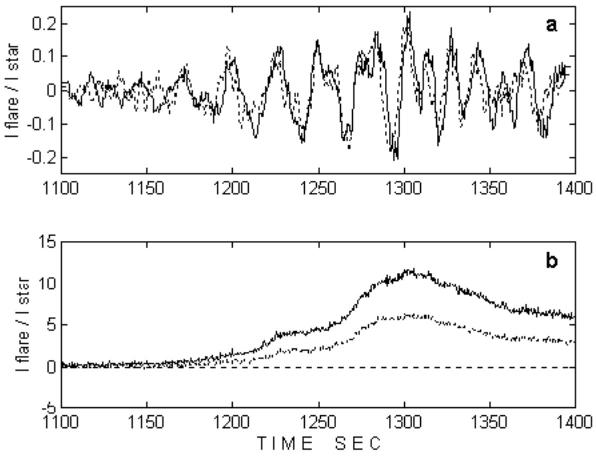

Figure 1: (left) Portions of the high-frequency B-band remains (upper panel) and of the main light curve (lower panel) from the sets of EV Lac data obtained with the Crimean (solid line) and Greek (dotted line) telescopes on September 11, 1998, 21:55:02 UT (max)

Figure 2: (right) Time variations in high-frequency oscillations in the U (solid) and B (dotted) bands from the same sets of EV Lac data obtained at Crimea (upper panel). The lower panel represents the raw main U and B light curves. Both B curves are magnified by a factor of 5

Figure 1a shows the simultaneous observations of the oscillations on EV Lac at the Crimean and at the Stephanion observatories. Figure 1b shows the main flare curve in B band with sampling time of 1.2 s. A comparison between these two measurements obtained from synchronous observations at different sites showed obvious correlations significant at greater than 99% confidence level. A period of 12.8 $\pm$ 0.7 s (0.078 Hz) was obtained from the times of maxima and a mean amplitude of 0.025 mag was calculated. From these facts we can be assured that both an atmospheric and an instrumental origin for the high-frequency oscillations can be ruled out with a high degree of confidence. Figure 2 gives some insight into the way in which high-frequency oscillations arise and develop during the progress of a flare. An illustrative example of a strong excitation of oscillations is furnished by Figure 2a. These oscillations first arise at the earliest stage of the flare development, with a frequency of 0.039 Hz (the period = 25.7 $\pm$ 1.8 s). Some time later they transform into a wave of a twofold frequency. Their amplitudes may reach 10% of the quiescent intensity in the U band and about five times lower in the B.

As the data of Figure 2 suggest, the UB color indices of the mean flare light curve differ significantly from those of the oscillations. They are as follows: U–B = -0.99 ± 0.06 , B–V = -0.46 ± 0.07 and U–B = -0.42, B–V = 0.07, respectively. The color indices do not show variations with time in the vicinity of the brightness maximum and on the portion of the descending light curve to an accuracy of 0.07 mag.

REFERENCES

[1] *Kaiser J. F.* Nonrecursive Digital Filter Design Using the – sinh Window Function // Proc. 1974 IEEE Symp. Circuits and Syst.–1974.–P. 20–23.

[2] *Rabiner L. C. and Gold B.* Theory and Application of Digital Signal Processing // Prentice-Hall, Englewood Cliffs, NJ, 1975.

[3] *Rodonó M.* Short-lived Flare Activity of the Hyades Flare Star HII 2411 // Astron. and Astrophys.–1974.–**32**, N 3.–P. 337–341.

STRUCTURES OF THE QUIET CHROMOSPHERE AND FLARES OF RED DWARF EV LAC OBTAINED FROM OBSERVED EMISSION SPECTRA

E. A. Baranovsky, R. E. Gershberg, and D. N. Shakhovskoy

Crimean Astrophysical Observatory, Ministry of Ukraine for Education and Science
Naukove, 98409 Crimea, Ukraine
e-mail: gershberg@crao.crimea.ua

During spectral observations of the flare red dwarf star EV Lac, carried out at the 2.6-m Shajn reflector, emission profiles of the hydrogen and helium lines have been registered both for the quiet state of the star and for flares. Using the Crimean computation algorithm, the hydrostatic models have been calculated for a homogeneous stellar chromosphere, for a set of active regions on the star and for stellar flares. In all cases regions of a very small temperature gradient were found, and these temperature plateaux are the main contributors to the Balmer emission. Physical parameters, sizes and locations of these regions are confronted with similar structures in the solar atmosphere.

Results of this study are published in Astronomy Reports.

FLARES ON SINGLE ACTIVE GIANTS

R. Konstantinova-Antova and A. Antov

Institute of Astronomy, Bulgarian Academy of Sciences
72 Tsarigradsko shosse blv., BG-1784 Sofia, Bulgaria
e-mail: antovi@astro.bas.bg

Flare activity in single late giants was studied as a part of the programme for chromospheric activity investigation in late-type evolved stars.
Electrophotometric UBV observations and U-filter patrol monitoring with an integration time of 1 sec were carried out at the Belogradchik Observatory, in the period 1993–1998.
The short-lived flares were observed during 3 nights on V390 Aur and HD112989. An event with a longer duration was detected on OP And. Some brightenings of HD112989 and OP And in the limits of one-two nights observations that seem to indicate for presence of flare-like events were observed too.
The reported results reveal that single active giants also exhibit flares with different duration, in spite of the fact that these stars flare more rarely than the active dwarfs and RS CVn binaries.

INTRODUCTION

Magnetic activity in the cool half of the H–R diagram presents in stars at different evolutionary stages, single and binary ones. There are much signatures of it, scattered throughout the electromagnetic spectrum. It is widely accepted that the dynamo, powered by the convection and catalyzed by the stellar rotation is the reason for this activity.

A scanty group of apparently single low and intermediate mass giants with evidences of dynamo-driven activity was formed in the beginning of the last decade. However, this group undergo slow enrichment with new members during the last years.

According to Simon & Drake (1989) such stars evolved to the red giant branch acquire magnetic activity due to rapid spin-up as their convection zones advance upon the faster rotating stellar interiors. An alternative recent hypothesis proposes the engulfment of the angular momentum of close-in brown dwarf or “hot Jupiter” on the ascent to the red giant tip or later ascent of the asymptotic giant branch (Siess & Livio, 1999) as the reason for the dynamo action in these stars.

The aim of our research was a systematic study of the activity properties in such single giants reached with our equipment – the 2-m telescope with Coude spectrograph at the Rozhen Observatory and the 60-cm telescope with electrophotometer at the Belogradchik Observatory.

Table 1: Data for the detected flares

Star	*Date*	*EventNo.*	*Filter*	Δm	σ	$U.T._{max}$	*Duration*
OP And	17.12.1993	1	U	0.24	0.015	$21^h50^m05^s$	$> 1^h$
			B	0.23	0.010	21 51 10	
			V	0.24	0.010	21 52 31	
V390 Aur	01.01.1998	1	U	0.12	0.015	$20^h47^m34^s$	11^s
		2	U	0.18	0.015	20 47 58	1^s
		3	U	0.17	0.015	20 48 18	9^s
		4	U	0.14	0.015	20 48 59	9^s
		5	U	0.13	0.015	20 52 09	3^s
		6	U	0.06	0.015	20 52 53	11^s
	22.02.1998	1	U	0.29	0.020	$21^h24^m07^s$	6^s
		2	U	0.18	0.020	21 24 11	2^s
		3	U	0.12	0.020	21 24 14	4^s
37 Com	22.02.1998	1	U	0.12	0.010	$01^h36^m25^s$	5^s

OBSERVATIONS

U-band patrol monitoring and UBV measurements were carried out for 5 known as active and suspected in activity single G and K giants. Spectral and photometric activity signatures were found in 4 of these stars. They are as follows: OP And=HD9746, V390 Aur=HD33798, 37 Com=HD112989 and HD145001. Their activity properties and evolutionary stage are described by Fekel & Marshall (1991), Fekel & Balachandran (1993), Konstantinova-Antova *et al.* (1995), De Medeiros (1999) and De Medeiros & Konstantinova-Antova (2000).

The photometric observations for these stars were carried out at the Belogradchik Observatory. The 60-cm Cassegrain telescope, with a single-channel electrophotometer (Antov & Konstantinova-Antova, 1995) was used. The integration time was 1 sec for all the observations. The differential photometry method was applied. The APR program package (Kirov *et al.*, 1991) was used for data processing.

RESULTS

The three of the active giants mentioned above were found to flare: OP And, V390 Aur and 37 Com.

OP AND = HD9746

This star is an appr. 6 magnitude single K1 giant of appr. 1.5 $M_\odot$, according to recent Hipparcos data and Schaller *et al.* (1992) evolutionary tracks for solar chemical composition.

Serious proofs for chromospheric activity and mass loss were found in this giant: strong CaII K&H emission cores, filled-in and variable H_α, presence of coronal and transition region emission lines and periodic photometric variability interpreted as presence of spots on the surface of the star. Changes in the spots configuration from season to season were found too.

UBV measurements and U-patrol monitoring were completed for OP And in the period 1993–1996. The effective total monitoring time was more than 30 hours. HD9057 was used as a comparison star during all these observations.

A flare was detected on December 17, 1993 during UBV patrol monitoring. Data for the event are presented in Table 1 and in Figures 1a and 1b, respectively. Despite we couldn't determine the exact duration of this flare it is visible that it is a long-lived one.

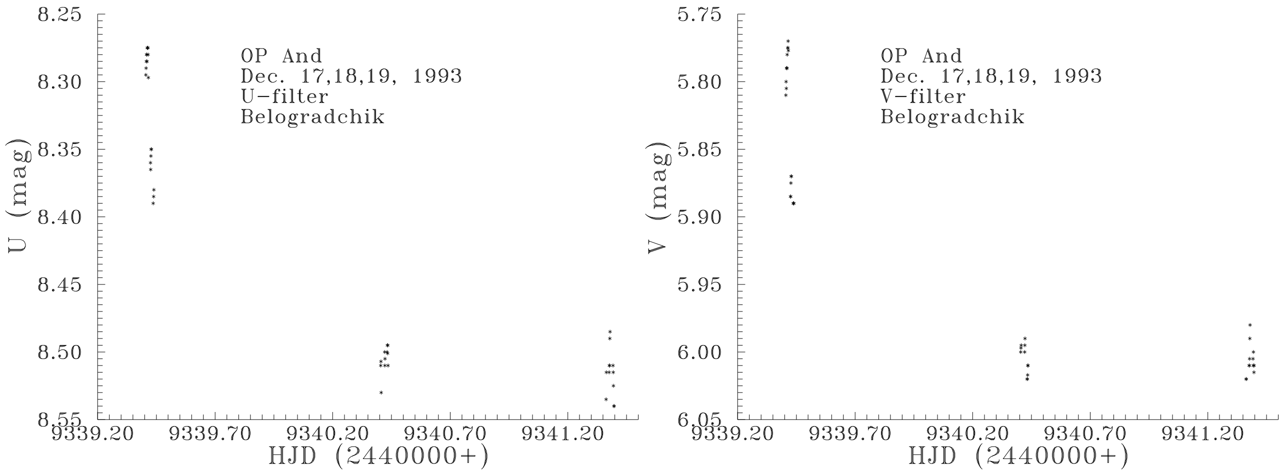

Figure 1: The detected flare on OP And, observed in U- and V-filters

An inspection of the OP And UBV measurements where the average values for the relevant nights are presented reveals that some other isolated points of brightening exist. Such kind brightenings of OP And are also shown by Strassmeier & Hall (1988). These events might be also flares similar to the detected by us.

Such brightenings are observed not only on OP And, but on another active giants too. An example is 37 COM.

37 COM = HD112989

This star is an appr. 5 magnitude G9 single giant of about 5 $M_\odot$, according to Hipparcos data. Activity signatures were also found on this star: moderate and variable CaII emission cores, fairly high X-ray emission and photometric variability interpreted as presence of spots. A long-term period was found for this star too (Donahue, 1996).

Our UBV observations were completed in the period of 1996–1998. HD113493 and HD113494 stars were used for comparison and clarification, respectively. We found one-two night brightenings with amplitudes 0.1–0.2 magnitude,which are similar to those ones reported in OP And. They also might be flares.

On the other hand, one short-lived flare-like event was detected on 37 Com during about 11-hours total monitoring time in U-filter, obtained in the period of 1997–1998. The data are presented in Table 1 and the detail lightcurve could be found by De Medeiros *et al.* (1999). The short life and unusual structure of this event are somewhat unexpected for a giant star. According to the gas-dynamic model (Katsova & Livshits, 1991) giants should not demonstrate such kind of short-duration flares.

However, events with a similar duration were also detected on another active giant – V390 Aur.

V390 AUR = HD33798

This appr. 7 magnitude star of about 2 $M_{\odot}$ was classified as chromospherically active giant by Fekel & Marshall (1991). Moderately strong CaII emission cores and a periodic photometric variability were reported for it. Photometric data are presented by Hooten & Hall (1990) and an isolated night of brightening was detected by them too.

UBV observations and patrol U-monitoring were carried out for this star in the period of December, 1997 – March, 1999. HD34533A was used as a comparison star. The short-lived flares were detected during appr. 24-hours total monitoring time. More than 9 such events were observed during 2 nights. The data are presented in Table 1 and in Figs. 2 and 3, respectively.

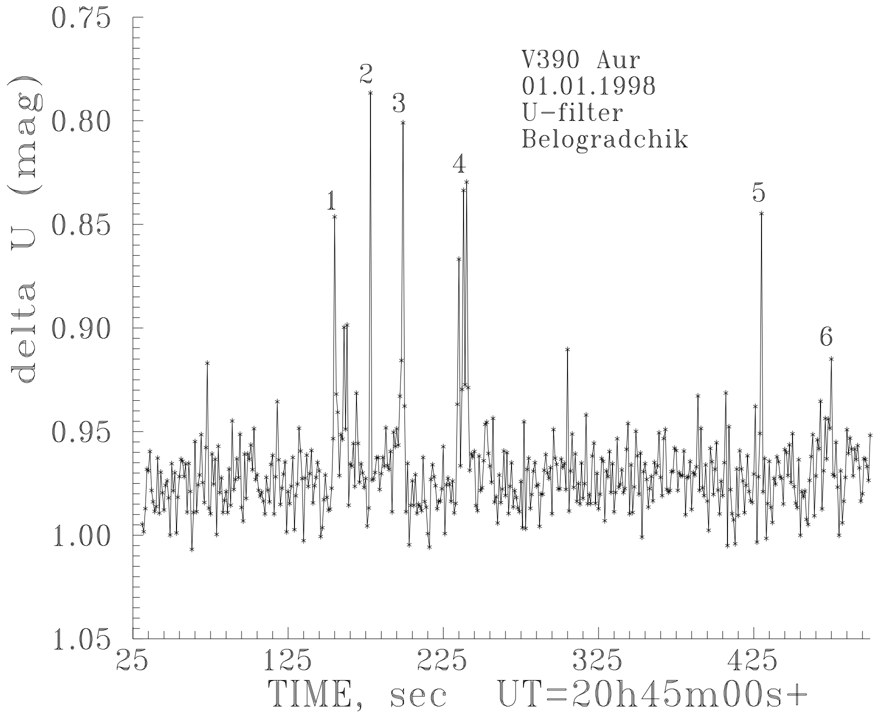

Figure 2: Flares detected on V390 Aur on January 1, 1998

However, a secondary star located at 0.4 arcsec away from V390 Aur with amplitude fainter 3.3 magnitude was reported by Van Biesbroeck (1974) and the Hipparcos mission confirmed his measurement. These stars cannot be separated in the photometer diaphragm. They were observed together with our equipment. But, taking into account the duration of events, the shape of the lightcurves and the fact that the secondary star should be late F or early G dwarf we came to the conclusion that it is more likely for these events to be happened on the primary star, V390 Aur. Moreover, if we assume that flares with such resulting amplitudes are produced by the secondary star, then their real amplitudes should be greater (or equal) 1.5 magnitude. Flares with similar U-amplitudes and a duration of appr. 10 sec were detected on active red dwarf stars. However, a set of events with such characteristics occurs very rarely and moreover on early G dwarfs.

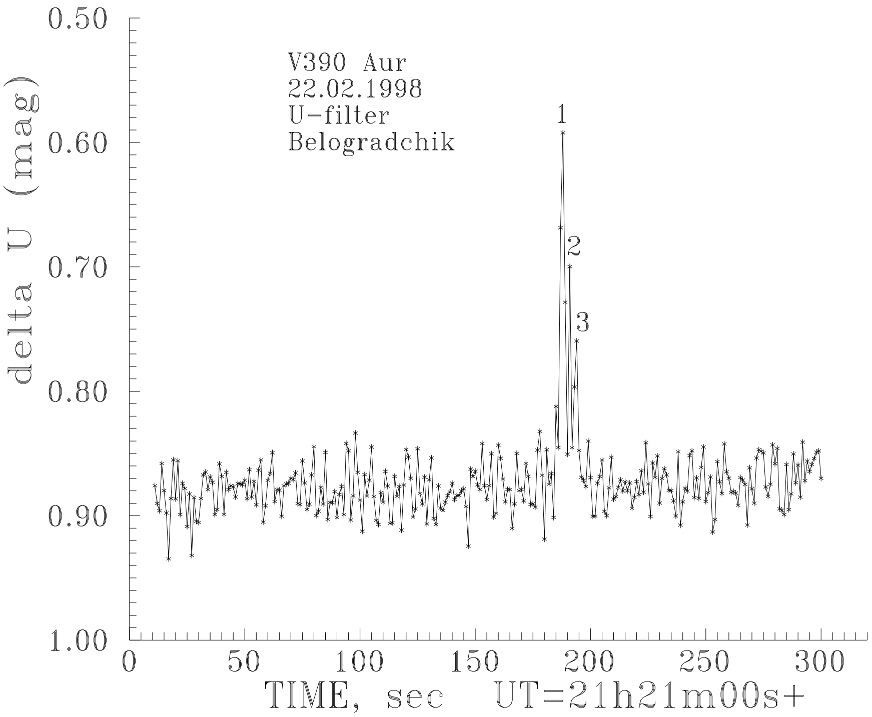

Figure 3: The events observed on V390 Aur on February 22, 1998

DISCUSSION

Our results revealed that both short-lived and longer duration flares appear in single active G and K giants but these events happen not very often.

The bibliographic search also confirms this result. A few events in X-ray and in some UV lines, that seems to be flares are reported by Huensch & Reimers (1995), Haish & Schmitt (1994), Ambruster *et al.* (1997) and Ayres *et al.* (1999). No firmly proofs for optical flares in single giants were reported till now. The earlier reviews on this topic by Pettersen (1989) and Schaefer (1989) pointed out a few stars (ν Oph, τ CrB, V654 Her) as flaring giants candidates. Our study of the chromospheric activity indicators and U-patrol monitoring revealed no sign of activity and flares in these stars (Konstantinova-Antova *et al.*, 1995). So, after a careful analysis we could not exclude the possibility for these events to be artificial ones.

Our recent systematic photometric study of active single giants found that optical flares happen on them, but RARELY. This fact could be explained either with their lower activity level, or with the specific properties and structure of the active regions in these stars.

Short-lived optical flares, especially, could not be easily explained by the Katsova and Livshits gas-dynamic model. A possible explanation could be given under the assumption of influence of accelerated particles into the more dense chromospheric and upper photospheric layers. Their unusual spike structure needs a further investigation. In future, a high-speed simultaneous patrol monitoring is required to refine our knowledge on the properties of these events.

Aknowledgements. This work is partially supported by the Bulgarian National Science Foundation under contract F-716/1997.
The Hipparcos Catalogue was used.

REFERENCES

[1] *Antov A. P., Konstantinova-Antova R. K.* // Robotic Observatories / Ed. M. F. Bode.–Chichester, England: Praxis Publishing Ltd., 1995.–P. 69.

[2] *Ambruster C. W., Fekel F. C., Guinan E. F., Hrivnak B. J.* // Astrophys. J.–1997.–**479**.–P. 960.

[3] *Ayres T. R., Osten R. A., Brown A.* // Astrophys. J.–1999.–**526**.–P. 445.

[4] *de Medeiros J. R., Konstantinova-Antova R. K.* in preparation.

[5] *de Medeiros J. R., Konstantinova-Antova R. K., Da Silva J. R. P.* // Astron. and Astrophys.–1999.–**347**.–P. 550.

[6] *Fekel F. C., Marshall L. A.* // Astron. J.–1991.–**102**.–P. 1439.

[7] *Fekel F. C., Balachandran S.* // Astrophys. J.–1993.–**403**.–P. 708.

[8] *Haisch B., Schmitt J. H. M. M.* // Astrophys. J.–1994.–**426**.–P. 716.

[9] *Hooten J. T., Hall D. S.* // Astrophys. J. Suppl. Ser.–1990.–**74**.–P. 225.

[10] *Hunsch M., Reimers D.* // Astron. and Astrophys.–1995.–**296**.–P. 509.

[11] *Katsova M. M., Livshits M. A.* // Sov. Astron.–1991.–**35**.–P. 65.

[12] *Kirov N. K., Antov A. P., Genkov V. V.* // Comt. Rend. Acad. Bulgare Sci.–1991.–**44**, N 11.–P. 5.

[13] *Konstantinova-Antova R. K., Ivanov M. M., Antov A. P.* // Flares and Flashes: Proc. IAU Coll. 151 / Eds J. Greiner, H. W. Duerbeck and R. E. Gershberg.–Lecture Notes in Physics.–1995.–**454**.–P. 98.

[14] *Konstantinova-Antova R. K., Ivanov M. M., Antov A. P.* // Stellar Surface Structure: Poster Proc. IAU Symp. 176 / Ed. K. G. Strassmeier.–University of Wien Press, 1995.–P. 178.

[15] *Pettersen B. R.* // Solar Phys.–1989.–**121**.–P. 299.

[16] *Schaefer B. E.* // Astrophys. J.–1989.–**337**.–P. 927.

[17] *Schaller G., Schaerer D., Meynet G., Maeder A.* // Astron. and Astrophys. Suppl. Ser.–1992.–**96**.–P. 269.

[18] *Siess L., Livio M.* // Mon. Notic. Roy. Astron. Soc.–1999.–**308**.–P.1133.

[19] *Simon T., Drake S. A.* // Astrophys. J.–1989.–**346**.–P. 303.

[20] *Strassmeier K. G., Hall D. S.* // Astrophys. J. Suppl. Ser.–1988.–**67**.–P. 453.

[21] *Van Biesbroeck G.* // Astrophys. J. Suppl. Ser.–1974.–**28**.–P. 413.

THE DEPENDENCE OF THE BY DRA–TYPE VARIABLE SPOTTEDNESS ON GENERAL STELLAR PARAMETERS

I. Yu. Alekseev and R. E. Gershberg

Crimean Astrophysical Observatory, Ministry of Ukraine for Education and Science
Naukove, 98409 Crimea, Ukraine
e-mail: gershberg@crao.crimea.ua

Within the framework of the zonal spottedness model for red dwarf stars that was proposed and developed in Crimea, a spottedness of a star is approximated with two belts parallel to a stellar equator with a linear variation of darkness along the belt. Using $UBVRI$ observations of 25 stars for 342 observational epochs such models have been calculated for all these photometric data. Here we confront model parameters with global characteristics of stars under consideration – absolute luminosities, the Rossby numbers, rotational velocities. A set of good correlations is found, and the Sun fits to all of them.

In our papers (Alekseev & Gershberg, 1996ab) we proposed and developed a new approach to analyse the surface inhomogeneities of red dwarf stars based on the multicolour broad band photometry. Instead of trying to explain the observed photometric effects in the traditional way by estimating parameters of one or two – three large separate spots, we consider general characteristics of spotted regions on a star. We approximate the aggregate of stellar spots by two spotted belts located symmetrically relative to the stellar equator with variable linearly along stellar longitudes filling factor of the dark regions inside these belts.

This model can be described by four independent parameters: a distance of the belts from the equator $\pm\phi_0$, a width of the belts $\Delta\phi$, a lower limit of a range $(f_{min}, 1)$ for a filling factor into a belt and a spot/photosphere contrast β_V. The main advantage of our zonal model is a possibility to reproduce a spottedness picture similar to the solar one.

We used our algorithm to analyse all photometric observations of 25 red dwarf stars for 342 epochs (Alekseev & Gershberg, 1996c; Alekseev, 1998; Alekseev, 2000; Alekseev & Bondar', 1998; Alekseev & Grankin, 2001; Alekseev & Kozlova, 2000; Alekseev & Kozlova, 2001).

These stars occupy the wide ranges of spectral classes ($dG1e \div dM4.5e$), luminosities ($M_V = 4\overset{m}{.}80 \div 12\overset{m}{.}24$) and equatorial rotation velocities ($v_{rot} = 4 \div 25$ km/s). Therefore, we can draw preliminary conclusions about general regularities of the red dwarfs' spottedness.

It is known that the solar-type activity is determined by general structure and rotation of a star. The stellar structure primarily depends on its mass or on color index as an indicator of the mass. We compare our model parameters with the color index $V - I$.

Stellar rotation is characterized by its linear velocity v_{rot}, which can be determined from the observed period and stellar radius. The kinematics of stellar internal layers is determined by the Rossby number. Figure 1 presents comparisons of some zonal model parameters with these general stellar parameters $V - I$, v_{rot} and Ro. The vertical line in Fig. 1b corresponds to the range of spot latitudes on the Sun. The value $< \phi >= \phi_0 + \Delta\phi/2$ is a mean latitude of starspots.

The main results of the comparison of spottedness model parameters with general stellar characteristics are following:

– For all stars with $V - I > 1\overset{m}{.}5$, *i.e.*, with $T_{phot} < 4700\ K$, $\phi_0 = 0$ at all epochs. In other words, the two spot belts merge into a single equatorial belt. Such spottedness picture is directly confirmed for a single rapidly rotating star $LQ\ Hya$ studied by the Doppler Imaging (Rice & Strassmeier, 1998).

– The spotted belt width $\Delta\phi$ decreases to the hot end of the our sample. The hottest star of our sample $BE\ Cet$ of the same spectral class as the Sun has the lowest value of $\Delta\phi$, which is the closest to the situation on the Sun.

– The values $< \phi >$ show that starspots concentrate near the stellar equators on cool stars and near middle latitudes on the solar type stars. On latter stars the starspot latitude distribution is similar to the solar one. It should be noted that our algorithm did not impose any restriction on definable spot latitudes but in no case the latitudes $\phi_0 + \Delta\phi$ turned out to be more than 60°. Therefore, we did not found either very high latitude or

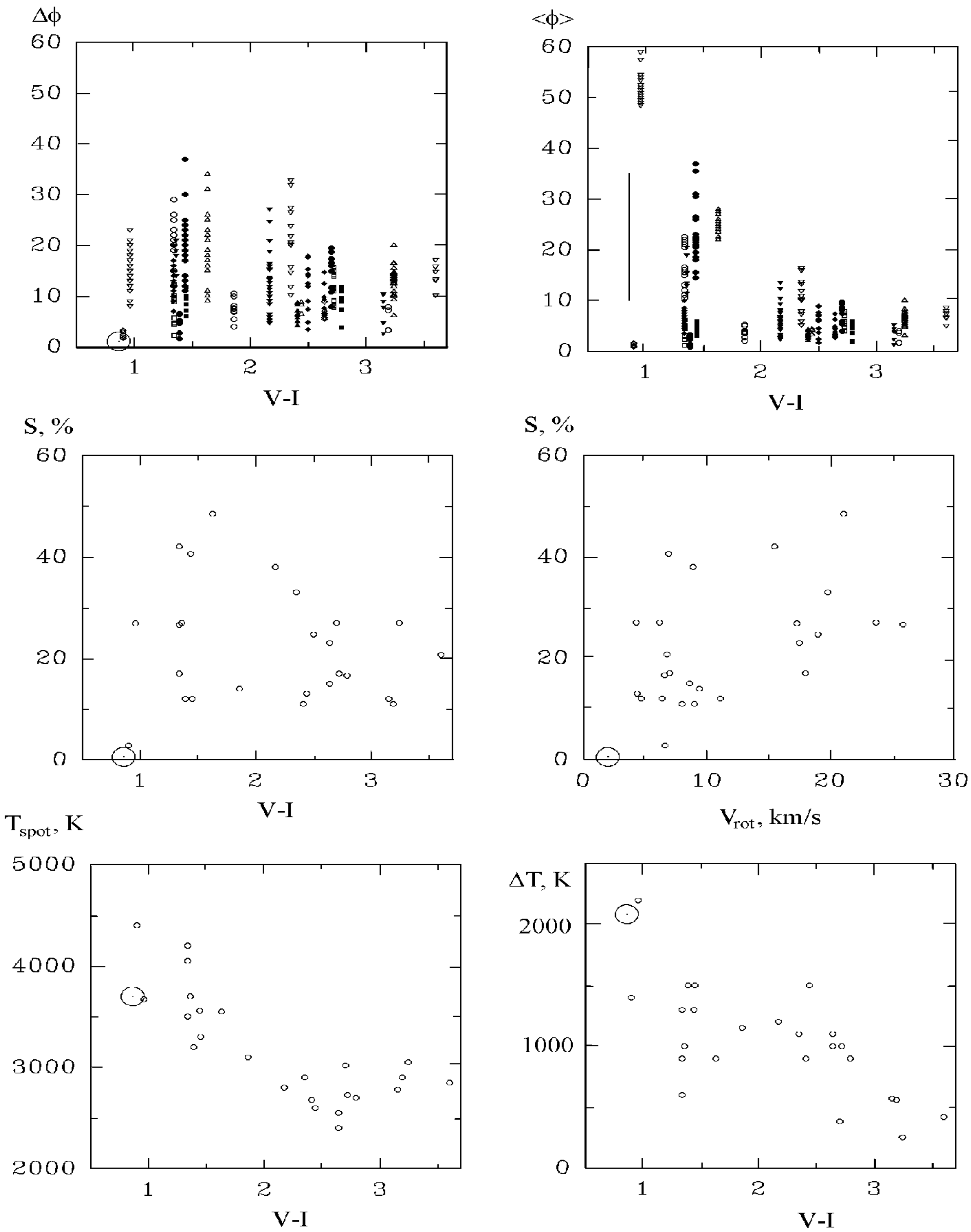

Figure 1: The comparison of model parameters with general stellar characteristics

circumpolar starspots.

– The coverage parameter f_{min} does not depend on any general stellar characteristics.

– The combination of ϕ_0, $\Delta\phi$ and f_{min} gives us the value of total spotarea S in each epoch measured in percents of the total stellar surface. The maximum S values for each star given in Figs. 1c, 1d demonstrate a tendency to increase S, when the rotation velocity grows. The largest spotarea values take place at the rotation velocity $v_{rot} \sim 15-20$ km/s. In this case spotted regions occupy up to 50% of the total stellar surface.

– The dependence of S on $V-I$ shows that the maximum spotarea takes place for stars with the spectral classes K. $BE\ Cet$, whose characteristics are the closest to solar ones, has the lowest spottedness degree approaching to the solar value.

– The mean starspot temperatures indicate well the defined statistical dependence: the coolest spots are on the coolest stars (Fig. 1e). The starspot temperatures are from 4000 K on solar-like G stars to $2500-3000$ K on the coolest M stars. The mean temperature difference ΔT between the quiet stellar photosphere and starspots is from 2000 K on the hottest stars to 300 K on the coolest stars (Fig. 1f).

– The sunspots fit to all these dependences.

In other words, we see a tendency for parameters of our models to match the characteristic parameters of solar spottedness. This matching leads us to believe that our zonal models indeed reflect fundamental properties of the red dwarf stars' surface inhomogeneities.

We intend to apply our model to the $T\ Tau$ and $RS\ CVn$ type variables, where the Doppler Imaging shows systematically an existence of high latitude or circumpolar starspots.

REFERENCES

[1] *Alekseev I. Yu.* // Astron. Rep.–1998.–**42**.–P. 649.

[2] *Alekseev I. Yu.* // Astron. Rep.–2000.–**44**.–P. 178.

[3] *Alekseev I. Yu., Bondar' N. I.* // Astron. Rep.–1998.–**42**.–P. 655.

[4] *Alekseev I. Yu., Gershberg R. E.* // Astron. Rep.–1996a.–**40**.–P. 528.

[5] *Alekseev I. Yu., Gershberg R. E.* // Astron. Rep.–1996b.–**40**.– P. 538.

[6] *Alekseev I. Yu., Gershberg R. E.* // Astrophysics.–1996c.–**39**.–P. 33.

[7] *Alekseev I. Yu., Gershberg R. E.* // Astron. Rep.–1997.–**41**.–P. 207.

[8] *Alekseev I. Yu., Grankin K. N.* // 2001.–in preparation.

[9] *Alekseev I. Yu., Kozlova O. V.* // Astrophysics.–2000.–**43**.–P. 339.

[10] *Alekseev I. Yu., Kozlova O. V.* // 2001.–in preparation.

[11] *Rice J. B., Strassmeier K. G.* // Astron. and Astrophys.–1998.–**336**.–P. 972.

Session 3. Stellar Variability and Abundances

Convener: Prof. Werner W. Weiss
(Inst. for Astronomy, Univ. of Vienna, Austria)

SPECTRUM ANALYSIS OF HD 83368 AND HD 60435 WITH LITHIUM SPOTS

A. V. Shavrina[1], V. Tsymbal[2], V. Khalack[1], N. S. Polosukhina[3], J. Zverko[4], J. Žižňovský[4], M. Hack[5], P. North[6]

[1] *Main Astronomical Observatory, NAS of Ukraine*
27 Akademika Zabolotnoho St., 03680 Kyiv, Ukraine
e-mail: shavrina@mao.kiev.ua, khalack@mao.kiev.ua

[2] *Tavrian National University, 95000 Simpheropol, Ukraine*
e-mail: VAD@ccssu.crimea.ua

[3] *Crimean Astrophysical Observatory, Naukove, 98409 Crimea, Ukraine*
e-mail: polo@crao.crimea.ua

[4] *Astronomical Institute, Slovak Academy of Sciences, 059 60 Tatranská Lomnica, Slovakia*
e-mail: zve@ta3.sk, ziga@ta3.sk

[5] *Dept. of Astronomy, Trieste Univ., I-34131 Trieste, Italy*
e-mail: hack@ts.astro.it

[6] *Inst. d'Astronomie, Univ. Lausanne, CH-1290 Chavannes-des-Bois, Switzerland*
e-mail: Pierre.North@obs.unige.ch

We present results of abundance determination of some elements in the roAp star HD 60435 and compare them with the results obtained for HD 83368. Lithium spots were distinguished on HD 60435 and their parameters were derived. For the first time the values of the rotational axis inclination i and surface magnetic field H_s were determined for HD 60435.

INTRODUCTION

The behaviour of the Li line at 6708 Å in spectra of several magnetic CP stars was studied by Polosukhina *et al.* [6] in the framework of the "Lithium in CP stars" project. A distinguished behaviour of the 6708 Å line which divided the stars into four different groups, was explained in terms of the oblique rotator model with magnetic field and occurence of Li spots at the magnetic poles. HD 60435 and HD 83368 studied here belong to the group I, for which we observe two lithium spots on a rotating star, that can be explained in the frame of magnetic dipole model with significant inclination of its magnetic axis to the rotational one.

SPECTRUM ANALYSIS

Primary data reduction was made by one of us (PN) using the standard IHAP procedure. Subsequent evaluation of the spectra were performed with SPE, a code written by Sergeev. The quantitative analysis was carried out by means of synthetic spectra using STARSP code and Kurucz's model atmospheres [3]. Line lists with atomic data were those by Kurucz (CDROM 23) and VALD [2, 5] accessible through INTERNET. Computations of spots' parameters (size, location and elemental abundance) were performed with the ROTATE code of Tsymbal.

The values of T_eff, $\log g$ and $v \sin i$ were determined in [7, 10]. For HD 83368 the best agreement in the abundances computed from the Fe I and Fe II lines was achieved for the model $T_\mathrm{eff} = 7750$ K, $\log g = 4.0$. For HD 60435 the best agreement between the abundances computed from the Fe I, Fe II and Cr I, Cr II lines was reached for the model $T_\mathrm{eff} = 8250$ K, $\log g = 4.5$. For the line profile calculations we used $v \sin i = 11$ km s^{-1} for HD 60435 and $v \sin i = 34$ km s^{-1} for HD 83368. Models with [M/H] = 0.0 were the best ones.

Table 1: Elemental abundances for HD 83368 and HD 60435 as compared with data by Zverko *et al.* [11] for HD 60435, Grevesse & Sauval [1] for the Sun and Roby & Lambert [8] and Ryabchikova *et al.* [9] for HD 24712

El	HD 83368 max	HD 83368 min	HD 60435 max	HD 60435 min	N lines	error (dex)	HD 60435 m1^b	HD 60435 m2^c	Sun	HD 24712	
1	2	3	4	5	6	7	8	9	10	11	12
C I	-3.8	-4.5	-3.6	-3.8	6	.3			-3.52	-4.5	
N I	-3.0	-4.0	-3.2	-3.4	10	.3			-4.09	-4.4	
O I	-3.4	-4.3	-3.9	-4.5	2	.3	-4.0	-4.0	-3.21	-3.8	
Na I	-6.1	-6.1	-5.8	-5.8	2	.3		-5.9	-5.72		
Al I	-6.0	-6.6	-6.2	-6.2	1	.2		-6.8	-5.57	-5.53	
Si I	-3.9	-4.9	-3.6	-4.4	5	.2		-4.9	-4.48	-4.43	
S I	-5.2	-5.2			5	.3			-4.84		
Ca I	-5.1	-5.6	-4.7	-5.1	2	.1	-5.4	-5.4	-5.69	-5.69	
Ca II	-5.3	-5.8	-5.8	-5.8	3	.3				-5.22	-4.88
Ti II	-6.8	-7.3	-7.2	-7.3	2	.2			-7.10	-7.22	-7.29
Cr I	-4.1	-5.0	-4.3	-4.4	4	.2			-6.35	-5.93	-5.80
Cr II	-4.2	-4.6	-4.6	-4.6	4	.3	-4.9	-5.0		-5.58	-5.33
Fe I	-4.6	-4.9	-4.1	-4.2	4	.1	-4.4	-4.5	-4.54	-4.77	-4.88
Fe II	-4.3	-4.7	-4.3^a	-4.3^a	10	.2	-4.4	-4.5		-4.80	-5.11
Co I	-5.5	-6.3			1	.3		-5.7	-7.13	-5.88	-5.57
Y I	-6.4	-7.0			4	.2		-8.5	-9.81	-7.80	-7.80
Ba II	-9.1	-9.1	-9.1^a	-9.1^a	1	.2	-9.5	-10.0	-9.82	-9.12	-8.98
La II	-8.4	-9.2			3	.4		-10.3	-10.82	-9.40	-8.75
Ce II	-8.1	-8.7			2	.2		-9.4	-10.41	-9.18	-8.90
Pr II	-9.3	-9.3	-9.3	-9.3	4	.2			-11.24	-10.15	-9.60
Pr III	-8.5	-9.1	-8.4	-8.8	2	.2					
Nd II	-8.2	-9.3	-7.9	-8.6	4	.3		-9.2	-10.55	-9.13	-8.64
Nd III	-7.2	-8.0	-7.5	-8.0	2	.2					
Sm II	-8.4	-9.1	-8.1	-8.4	3	.2		-9.9	-11.06	-9.75	-9.16
Eu II	-9.8	-9.8			2	.2		-9.5	-11.07	-9.50	-9.00
Gd II	-8.4	-8.9			6	.3	-8.2		-10.95	-9.11	-8.70
Er II	-8.1	-8.6			1	.3			-11.07	-9.79	-9.53
Yb II			-9.3	-9.4	1	.3			-11.08	-8.30	-8.30
Lu II	-9.2	-9.2	-9.4	-9.4	1	.2			-11.91		

a) - from spectral range 6120–6180 Å;
b) - $T_{\rm eff} = 8250$ K, $\log g = 4.5$, $v \sin i = 11$ km s^{-1} and [M/H]=0.0;
c) - $T_{\rm eff} = 7750$ K, $\log g = 3.0$, $v \sin i = 11$ km s^{-1} and [M/H]=0.0.

Comparing the synthetic spectra with the observed ones at individual rotational phases, we derived abundance variations of several elements with rotation. The maximum and minimum values of log(N/H) for the corresponding phases are given in Table 1 for HD 83368 (column 2 and 3) and for HD 60435 (column 4 and 5). The number of lines used and the errors for each element are given in columns 6 and 7, respectively. The procedure of fitting the observed and calculated spectra was repeated until the disagreement in abundances for all the analysed lines of each element has been reached its minimum.

MAGNETIC FIELD

In the previous paper we estimated the value of the surface magnetic field to be equal to ~ 2 kG that varies by $\pm$ 300 G over the rotation of the star. We attempted also to determine the value of the surface magnetic field from the Fe II 6147 Å and 6149 Å line profiles. We computed the synthetic profiles taking into account magnetic splitting for two values of the magnetic field, namely 2 kG (Zeeman splitting), and 11 kG (Paschen-Back effect) [4]. The profiles shown in Fig. 1a were computed for $H_{\rm s} = 2$ kG taking into account spots of the Fe II located at the longitudes $l_1 = 110°$ and $l_2 = 170°$ and of the Pr II ($l = 100°$), where $l = 0°$ corresponds to the subsolar point on the stellar surface at the photometric phase zero [7].

We completed the same calculations for $H_{\rm s} = 11$ kG and a significantly worse agreement with observed line profiles was derived. Due to this reason we consider the value $H_{\rm s} = 2$ kG to be more convenient. This value is confirmed also by a good fit of the computed profiles of the Eu II 6645.46 Å, Nd III 6145.07 Å and Ba II 6141 Å lines to the observed ones, taking into account the surface spot structure (see Fig. 2a).

Contrary to the case of HD 83368, there are no original measurements of magnetic field for HD 60435. Considering the similarity of these two stars we followed the same way for HD 60435.

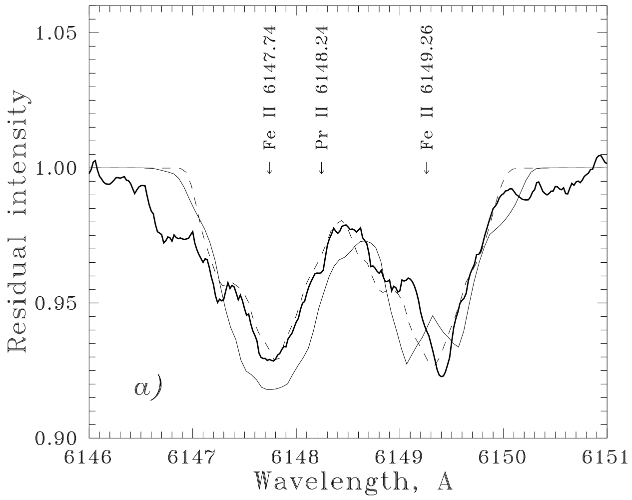

Figure 1: Profiles of Fe II 6147.74 and 6149.26 Å. Full line: observed spectrum. **a)** HD 83368, phase 0.320; dashed line: 2 kG (Zeeman splitting), thin line: 11 kG (Paschen-Back effect), spotted surface. **b)** HD 60435, phase 0.005; dashed line: 3 kG (Zeeman splitting)

We computed profiles of the lines mentioned for the corresponding orientation of the magnetic field with Zeeman splitting for a set of values of H_s in the range 2–8 kG and $v \sin i = 11 \pm 2$ km s^{-1}. The best fit of the computed profiles to the observed ones was achieved for $H_s = 2$ kG in the case of the Fe II lines and for $H_s = 3.5$ kG in the case of the Ba II lines (Fig. 2b). We derived a good fit for both elements simultaneously: for a single value $H_s = 3$ kG, but only if $v \sin i = 9$ km s^{-1} for the Fe II lines (Fig. 1b), and if $v \sin i = 13$ km s^{-1} for the Ba II line. Thus, our estimate of the surface magnetic field of HD 60435 is $H_s = 3 \pm 1$ kG with $v \sin i = 11 \pm 2$ km s^{-1}.

CONCLUSIONS

We find that abundances of elements in both stars differ from each other and differ considerably from the solar one, which is a common feature of CP stars. As compared with the other roAp star HD 24712, almost all elements studied show overabundances, while Al is deficient in both stars. In HD 60435 the O and Yb are underabundant too.

In HD 83368, the abundances of the elements studied vary with rotation by up to 0.9 dex in general, while in HD 60435 the most prominent variations (up to 0.7 dex) are shown by REE and some of the light elements (O, Si). The main difference between these two stars is that the iron peak elements in HD 60435 are non-variable within the abundance errors.

In HD 83368, the abundance maximum of the most variable elements occurs at phases when the Li line is outside of its extrema. From this we deduce that some of the other elements (mainly REE) may form the ring-like features surrounding the lithium spots. A similar structure can be expected for HD 60435.

In HD 83368 the behaviour of the Li line profile and magnetic field shows that lithium spots approximately coincide with magnetic poles. The positions l_1, l_2 of the two lithium spots correspond to a lag between magnetic poles and spots of $\sim 23°$ which is in a good agreement with the lag derived in [7]. At the same time the values of l_1, l_2 show that the lithium spots are possibly not exactly 180° apart. In HD 60435 we derived from the line profile variations the positions of the lithium spots, which similarly do not lie strictly at opposite sites. Like on the former star, we suppose that magnetic poles may coincide approximately with the lithium spots.

For HD 83368 the determination of inclination i was described in [7] and it has to be close to 90°. For HD 60435 using the HIPPARCOS data we derived $i = 133° \pm 23°$ (or $47° \pm 23°$). Under these conditions our analysis of profiles of magnetically sensitive Fe II lines (6147 Å, 6149 Å) leads to the surface field value $H_s = 3$ kG for HD 60435 and $H_s = 2$ kG for HD 83368.

Acknowledgements. We are grateful to S. Sergeev for SPE code for spectra analysis, to Ch. Cowley for numerous consultations and for sending us the rare earth element data, to M. Ya. Orlow for discussion, to D. Bord and J. Sugar for suggestions and advices to use their data. The data from Kurucz's CDROM 23,

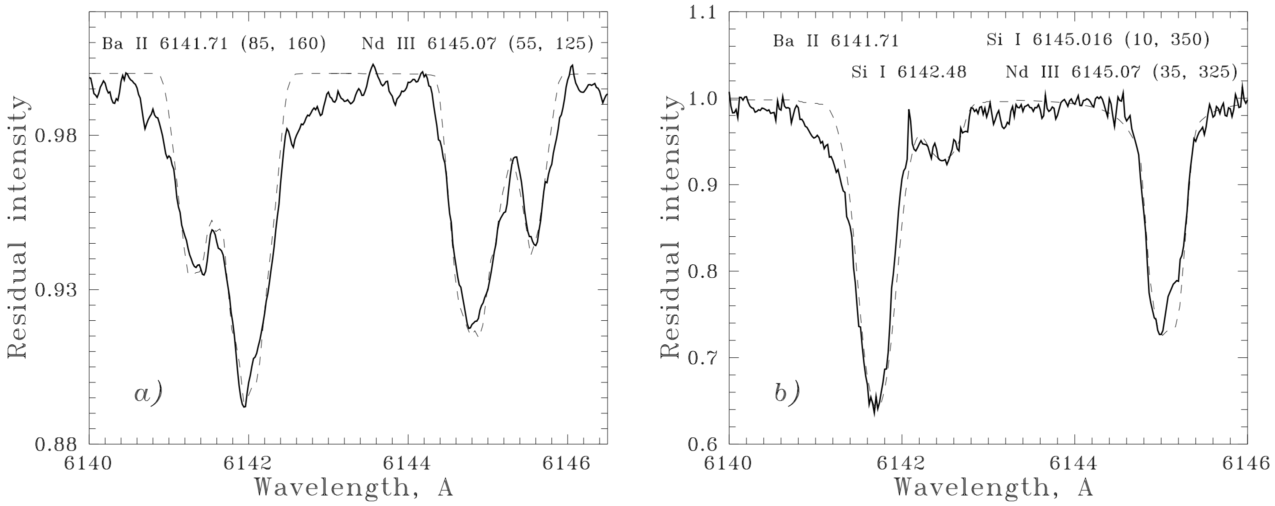

Figure 2: Profile of the Ba II 6141.71 Å line with Zeeman splitting. Full line: observed spectrum, dashed line: synthetic spectrum. **a)** HD 83368, two spots at $l = 85^\circ$ and $l = 160^\circ$, 2 kG. **b)** HD 60435, 3.5 kG, $v \sin i = 11$ km s^{-1}

NASA ADC, VALD and NIST were used and we thank the administrators of these databases, accessible through INTERNET. A partial support of VEGA grant No. 7107 is acknowledged. V. Tsymbal thanks Mr. Yakushechkin for his support. P. North thanks the Swiss National Science Foundation for its support. V. Khalack is grateful to the Ukrainian Astronomical Association for financial support.

REFERENCES

[1] *Grevesse N., Sauval A. J.* Standard solar composition // Space Sci. Rev.–1998.–**85**.–P. 161–174.

[2] *Kupka F., Piskunov N., et al.* VALD-2: Progress of the Vienna Atomic Line Data Base // Astron. and Astrophys. Suppl. Ser.–1999.-**138**.-P. 119–133.

[3] *Kurucz R. L.* // CDROM13, CDROM23–1993.

[4] *Mathys G.* Spectropolarimetry of magnetic stars. V. The mean quadratic magnetic field // Astron. and Astrophys.–1995.–**293**, N 3.–P. 746–763.

[5] *Piskunov N. E., Kupka F., et al.* VALD: The Vienna Atomic Line Data Base // Astron. and Astrophys. Suppl. Ser.–1995.-**112**.-P. 525–541.

[6] *Polosukhina N. S., Kurtz D., et al.* Lithium on the surface of cool magnetic CP stars. I. Summary of spectroscopic observations with three telescopes // Astron. and Astrophys.–1999.–**351**.–P. 283–291.

[7] *Polosukhina N. S., Shavrina A. V., et al.* Preliminary spectroscopic analysis of the "spotted" roAp star HD 83368 in the Li I 6708 Å region // Astron. and Astrophys.–2000.–**357**.–P. 920–930.

[8] *Roby S. N., Lambert D. L.* Carbon, nitrogen, and oxygen abundances in the chemically peculiar stars of the upper main sequence // Astrophys. J. Suppl. Ser.–1990.–**73**.–P. 67–102.

[9] *Ryabchikova T. A., Landstreet J. D., et al.* Abundance analysis of roAp stars. IV. HD24712 // Astron. and Astrophys.–1997.–**327**.–P. 1137–1146.

[10] *Zverko J., Žižňovský J., North P.,* Spectrum variability of the roAp star HD 60435 in the red region // Contr. Astron. Obs. Skalnate Pleso.–1998.–**28**.–P. 109–120.

[11] *Zverko J., Žižňovský J., North P.* // private communication.–2000.

LITHIUM AND REE SURFACE STRUCTURE OF TWO roAp STARS, HD 83368 AND HD 60435. PRELIMINARY RESULTS

A. V. Shavrina[1], V. Tsymbal[2], N. S. Polosukhina[3], J. Zverko[4], V. Khalack[1], J. Žižňovský[4], M. Hack[5], P. North[6]

[1] *Main Astronomical Observatory, NAS of Ukraine*
27 Akademika Zabolotnoho, 03680 Kyiv, Ukraine
e-mail: shavrina@mao.kiev.ua, khalack@mao.kiev.ua

[2] *Tavrian National University, 95000 Simpheropol, Ukraine*
e-mail: VAD@ccssu.crimea.ua

[3] *Crimean Astrophysical Observatory, Naukove, 98409 Crimea, Ukraine*
e-mail: polo@crao.crimea.ua

[4] *Astronomical Institute, Slovak Academy of Sciences, 059 60 Tatranská Lomnica, Slovakia*
e-mail: zve@ta3.sk, ziga@ta3.sk

[5] *Dept. of Astronomy, Trieste Univ., I-34131 Trieste, Italy*
e-mail: hack@ts.astro.it

[6] *Inst. d'Astronomie, Univ. Lausanne, CH-1290 Chavannes-des-Bois, Switzerland*
e-mail: Pierre.North@obs.unige.ch

We determined the Li and REE surface distribution on two roAp stars by computing line profiles in the region near Li I line 6708 Å using high resolution spectra in different rotation phases.

INTRODUCTION

The quantitative analysis of two roAp stars atmospheres was completed by means of synthetic spectra using STARSP code (Tsymbal) and Kurucz's model atmospheres. Line lists with atomic data were those by Kurucz (CDROM 23) and VALD Computations of spots' parameters (size, location and elemental abundance) were performed with the ROTATE code of Tsymbal allowing to calculate the line profiles for a rotating star.

For HD 83368 the best agreement in the abundances computed from the Fe I and Fe II lines was achieved for the model $T_{\rm eff} = 7750$ K, $\log g = 4.0$. For HD 60435 the best agreement between the abundances computed from the Fe I, Fe II and Cr I, Cr II lines was reached for the model $T_{\rm eff} = 8250$ K, $\log g = 4.5$. Also for HD 60435 we used $v \sin i = 11$ km s^{-1} and for HD 83368 $v \sin i = 34$ km s^{-1}. Models with [M/H] = 0.0 were the best ones.

RARE EARTHS

Spectra of these roAp stars are rich in REE lines. Especially strong lines are the ones of Nd II, Pr II and Pr III lines. The most significant abundance variations are shown by La II, Ce II, Nd III, Sm II, Gd II and Er II lines in HD 83368, and by Nd II and Nd III lines in HD 60435.

As it was shown in [1], REE create ring-like structures surrounding the Li spots in HD 83368. In the same way we tried to determine the position of REE spots on HD 60435 using the lines of ionized rare earth elements near the Li line (Pr III, Sm II and Ce II) and Pr III 6160.22 Å and 6161.24 Å (spectral region 6120-6180 Å) for the phase 0.005. For insufficient phase coverage, our results can be considered as preliminary ones only.

The lithium spots parameters for HD 83368 [1] are following:

- spot 1: $l_1 = 173 \pm 6°, \varphi = 0 \pm 6°, R = 33 \pm 6°, \log(N_{\rm Li}/N_{\rm H}) = -8.4 \pm 0.2$.
- spot 2: $l_2 = 337 \pm 6°, \varphi = 0 \pm 6°, R = 35 \pm 6°, \log(N_{\rm Li}/N_{\rm H}) = -8.5 \pm 0.2$.

where l is the longitude, φ the latitude and R the radius of the spot ($R = 90°$ is corresponding to a whole hemisphere). The resulting lithium spots parameters for HD 60435 are following:

- spot 1: $l_1 = 205 \pm 10°, \varphi = 15 \pm 5°, R = 40 \pm 7°, \log(N_{\rm Li}/N_{\rm H}) = -9.3 \pm 0.2$.
- spot 2: $l_2 = 11 \pm 6°, \varphi = -15 \pm 5°, R = 44 \pm 3°, \log(N_{\rm Li}/N_{\rm H}) = -8.2 \pm 0.2$.

Table 1: REE spots data for HD 83368 and HD 60435

El, λ_{lab}, Å	HD 83368 λ_{obs}, Å	longitude, l_{sp}	Radius, R_{sp}	$\log N_{El}$, dex	HD 60435 λ_{obs}, Å	longitude, l_{sp}	latitude, φ_{sp}	Radius, R_{sp}	$\log N_{El}$ dex
	Phase = 0.689 (248.°04)				Phase = 0.743 (267.°48)				
Ce II	6705.5	$305 \pm 10°$	$30 \pm 10°$	-8.5 ± 0.3	6706.1	$230 \pm 10°$	$15 \pm 10°$	$15 \pm 10°$	-8.7 ± 0.3
6706.051	6706.1	$240 \pm 10°$	$10 \pm 10°$	-8.1 ± 0.3	6706.2	$180 \pm 10°$	$15 \pm 10°$	$40 \pm 10°$	-8.3 ± 0.3
Ce II	6707.6	$305 \pm 10°$	$26 \pm 10°$	-8.5 ± 0.3	6708.2	$230 \pm 10°$	$15 \pm 10°$	$15 \pm 10°$	-8.7 ± 0.3
6708.099	6708.0	$250 \pm 10°$	$15 \pm 10°$	-8.2 ± 0.3	6708.3	$180 \pm 10°$	$15 \pm 10°$	$40 \pm 10°$	-8.3 ± 0.3
Pr III	6706.1	$305 \pm 10°$	$15 \pm 10°$	-8.8 ± 0.3	6706.9	$170 \pm 10°$	$15 \pm 10°$	$40 \pm 10°$	-8.3 ± 0.3
6706.705	6706.8	$240 \pm 10°$	$30 \pm 10°$	-8.5 ± 0.3	6706.8	$270 \pm 10°$	$10 \pm 10°$	$40 \pm 10°$	-9.1 ± 0.3
	6707.3	$195 \pm 10°$	$15 \pm 10°$	-8.0 ± 0.3	6706.5	$330 \pm 10°$	$-5 \pm 10°$	$40 \pm 10°$	-8.3 ± 0.3
Sm II	6707.6	$235 \pm 10°$	$20 \pm 10°$	-8.2 ± 0.3	6707.6	$190 \pm 10°$	$10 \pm 10°$	$40 \pm 10°$	-7.3 ± 0.3
6707.473	6708.0	$207 \pm 10°$	$20 \pm 10°$	-7.8 ± 0.3	6707.5	$265 \pm 10°$	$10 \pm 10°$	$40 \pm 10°$	-7.5 ± 0.3
	Phase = 0.320 (115.°2)				Phase = 0.005 (1.°8)				
Pr III	6160.0	$145 \pm 10°$	$25 \pm 10°$	-8.0 ± 0.3	6160.2	$310 \pm 10°$	$0 \pm 10°$	$30 \pm 10°$	-8.3 ± 0.3
6160.243	6160.2	$120 \pm 10°$	$15 \pm 10°$	-8.0 ± 0.3	6160.3	$55 \pm 10°$	$0 \pm 10°$	$30 \pm 10°$	-8.3 ± 0.3
	6160.8	$65 \pm 10°$	$20 \pm 10°$	-8.3 ± 0.3					
	6160.9	$45 \pm 10°$	$20 \pm 10°$	-8.3 ± 0.3					
Pr III	6160.9	$145 \pm 10°$	$25 \pm 10°$	-8.0 ± 0.3	6161.2	$310 \pm 10°$	$0 \pm 10°$	$30 \pm 10°$	-8.3 ± 0.3
6161.224	6161.1	$120 \pm 10°$	$15 \pm 10°$	-8.0 ± 0.3	6161.3	$55 \pm 10°$	$0 \pm 10°$	$30 \pm 10°$	-8.3 ± 0.3
	6161.7	$65 \pm 10°$	$20 \pm 10°$	-8.3 ± 0.3					
	6161.8	$45 \pm 10°$	$20 \pm 10°$	-8.3 ± 0.3					

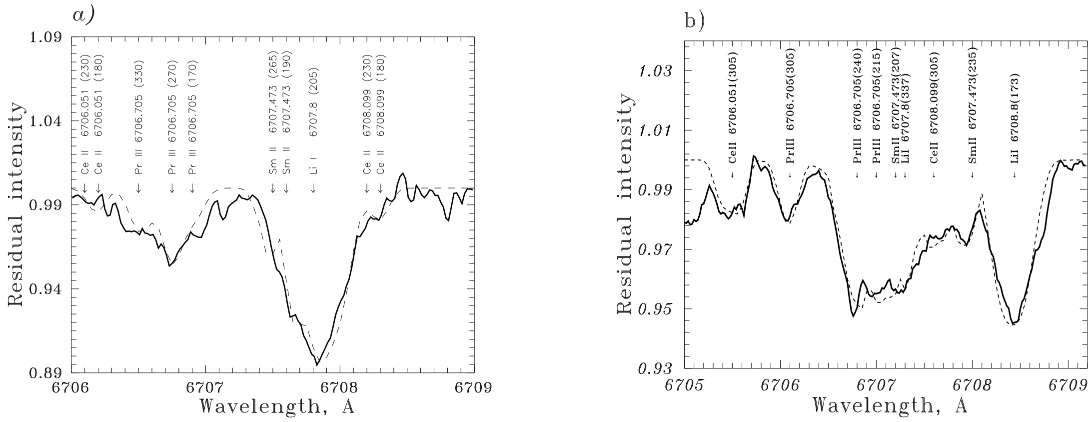

Figure 1: The calculated and observed spectrum a) for HD 60435, phase 0.743, and b) for the HD 83368, phase 0.689

Our results of location for some REE from their lines in the Li I 6708 Å region and from the Pr III lines 6160 Å and 6161 Å are given in Table 1. The calculated and observed spectra for selected phase of each star are shown in Fig. 1.

CONCLUSION

In HD 83368 the behaviour of the Li line profile and magnetic field shows that lithium spots approximately coincide with magnetic poles. Some of the other elements (mainly REE) may form the ring-like features surrounding the lithium spots. A similar structure is revealed for HD 60435.

Acknowledgements. We are grateful to S. Sergeev for SPE code for spectra analysis, to Ch. Cowley for numerous consultations and for sending us the rare earth element data, to M. Ya. Orlow for discussing our work, to D. Bord and J. Sugar for suggestions and advices to use their data. The data from Kurucz's CDROM 23, NASA ADC, VALD and NIST were used and we thank the administrators of these databases, accessible through INTERNET. A partial support of VEGA grant N 7107 is acknowledged. V. Tsymbal thanks Mr. Yakushechkin for his support. P. North thanks the Swiss National Science Foundation for its support. V. Khalack is grateful to the Ukrainian Astronomical Association for financial support.

REFERENCES

[1] *Polosukhina N. S., Shavrina A. V., et al.* Preliminary spectroscopic analysis of the "spotted" roAp star HD 83368 in the Li I 6708 Å region // Astron. and Astrophys.–2000.–**357**.–P. 920–930.

MAGNETIC FIELD MODELLING ON THE CP STARS

V. R. Khalack[1], Ju. N. Khalack[2], A. V. Shavrina[1], N. S. Polosukhina[3]

[1] *Main Astronomical Observatory, NAS of Ukraine*
27 Akademika Zabolotnoho, 03680 Kyiv, Ukraine
e-mail: khalack@mao.kiev.ua, shavrina@mao.kiev.ua

[2] *Physics Faculty, Taras Shevchenko National University, 03022 Kyiv, Ukraine*
e-mail: khalack@phys.univ.kiev.ua

[3] *Crimean Astrophysical Observatory, Naukove, 98409 Crimea, Ukraine*
e-mail: polo@crao.crimea.ua

The modulus and longitudinal component of the surface magnetic field of a star are constructed applying the model of artificially introduced magnetic charges with their superposed potentials that are spatially distributed in the stellar interior. In the dipole approximation the expression for the mean longitudinal magnetic field given by the proposed model is of the same form as obtained previously by another authors. Such straight-forward calculations of the magnetic field allow one to reconstruct most of possible magnetic field configurations on the stellar surface.

INTRODUCTION

A comprehensive study of chemically peculiar (CP) stars spectra and elements abundance analysis at their surfaces should take into account all the possible physical processes, which contribute to the spectral line broadening. For the magnetic CP stars one of these processes is a magnetic broadening due to the Zeeman or Pashen-Back effects. In order to estimate this contribution we have to know the structure of surface magnetic field at the CP stars.

Most of our knowledge about magnetic field structure at these stars is based on the measurements of *a mean longitudinal magnetic field* variation with rotation of the star. Many observational data were obtained recently by Mathys & Hubrig [4] as a result of observation campaign of magnetic CP stars.

The modelling of the magnetic structure of CP stars was initially based on the *oblique rotator model* with dipolar field that allowed to explain the sine character of mean longitudinal field variation with the phase of star rotation $\langle B_z\rangle(\varphi)$. But most of the observational data testify that there are some deviations from the sine form. To describe these observable deviations Hensberge *et al.* [2] propose *the decentered dipole model.* Recently, Landolfi *et al.* [3] developed a (non-axisymmetric) *multi-polar model* for explanation of the detected mean longitudinal field variations. But not all the observable features of $\langle B_z\rangle(\varphi)$ could be explained in the frame of the mentioned models.

From the other point of view Gerth *et al.* [1] proposed *the model of the spatially distributed point-like field sources* with *virtual magnetic charges.* Though the isolated magnetic charges have not been found in the nature, we, however, can artificially introduce such *a system of the point-like field sources* distributed throughout the volume **D** (see Fig. 1) somewhere in the *interior* of a stellar body for the best recovering the magnetic field structure at the star surface. Due to the disruption of magnetic field lines in the vicinity of such sources and the presence of some *whirls* inside the **D**-volume, the results of magnetic field modelling are valid only outside this volume, where $\mathbf{div}\,\vec{\mathbf{B}} = 0$ and $\mathbf{rot}\vec{\mathbf{H}} = 0$. In such a way for the surface magnetic field modelling the **D**-volume should be located in the stellar interior.

The superposition of potentials of artificially introduced virtual magnetic charges results in the scalar magnetic potential for any surface point **M** (see Fig. 1):

$$U = \sum_j \frac{Q_j}{|\vec{\mathbf{r}}_j|}, \qquad (1)$$

where Q_j is a virtual magnetic charge of the j-source and $|\vec{\mathbf{r}}_j|$ is a distance from this field source to the surface point [1]. In order to provide a zero magnetic flux trough the star surface ($\oint \vec{\mathbf{B}}\mathbf{d}\vec{\mathbf{S}} = 0$), the sum of virtual

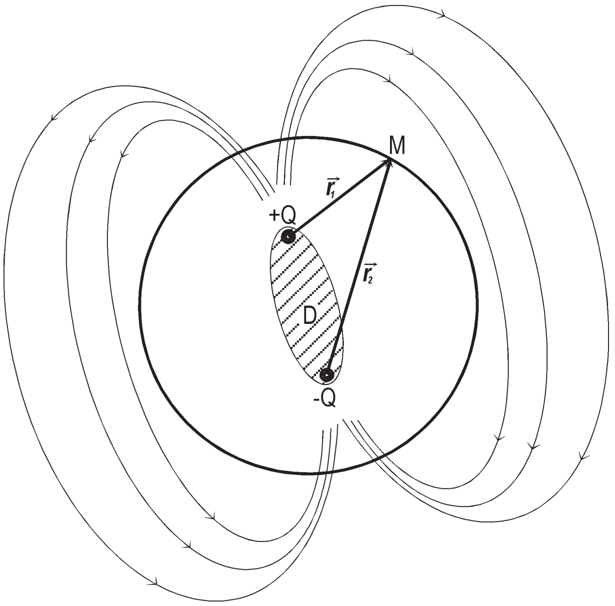

Figure 1: System of the point-like field sources artificially introduced inside the star for modelling the surface magnetic field structure

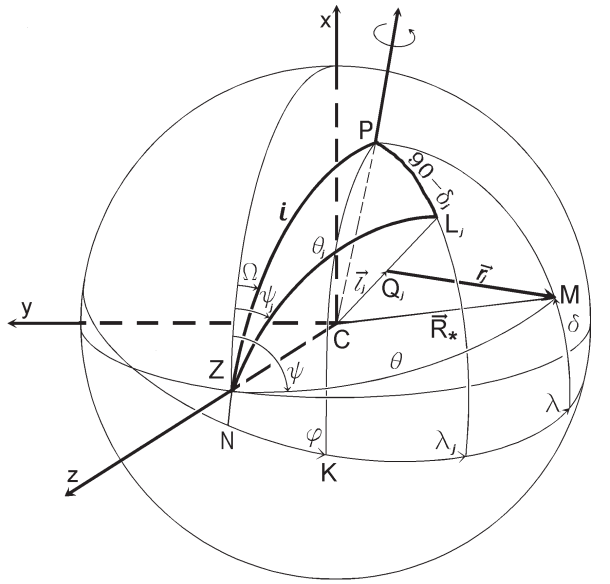

Figure 2: Geometry of the oblique rotator model with one probe point-like magnetic field source

magnetic charges should be kept

$$\sum_j Q_j = 0. \tag{2}$$

Then, the surface magnetic magnetic field vector is determined by the *gradient of potential*:

$$\vec{\mathbf{B}} = -\vec{\nabla} U = \sum_j \frac{Q_j}{|\vec{\mathbf{r}}_j|^3} \vec{\mathbf{r}}_j. \tag{3}$$

METHOD

Let us consider the geometry of oblique rotator model with one probe point-like field source Q_j with the help of three different coordinate frames (see Fig. 2). The first one is a *right-handed Cartesian frame* (x, y, z) with the origin in the centre of the star **C**, the z-axis is directed along the line of sight (pointing to the observer) which crosses star surface in the *subsolar point* **Z**, and the x-axis is in the direction of the *North celestial pole*. The second one is a spherical frame relative to the observer with coordinates (R, θ, ψ) connected with the Cartesian frame coordinates (x, y, z) by the following expressions:

$$\left\{ \begin{array}{ll} x = & R \sin\theta \cos\psi, \\ y = - & R \sin\theta \sin\psi, \\ z = & R \cos\theta. \end{array} \right. \tag{4}$$

In this frame the *positive rotation pole* **P** (the star rotates, by definition, in the counterclockwise direction as shown by the arrow) is specified by the inclination angle i and the azimuth angle Ω, measured from the central meridian in the clockwise direction (see Fig. 2).

The third coordinate frame is the spherical one relative to the star with the origin in its centre **C**. In this frame any surface $(R = R_\star)$ point **M** could be specified by latitude δ and longitude λ, measured from the *zero meridian* in the counterclockwise direction (see Fig. 2). As it follows from spherical triangle $\mathbf{ZPL}_1$ and taking into account the angles i and Ω the relation between these two spherical coordinate frames is specified by the following expressions:

$$\left\{ \begin{array}{l} \cos\theta = \sin\delta \cos i + \cos\delta \sin i \cos(\varphi + \lambda), \\ \sin\theta = \sqrt{1 - \cos^2\theta}; \end{array} \right. \tag{5}$$

$$
\begin{cases}
\cos(\psi-\Omega) = \dfrac{\sin\delta - \cos i \cos\theta}{\sin\theta \sin i}, \\
\\
\sin(\psi-\Omega) = \cos\delta \, \dfrac{\sin(\varphi+\lambda)}{\sin\theta},
\end{cases}
\tag{6}
$$

where φ is the angle between zero meridian and **PZ** meridian (see Fig. 2).

Let one the probe point-like field source be located at the point Q_j at the distance l_j from the centre. Vector $\vec{\mathbf{l}}_j$ crosses star surface in the point L_j, characterized by coordinates (θ_j, ψ_j) or (δ_j, λ_j). Distance between the source location Q_j and surface point **M** is $|\vec{\mathbf{r}}_j| = |\vec{\mathbf{R}}_\star - \vec{\mathbf{l}}_j|$. In spherical coordinates relative to the observer it reads (see Eq. (4)):

$$
|\vec{\mathbf{r}}_j| = R_\star \sqrt{1 + a_j^2 - 2a_j(\sin\theta \sin\theta_j \cos(\psi-\psi_j) + \cos\theta\cos\theta_j)},
\tag{7}
$$

where $a_j = l_j/R_\star$.

In such a way, for any surface point **M** the components of the magnetic field vector (see Eq. (3)) in the Cartesian frame (x, y, z) are given by the following expressions (see Eq. (4, 7)):

$$
\begin{cases}
B_x = R_\star \sum\limits_j \dfrac{Q_j}{|\vec{\mathbf{r}}_j|^3} (\sin\theta\cos\psi - a_j \sin\theta_j \cos\psi_j), \\
\\
B_y = - R_\star \sum\limits_j \dfrac{Q_j}{|\vec{\mathbf{r}}_j|^3} (\sin\theta\sin\psi - a_j \sin\theta_j \sin\psi_j), \\
\\
B_z = R_\star \sum\limits_j \dfrac{Q_j}{|\vec{\mathbf{r}}_j|^3} (\cos\theta - a_j \cos\theta_j).
\end{cases}
\tag{8}
$$

Assuming a *limb-darkening law* of the form $1 - u + u\cos\theta$ (where $0 \le u \le 1$), we average B_z over the visual stellar disk according to Landolfi *et al.* [3] and obtain expression for the observable mean longitudinal magnetic field:

$$
\langle B_z \rangle = \frac{3}{\pi(3-u)R_\star^2} \sum_j Q_j \int\limits_0^{2\pi} d\psi \int\limits_0^{\pi/2} \frac{\sin\theta\cos\theta(1-u+u\cos\theta)(\cos\theta - a_j\cos\theta_j)d\theta}{[1 + a_j^2 - 2a_j(\sin\theta\sin\theta_j\cos(\psi-\psi_j) + \cos\theta\cos\theta_j)]^{\frac{3}{2}}}.
\tag{9}
$$

Correspondingly, the *magnetic field modulus* averaged over the visual stellar disk is given by

$$
\langle |\vec{\mathbf{B}}| \rangle = \frac{3}{\pi(3-u)} \int\limits_0^{2\pi} d\psi \int\limits_0^{\pi/2} \sin\theta\cos\theta(1-u+u\cos\theta)\sqrt{B_x^2 + B_y^2 + B_x^2}\, d\theta.
\tag{10}
$$

The complete expression for $\langle |\vec{\mathbf{B}}| \rangle$ is too cumbersome, so it is not given here.

For the system of the two point-like field sources (magnetic dipole) the proposed model has 11 free parameters:

$$
\begin{cases}
Q, |\vec{\mathbf{R}}_\star|; \\
0 \le a_1, a_2 < 1; \\
0 \le u \le 1; \\
0^\circ \le i < 180^\circ; \\
0^\circ \le \lambda_1, \lambda_2, \Omega < 360^\circ; \\
-90^\circ \le \delta_1, \delta_2 \le 90^\circ,
\end{cases}
\tag{11}
$$

taking into account the Eq. (2). Two (Ω, i) of these parameters specify the orientation of star rotation axis relative to the observer, next two ones $(u, |\vec{\mathbf{R}}_\star|)$ determine the stellar characteristics and the rest seven parameters determine the virtual charges and the location of point-like sources in stellar interior. Varying these free model parameters we try to achieve the best agreement between the observed and simulated characteristics of a surface magnetic field.

SYMMETRIC DIPOLE APPROXIMATION

For the central magnetic dipole in the star with $u = 0.6$, $R_\star = 2R_\odot$ the following assumptions are valid:

$$a_1 = a_2 = a \ll 1,\ Q_1 = -Q_2 = Q,\ \delta_1 = -\delta_2 = \delta,\ (\lambda_1 = \lambda)\ \lambda_2 = 180^\circ + \lambda.$$

As indicated by Landolfi *et al.* [3], in the case of symmetric dipole the value of $< B_z >$ does not depend on the angle Ω. Therefore, without losing in generality, we can keep $\Omega = 0^\circ$ through the rest of calculations. Following to Hensberge *et al.* [2] we use the angle β ($\beta = 90^\circ - \delta$) between the magnetic dipole and rotational axes. The z-component of the magnetic field for the surface point $\mathbf{M}(\theta, \psi)$ is proportional to

$$B_z \sim \left\{ \frac{\cos\theta - aZ}{[1 + a^2 - 2a(A\sin\theta + Z\cos\theta)]^{\frac{3}{2}}} - \frac{\cos\theta + aZ}{[1 + a^2 + 2a(A\sin\theta + Z\cos\theta)]^{\frac{3}{2}}} \right\},$$

where $A = X\cos\psi + Y\sin\psi$ and

$$\left\{ \begin{array}{l} X = \cos\beta\sin i - \sin\beta\cos i\cos(\varphi + \lambda); \\ Y = \sin\beta\sin(\varphi + \lambda); \\ Z = \cos\beta\cos i + \sin\beta\sin i\cos(\varphi + \lambda). \end{array} \right. \tag{12}$$

Since the value of $a \ll 1$, we decompose expression for B_z into the series for small parameter a and obtain finally

$$B_z \sim 2a[Z(3\cos^2\theta - 1) + 3A\sin\theta\cos\theta],$$

that after averaging over the visible stellar disk (Eq. 9) results in

$$\langle B_z \rangle \sim \frac{15 + u}{20(3 - u)} Z. \tag{13}$$

The last expression is the same as given in the paper of Hensberge *et al.* [2] for mean longitudinal magnetic field in the case of central symmetric dipole. As it follows from Eq. (12) and Fig. 2, $Z = \cos\alpha$, where α is an angle between the dipole axis and line of sight. In such a way the case of central symmetric dipole is a special case of the model proposed here.

SUMMARY

Basing on the approach developed by Gerth *et al.* [1] we propose the modified method for surface magnetic field modelling. Due to the appropriate choice of orientation of the Cartesian and spherical coordinate frames we obtain the simple expression for the components of surface magnetic field vector $\vec{\mathbf{B}}$ (see Eq. (3)).

The proposed method involves the *point-like field sources* for modelling of the surface magnetic field structure on CP stars. In reality the point-like field sources have not been found. They are introduced into the model artificially as the auxiliary objects only for the best description of the observed characteristics of a surface magnetic field with the least number of model parameters.

In the dipole approximation the expression for $\langle B_z \rangle$ given by the proposed model is of the same form as obtained by Hensberge *et al.* [2].

In principle, any magnetic field configuration can be represented with the help of such artificially introduced *point-like field sources*, while the sum of their magnetic charges is zero. The advantage of this approach consists in arbitrary location of field sources in the interior of a stellar body. Its application is limited only by their number.

Acknowledgements. V. Khalack is grateful to the Ukrainian Astronomical Association for financial support and to Dr. S. Plachinda for consultation and useful advice.

REFERENCES

[1] *Gerth E., Glagolevskij Yu. V., Scholz G.* Integral representation of the stellar surface structure of the magnetic field // Contr. Astron. Obs. Skalnate Pleso.–1998.–**27**.–P. 455–457.

[2] *Hensberge H., van Rensbergen W., Goossens M., Deridder G.* On the orientation of magnetic and rotation axes in Ap stars // Astron. and Astrophys.–1977.–**61**.–P. 235–245.

[3] *Landolfi M., Bagnulo S., Landi Degl'Innoncenti E.* Modelling of magnetic fields of CP stars // Astron. and Astrophys.–1998.–**338**.–P. 111–121.

[4] *Mathys G., Hubrig S.* Spectropolarimetry of magnetic stars // Astron. and Astrophys. Suppl. Ser.–1997.–**124**.–P. 475–497.

LITHIUM ABUNDANCES IN ATMOSPHERES OF PMS STARS FN TAU AND V927 TAU

Yu. Lyubchik and Ya. Pavlenko

Main Astronomical Observatory, NAS of Ukraine
27 Akademika Zabolotnoho, 03680 Kyiv, Ukraine
e-mail: `lyu@mao.kiev.ua`, `yp@mao.kiev.ua`

We present the fits of synthetical spectra to the observed spectra of the young pre-main sequence stars V927 Tau (M5.5IV) and FN Tau (M5IV). The profiles of K line at $\lambda\,7699\,\text{Å}$, resonance and subordinate doublets of Li at $\lambda\,6708\,\text{Å}$ and $\lambda\,8126\,\text{Å}$ are simulated. The model atmospheres of Alard and Hauschildt (1995) are used to compute the spectra. Rotational velocities for FN Tau $v\sin i = 13\,\text{km/s}$ and $22\,\text{km/s}$ for V927 Tau are adopted. We determine $\log g = 4.0$ for V927 Tau and $\log g = 3.5$ for FN Tau for $T_{\text{eff}} = 3100\,\text{K}$, using the K line profile fits. For V927 Tau $\log N(Li) = 2.5$ for $\lambda\,6708\,\text{Å}$ and 2.7 for $\lambda\,8126\,\text{Å}$ region, and for FN Tau 3.0 and 3.3, respectively were obtained.

INTRODUCTION

Substantial progress has been achieved over the last few years due to observational and theoretical efforts devoted to studies of the lithium depletion in pre-main sequence (PMS) stars. Investigations of cool PMS stars [3, 4] give strong arguments that lithium has been effectively depleted during the early evolution of low-mass stars. But low-mass PMS stars are expected to preserve their initial lithium content during their first few million years of existence ([2], see also [3, 5]).

Here we present fits of synthetical spectra to the observed spectra of the two young PMS stars V927 Tau (M5.5 IV) and FN Tau (M5 IV).

PROCEDURE

The high resolution ($\lambda/\delta\lambda$=45000) observational data were obtained with Keck Telescope in 1994. For calculations of synthetical spectra we used the WITA6 program by Pavlenko [6]. Calculations were completed in classical approaches: LTE, hydrostatic equilibrium for one-dimensional model atmospheres, absence of energy sources and flowings. Equations of ionization-dissociation equilibrium were solved for the environment of atoms, ions and molecules. The molecular data used in these calculations were taken from [12]. The data on atomic lines were from VALD [8]. The calculations of molecular opacity were completed in JOLA and LBL approximations. For latter one we took the line-lists by Plez [9] and Shwenke [11]. We used the model atmospheres of Allard and Hauschildt [1] with $T_{\text{eff}} = 3000$–$3300\,\text{K}$, $\log g = 3.5$–5.0 and metallicity $\mu = 0$.

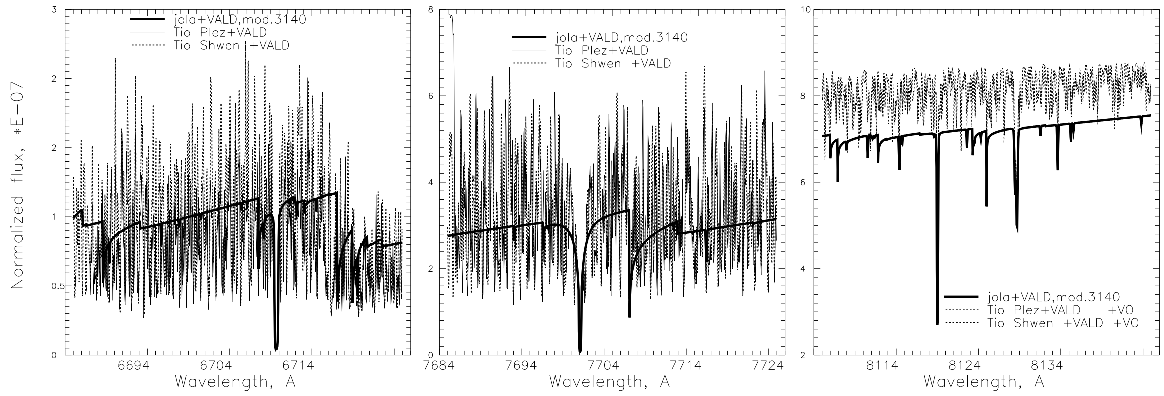

Figure 1: Theoretical spectra of M-dwarfs computed with different approximations of molecular opacity

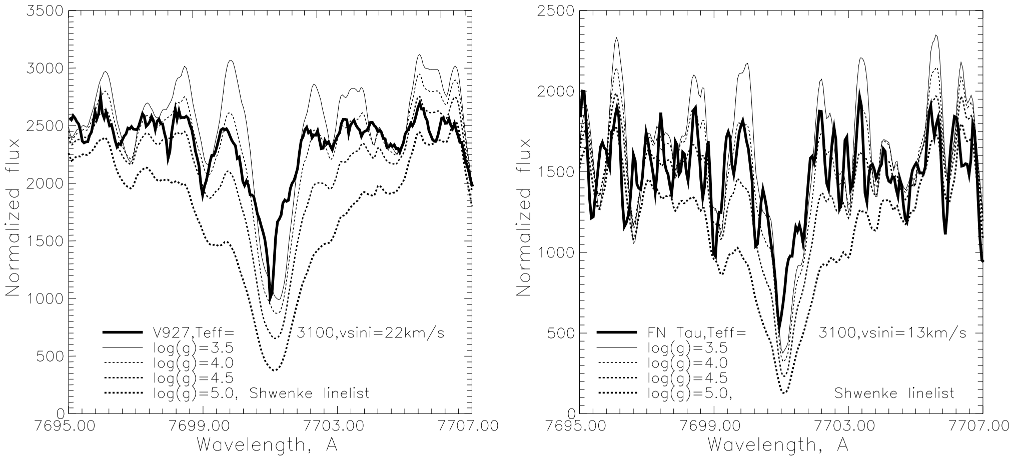

Figure 2: Fit of observed spectra to synthetical ones, computed with different $\log g$ for region centred at KI line λ=7699 Å

RESULTS

Spectra of late M stars is formed mainly by the molecular bands of TiO and VO, but there are number of strong atomic lines, which can be used in quantitative analysis. Here we consider the regions of Li λ 6708 Å and λ 8126 Å and KI λ 7699 Å.

In the frame of this work we examine two approaches of molecular opacity – JOLA (just overlap line approximation) and line-by-line, with two independently obtained line-lists of TiO by Plez [9] and Shwenke [11]. Comparison of the results shows rather good coincidence of these approaches in λ 6708 Å and λ 7699 Å regions and some lack of agreement in λ 8126 Å region (Fig. 1). To our mind the Shwenke's line-list of TiO is more full then Plez's one, and reproduce observational spectra more accurate. That's why in further calculations we use only this line-list of TiO.

For the region centred at the KI line, λ 7699 Å, we examine the flux dependence on temperature. It is proved to be rather weak. Also, for the KI line region for both stars we carried out the calculations of flux dependence on $\log g$. Synthetical spectra were computed for $\log g = 3.5$, 4.0, 4.5 and 5.0 for $T_{\rm eff}$ = 3100 K. It is worth to note that this dependence is rather strong, and it can be used to define $\log g$ in stars along with the well known gravity test based at the sodium subordinate doublet at $\lambda\lambda$ 8183, 8195 Å [10]. The best fit to observed spectra was obtained for the synthetical spectra with $\log g = 4.0$ for V927 Tau and $\log g = 3.5$ for FN Tau (Fig. 2).

Lithiun lines in spectra of V927 Tau and FN Tau are broadened by rotation. We assume the values of $v \sin i = 22$ and 13 km/s for V927 Tau and FN Tau, respectively [7]. For calculations of synthetical spectra we used 3100/4.0/0 model atmosphere for V927 Tau and 3100/3.5/0 for FN Tau.

For V927 Tau we obtained Li abundances – 2.5 for λ 6708 Å region, and $\log N(Li) = 2.7$ for λ 8126 Å (Fig. 3).

For FN Tau we determine $\log N(Li) = 3.0$ and 3.4 for λ 6708 Å and λ 8126 Å, respectively (Fig. 4).

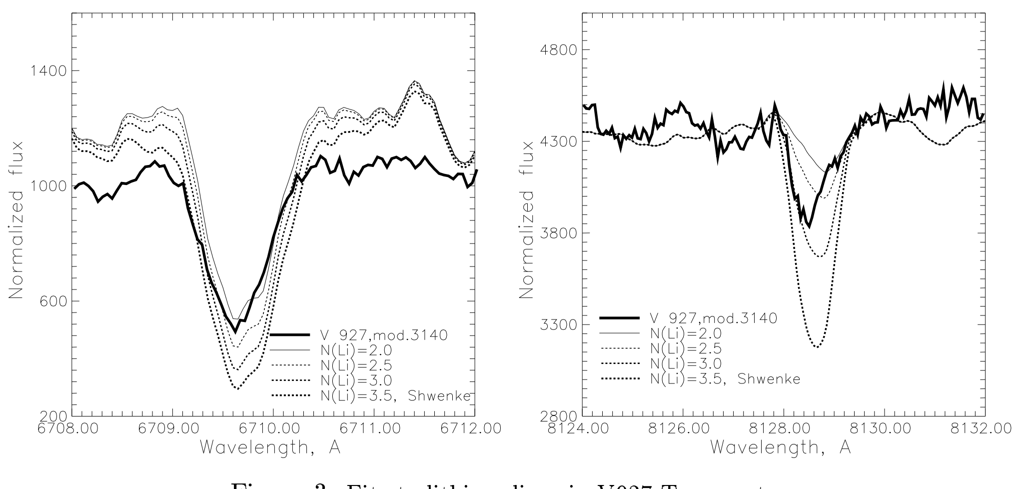

Figure 3: Fits to lithium lines in V927 Tau spectrum

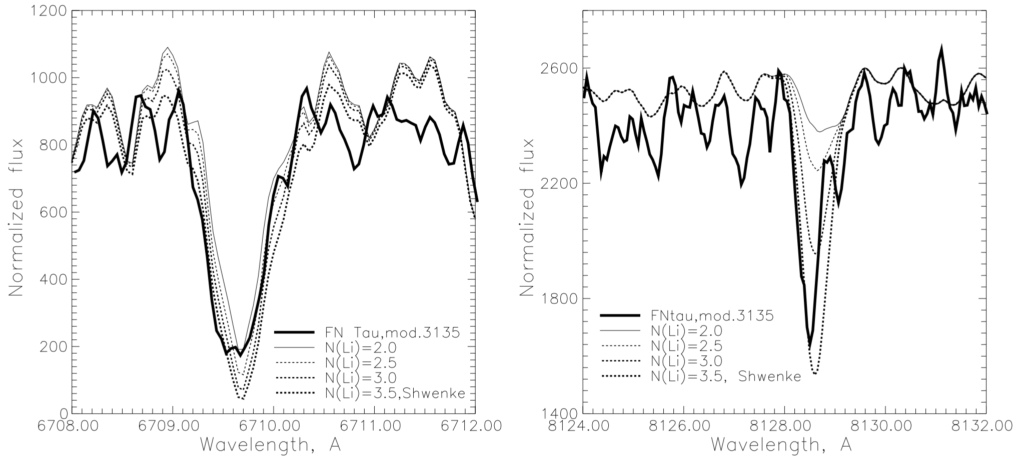

Figure 4: Fits to lithium lines in FN Tau spectrum

Thus, the main results of the work are following:
— two approximations of molecular opacity – JOLA and LBL are compatible;
— Shwenke's line-list of TiO is more accurate to reproduce the observational spectrum than Plez's one;
— synthetical spectrum dependence on $T_{\rm eff}$ is not strong for region centred at K line, λ=7699 Å;
— dependence of K line (λ=7699 Å) profile on $\log g$ is rather strong. Finally, we determine the $\log g = 4.0$ for V927 Tau and $\log g = 3.5$ for FN Tau;
— we determine the abundances of Li using two regions for V927 and FN Tau. They are for regions λ=6708 Å and λ=8126 Å, $\log N(Li) = 2.5$ and 2.7 for V927 and $\log N(Li) = 3.0$ and 3.4 for FN Tau, respectively.

REFERENCES

[1] *Allard F., Hauschildt P.* Model atmospheres for M (sub)dwarf stars. I. The base model grid // Astrophys. J.–1995.–**445**, N 1.–P. 433–450.

[2] *D'Antona F., Mazzitelli I.* Lithium depletion in stars. Pre-main sequence burning and extra-mixing // Astron. and Astrophys.–1984.–**138**, N 2.–P. 431–442.

[3] *Magazzu A., Rebolo R., Pavlenko Ya.* Lithium abundances in classical and weak T Tau stars // Astrophys. J.–1992.–**392**, N 1.–P. 159–171.

[4] *Martin E., Rebolo R., Magazzu A., Pavlenko Ya.* Pre-main sequence lithium burning. I. Weak T Tauri stars // Astron. and Astrophys.–1994.–**282**, N 2.–P. 503–517.

[5] *Oppenheimer B., Basri G., Nakadjima T., Kulkarni S.* Lithium in very low mass stars in the Pleiades // Astron. J.–1997.–**113**.–P. 296–305.

[6] *Pavlenko Ya. V.* Lithium lines in the spectra of M dwarfs: UX Tau C // Astron. Rep.–2000.–**44**, N 4.–P. 219–226.

[7] *Pavlenko Ya. V., Oppenheimer B.* Lithium abundances in the young PMS stars FN Tau and V927 Tau: an interplay of observations and theory // 10th Cambridge Workshop on Cool stars, stellar systems and the Sun / Eds R. A. Donahue, J. A. Bookbinder.–ASP Conf. Ser. 154, 1998.–P. 1764.

[8] *Piskunov N. E., Kupka F., Ryabchikova T. A., et al.* VALD: The Vienna atomic line data base // Astron. and Astrophys. Suppl. Ser.–1995.–**112**.–P. 525–534.

[9] *Plez B.* A new TiO line list // Astron. and Astrophys.–1998.–**337**.–P. 495–500.

[10] *Rebolo R., Martin E., Magazzu A.* Spectroscopy of a brown dwarf candidate in the α Per cluster // Astrophys. J. Lett.–1992.–**389**.–P. L83–L86.

[11] *Shwenke D.* Opacity of TiO from a coupled electronic state calculation parametrized by ab initio and experimental data // Faraday Discuss.–1998.–**109**.–P. 321–334.

[12] *Tsuji T.* Molecular abundances in stellar atmospheres. II // Astron. and Astrophys.–1973.–**23**.–P. 411–431.

THE ENERGY DISTRIBUTIONS IN SPECTRA OF 111 LATE TYPE STARS

V. Burnashev[1], S. Guziy[2]

[1] *Crimean Astrophysical Observatory, Ministry of Ukraine for Education and Science Naukove, 98409 Crimea, Ukraine*

[2] *Kalinenkov Astronomical Observatory of the Mykolaiv Pedagogical State University 24 Nikolska St., Mykolaiv, Ukraine*
e-mail: gss@aok.mk.ua

The energy distributions data in the spectra of 111 late-type stars have been obtained in the spectral range 320–790 nm with the resolution near 3 nm. The observations were completed by means of the stellar scanning spectrophotometer mounted on the 80-cm telescope at the Crimean Astrophysical Observatory. The absolute calibration is based on the energy distribution of Vega published by Hayes (1985).

In 1990–1996 the observations of stellar radiation were completed in the Crimean Astrophysical Observatory by means of the scanning spectrophotometer mounted on the 80-cm telescope in the spectral range 320–790 nm with the resolution near 3 nm (Burnashev *et al.*, 1996). The energy distribution in the spectrum of the BS 8585 star obtained by authors was used for the absolute calibration. The absolute calibration based on the energy distribution of Vega is published by Hayes (1985).

The stellar spectrophotometric catalogue contains of the energy distributions data of 111 stars. The list of BS and HD numbers of stars and number of observations for each star is given. The comparison of these data with the published ones was done (Kharitonov *et al.*, 1988; Glushneva *et al.*, 1982; Komarov *et al.*, 1995; Alekseeva *et al.*, 1997). The mean discrepancies not exceed 5% in the spectral range 400–700 nm, and are of about 10% at the edges of the observed spectral range.

Table 1: The list of catalogue stars (BS or HD numbers and the number of the observations)

BS	*BS*	*BS*	*BS/HD*	*BS*	*BS*	*BS*	*BS/HD*
163(6)	5602(10)	7314(6)	8252(8)	918(8)	6688(8)	7660(8)	8780(6)
253(4)	5635(6)	7328(8)	8308(8)	937(8)	6695(10)	7685(14)	8796(8)
265(8)	5681(10)	7462(10)	8313(8)	941(6)	6705(10)	7744(4)	8819(6)
294(8)	5823(8)	7479(10)	8317(6)	1101(8)	6853(8)	7770(4)	8832(12)
351(6)	5868(6)	7488(8)	8414(8)	1346(8)	6860(6)	7834(8)	8852(8)
402(4)	5889(6)	7503(6)	8426(10)	1409(4)	6895(6)	7897(6)	8878(6)
437(10)	5968(8)	7504(6)	8430(8)	1411(8)	6927(8)	7995(12)	8916(10)
464(12)	6132(8)	7525(8)	8498(10)	1907(8)	6945(10)	8079(6)	8930(10)
483(6)	6152(8)	7576(10)	8538(10)	2012(4)	7061(4)	8085(4)	8943(4)
617(8)	6200(6)	7582(6)	8551(8)	3905(6)	7125(10)	8086(6)	9008(4)
649(10)	6299(6)	7602(8)	8626(10)	4932(10)	7192(6)	8089(8)	9088(10)
774(6)	6536(6)	7606(14)	8632(8)	5102(4)	7218(6)	8173(8)	HD
799(8)	6574(6)	7615(10)	8667(8)	5464(10)	7300(6)	8228(6)	122563(12)
834(6)	6623(6)	7635(8)	8694(8)	5502(8)	7310(6)	8232(14)	151937(10)

REFERENCES

[1] *Alekseeva G. A., et al.* // Baltic Astron.–1997.–**6**.–P. 481.

[2] *Burnashev V. I., et al.* // Izv. Krim. Astrofiz. Obs.–1996.–**93**.–P. 157.

[3] *Glushneva I. N., et al.* Bright stars spectrophotometry.–Moscow: Nauka, 1982.–256 p.

[4] *Hayes D. S.* // IAU Symposium N 111.–1985.–P. 225.

[5] *Kharitonov A. V., et al.* The stellar spectrophotometric catalogue.–Alma-Ata: Nauka, 1988.–477 p.

[6] *Komarov N. S., et al.* // Odessa Astron. Publ.–1995.–**8**.–P. 3.

ABOUT THE HEAVY ELEMENTS ABUNDANCES IN SIRIUS A

V. F. Gopka

Astronomical Observatory, Odesa National University
T. G. Shevchenko Park, 65014 Odesa, Ukraine
e-mail: gopka@lens.tenet.odessa.ua

We have identified the absorption lines of Cu, Zn, Ga, Y, Zr, Nb, Mo, Cd, Sn, Hf, Ta, W, Re, Os, Hg, Pb, Th, U by comparing an atlas of the Sirius A spectrum with the synthetic one computed in the near-UV region (between 1649 Å an 3170 Å). The synthetic spectrum technique was used to determine the abundances of these elements in the Sirius A atmosphere. A summary table of the abundances of heavy elements is given. It is noted that abundances of gallium, tin, thorium, uranium were not studied early. The detected overabundances of heavy elements are in the range of 0.4–3.2 dex with respect to the meteoritic abundances.

The Am stars were first recognized as a group of peculiar stars of the main sequence by Titus & Morgan in 1940 [13]. They found that Ca K lines did not lead to the same classification as the hydrogen lines for some of the Hyades A stars. The abundances of CNO are generally below solar, while those of iron-peak elements are generally above solar, and the species in between can be either under- or overabundant [13]. The classical metallic-line A stars are characterized by a general enhancement of the metallic lines but a marked weakness of the lines of Ca and Sc when compared to normal A stars at the resolution of classification spectra. Heavy elements are systematically enhanced for most Am stars relative to the Sun. The best studied Am star is Sirius (HD 48915) – the brightest star in the sky. This star is a hot Am star. The Sirius is often used as a reference star in analysis of A-type stars. Parameters of atmosphere $T_{\rm eff}$ and $\log g$ are exceptionally well studied. Of all the fundamental stars, only Sirius and Procyon have truly fundamental values of both effective temperature and surface gravity. Chemical composition cannot be obtained in fundamental manner [12]. The present study is intended to determine the abundances of elements with atomic number $Z > 29$ in the atmosphere of Sirius A (Sirius B is white dwarf). The spectral lines of heavy elements are mainly populated the UV region of the spectrum. That is why the Copernicus Ultraviolet spectral Atlas of Sirius [7] was used as an observational spectrum. The Atlas covers the wavelength region from 1649 Å to 3170 Å, the spectral resolution is equal to 0.1 Å, and signal to noise ratio can reach 100.

Table 1: Lines of elements in the spectrum of Sirius and abundances of elements in the atmosphere of Sirius

Z	Ion	λ (Å)	$\log gf$	$\Delta \log N$	$* - \odot$	σ
29	Cu II	1989.855	-0.751	0.69	0.94	0.15
	Cu II	2037.127	-0.241	1.09		
	Cu II	2054.979	-0.177	1.04		
	Cu II	2104.796	-0.482	0.96		
30	Zn II	2099.937	-0.032	1.14	1.14	
31	Ga II	2090.771	-3.020	0.83	0.83	
39	Y II	2422.188	-0.200	0.93	0.92	
40	Zr II	2745.854	-0.270	0.77	0.91	0.14
	Zr II	3054.837	0.180	1.08		
	Zr II	3129.763	-0.650	0.76		
	Zr II	3138.683	-0.460	0.76		
	Zr II	3164.303	-0.180	0.87		
41	Nb II	2451.880	-0.280	1.51	0.49	
42	Mo II	2020.324	-0.900	1.94	2.08	0.13
	Mo II	2502.828	-1.090	2.25		
	Mo II	3152.813	-0.010	2.05		
48	Cd II	2265.018	-0.340	1.70	1.70	
50	Sn II	1899.898	-0.196	0.39	0.39	
72	Hf II	2496.993	-0.300	2.63	1.63	
73	Ta II	2400.637	1.650	2.87	1.87	
74	W II	2702.131	-0.230	2.89	2.89	
75	Re II	2504.563	1.000	2.02	2.25	
	Re II	2608.497	1.350	1.96		
76	Os II	2067.230	1.200	0.96	2.24	
	Os II	2580.024	1.620	1.16		
77	Ir II	2242.631	2.14	3.15 :	1.80	
80	Hg II	1942.313	-0.140	1.56	1.56	
82	Pb II	2203.534	-0.095	2.39	2.38	
90	Th II	2508.278	-0.020	3.08	3.20	0.11
	Th II	2774.066	-0.740	3.61		
	Th II	3019.422	-0.570	3.15		
	Th II	3080.217	0.238	3.11		
	Th II	3124.387	-0.406	3.32		
	Th II	3139.307	0.009	3.34		
92	U II	3111.618	-0.147	3.04	3.04	
	U II	3039.258	-0.260	3.04		

The abundance analysis is based on technique of synthetic spectra and comparison of synthetic spectrum with observed one. To study abundances in the atmosphere of Sirius we used the atmosphere model [4] with the following parameters: $T_{\rm eff} = 10000$ K, $\log g = 4.3$, $v_{\rm turb} = 2$ km/s. We calculated the synthetic spectra of Sirius in the wavelength region covered by observed spectrum using [14] program. The values of abundances of elements were adopted from previous investigations of this star. The abundances of the uninvestigated heavy elements were adopted as a function of atomic number. The values of this function varied from [A/H] = 1 for Z = 29 to [A/H] = 3 for Z = 92. We identified the lines of heavy elements. Abundances of selected elements were derived using URAN software for automatic spectrum synthesis [16]. We used SYNTHE code [4] for calculations of synthetic spectra in the region of line investigation. In each case the synthesis was performed taking into account all possible blending by atomic lines with measured wavelengths and oscillator strengths from [4] database (CD-ROMs 18, 23). Synthetic spectra were broadened by rotation and instrumental profile. The results are listed in Table 1. The designations in the table are following: the charge of nuclei (Z), identification of ion, wavelength, oscillator strength ($\log gf$), abundance in the scale $\log N(H) = 12.00$, mean relative abundances of the element in the Sirius atmosphere with respect to the solar system one [1] – $(* - \odot)$, σ – the square error of one measurement.

All elements we consider show overabundances with respect to the solar system values. It should be noted that measurable lanthanides lines are absent in UV region of the spectrum. Lines of these elements are quite weak or strongly blended in UV. Our data for abundances of heavy elements show a good agreement with other data from visual and UV regions of the spectrum [2, 3, 5], [9]–[12], [15]. The abundances of 19 elements are defined in this work. It is noted that abundances of gallium, tin, thorium, uranium were not studied early. Our results can be used for testing various theories on the nature of Am phenomena. For example, the diffusion theory developed by Richer & Michaud [6] for light elements ($Z < 28$). We should to note that the total abundance pattern for Sirius A is 50 elements. It is the third abundance pattern after Sun and Procyon.

REFERENCES

[1] *Anders E. and Grevesse* Abundances of the elements: Meteoritic and solar // Geochimica et Cosmochimica Acta Astrophys.–1989.–**53**, N 1.–P. 197–214.

[2] *Hill G. M.* Compositional differences among the A-type stars. // Astron. and Astrophys.–1995.–**294**, N 2.–P. 536–546.

[3] *Hill G. M. and Landstreet J. D.* Compositional differences among the A-type stars // Astron. and Astrophys.–1993.–**276**, N 1.–P. 142–160.

[4] *Kurucz R. L.* An atomic and molecular data // Astron. Soc. Pacif. Conf. Ser.–1995.–**81**, N 2.–P. 583–588.

[5] *Lemke M.* Abundance anomalies in main sequence A stars. // Astron. and Astrophys.–1990.–**240**, N 2.–P. 331–345.

[6] *Richer J. and Michaud G.* The evolution of AmFm stars, abundance anomalies, and turbulent transport // Astropys. J.–2000.–**529**, N 1.–P. 338–356.

[7] *Rogerson J. B.* COPERNICUS ultraviolet atlas of Sirius // Astrophys. J. Suppl. Ser.–1987.–**63**.–P. 369–455.

[8] *Sadakane K.* Abundances of heavy elements in Sirius // Publs Astron. Soc. Pacif.–1991.–**103**, N 662.–P. 355–358.

[9] *Sadakane K. and Jugaku J., et al.* Abundances of mercury in Sirius and Vega // Publs Astron. Soc. Pacif.–1988.–**100**.–P. 811–814.

[10] *Sadakane K. and Ueta M.* Abundance analysis of Sirius in blue-violet region // Publs Astron. Soc. Jap.–1989.–**41**, N 2.–P. 279–288.

[11] *Savanov I. S.* Abundance of atmosphere metallic-line star Sirius // Izv. KrAO –1987.–**76**.–P. 37–40.

[12] *Smolley B.* The determination of effective temperature and surface gravity for B to G stars // Astron. Soc. Pacif. Conf. Ser.–1996.–**108**.–P. 43–55.

[13] *Titus J., Morgan W. W.* On the classification of the A stars // Astrophys. J.–1940.–**92**.–P. 256–261.

[14] *Tsymbal V. V.* STARSP: a software system for the analysis of the spectra of normal stars // Astron. Soc. Pacif. Conf. Ser.–1996.–**108**.–P. 198–199.

[15] *Yushchenko A. V.* Abundances of heavy elements in Sirius // Odessa Astron. Publ.–1996.–**9**, N 1.–P. 84–85.

[16] *Yushchenko A. V.* URAN: a software system for the analysis of stellar spectra // Proc. 29th Conf. on Variable Star Research, Brno, Czech Republic, November 5–9, 1997 / Eds J. Dusek, M. Zeida.– Brno: Nicholas Copernicus Obs., 1998.–P. 202–204.

DUST AND MOLECULES ENVELOPE AROUND OF RW CYG

V. Kuz'kov

Main Astronomical Observatory, NAS of Ukraine
27 Akademika Zabolotnoho, 03680 Kyiv, Ukraine
e-mail: kuzkov@mao.kiev.ua

IR observations are important for selection dust and molecules in carbon stars. Near IR observations of RW Cyg were obtained by a small IR photometer. Observations were performed at the Peak Terskol Observatory (the Caucasus, H = 3100 m). IR observations confirm the existence of the large dust and molecules envelope with the maximum radiation at 10 micron. Comparison with radio emissions maps and far infrared survey was performed. IR excess may be caused by the C_2, CN, HCN molecules and emissions by the CO. Cooperative IR/mm waves observations will be useful for further study of this envelope.

INTRODUCTION

The RW Cyg star with the coordinates (1950) RA $= 20^h27^m01^s$, DEC $= 39°48'52''$ is situated near NGC 6913 stars formation. This is a variable star of the SR_c type with period near 586 days and amplitude $1\overset{m}{.}73$ B in range $10\overset{m}{.}65 \div 12\overset{m}{.}38$ B and with M3 Ia (M3-4 Ia-ab [1]) spectral class.

The B, V photometrical parameters for RW Cyg are following: V $= 8\overset{m}{.}4$, B $= 11\overset{m}{.}5$, Sp.M5, B − V $= 3\overset{m}{.}1$ [2]. For stars of M5I type the standard color is equal to $(B - V)_0 = 1\overset{m}{.}80$ and the resulting color excess is equal to $E_{B-V} = 1.3$. This excess can be explained by interstellar extinction in this direction or by dust and molecules envelope around of RW Cyg.

Study of the distribution of interstellar extinction in this direction performed in paper [3] has indicated the absence of extreme interstellar extinction in this direction. The data of viewing the nearest stars around of RW Cyg in according with catalogue [2] indicate also to this fact. Assuming that the absolute star magnitude of RW Cyg is $M_V = -7^m$, and in according with expression: $m - M = 5\log r - 5 + R\,E_{B-V}$ and $R = 3.0$ we get the result: $r = 1995$ nc. But absence of viewing stars in the nearest region around RW Cyg at distances larger 620 nc indicates that the distance to the RW Cyg is smaller and infrared excess is determined by proper dust and molecular envelope around this star.

The observations in IR bands [4] and IR spectroscopy of RW Cyg [1] confirm the existence of large envelope with extreme radiation at 10 microns. The mass loss estimated for RW Cyg is of about $5\times10^{-6}\ M_\odot$/year.

NEAR IR OBSERVATIONS RW CYG

The near infrared observations of RW Cyg were performed by a small IR photometer [5] on the Zeiss-600 telescope at the Peak Terskol Observatory (the Caucasus, H = 3100 m). The detector was cooled by liquid nitrogen. The aperture photometer was as 10 arcsec. A modulation of star-background-star was performed by amplitude 30 arcsec. The instrument photometry system in compare with the standard photometry system was described in [6]. It is similar to Johnson-Mendoza-Lee photometry systems. We used GAM Cyg as a standard star. The star has Sp.F8Ib and situates at of about 9 arcmin from RW Cyg. In this way we reduced the influence of extinction and color difference from standard photometry system. The results of observations compared with data of T. Lee are in Table 1.

Table 1: Near IR data of RW Cyg

I	J	H	K	J.D.	author
3.38	2.11	0.94	0.45	2440120	[7]
–	2.12	0.97	0.47	2446686	Kuz'kov
–	±0.02	±0.02	±0.05		

Absence of the observed variability of IR data indicates that the IR radiation of large envelope greater then proper variable IR emission of the star.

THE OBSERVED MOLECULES IN ENVELOPE OF RW CYG

The observation of silicon monoxide (SiO) in the envelope of RW Cyg was performed in the spectral region 3.98 – 4.07 microns, which includes the (2.0) and (3.1) rotation-vibration bands [8]. The observation has indicated the absorption at 4.00 and 4.05 microns. Comparison with synthetic spectra was performed too.

The measurements of the strength of the CO absorption band [2.35]–[2.2] Color index of RW Cyg were performed by Kenyon S. J. [9] using CVF infrared photometry. Color index [2.35]–[2.2] is measured as +0.50. The same observations of the CO absorption of RW Cyg were performed by using the two narrow band ($\Delta\lambda = 0.10\,\mu$m) filters centered at 2.17 and 2.4 microns [10].

THE FAR IR CHARACTERISTICS (IRAS)

The far infrared observations of RW Cyg were performed by IRAS too. Far infrared fluxes in Janskys are [11] as follows:

	$12\,\mu$m	$25\,\mu$m	$60\,\mu$m	$100\,\mu$m	V–K
1.	298.40	189.80	60.69	96.93	7.67
2.	298.14	202.44	53.82		

The interesting fact is that the far infrared flux at $100\,\mu$m is greater than at $60\,\mu$m. It can be explained by the additional emission of some molecules in far infrared band, for example, emission of OH at 3000 GHz. The characteristics of circumstellar shells at $60\,\mu$m derived by IRAS have indicated the absence of the extended envelope or this envelope has been not resolved by IRAS. But a peak intensity is estimated as 150×10^{-14} W m^{-2}. What is the source of this intensity?

The low resolution infrared spectrometer quantity f8 μm/f13 μm is equal to 1.40 and blackbody temperature is equal to 325 K.

THE RADIO MAPS AND IR/MM LINES

A comparison with the far infrared survey [12] and radio maps was performed. The FIR6 source exists near RW Cyg which is associated with 2.7 GHz radio continuum emission.

Comparison with the maps of various velocity ranges of the CO line has indicated that there are not a direct association with the CO molecular clouds.

Another IR and radio lines [13], for example, which can be observed in the envelope of RW Cyg are as follows:
C_2 transitions at 1.46 μm, and at 1.78 μm; CN transitions at 1.10 μm, and at 1.45 μm; CO_2 transition at 4.25 μm; HCN transition J=4-3 rot at 840 μm; H_2CO 5(1.5)–4(1.4) at 351.77 GHz (0.85 mm); HCN J(1-0) at 88.6 GHz (3.4 mm); H_2S 1_{10}-1_{01} at 169 GHz (1.8 mm); H_2S 2_{20}-2_{11} at 217 GHz (1.4 mm); H_2CO 3_{12}-3_{11} at 226 GHz (1.3 mm); HCN J(3-2) at 266 GHz (1.1 mm).

COOPERATIVE RADIO AND IR INVESTIGATIONS

Due to a close displacement of lines of various molecules in the IR band, it is difficult to perform the identification of these lines without observations in radio and optical bands. Future far infrared and mm/submm space telescope missions will be useful for the further investigation of these molecules.

There are some opportunities in performance of the onground observations. The optical mirror of the telescope is the ideal one in far IR and short mm wave bands, when the diffraction limit resolution is achieved simultaneously. The dichroic element would be a photolitography grate reflecting all waves larger 0.8 mm towards the second channel. The IR/visible waves pass across the dichroic element at the first channel. We could use infrared detectors in the first channel and radiometer mm detectors in the second one [14]. The cooperative synchronized observations in the short mm and IR bands will be performed in this way by using the ordinary optical telescope. The further IR/mm studies of the RW Cyg envelope will be useful too.

REFERENCES

[1] *Merrill K. M., Stain N. A., et al.* 2-14 micron Stellar Spectrophotometry // Publs Astron. Soc. Pacif.–1976.–**88**, N 2.–P. 285–293.

[2] *Voroshilov V. I., Guseva N. G., et al.* Catalogue B-V data and spectral classification of 18000 stars before 12^m.–Kiev, 1976.

[3] *Kalandadze N. B., Kolesnik L. N., et al.* Space distribution of stars and dust in the direction l=76°.9, b=+0°.6 // Astrometry and Astophys.–1977.–N 32.–P. 57–67.

[4] *Gehrz R. D., Woolf N. J., et al.* Mass Loss from M-stars // Astrophys. J.–1971.–**165**.–P. 285–294.

[5] *Kuz'kov V. P., et al.* J, H, K, L Photometer for Field Use // Kinematics and Physics of Celestial Bodies.–1989.–**5**, N 2.–P. 74–76.

[6] *Kuz'kov V. P., et al.* J, H, K photometry of CH star HD188650 // Kinematics and Physics of Celestial Bodies.–1997.–**13**, N 5.–P. 93–95.

[7] *Lee T. A., et al.* Photometry of High Luminosity M-type Stars // Astrophys. J.–1970.–**162**.–P. 217–238.

[8] *Rinsland C. P., Wing R. F., et al.* Observations of the First-Overtone Silicon Monoxide Bands in Late Type Stars // Astrophys. J.–1982.–**262**, N 1.–P. 201–212.

[9] *Kenyon S. J. and Gallagher J. S., et al.* Infrared Spectroscopy of Symbiotic Stars and nature of their cool components // Astron. J.–1983.–**88**, N 5.–P. 666–673.

[10] *Kenyon S. J., et al.* The Cool Components of Symbiotic Stars II. Infrared Photometry // Astron. J.–1988.–**96**, N 1.–P. 337–345.

[11] *Stencel R. E., Pesce J. E., et al.* Infrared circumstellar shells: origins and clues to the evolution of massive stars // Astron. J.–1989.–**97**, N. 4.–P. 1120–1138.

[12] *Campbell M. F., Hoffmann W. F., Thronson H. A., et al.* Far Infrared Survey of Cygnus X // Astrophys. J.–1980.–**238**.–P. 122–132.

[13] *Feston M. C., Rickman H., West R. M., et al.* Comets // ESO Scientific preprint.–1993.–N 960.

[14] *Kuz'kov V. P., Kudelja A. M., Larkin S. Yu., et al.* The rapid multichannel system for infrared and mm wave investigations // Proc. SPIE Intern. Conf, Kyiv, Ukraine, 1995.–**2648**.–P. 761–764.

TEMPORAL CHANGES OF SED'S OF SAKURAI'S OBJECT (V 4334 SGR)

Ya. Pavlenko and L. A. Yakovina

Main Astronomical Observatory, NAS of Ukraine
27 Akademika Zabolotnoho, 03680 Kyiv, Ukraine
e-mail: yp@mao.kiev.ua, yakovina@mao.kiev.ua

Results of the computation of spectral energy distributions (SED) in spectra of Sakurai's object (V4334 Sgr) are discussed. Hydrogen deficient and carbon-reach model atmospheres with $T_{\rm eff}$ 4000–6200 K and $\log g = 1.0 - 0.0$ are computed by the technique of opacity sampling taking into account molecular and atomic absorption for abundances determined by Asplund *et al.* (1997) and T. Kipper & Klochkova (1997). The computed SED's ($\lambda\lambda$ $300 - 1000$ nm) are fitted to the observed ones. Our conclusion is as follows: a) the theoretical SED's of Sakurai's object show a strong dependence on $T_{\rm eff}$; b) in the frame of our self-consistent approach we estimate $T_{\rm eff}$, $\log g$, $E_{\rm B-V}$ from the fit of computed SEDs to the observed spectra.

INTRODUCTION

Sakurai's object (SO, V4334 Sgr) was discovered on February 20, 1996 (Nakano *et al.*, 1996). The character of observable processes testifies that the SO is at a final stage of helium flare source (Duerbeck & Benetti, 1996). The abundances in SO atmosphere are peculiar. There are found a hydrogen deficit, C/O > 1 and low $^{12}C/^{13}C = 5$ (Asplund *et al.*, 1997; T. Kipper & Klochkova, 1997). The SO is increased in optical luminosity already from 1995. Then, in early 1998, abrupt declines of brightness at all colours have occurred. They are interpreted as onsets of dust formation, which are very similar to those observed in R CrB variables. We study the changes of SEDs of the SO to determine some atmosphere parameters of the SO from April 1997 to August 1998.

In our work we use the spectra of the SO, taken on April 29, 1997 (range 300–1000 nm) and August 12, 1998 (range 355–1000 nm). The spectra corrected by $E_{\rm B-V} = 0.7$ (for April 1997) and $E_{\rm B-V} = 1.3$ (for August 1998) were kindly provided by Dr. H. Duerbeck.

In August 1998 the SO spectrum was taken shortly before the onset of the $\approx 6^m$ decline, but at a time when V4334 Sgr was obviously already suffering by dust formation $\approx 1^m$ of visual dust obscuration.

PROCEDURE

Numerical computations are completed within the framework of classical approaches. Chemical abundances by Asplund *et al.* (1997) and T. Kipper & Klochkova (1997) are used. Absorption by atoms, ions and molecules is calculated. Opacity sampling model atmospheres and SEDs of the SO are computed by the SAM941 program and WITA6 (see Pavlenko *et al.* (2000) for more details).

Note that SEDs of the SO are computed also for the real isotopic ratio $^{12}C/^{13}C$. Molecular constants for isotopic species are calculated by Pavlenko's ISOTOPC program based on Graybeal (1988) formulae. We used $^{12}C/^{13}C = 5$ derived by Asplund *et al.* (1997).

RESULTS

Recently Pavlenko *et al.* (2000) shown that the overall shape of the SED of the SO is governed by the C_2 and CN band systems. In the near UV ($\lambda < 400$ nm) the atomic absorption becomes important. The best fit to the observed SED for April 1997 is obtained for an $T_{\rm eff} \sim 5500$ K and $\log g \sim 1$, but for August 1998 – for $T_{\rm eff} \sim 5250$ K and the $\log g = 0$ (Fig. 1).

SUMMARY

- From April 1997 to August 1998, $T_{\rm eff}$ of the SO had declined by only ≈ 250 K (from 5500 K to 5250 K). The interstellar reddening $E_{\rm B-V}$ was increased from 0.7 to 1.3.

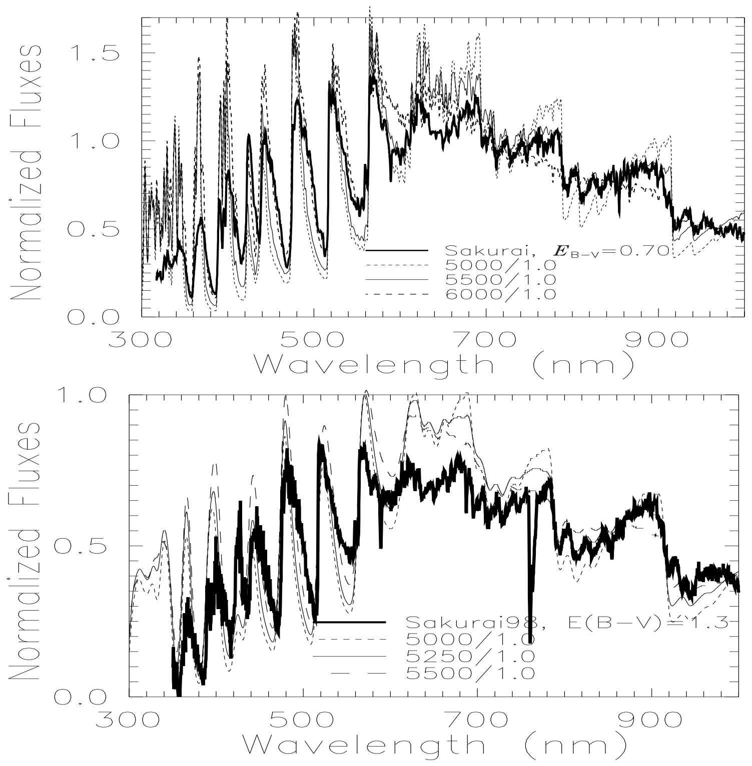

Figure 1: The best fits to the SO spectra in April 1997 (top) and August 1998 (bottom)

- The account of isotopic relation $^{12}C/^{13}C = 5$ does not change the calculated SED for our resolution 0.5 nm due to small shifts in wavelengths of the heads of the CN and C_2 isotopic bands.

Acknowledgements. We are grateful to Dr. Hilmar Duerbeck for the fruitful collaboration and providing the spectra of SO in digital form and Drs. T. Kipper and M. Asplund for helpful discussions. Partial financial support of the project was provided by the Small Research Grant of the American Astronomical Society.

REFERENCES

[1] *Asplund M., Gustafsson B., Lambert D. L., Rao N. K.* A stellar endgame - the born-again Sakurai's object // Astron. and Astrophys.–1997.–**321**.–P. L17–L20.

[2] *Duerbeck H. W., Benetti S.* Sakurai's object – a possible final helium flash in a planetary nebula nucleus // Astrophys. J.–1996.–**468**.–P. L111–L114.

[3] *Graybeal J. D.* Diatomic vibrotor states and selection rules // Molecular spectroscopy.–New York: McGraw-Hill Book Company, 1988.

[4] *Kipper T., Klochkova V.* The chemical composition of Sakurai's Object // Astron. and Astrophys.–1997.–**324**.–P. L65–L68.

[5] *Nakano S., Sakurai Y., et al.* // IAU Circ.–1996.–N 6322.

[6] *Pavlenko Ya. V., Yakovina L. A., Duerbeck H. W.* Modeling the spectrum of V4334 Sgr (Sakurai's object) // Astron. and Astrophys.–2000.–**354**.–P. 229–235.

Session 4. Interacting Binaries and Pulsating Variables

Convener: Prof. Ivan Andronov (ONU, Ukraine)

ASTEROSEISMOLOGY: A CHALLENGE FOR INTERNATIONAL COLLABORATION [1]

W. W. Weiss

Institute for Astronomy
University Vienna
Türkenschanzstrasse 17, A-1180 Wien, Austria
e-mail: weiss@astro.univie.ac.at

Asteroseismology is rather new diagnostic tool for investigating the interior and evolutionary status of stars. The potential for testing stellar models is already successfully demonstrated for our sun. Helioseismology, *e.g.*, allowed to investigate the rotation in the solar interior, the settling of helium, mixing and overshooting effects at the bottom of the convection zone, vertical extensions of active regions and to monitor them also on the hemisphere not visible from ground.
Of the various groups of pulsating stars, asteroseismology has been successfully applied to subdwarf B-type stars (sdB), pulsating white dwarfs (DA and DB), and to some extent also to rapidly oscillating Ap (roAp) stars. It has not yet been possible to model the observed pulsation frequency spectra of δ Scuti stars to satisfaction (*e.g.*, FG Vir), but experts expects a break-through in the near future, at the latest when observations from space will be available. γ Doradus and λ Bootis stars share this situation, and to some extent also β Cephei and the Slowly Pulsating B-type (SPB) stars. For the latest reviews in this field consult [1].
Two satellites, specialized for high precision photometry, will be launched in the next years, MOST in 2002 and COROT in 2004. A third one, the ESA mission EDDINGTON, has good chances for a launch around 2010, and the Danish project MONS is in a study phase.

POTENTIAL AND PROBLEMS OF ASTEROSEISMOLOGY

Many stars (*all* stars ?) pulsate with amplitudes ranging from about a magnitude to a thousandth of a magnitude or even less. Fig. 1 shows the Hertzsprung-Russell diagramme based on the HIPPARCOS observations plotted together with various classes of pulsating stars (ESA-SCI(2000)8).

Oscillations of stars are determined by their internal dynamics and structure. A precise determination of pulsation frequencies, therefore, allows to derive information about the interior of stars and the evolutionary status. This technique is called asteroseismology and its importance for modern astrophysics can be compared to that of X-ray techniques for medical or material sciences.

Asteroseismology can be defined as a method of testing stellar structure and evolution theory, using all available pulsation data, including also growth rates, phases, the fact that mode exists, and sometimes are transient, *etc.* [2]. In the present status of theory, a stellar model is typically characterized by five parameters (mass, age, initial compositions in helium and metals, and mixing length – a parameter describing the convective transport of energy) for which we usually have only two observables (effective temperature and surface gravity). Consequently, stellar models cannot be adequately tested without introducing additional assumptions. Moreover, we have some reasons not to trust our description of stellar interiors.

When open clusters or binary systems are observed for which independent constraints on some astrophysical parameters are available (same age and same initial composition for each star in the ensemble), it is usually impossible to reproduce the observed properties of the stars with the same value of the mixing length. This

Invited paper.
[1] Dedicated to Prof. Karl D. Rakosch, the pioneer of space astronomy in Austria, at his 75th birthday.

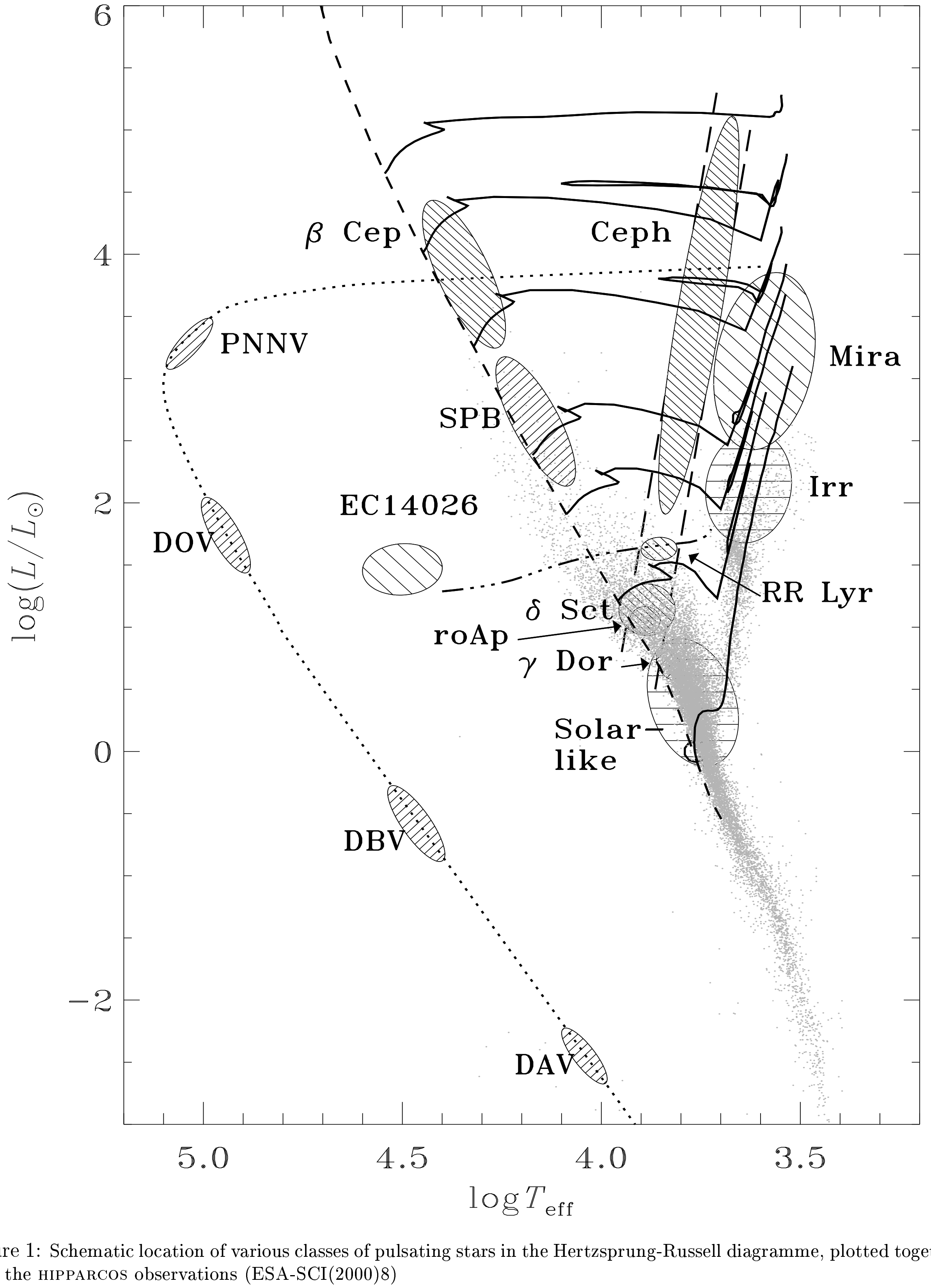

Figure 1: Schematic location of various classes of pulsating stars in the Hertzsprung-Russell diagramme, plotted together with the HIPPARCOS observations (ESA-SCI(2000)8)

confirms that the representation of convective transport by the mixing length theory is not adequate. This is only one example of many others which illustrate that an improvement of stellar modelling is clearly necessary. However, such an improvement is possible only if adequate tests for current models can be provided. Asteroseismology is this new tool for this purpose.

Pulsating stars have already been known since 1784, when δ Cephei was discovered as a variable star. It took nearly 200 more years to understand the reasons for this type of stellar variability. A more recent example for observations of a pulsating star, the λ Bootis star 29 Cyg, is presented in Fig. 2. The data were obtained during an international multisite campaign in 1997.

Eigenmodes of pulsations carry a wealth of information on the state of the interior of stars. A mode of a given degree ℓ and order (overtone) n is confined to a given cavity within the star. High degree modes are restricted to sub-surface layers, while low degree modes propagate all the way to the center of the star. Surface harmonics, $Y_{\ell,n,m}$, usually help to describe the oscillation modes, where the azimuthal order m is degenerate for a spherical symmetric star.

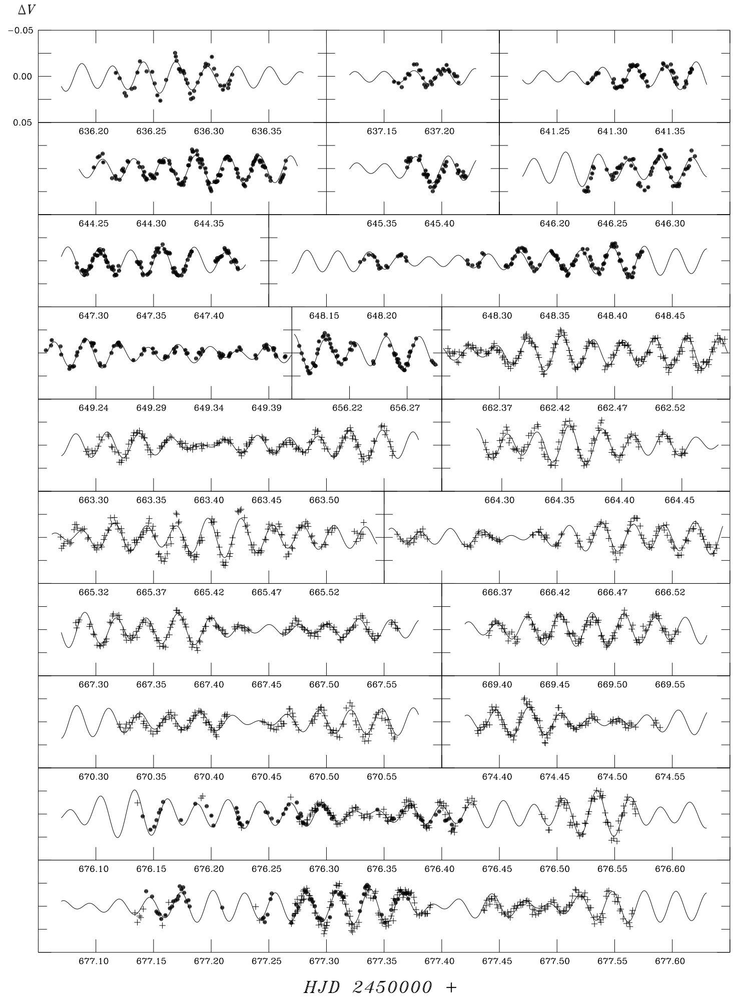

Figure 2: Photometric light curve for 29 Cyg obtained during a multisite campaign in 1997 with 5 observatories in America, Europe and Asia participating

So far, the method seems to be fairly simple. Given is a set of the observed frequencies and one has "only" to find a model which reproduces these frequencies within the errors. The limits of this approach are quickly evident, if evolved and rotating stars are investigated, as it is shown in Fig. 3 for the two λ Bootis stars HD 111786 and HD 142994 [3]. Obviously, it is impossible to identify ℓ, n and m clearly for the modes observed with the given frequencies. Without knowledge of these parameters an inversion is impossible and asteroseismic techniques cannot be directly applied.

Stellar rotation and evolution of stars are not the only ingredients which affect stellar models and hence the observable frequency spectra. Physical effects which render the application of asteroseismic techniques difficult, *e.g.*, are convection in the stellar envelope, core overshooting, hydrogen abundance, and heavy element abundances. An excellent review on this subject for δ Scuti stars is given in [4].

REQUIREMENTS FOR AN ASTEROSEISMIC ANALYSIS

Concluding the previous section, we identify the following problem. A direct mode identification is very difficult, because there are too many free parameters to fit relatively few frequencies. The following remark made by W. Dziembowski [5] sounds very pessimistic: *...without understanding mode selection we will never be able to make use of non radial mode frequencies for seismic probing...*

But what can be done to win the race against the odds? The asymptotic theory shows [6] that certain pattern can be expected in the frequency spectrum of a star which is pulsating in several modes, if $\ell \ll n$. Basically, one finds frequencies separated by the so-called "large separation", Δ, which for solar like stars typically ranges between 100 and 150 μHz, and the "small separation", δ, ranging from few to 20 μHz. Δ is inverse proportional to the sound travel time across a star and hence is sensitive to the global properties. δ, on the other hand, is proportional to the gradient of the sound speed weighted with the distance to the surface. Therefore, this quantity is sensitive to the interior of a star close to the core and hence also depends on the age. For our sun, data obtained from space by, *e.g.*, IPHIR or VIRGO, or from ground by BISON, IRIS or GONG, clearly show these periodicities (*e.g.*, [7]).

In conclusion, information about the structure of a star can be deduced from a pulsation frequency spectrum even without identifying individual modes, provided that characteristic frequency *pattern* can be determined.

In the case of a frequency identification close to the noise level, it can be helpful if the so-called combination modes can be identified in the frequency spectrum. These combination modes with frequencies $f = f_i \pm f_k$ are not observational artifacts but intrinsic to the star [8]. These modes, however, are expected at low frequencies what requires a very stable instrument for detection, and at high frequencies, requiring short integration times.

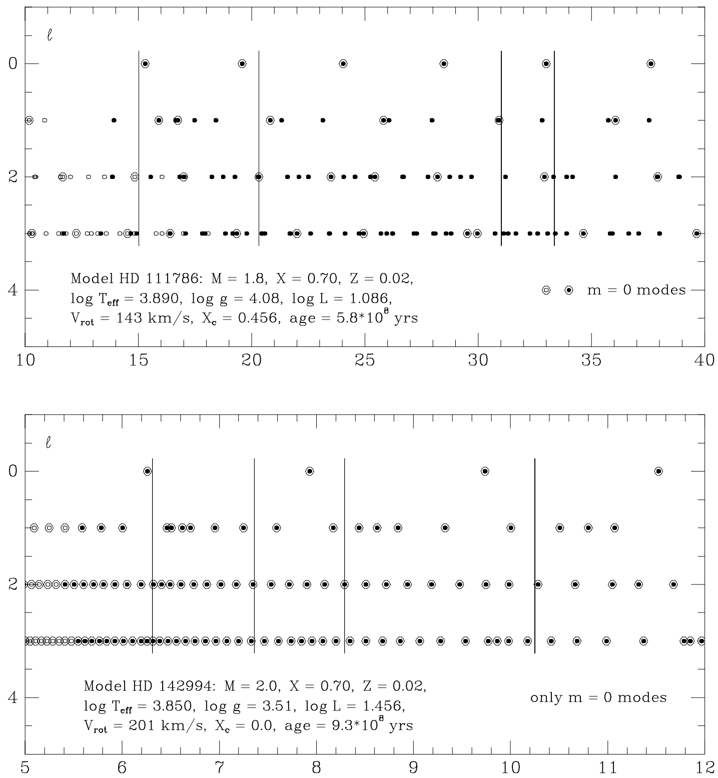

Figure 3: Computed frequency spectra of low-degree oscillations including frequency shifts due to rotation. Horizontal sets of points correspond to fixed values of spherical harmonic degree. Filled circles mark unstable modes. Vertical lines are the observed frequencies [3]

A further help for proper mode identification can come from multicolor photometry of pulsating stars. The amplitude and phases of light and color variations obtained with properly chosen filters can be related to luminosity and temperature variations due to pulsation. A phase lag between temperature and luminosity variation can be helpful for a mode identification.

Finally, if higher pulsation orders, ℓ, can be observed, different parts of the stellar interior can be analyzed and hence the choice of models can be restricted.

In conclusion, there are indeed some possibilities to apply asteroseismic techniques, even if a direct mode identification is not possible. The requirements for the needed observations are following:

- low noise of the pulsation frequency spectrum
- large frequency range
- high frequency resolution
- supplementary observations from ground, in particular spectroscopy
- restriction of the number of free parameters

what can be summarized in the popular saying: *The best possible may be barely sufficient.*

The low noise is important, because we want to detect a sufficient number of frequencies for deriving the characteristic frequency spacings. As the amplitudes tend to decrease outside a characteristic frequency range, the detection threshold has to be quite low in order to identify these additional frequencies in the noise.

Asteroseismic information is buried in a large frequency range, if also combination modes are considered. To obtain reliable data in such a large range requires an extremely stable instrument in an excellent observing site. This is a rather rare combination.

For identifying frequency splitting due to, *e.g.*, rotation or a magnetic field, a high frequency resolution is needed, which means long and uninterrupted observations. Large gaps in the data result in a poor "window" function which increases the noise level and ambiguity in the identification of correct frequencies.

Whereas photometry is sensitive to low order modes, because we integrate over the visible stellar hemisphere, spectroscopy allows to observe higher orders. Due to the Doppler effect the various velocity fields on the stellar surface appear as wavelength shifts in spectral line profiles. Hence, spectroscopy is a very important complement to photometry of pulsating stars.

We have already mentioned earlier that presently stellar models typically are characterized by mass M, age t, initial compositions in helium Y and metals Z, and α – a parameter describing the convective transport of energy. To determine these quantities we usually have only observables which have to be extracted from spectroscopic and photometric observations of the stellar atmosphere, like temperature T, metallicity Z, and surface gravity g, and also the parallax p for nearby stars. Consequently, stellar models in general cannot be adequately tested and additional information is needed, like that obtained from pulsation frequency spectra of oscillating stars, which carry information about the internal physical conditions of stars.

Asteroseismology of members of star clusters or multiple stellar systems has the advantage of similar parameter values for all the pulsating stars in the ensemble, like age, metallicity or the MLT parameter α. Unfortunately, suitable clusters are already quite faint for the telescopes available for typical ground based multisite campaigns of many weeks.

TOWARDS NEEDED DATA

The observational requirements needed for a determination of a rich pulsation frequency spectrum have been listed in the previous section. How to obtain these data?

The photometric noise can be reduced by increasing the number of registered photones (more observations, larger telescopes), whereas the scintillation noise can be reduced by using large telescopes (4-m class and larger). A total elimination is only possible by going to space. Another annoying noise source are large gaps in the data. A poor window function increases the noise level in frequency space and due to the aliasing problem it increases the danger of misidentification of intrinsic frequencies.

To obtain reliable data in a large frequency range requires extremely stable instrumentation, access to observing sites with a very homogeneous atmosphere – or to go to space.

A high frequency resolution can only be achieved with a long time base of the observations. There are two strategies possible. Either to organize international observing campaigns with participation of observatories distributed over all continents, or to obtain the data from a spacecraft with an appropriate orbit. Both strategies are followed at our institute. The δ Scuti network (M. Breger *et al.*) also in combination with WET (Whole Earth Telescope: D. Winget *et al.*) or CAN (Central Asian Network: D. Mkrtichian *et al.*) provided already excellent data sets. The other strategy is to participate in the development of space experiments dedicated to high precision photometry, where the author is involved in COROT, MOST and EDDINGTON. In any case, a substantial international collaboration is needed for networks as well as for space experiments.

At this point it should be mentioned that probably no pure asteroseismic space mission would have been funded, if not the search for terrestrial planets circling around stars other than our sun would not have had similar technical requirements: a continuous high precision photometric monitoring of stars over many months and up to few years.

In the following we briefly will describe the mentioned space experiments.

COROT: COROT stands for *CO*nvection, *RO*tation and *T*ransits. This mission currently is in phase C/D and is a project of the French space agency, CNES, with bilateral cooperation of Austria, Belgium, ESA, Italy, and Spain. It will realize both a first exploratory step, to detect oscillations in a large variety of stars to classify the asteroseismic properties of stars in the HR-diagramme and a more specific one, centered on a detailed study of a few objects, specially chosen to test the hydrodynamics of the internal layers and the physical state of the stellar cores.

An exploratory programme will determine the domain of stellar parameters for which oscillations are detectable, and will investigate the relation between the amplitudes of the solar-like oscillators and their astrophysical parameters. Though several theoretical predictions of the amplitudes of oscillations excited stochastically by convective motions exist, a large uncertainty remains, in particular on the treatment of the superadiabatic external layers and on the scaling of the turbulent velocity field.

To match the scientific goal of COROTs exploratory programme one has to observe a sample of objects with a variety of stellar parameters, *i.e.*, mass, age, chemical composition, state of rotation, *etc.*, but only a moderate signal to noise ratio is needed. A substantial ground based support programme has been developed to provide information on most of these parameters for the target star candidates, primarily based on spectroscopic observations. A frequency resolution of $0.5\,\mu$Hz is sufficient for the exploratory programme, corresponding to observing runs of 10 to 20 days. Stars down to the 9th magnitude are appropriate targets; 5 to 10 targets will be observable at the same time. Several tens of stars will have to be checked, corresponding to a total observing time within the exploratory programme of at least 2 to 4 months. Up to now COROT is the only project which is able to observe several (ten) stars simultaneously in its seismologic mode.

The so-called Central Programme is more ambitious and more time consuming than the exploratory one, it corresponds to the second step in the development of space asteroseismology and aims at observing very precisely a small set of objects, selected for their diagnostic power. The choice of these targets will be partly based on the results of the exploratory phase. Based on the solar case, the accuracy of the frequency measurement is chosen to be $0.1\,\mu$Hz to have access to mode profiles and rotational splitting and to measure precisely the distribution of the mode frequencies. For a 6th magnitude star, the detection threshold will be less than 1 ppm. For A and F type stars close to the main sequence, it will then be possible to measure the size of the convective cores, the size of the outer convective zones and their helium content or the rotation profile of δ Scuti stars.

A least 5 runs, each about 150 days long are planned, during which one bright star (the main target) and a few stars in the surrounding field of view will be followed.

The Institute for Astronomy is participating in the development of a flight hardware thanks to a substantial research grant of the Bundesministerium für Unterricht, Wissenschaft und Kultur (BMUWK). This grant covers only the expenses for our hardware contribution and the scientific activities have to be funded through the Fonds zur Förderung der wissenschaftlichen Forschung (FWF).

COROT is scheduled for launch in the year 2004.

MOST: MOST (*M*icrovariability & *O*scillations of *ST*ars) is a Canadian project currently in phase C/D and with a possible Austrian participation. The scientific aim is to perform seismology of sun-like and magnetic stars from space, as well as to study microvariability in Wolf-Rayet winds and other pulsating targets. The main scientific goals of MOST are, therefore, similar to COROT.

A 15-cm Maksutov telescope is mounted on a micro satellite bus only 50 kg in mass and with dimensions of about 60×60×24 cm. The microsat will be launched into a polar sun-synchronous orbit ≈ 800 km high, as a secondary payload (possibly aboard a Delta rocket with Radarsat II). From that vantage point, MOST will be able to monitor certain stars in Continuous Viewing Zones for up to 7 weeks without interruption. The satellite will be stabilized by a set of miniature reaction wheels which will point the telescope to an accuracy of about 10 arcsec. This sounds like poor tracking, but until now, any microsat of comparable size could only be stabilized to within 2 – 3 degrees! The current design is expected to reach photometric precision of better than a few micro mag in stars as faint as V = 6 in about ten days of observation. Launch is expected for 2002. It is very pleasing to mention here that a former student of our institute, Dr. Rainer Kuschnig, serves as the instrument scientist for MOST.

EDDINGTON: This is an ESA F-type mission which will be developed parallel to the NGST (New Generation Space Telescope) project and was selected in October 2000. The EDDINGTON mission has two primary goals (ESA-SCI(2000)8), similar to COROT and MOST, to provide data on the evolution and age of stars using asteroseismic techniques, and to find habitable planets outside of our solar system using the transit method.

The lifetime of EDDINGTON will be divided into two phases, one dedicated mainly to asteroseismology (the first 2 yrs of the mission) and the other mainly to planetary transit detection (the following 3 yrs of the mission). Each of the two primary science goals will, however, continue throughout the whole mission's lifetime, although they will have a lower priority when the other science is "prime".

Thanks to its large field of view, EDDINGTON will acquire data simultaneously on a large number of targets: asteroseismic data will be collected on some 50 000 stars, while planetary transits will be searched for on some 700 000 stars. Also, its larger collecting area will allow it to observe crucial stages of stellar evolution which are not available among the bright stars in the sky. These facts will allow EDDINGTON to achieve qualitatively different science goals than the small national projects (COROT, MONS, MOST) which are currently under development and which can be considered at some level as its precursors.

In addition, to the two primary science goals, the EDDINGTON data will allow several other scientific programs to be carried out, both in the field of stellar physics as well as in the field of galactic dynamics and evolution.

EDDINGTON features a simple, single payload: a lightweight, wide field-of-view 1.2-m diameter optical telescope, with twin mosaic CCD cameras (Fig. 4). The key requirement imposed on the mission by the observing program is one of long, uninterrupted observations, thus favouring deep orbits – L2 being currently the one base.

The launch date is expected between 2007 to 2013, depending on the development of the ESA Science programme.

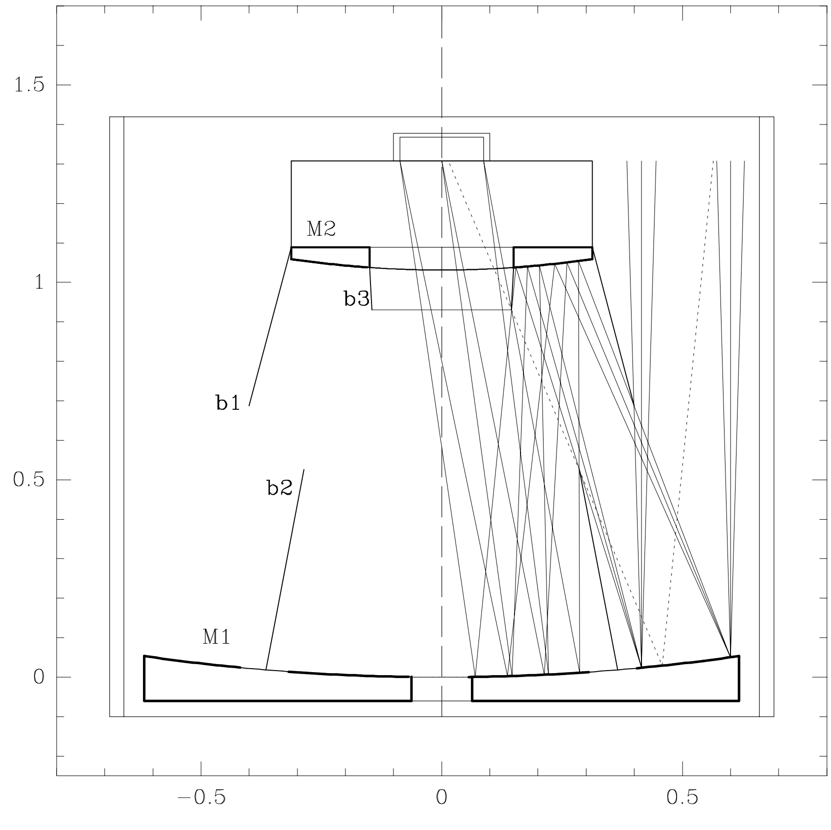

Figure 4: Optical scheme of the EDDINGTON three mirror system

MONS: MONS was selected in August 1998 to undergo a pre-Phase A study under the Danish Small Satellite Programme (DSSP). A proposal was submitted on April 1, 1999, and currently it is studied in a merged version with BALERINA, a mission dedicated to observe γ-ray bursters.

MONS will measure oscillations in about 25 nearby stars by monitoring the brightness and color fluctuations in each star for about one month. The spacecraft has overall dimensions of $60\times60\times80$ cm, a mass of 65 kg, and a power budget of 60 W. The orbit is elliptical with a high apogee, to allow (i) almost continuous observations of each star, and (ii) access to the whole sky during the course of a year. The baseline is a Molniya orbit, with a high inclination that will minimize radiation exposure, with a mission lifetime of two years.

The attitude control system will be 3-axis stabilized, with a required precision of about 0.02 degree rms (1.2 arcmin). This will be achieved using momentum wheels, with attitude sensing via two wide-field star imagers. The star imagers will also serve as secondary scientific instruments, providing photometry for about 10 000 stars over the mission.

The telescope is a 34-cm reflector, with a dichroic beamsplitter to form side-by-side blue and red stellar images. Each stellar image is highly defocussed to avoid saturating the CCD detector and minimize sensitivity to attitude movements.

Data frames will be taken every 4 seconds and on-board data processing will measure the brightness of stars every 20 seconds. The down-link rate, including house keeping, will be below 4 Mbyte per day.

Acknowledgements. Participation in the development of the space projects mentioned is funded mainly by the Austrian *Fonds zur Förderung der wissenschaftlichen Forschung* (S-7303-AST) and the *Bundesministerium für Unterricht, Wissenschaft und Kultur.*

REFERENCES

[1] *Breger M., Montgomery M. H.* δ Scuti and related stars // ASP Conf. Ser.–**210**.

[2] *Däppen W., Dziembowski W., Sienkiewicz R.* // Advances in Helio- and Asteroseismology: IAU Symp.–**123**.–P. 233.

[3] *Paunzen E., Weiss W. W., Martinez P., et al.* Pulsation of the λ Bootis stars HD 111786 and HD 142994 // Astron. and Astrophys.–1998.–**330**.–P. 605.

[4] *Pamyatnykh A.* Pulsational Instability Domain of δ Scuti Variables // ASP Conf. Ser.–2000.–**210**.–P. 215.

[5] *Dziembowski W.* Sounding Stellar Interiors // IAU Symp. 181.–Dordrecht: Kluwer Acad. Publ., 1998.–P. 317.

[6] *Tassoul M.* Asymptotic approximations for stellar nonradial pulsations // Astrophys. J. Suppl. Ser.–1980.–**43**.–P. 469.

[7] *Appourchaux T., et al.* VIRGO-The solar monitor experiment on SOHO // Astron. Soc. Pacif. Conf. Ser.–1995.–**76**.–P. 408.

[8] *Breger M.* δ Scuti Stars (Review) // ASP Conf. Ser.–2000.–**210**.–P. 3.

UKRAINE IN INTERNATIONAL ASTEROSEISMIC PROJECTS

D. E. Mkrtichian[1], **A. V. Kusakin**[2], **A. P. Hatzes**[3], **A. Kanaan**[4], **V. E. Panchuk**[5], **W. W. Weiss**[6], **E. Paunzen**[6], **V. Koval**[1], **A. Gamarova**[1], **E. B. Janiashvili**[7]

[1] *Astronomical Observatory of Odesa National University, T. Shevchenko Park, 27014 Odesa, Ukraine*
e-mail: davidm@te.net.ua

[2] *Sternberg State Astronomical Institute, Universitetsky prospect, 13, Moscow, 119899, Russia*

[3] *Thüringer Landessternwarte Tautenburg, D-07778 Tautenburg, Germany*

[4] *Departamento de Física, Universidade Federal de Santa Caterina, Campus Universitário 88040-900, Florianópolis, Brazil**

[5] *Special Astrophysical Observatory, Russian Academy of Sciencies, Nijnij Arkhuz, Russia*

[6] *Institut für Astronomie der Universität Wien, Türkenschanzstr. 17, A-1180 Wien, Austria*

[7] *Abastumani Astrophysical Observatory, Mt. Kanobili, Abastumani, Georgia*

This brief summarizes the results of international asteroseismic projects with Ukrainian participation on pulsating λ Bootis, rapidly-oscillating Ap stars, and pulsating components of eclipsing binaries.

INTRODUCTION

Application of seismic techniques to A–F spectral type pulsating stars is possible if the dense spectrum of opacity driven acoustic and gravity modes can be detected and their spatial structure (which is determined by the ℓ, m, n quantum numbers of spherical harmonics) be identified, as was done for the majority of convection driven modes in the Sun. The detection and identification of excited modes in pulsating stars require high-quality, continuous photometric and spectroscopic data obtained from space or from the ground, of which the latter requires the organization of international world-wide asteroseismic campaigns from observatories at good weather sites distributed uniformly in geographic longitudes. In 1994 Ukraine started an active participation in such projects.

THE CENTRAL ASIAN NETWORK COLLABORATION

In 1994 the newly created Central Asian Network (CAN) collaboration of astronomers (Mkrtichian *et al.*, 1998a) informally began activity among scattered groups of the former SU astronomers within the framework of asteroseismic campaigns and networked observations of variable stars. The coordinated rapid-response (Euro)Asian network includes astronomers from the Astronomical Observatory of Odesa National University (Ukraine), Sternberg State Astronomical Institute (Russia), Tien-Shan Astronomical Observatory (Kazakhstan), Mt. Dushak-Erekdag Observatory (Turkmenistan) and Abastumani Astrophysical Observatory (Georgia). They effectively cover the Central Asian gap in distribution of observatories over the northern hemisphere. The main objectives of CAN are deep investigations of the spectra of oscillating stars and the development of approaches for understanding their internal structure and evolution. These objectives are approached by carrying out continuous multi-longitude, global asteroseismic photometric and spectral observations on target stars. The first worldwide campaigns organized by Central Asian Network collaboration showed highly effective collaboration between the Eastern and Western European, Asian, North America institutions, and other international groups (see Weiss *et al.*, 1998; Mkrtichian *et al.*, 1998b).

ASTEROSEISMOLOGY OF λ BOOTIS STAR 29 CYG

The 29 Cyg is the first among λ Boo-type stars in which the well defined pulsations were detected and studied (Gies & Percy, 1977; Kusakin & Mkrtichian, 1996). 29 Cyg was selected as a key object to investigate the pulsational characteristics of λ Boo–type stars. The 1996, 1997 and 1998 global multisite campaigns were initiated by CAN in a wide international collaboration of institutes from Austria, Canada, Hungary, Mexico,

*CNPq Fellow.

Russia, Spain, Turkey, Ukraine, and USA. As a result, CAN's strategy led to significant progress in the detection and study of the seismic spectra of λ Boo stars. The first results on this project, which are based mainly on results of the 1996 campaign, can be summarized as follows:

- We established a multiperiodicity in 29 Cyg and determined frequencies and amplitudes for 10 high-amplitude (A> 1 mmag) modes. These are related to consecutive $2, 3, 4$ and 5 overtone low-degree ℓ modes (see Fig. 1).
- We found in 29 Cyg the long-term and short-term variability of amplitudes for all of these modes.
- For the first time in λ Boo stars we detected pulsational multiperiodic radial velocity variations (Mkrtichian *et al.*, 1998b). Based on spectroscopic radial velocity and line-profile data obtained during 1996, 1997 and 1998 campaigns we found that both low and high–degree nonradial modes are excited.
- For the first time in λ Boo stars, based on multicolor W, B, V, R photometry, we determined the amplitude-wavelength dependency for high-amplitude low-degree modes in 29 Cyg.
- The photometric behavior of the 29 Cyg shows a close similarity to the pulsational characteristics δ Scuti-type stars.

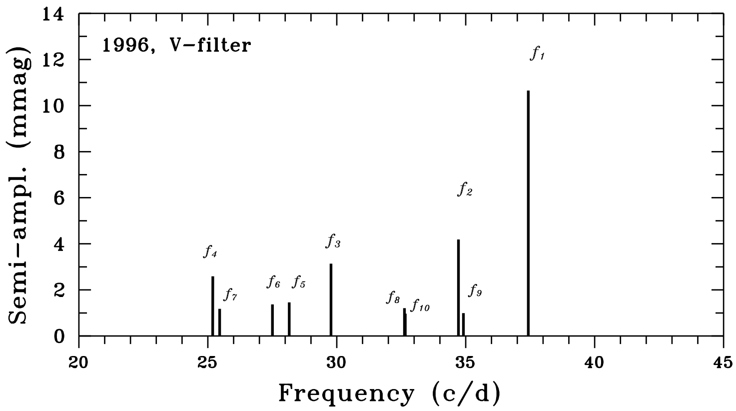

Figure 1: The schematic of pulsation frequency spectrum detected during 29 Cyg 1996 global campaign

ASTEROSEISMOLOGY WITH SPATIAL RESOLUTION

The rapidly oscillating magnetic chemically-peculiar (roAp) stars exhibit low-amplitude photometric variations ($<$ 2–5 mmag) with periods ranging from 5 to 15 minutes. These variations are thought to be due to low order ($\ell < 4$) nonradial pulsations, but the excitation mechanism remains unknown (Kurtz, 2000). Like their non-oscillating Ap counterparts these stars have strong chemical anomalies that are distributed inhomogeneously on the stellar surface (Hatzes, 1993) and a large, global dipole (quadruple and more complex in some cases) magnetic field whose axis is inclined with respect to the rotation axis. roAp stars (as the eclipsing binaries) are unique objects for which the technique of spatial filtration of nonradial modes is applicable (Mkrtichian, 1994).

We began the "Asteroseismology with Spatial Resolution" program for use of the precise stellar radial velocities (RV) to study rapidly oscillating Ap stars (roAp). This program united for the first time astronomers from the U.S.A. (McDonald Observatory, The University of Texas at Austin), Ukraine (Astronomical Observatory of Odesa State University), Brazil (Departamento de Física, Universidade Federal de Santa Caterina), and Russia (Special Astrophysical Observatory), in a collaborative effort for studying an important class of objects to understand the basic stellar problems such as origin of strong chemical anomalies and rapid pulsations. We were one of the first researchers to use an iodine gas absorption cell to study the pulsational RV behavior of roAp stars over a wide spectral range and with a high precision. Our RV measurements can achieve a velocity precision of 10-30 m/s for the brighter roAp stars. Some of the highlights of the first results from this ongoing project include:

- The first detailed investigation in 33 Lib of atmospheric standing acoustic waves – a new phenomenon for stellar atmospheres (Hatzes *et al.*, 2001).

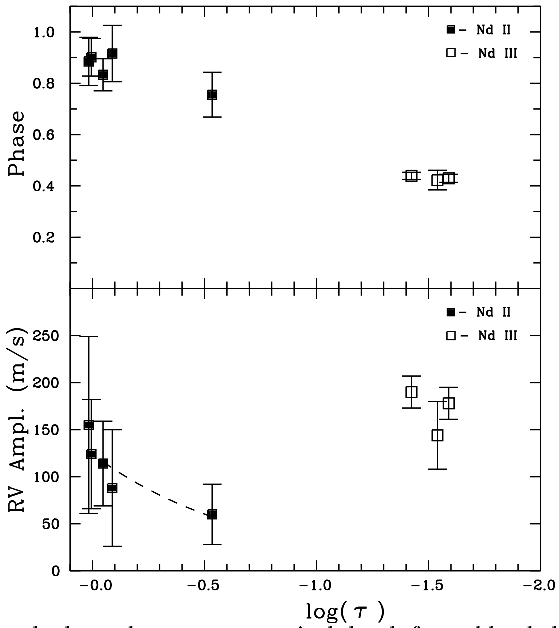

Figure 2: The phase and amplitude dependence versus optical depth for unblended or weakly blended Nd II and Nd III lines showing the acoustic cross-section of the atmosphere in 33 Lib. We can see the different formation heights for Nd II and Nd III lines. The latter shows a very small phase scatter that may be a strong indication of formation of Nd III lines in a thin upper atmospheric layer on another side of vertical pulsation node, which have the opposite pulsation phase respect lower layers where the Nd II lines are formed

- The detection of pulsational radial velocity variations in three roAp stars for which the RV variations have been found in the past but with better precision. The detection of RV variations in two additional roAp stars HD 122970 and HD 134214 (Hatzes *et al.*, 1999b).
- The oscillation spectrum of HR1217 entirely from RV data are derived.
- It is established that the pulsation RV amplitude depends on the spectral line strength and thus the depth of formation of the line. It has been seen in all roAp stars and indicates the presence of a radial node in the stellar atmosphere.
- We were the first to establish that the pulsation RV amplitude depends on the atomic species, which is interpreted as arising from the inhomogeneous distribution of elements in atmospheres of roAp stars. This gives a firm basis to our concept of periodic spatial filters.
- Two-site high-resolution spectroscopic campaign on γ Equ using the 2.7 McDonald and 6.0-m SAO telescopes were successfully performed.
- For the first time we detected that the pulsational phase of spectral lines depends on the Lande factors in 33 Lib (Hatzes *et al.*, 2001). This indicates strongly the influence of the magnetic field on the effective heights of formation of spectra lines and also reflects the existence of a radial node in stellar atmosphere. Investigations of the Lande g-factor versus pulsation phase in other roAp stars may prove fruitful.

SURVEY OF PULSATING ECLIPSING BINARY STARS

The asteroseismology of pulsating components (PC) in eclipsing binary systems (EBS) is expected to be very powerful and attractive tool for investigation of the inner structure of these stars. The advantages of studying PC in EBS with respect to single stars are the high accuracy in determination of the basic stellar parameters of components that is necessary for the precise tuning of theoretical models and also for the possibility of spatial filtration and identification of modes during the eclipse phases. Only five firm discoveries of δ Scu–type PC in EBS until 2000 year were made, among them only three stars are in the semi-detached (SD) systems.

The remarkable peculiarity of PCs in SD systems is a mass accretion on a pulsating gainer in an SD system. The mass accretion may lead to accretion-driven period changes of the pulsation modes. The observed period changes may be used as a tool for asteroseismic accretion rate estimation in binary system (Mkrtichian, 2001).

This expected phenomenon needs more detailed theoretical and comparative observational investigations in components of SD and detached systems. The pulsation spectra of stars in these sub-groups have not been studied well. Within the frames of CAN collaboration we started a project on an asteroseismic study and survey for new PC in the detached and SD eclipsing binary stars. The first results of our project on the study of PC in EBS can be summarized as follows:

- During the first stages of our survey we discovered the 24.4 min pulsations in A3 V primary, component of SD EBS AS Eri (Gamarova *et al.*, 2000). The calculated pulsation constant $Q = 0.01194$ relates this pulsation mode to the sixth-seventh overtone of low degree modes.
- We discovered the 67.89 min first overtone pulsations in a primary F0 V component of the well studied semi-detached EBS R CMa (Mkrtichian and Gamarova, 2000).
- During the survey we also confirmed the rapid pulsations in a primary A3 V component of SD EBS RZ Cas with a period 22.43 min and interpreted the excited mode as sixth overtone of low degree modes.
- We have carried out the intensive set of theoretical modeling of nonradial pulsations demonstrating the effect of apparent changes in the pulsation amplitude and phase during the eclipse of the pulsating component. This confirms the possibility and the high efficacy of using a spatial filtration of modes during the eclipse.

Acknowledgements. “Asteroseismology with Spatial Resolution” project was supported by US CRDF grant UP2-317. EP and WWW acknowledge support from FWF project S7303-AST.

REFERENCES

[1] *Gamarova A. Yu, Mkrtichian D. E. and Kusakin A. V.* Discovery of rapid pulsations in the A3 component of the eclipsing binary system AS Eri // IBVS.–2000.–N 4837.–P. 1–4.

[2] *Gies D. R. and Percy J. R.* Photometric variability of 29 Cygni // Astron. J.–1977.–**82**.–P. 166–168.

[3] *Kurtz D. W.* An Introduction to Ap Stars, roAp Stars and the Asteroseismology of roAp stars // Variable Stars as Essential Astrophysical Tools.–Kluwer Acad. Publ., 2000.–P. 313–338.

[4] *Hatzes A. P.* Mapping the Surface Distribution of Elements on Ap Stars Using the Maximum Entropy Method // Peculiar Versus Normal Phenomena in A-type and Related Stars: Proc. IAU Coll. N 138 / Eds M. M. Dworetsky, F. Castelli, R. Faraggiana.–1993.–P. 257

[5] *Hatzes A. P., Kanaan A., Mkrtichian D. E.* Radial Velocity Observations of Non-radially Pulsating Stars // Precise Stellar Radial Velocities: Proc. IAU Coll. N 170, Victoria, BC Canada, 1998 / Eds J. B. Hearnshaw, C. D. Scarfe.–ASP Conf. Ser.–1999.–**185**.–P. 166–176.

[6] *Hatzes A. P., Mkrtichian D. E. and Kanaan A.* // Variable Stars as Essential Astrophysical Tools: Proc. NATO/ASI Conf., Cesme, Turkey, 1999 / Ed. C. Ibanoglu.–1999.–P. 397–404.

[7] *Hatzes A. P., Mkrtichian D. E. and Kanaan A.* Radial Velocity Variations in Pulsating Ap Stars. II. 33 Librae // Mon. Notic. Roy. Astron. Soc.–2001.–submitted.

[8] *Mkrtichian D. E.* “Star As a Sun” observations in seismology of distant stars // Solar Phys.–1994.–**152**.–P. 275–282.

[9] *Mkrtichian D. E., Kusakin A. V., Janiashvili E. B., et al.* Central Asian Network (CAN) – the history and present status // Contr. Astron. Obs. Skalnate Pleso.–1998a–**27**.–P. 238–242.

[10] *Mkrtichian D. E., Kusakin A. V., Malanushenko V. P., et al.* 1996 multisite photometric and spectral campaign on the Lambda Boo star 29 Cyg // Contr. Astron. Obs. Skalnate Pleso.–1998b–**27**.–P. 476.

[11] *Mkrtichian D. E.* The asteroseismic approach for mass-accretion rate estimation in eclipsing binaries // Astron. and Astrophys.–2001.–submitted.

[12] *Mkrtichian D. E., Gamarova A. Yu.* RCMa – a new pulsating eclipsing binary star // IBVS.–2000.–N 4836.–P. 1–4.

[13] *Weiss W. W., Kuschnig R., Mkrtichian D. E., et al.* Photometry of ET And and pulsation of HD 219891 // Astron. and Astrophys.–1998.–**338**.–P. 919.

PERIODIC AND APERIODIC VARIABILITY OF THE INTERACTING BINARY AND LONG–PERIODIC STARS

I. L. Andronov[1], **A. V. Baklanov**[1], **L. L. Chinarova**[1], **D. Chochol**[2], **K. Gazeas**[3], **A. V. Halevin**[1], **S. V. Kolesnikov**[1], **L. S. Kudashkina**[1], **V. I. Marsakova**[1], **P. A. Mason**[4], **P. G. Niarchos**[3], **L. Patkos**[5], **E. P. Pavlenko**[6], **N. M. Shakhovskoy**[6], **L. L. Shapovalova**[1], **J. Tremko**[2], **S. Zola**[7,8]

[1] *Department of Astronomy and Astronomical Observatory of Odesa National University, Odesa, Ukraine*
e-mail: il-a@mail.od.ua, astro@paco.odessa.ua, *WWW:* www.paco.odessa.ua/~il-a

[2] *Astronomical Institute of the Slovak Academy of Sciences, Tatranska Lomnica, Slovakia*
e-mail: chochol@ta3.sk, tremko@ta3.sk

[3] *Section of Astronomy, Astrophysics and Mechanics, University of Athens, Greece*
e-mail: pniarcho@atlas.cc.uoa.gr

[4] *Department of Astronomy, New Mexico State University, USA*
e-mail: pmason@nmsu.edu

[5] *Konkoly Observatory, Hungarian Academy of Sciences, Budapest, Hungary*
e-mail: patkos@konkoly.hu

[6] *Crimean Astrophysical Observatory, Naukove, Crimea, Ukraine*
e-mail: shakh@crao.crimea.ua

[7] *Mt. Suhora Observatory, Pedagogical University, Kraków, Poland*

[8] *Astronomical Observatory, Jagiellonian University, Kraków, Poland*
e-mail: sfzola@cyf-kr.edu.pl

Recent results obtained within the framework of the international observational and research campaigns are reviewed. The main topics are following:

magnetic cataclysmic variables: synchronization of the spin and orbital period of the white dwarf; observational evidence on the switching of the accretion from one pole to another; non-dipole configuration of the magnetic field; "swingings" of the orientation of the magnetic axis in the "synchronous systems"; instability of the accretion and the "red noise"; long-term luminosity changes; UV Cet – like flares; two-pole accretion in the intermediate polars;

weakly- and non- magnetic cataclysmic variables: negative and positive superhumps in the nova–like variables; "red noise" and/or quasi–periodic oscillations; unprecedented switch of the superhump period in TT Ari; the luminosity dependence of the superhump period in BZ Cam and V725 Aql; long-term variations of the outburst characteristics of dwarf novae and luminosity of old novae – magnetic activity of the red secondary vs third body orbiting around a cataclysmic variable;

symbiotic binaries: light curve variations in symbiotic novae and stars with a pulsating component;

long–periodic pulsating variables: statistical study of the characteristics of the mean phase curves and of the individual cycles; additional classification criteria for the Mira–type and semi–regular stars.

Some of the original papers are available at *http://www.paco.odessa.ua/~il-a* and *http://ila.webjump.com*

INTRODUCTION

The variety of physical mechanisms taking place in stars leads to a variety of their observational appearance. Thus, a monitoring study of long–term variations of the characteristics of variability is needed, which may give an important information on the structure and evolution of the underlying objects, in addition to the short–term studies at different instruments. A year–scale cyclic or aperiodic modulation is observed in magnetic and non–magnetic cataclysmic binary systems, in symbiotic binaries and long–period pulsating variables.

In this review, we list the highlights of the study carried out by the authors and we point out some problems, which are the subjects for further investigations.

Invited paper.

MAGNETIC BINARY SYSTEMS: POLARS

AM Her–type stars, or polars, are characterized by a strong magnetic field of the white dwarf capturing the accretion flow and preventing the disk formation. The standard model and its extensions have been discussed by Andronov (1987).

AM Her has been monitored photometrically since 1978 and polarimetrically since 1989. The 186-min spin-orbital variability was studied by using various complementary methods. Long-term variations of the shape of the light curve were found, which are caused by switches of luminosity between high, intermediate and low states. The amplitude either of the orbital variability, or the "red noise" variability, statistically depends on luminosity, being the largest in the intermediate state.

The interrelations between the luminosity, colors of the mean flux, orbital and "red noise" variability will be discussed separately.

The following linear ephemeris was derived by using 267 photometric minima from various sources, which cover 65097 cycles (1976-1999): $MinHJD = 2446637.05101(\pm 0.00058) + 0.12892711(\pm 3{\times}10^{-8}){\times}(E - 28096)$. Here the initial epoch is close to the mid–observations and thus is much more accurate than that corresponding to the zero's cycle length.

The polarimetric ephemeris is based on the 19 main minima of the circular polarization in R: $HJD = 2450304.83379(\pm 0.00043) + 0.128927088(\pm 66{\times}10^{-9}){\times}(E - 56545)$.

There are cyclic variations of the phase with an effective cycle duration of $977 - 1288^d$, thus the seasonal value of the period may vary by $5{\times}10^{-5}P$. These changes are interpreted within the "swinging dipole" model (Andronov, 1987) of cyclic 2D variations of the orientation of the magnetic axis (both in longitude and latitude) of the white dwarf in respect to the line of centers.

The characteristics of the outbursts produced by the accretion events and the UV Ceti – type flares in AM Her, QQ Vul and BY Cam have been discussed separately (Halevin *et al.* (this volume), Bonnet–Bidaud *et al.* (2000), Shakhovskoy *et al.* (1993, 1999), Andronov (1999)). The spectral characteristics of AM Her at a low luminosity state as well as at an intermediate outburst have been discussed by Silber *et al.* (1996) based on the ultraviolet (IUE) and optical photometry.

MAGNETIC BINARY SYSTEMS: SYNCHRONIZING POLARS

Strong magnetic field of the white dwarf leads to a synchronization of its rotation with the orbital motion with the characteristic time scale of $\tau < 10^3$ years (Andronov, 1987). Nowadays, four slightly asynchronous polars are known. The most extensively studied object of this class is BY Cam, which was monitored from 1989. The observations completed during the "Noah project" (Silber *et al.*, 1997) and reanalyzed by Mason *et al.* (1998) have confirmed the asynchronism and have shown the "switches" of the accretion from one pole to another because of the "idling" of the white dwarf in respect to the red secondary. The characteristic time of the synchronization $\tau = 880 \pm 34$ years well agrees with the theoretical estimate.

Another asynchronous polar V 1500 Cyg (Nova Cygni 1975) was monitored since the explosion in 1975. Such a long–term database has allowed to detect variations of the rate of synchronization from $\dot{P}_{rot} = 1.8{\times}10^{-6}$ in 1977-1979 to $\dot{P}_{rot} = 2.7{\times}10^{-8}$ years. The last value corresponds to a characteristic time of 230 years (Pavlenko and Malanushenko, 1995). This allows to study a fine structure of the synchronization process.

MAGNETIC BINARY SYSTEMS: INTERMEDIATE POLARS

Circular polarization in two intermediate polars (RX J2107.9-0518 (=HU Aqr) and RX J0558+5353 (=V405 Aur)) was detected by Shakhovskoy and Kolesnikov (1993 and 1997, respectively). During the polarimetric period occur two photometric waves with a nearly same shape. This can be interpreted in terms of the model of two accretion columns located diametrical opposite above the surface of the magnetized white dwarf. The circular polarization crosses zero, when the column is effectively perpendicular to the line of sight. At this time, the brightness reaches its maximum. This argues either for the variations of the column's projected surface area, or for the minimal occultation of the column by the white dwarf. A small difference in the shape of the photometric pulses, as well as a small mean polarization argues for a small angle between the magnetic axis and the equator plane of the white dwarf, of about few degrees. This situation is opposite to classical polars, where the magnetic axis is usually well inclined to the orbital plane (Brainerd and Lamb, 1985).

SUPERHUMPS IN DWARF NOVAE: DEPENDENCE ON PERIOD AND LUMINOSITY

Dwarf novae are characterized by the outbursts with a cycle ranging from few days to few months or even years. The duration of this cycle, for a given star, may differ by few dozens per cent. Additionally, the so-called "supermaxima" (brighter and wider outbursts) are occurred in some binary systems, mainly with periods of

$\leq$ 2 hours. During these brighter and wider outbursts the photometric waves called the "superhumps" may be observed (*cf.* Warner, 1976). Only few groups in the world (in Japan, USA and our group in Ukraine) attempt to find the superhumps by using CCD in the stars, which are to be supposed to have superoutbursts. The period of superhumps P_{sh} is usually longer than the orbital one P_{orb} with a relative difference increasing with P_{orb}. Because of scatter, there are various forms of the $P_{sh}(P_{orb})$ relation. One of them is $\log P_{sh} = -0.0043(\pm 0.0033) + 1.077(\pm 0.006) \log P_{orb}$ (with a corrected zero–point) (Andronov, 1990). Here P_{sh} and P_{orb} are expressed in hours.

The superhumps are explained by the rotation of the elliptic accretion disk which is slower than the orbital motion. The spin/orbital resonance occurs in short–period cataclysmic variables owed to a low mass ratio (Whitehurst and King, 1991).

However, the observations have shown that the superhump period undergoes changes with luminosity. During a superoutburst in V725 Aql, the superhumps were detected with a period decreasing with luminosity from 160 to 80 minutes. This phenomenon was interpreted by a decrease of the rotational period of the tilted accretion disk with decreasing radius (Baklanov *et al.*, 2000). It is very interesting to note a similar dependence obtained for another *nova–like* star BZ Cam (Andronov *et al.*, 2000). The "switch" to a "negative superhump" at minimum was detected in other dwarf Nova V503 Cyg (Kuznetsova *et al.*, 1999).

Thus, the photometric period depends not only on the orbital period (despite at the superoutburst maximum, it depends statistically on P_{orb}), but on the luminosity as well. In this case, the photometric wave is caused by the rotation of the inhomogeneous disk rather than by the rotation of the "quasi-stable" disk. Further monitoring of the evolution of superhump during a decline is necessary for other SU UMa nova–like stars.

MULTI–CYCLIC ACTIVITY IN NON–MAGNETIC NOVA–LIKE BINARY SYSTEMS

Nova–like binary systems are cataclysmic variables with a high accretion rate leading to their "permanent outburst" state, which is rarely interrupted by excursions to a low or intermediate luminosity state.

TT Ari is the brightest object from this class and thus most extensively observed since 1965. One of the most prominent properties is the presence of quasi–periodic oscillations with a cycle length ranging mostly between 15 and 30 minutes. Recent studies (Tremko *et al.*, 1996; Andronov *et al.*, 1999) have shown that these variations occur at preferred time scales without a trend previously suggested. The power spectrum at higher frequencies obeys a power law with an index $\gamma_S = 1.51 \pm 0.04$ corresponding to a "red noise" often observed in accreting binaries. For different runs, the value of γ_S is ranging from 1.3 to 2.6.

The photometric period differs from the orbital one, being shorter, thus arguing for the so–called "negative superhumps". In different years, its value was ranged from $0\overset{d}{.}1326$ to $0\overset{d}{.}133160$ showing its uncoherency (Andronov *et al.*, 1999).

However, Tremko *et al.* (1996) predicted a value of the superhump period $P_{sh} = 0\overset{d}{.}1493 \pm 0\overset{d}{.}0007$ using the "orbital period – superhump period" relation by Andronov (1990). This value was justified in 1997, when the superhump period changed to $P_{sh} = 0\overset{d}{.}14926 \pm 0\overset{d}{.}00005$ (Skillman *et al.*, 1998). This switch has shown an existence of two types of disk motion in respect to the rotating frame: apsidal advance ("negative superhump") and nodal regression ("positive superhump").

The difference between the photometric and spectral periods may lead to a beat phenomenon corresponding to the period of changes of the orientation of the disk in respect to the red dwarf secondary. However, its amplitude is estimated to be twice smaller than of the primary photometric wave itself (Andronov *et al.*, 1999).

Another interesting phenomenon observed in TT Ari is the systematic trend of the effective colors of the mean flux, superhump variability and quasi–periodic oscillations towards higher color temperatures (Tremko *et al.*, 1996; Efimov *et al.*, 1998).

Kraicheva *et al.* (1999) confirmed the suggestion of Bianchini (1990) about the presence of 6–year cycle in the luminosity variations of TT Ari.

Such complicated behaviour needs extensive observational studies with an annual monitoring of a total duration at least ≈ 100 hours to study the origin of superhumps and other physical mechanisms causing variability at time scales from seconds to years.

Another nova–like system, *BZ Cam*, is usually in the state of a "permanent outburst". In 1999/2000, it underwent weakening by $\approx 1\overset{m}{.}3$ with slow decline and more rapid return at a rate (28 ± 2) days/mag in February-March, 2000. The primary photometric period usually interpreted as superhumps was variable, showing a statistical dependence $d \log P / d \log L = 1.0 \pm 0.2$ rather than a "switch" from a "negative" to "positive" superhump (Andronov *et al.*, 2000). The proposed interpretation was a response of the effective radius of the accretion disc on luminosity (*i.e.*, the mass transfer rate). Such a dependence resembles that described above for dwarf novae and thus shows a common origin of the photometric wave, despite these systems are located from different sides of the "2–3 hour period gap". This phenomenon is an excellent probe for the theories of non–stationary accretion discs and should be extensively studied.

“NON–MAGNETIC” (?) DWARF NOVAE

Dwarf novae are characterized by changes of the outburst cycle up to few dozens per cent. However, two types of possible season-to season changes can be occurred:

a) smooth variations of the cycle length (Bianchini, 1990);

b) abrupt switchings (Andronov and Shakun, 1990).

To study this phenomenon, the photographic observations on the negatives from the Odesa and Moscow plate collections were used as well as the visual estimates from the AFOEV and VSOLJ databases.

The star which is extensively covered by the observations is EM Cyg. The cycle of 3000^d in the cycle length variations, the amplitude and the mean brightness level have been discovered from the seasonal mean light curves by Andronov and Chinarova (1996) and then have been confirmed by using the data run covering 220 individual maxima and applying the wavelet analysis. The amplitude is correlated with the mean magnitude, thus the star shows only minor variations of the brightness at maximum at this timescale (despite the cycle–to–cycle changes are quite large from $11\overset{m}{.}9$ to $13\overset{m}{.}0$), despite the brightness at minimum shows a well pronounced $\sim 3000^d$ wave. The mean value of the cycle length is 25^d, the mean outburst curve shows an ascending branch of a duration of 10^d, whereas the descending branch lasts 14^d. The mean amplitude is $1\overset{m}{.}16$. The two main timescales of 25^d and 3000^d are in a good agreement with the optimal values of the filter half–width $\Delta t = 8^d$ and 1340^d obtained from the “running parabola” fits. The standstills at the light curve are present, during which the amplitude decreases drastically, confirming the UGZ classification of the star. One may note that the orbital period of EM Cyg is equal within few per cent to that of the prototypes of different subclasses of dwarf novae – SS Cyg and Z Cam.

In 5 other stars of the UGSS subtype, the few year–scale variations of the cycle length are found.

Such drastic changes of the cycle length are usually explained by variations of the accretion rate caused by a magnetic activity of the red dwarf (Bianchini, 1990; Andronov and Shakun, 1990). As an alternate explanation, one may suggest minor changes of the orbital separation owed to a third body orbiting near the cataclysmic binary. This model is indirectly confirmed by North (1999), who reported on a presence of a third star in EM Cyg. It would be desirable to make a more detailed study of this system and of similar objects.

SYMBIOTIC VARIABLES

The own photographic and the AFOEV and VSOLJ visual observations of the symbiotic variables R Aqr, TX CVn, UV Aur, V1016 Cyg, V 1329 Cyg are used for the time series and correlation analysis by applying the same methods to the systems with different types of variability are compared. The “scalegram” analysis is made by using the “running parabola” methods (Andronov, 1997) by the least–squares extension of the wavelet analysis (Andronov, 1998). The method of “running sines” (Chinarova *et al.*, 1994) allowed to study the slow variations of the mean, amplitude and phase of the pulsations. In the objects studied, these characteristics vary with time. Among the highlights are following:

UV Aur. The main oscillation with the period $P = 393\overset{d}{.}0 \pm 0\overset{d}{.}1$, full amplitude $1\overset{m}{.}32 \pm 0\overset{m}{.}02$ and asymmetry 0.43 ± 0.01 is superimposed onto a long–term variation with $P_2 = 6800 \pm 46^d$ and a full amplitude $1\overset{m}{.}20$. Suggesting that P_2 is a beat period between the orbital period P_{orb} and the pulsational period P_1, one may estimate $P_{orb} = 371\overset{d}{.}5$ (Chinarova, 1998). This suggestion of the beat phenomena in symbiotic binaries is to be checked.

TX CVn. The main oscillation with a characteristic cycle length of 500^d is characterized by highly variable semiamplitude from $\approx 0\overset{m}{.}2$ to zero within error estimate. This is characteristic for transient pulsations which may be caused by the red giant. A longer wave is characterized by a cycle length varying from $\approx 2000^d$ to $\approx 6000^d$.

V 1329 Cyg. The photometric behaviour in 1891–1997 years was characterized by a drastic change from the light curve with narrow eclipses to a slightly asinusoidal type of variability with the ephemeris

$$MinJD = 2446771(\pm 3) + 956.5(\pm 0.6) \cdot E.$$

The amplitude in U ($1\overset{m}{.}6$) is significantly larger than in the pg, B and V bands ($1\overset{m}{.}22$). After the outburst, the trend is superimposed onto the brightness variations at a rate being maximal in U: $dm/dt = (100 \pm 4) \times 10^{-6}$ mag/day. Besides this, a secondary period with the ephemeris $MaxJD = 2446711(\pm 9) + 553.1(\pm 1.9) \times E$ and the semi–amplitude $0.075 \pm 0\overset{m}{.}007$ is present, as well as a possible wave with a $\approx 5300^d$ cycle (Chochol *et al.*, 1999).

"RED NOISE" IN ACCRETING BINARY SYSTEMS

Cataclysmic variables are characterized by a high level of fast aperiodic variability called "flickering" (*cf.* Warner, 1976; Bruch, 1992). It is usually interpreted by inhomogeneity and instability of the emitting accretion structures. The main sources are following: a) the superposition of the individual outbursts caused by the accretion of the plasma inhomogeneities with a high overlapping causing the "shot noise" and b) chaotic motion of massive blobs and chaotic changes of the accretion disc structure.

The power spectra of these variations show a systematic decrease with frequency which may be called a "red noise" contrary to the "white noise", which is statistically independent on frequency. In a double logarithmic scale, such power spectra often have nearly linear parts corresponding to a power law $S(f) = A \cdot f^{-\gamma_S}$. For infinite time series, the values of $\gamma_S = 0$, 1 and 2 correspond to a "white noise", "flickering" and "random walks", respectively.

To study this phenomenon, we have elaborated a few complementary methods taking into account a finite length of irregularly spaced data which are listed by Andronov (1999) and based on the periodogram, wavelet, scalegram and auto-correlation analysis. In more detail, they will be described in the monograph by Andronov (2000, in preparation).

Results of study of the selected stars are briefly summarized by Andronov (1999) and Andronov *et al.* (1999). The characteristics of this variability are strongly dependent on the luminosity state of a given star and are different for objects with periodic modulation (intermediate polars), quasi-periodic oscillations (nova–like variables) and polars.

LONG–PERIOD PULSATORS

The statistical study of the characteristics of the individual pulsation cycles of 53 *Mira*–type stars has been carried out by using the visual observations of from the AFOEV and VSOLJ databases. Results of this study are presented separately in this volume by Marsakova and Andronov and will not be repeated here.

The periodogram analysis of 42 *semi-regular* stars was carried out. The algorithm was described by Andronov (1994). Three best fit frequencies were consequently determined for the original and "prewhitened" data. According to the periodograms and the shapes of the light curve, the stars may be preliminary subdivided into 5 groups:

1) "quasi-harmonic" (*e.g.*, T Ari with one dominating wave);

2) "quasi-multi-harmonic" (*e.g.*, U Del with 2 or 3 peaks at a periodogram corresponding to integer ratios of the period to a main one);

3) "multiperiodic" (*e.g.*, TX Dra with 2 or 3 periods differing by a few times);

4) "switching" periods (*e.g.*, AF Cyg with period ratio of 7/4);

5) "chaotic" (*e.g.*, X Her with a lot of peaks).

Possibly one may also distinguish the "modulated" stars (*e.g.*, S Per with highly variable amplitude of the main oscillation of a period by ≈ 10 times smaller than the cycle of mean brightness and amplitude modulation);

All waves have variable amplitude and phase and sometimes some "switchings" occur from one wave to another (*e.g.*, AF Cyg). These groups are not coinciding with the GCVS types, allowing possible additional phenomenological classification.

REFERENCES

[1] *Andronov I. L.* "Swinging Dipoles" in Magnetic Close Binary Systems // Astrophys. and Space Sci.–1987.–**131**.–P. 557–570.

[2] *Andronov I. L.* On "Orbital Period–Superhump Period" Relationship in Cataclysmic Variables of SU UMa-Type // Astron. Tsirk.–1990.–**1545**.–P. 15–16.

[3] *Andronov I. L.* (Multi-)frequency variations of stars. Some methods and results // Odessa Astron. Publ.–1994.–**7**.–P. 49–54.

[4] *Andronov I. L.* Method of running parabolae: spectral and statistical properties of the smoothing function // Astron. and Astrophys. Suppl. Ser.–1997.–**125**, N 1.–P. 207–217.

[5] *Andronov I. L.* Wavelet analysis of time series by using the method of least squares with supplementary weights // Kinematics and Physics of Celestial Bodies.–1998.–**14**, N 6.–P. 490–511.

[6] *Andronov I. L.* "Red noise" from the accreting magnetic white dwarfs // Astron. Soc. Pacif. Conf. Ser.–1999.–**169**.–P. 326–336.

[7] *Andronov I. L., Arai K., Chinarova L. L., et al.* A search for periodic photometric behavior in the cataclysmic variable TT Arietis // Astron. J.–1999.–**117**.–P. 574–586.

[8] *Andronov I. L., Chinarova L. L.* Outburst cycle length variations in the dwarf nova EM Cygni // Odessa Astron. Publ.–1996.–**9**.–P. 9–13.

[9] *Andronov I. L., Gazeas K., Kolesnikov S. V., Niarchos P. G., Shakhovskoy N. M.* Superhumps vs "red noise" in the cataclysmic binary BZ Camelopardalis in 2000 // Astronomy 2000: International Sci. Mem. Conf., Abstracts.–Odesa: Astroprint, 2000.–21 p.

[10] *Andronov I. L., Shakun L. I.* Alternating Cycle Durations in Dwarf Novae // Astrophys. and Space Sci.–1990.–**169**.–P. 237–240.

[11] *Baklanov A. V., Pavlenko E. P., Andronov I. L.* CCD and TV- photometry of cataclysmic variable stars // Astronomy 2000: International Sci. Mem. Conf., Abstracts.–Odesa: Astroprint, 2000.–21 p.

[12] *Bianchini A.* Solar-type cycles in close binary systems // Astron. J.–1990.–**99**, N 6.–P. 1941–1952.

[13] *Bonnet-Bidaud J. M., Mouchet M., Shakhovskoy N. M., et al.* Magnetic field and unstable accretion during AM Herculis low states // Astron. and Astrophys.–2000.–**354**.–P. 1003–1010.

[14] *Brainerd J. J., Lamb D. Q.* Orientations of AM Her stars from their polarization properties: the case of the missing AM Her stars // Astrophys. and Space Sci. Lib.–1985.–**113**.–P. 247–256.

[15] *Bruch A.* Flickering in cataclysmic variables: its properties and origins // Astron. and Astrophys.–1992.–**266**.–P. 237–265.

[16] *Chinarova L. L.* Time Series Analysis of the Periodic and Aperiodic Variations of the Symbiotic Star UV Aurigae // Proc. 29th Conf. Variable Star Res., Brno, Czech Republic / Eds J. Dusek, M. Zejda.–1998.–P. 38–44.

[17] *Chochol D., Andronov I. L., Arkhipova V. P., et al.* Long-term photometry of the symbiotic nova V1329 Cyg // Contr. Astron. Obs. Skalnate Pleso.–1999.–**29**.–P. 31–46.

[18] *Efimov Yu. S., Shakhovskoy N. M., Andronov I. L., Kolesnikov S. V.* UBVRI photometry and polarimetry of the cataclysmic variable TT Arietis // Izv. Krym. Astrophys. Obs.–1998.–**94**.–P. 263–266.

[19] *Kraicheva Z., Stanishev V., Genkov V., Iliev L.* TT Arietis: the 1985–1999 accretion disc behaviour // Astron. and Astrophys.–1999.–**351**.–P. 607–618.

[20] *Kuznetsova Yu. G., Pavlenko E. P., Sharipova L. M., Shugarov S. Yu.* Observations of typical, rare and unique phenomena in close binaries with extremal mass ratio // Odessa Astron. Publ.–1999.–**12**.–P. 197–200.

[21] *Mason P. A., Ramsay G., Andronov I., et al.* Evidence for pole switching in the magnetic cataclysmic variable BY Camelopardalis // Mon. Notic. Roy. Astron. Soc.–1998.–**295**.–P. 511–519.

[22] *North R. C.* EM Cygni: a compationable dwarf nova // Warner Symp. on Cataclysmic Variables, Cambridge, 1999.–P. 63.

[23] *Pavlenko E. P., Malanushenko V. P.* The peculiarity of V1500 Cyg synchronization // Astrophys. and Space Sci. Lib.–1995.–**205**.–P. 172.

[24] *Shakhovskoy N. M., Alexeev I. Yu., Andronov I. L., Kolesnikov S. V.* Unprecedented flare at red secondary component of AM Herculis // Annals of the Israel Phys. Soc.–1993.–**10**.–P. 237–240.

[25] *Shakhovskoy N. M., Andronov I. L., Kolesnikov S. V., Halevin A. V.* Blob parameters of accretion streams in magnetic cataclysmic variables // Odessa Astron. Publ.–1999.–**12**.–P. 242–244.

[26] *Shakhovskoy N. M., Kolesnikov S. V.* RXJ 2107.9-0518 // IAU Circ.–1993.–N 5891.–P. 1.

[27] *Shakhovskoy N. M., Kolesnikov S. V.* RXJ 0558.0+5353 // IAU Circ.–1997.–N 6760.–P. 1.

[28] *Silber A. D., Raymond J. C., Mason P. A., et al.* IUE and Optical Observations of AM Herculis in its Low State // Astrophys. J.–1996.–**460**.–P. 939–948.

[29] *Silber A. D., Szkody P., Hoard D. W., et al.* The Noah Project: detection of the spin-orbit beat period of BY Camelopardalis // Mon. Notic. Roy. Astron. Soc.–1997.–**290**.–P. 25–33.

[30] *Skillman D. R., Harvey D. A., Patterson J., et al.* Superhumps and accretion disk precession in TT Arietis // Astrophys. J. Lett.–1998.–**503**.–P. L67–L70.

[31] *Tremko J., Andronov I. L., Chinarova L. L., et al.* Periodic and aperiodic variations in TT Arietis. Results from an international campaign // Astron. and Astrophys.–1996.–**312**.–P. 121–134.

[32] *Warner B.* Observations of Dwarf Novae // The Structure and Evolution of Close Binary Systems, Dordrecht, Holland / Eds P. P. Eggleton, S. Mitton, J. A. Whelan.–1976.–P.85–140.

[33] *Whitehurst R., King A.* Superhumps, resonances and accretion discs // Mon. Notic. Roy. Astron. Soc.–1991.–**249**.–P. 25–35.

STUDIES OF X–RAY NOVAE
IN THE CRIMEAN ASTROPHYSICAL OBSERVATORY

E. Pavlenko

Crimean Astrophysical Observatory, Ministry of Ukraine for Education and Science
Naukove, 98409 Crimea, Ukraine
e-mail: pavlenko@crao.crimea.ua

The regular TV and CCD optical monitoring of the five X-ray novae (QZ Vul, V404 Cyg, V518 Per, J2123-058 and J1859+226) has been carried out in the Crimean Astrophysical Observatory. We made observations both immediately after announcement of the optical identification during the outburst decline and in a faint quiescent state in the close cooperation with colleagues from Russia, Spain, UK, and Japan. The review of campaign's achievements (discoveries of orbital and "superhumps" periods, quasi-periodic phenomena, studies of the nature of the binaries components) is presented.

INTRODUCTION

The X-ray novae or soft X-ray transients are a subclass of low-mass X-ray binaries. They are characterized by episodic X-ray outbursts lasting for several months. Their luminosity can increase by as much as a factor of 10^7, see [1]. Similar to the novae stars, X-ray novae show fast rise and slow exponential or linear decay. These objects are very promising targets in the field of searching for the neutron stars and black holes in the close binaries. Since the discovery of the first X-ray nova V616 Mon in 1975 there are currently 11 known X-ray novae with 8 black holes and 3 neutron stars as a primary components. The secondary star is the late-type star in such systems. Over more then ten years the optical studies of some X-ray novae have been carried out in the Crimean Astrophysical Observatory in the frame of international multilongitude campaigns. All our photometry was done at the TV complex of 0.5-m MTM-500 meniscus telescope [2] and at the 0.38-m Cassegrain telescope with SBIG ST-7 CCD camera [3]. Here we present a review of the main results of these campaigns.

QZ VULPECULAE = GS 2000 + 25

QZ Vul = GS 2000 + 25 was discovered in the X-ray outburst by the All Sky Monitor on the board the Ginga satellite telescope in 1988 [4]. We started our TV photometric monitoring immediately after announcement of the optical identification, when the brightness of nova was near ($B = 18^m$) and finished, when it reached $B = 19^m$. Our previous analysis of the 104 observations on 15 nights yields gives the existence of light variations with one of suspected periods (with 1-day aliasing): $0\overset{d}{.}532$, $0\overset{d}{.}348$ and $0\overset{d}{.}258$ [5]. Later we combined our data with CCD data obtained by Casares and Kidger at 1m JKT telescope on La Palma and found the period $0\overset{d}{.}347$ to be a real one that is close to one of our determinations. We suggested that these light variations display the possible superhump period similar to those of the SU UMa stars during the superoutbursts [6, 7].

Now QZ Vul is known as the X-ray nova that contains the black hole of 5.3–8.2 $M_\odot$ as the primary component [8].

V404 CYGNI = GS 2023+338

The X-ray nova V404 Cygni was also discovered by Ginga satellite during the 1989 outburst [9] and was identified with a known recurrent nova. Soon it was discovered as the strong black hole candidate by Casares *et al.* [10] from spectroscopic investigations: the mass function of V404 Cyg was found to be equal to 6.08 $M_\odot$. In 1991 in order to study V404 in the low brightness state we undertook a campaign on the photometric monitoring (CrAO, MTM-500) with spectroscopic observations (La Palma, 4.2-m William Hershel Telescope) simultaneously. The system that star was already in a quiet state ($B = 19^m$). Our observations shown the same period as the spectroscopic one (6.5 days) that was interpreted as the orbital period. The photometric light variations here are explained by the considerable ellipsoidal distortion of the secondary component caused by the massive primary component. The results of that campaign were the determination of the parameters of binary [11, 14] system: inclination $i = 45 - 70$, mass ratio $q = 4.5 - 2.6$, orbital separation of the components

$a = 46 - 39Ro$. The mass of the black hole was estimated of about 27–14 $M_{\odot}$ that later was defined more precisely by Shahbaz *et al.* as $\sim 12M_{\odot}$, [15].

Our long-term monitoring of V404 in quiescence yields the variations of ellipsoidal light curve from year to year that could be caused by some variations in accretion disk structure (may be, size) with time. Besides of the orbital variability, V404 Cyg also displayed 0.24 d quasi-periodic optical variations. We found that this phenomenon is persistent from year to year, however, the amplitude sometimes drops from $0^m_.14$ to the less than $0^m_.03$ [12, 13]. The source of these variations could be localized in the inner accretion disk surrounding the black hole and connected with some non-stationary accretion process.

V518 PERSEI = GRO J0422+32

This X-ray nova was first detected by the Burst and Transient Source Experiment (BATSE) on the Compton Gamma-Ray Observatory in 1992, Aug. 5 [16]. Since Aug. 11 the source has been observed by the all-sky X-ray WATCH monitor on the GRANAT satellite [17]. The optical counterpart was discovered at the TV complex of MTM-500 in the Crimean Astrophysical Observatory as the blue star of $13^m_.1$ [18]. It was done after visual inspection of each of the 36 fields that covered the whole 60' WATCH error box and after comparing with the corresponding Palomar Sky Survey plate. We have undertaken the simultaneous UBVR observations during the first 100 days after the outburst and found that the optical light has decayed at a rate of 0.0065 mag/day [19]. Similar to QZ Vul in the outburst decline, V518 Per also displayed the SU UMa-like superhumps (5.1 h) that were discovered by Kato [20]. At present time V518 Per is also known as the black hole candidate among X-ray novae. Casares *et al.* have found the mass of compact component is to be equal to 2.5–5.0 $M_{\odot}$, see [21].

XTE J2123-058

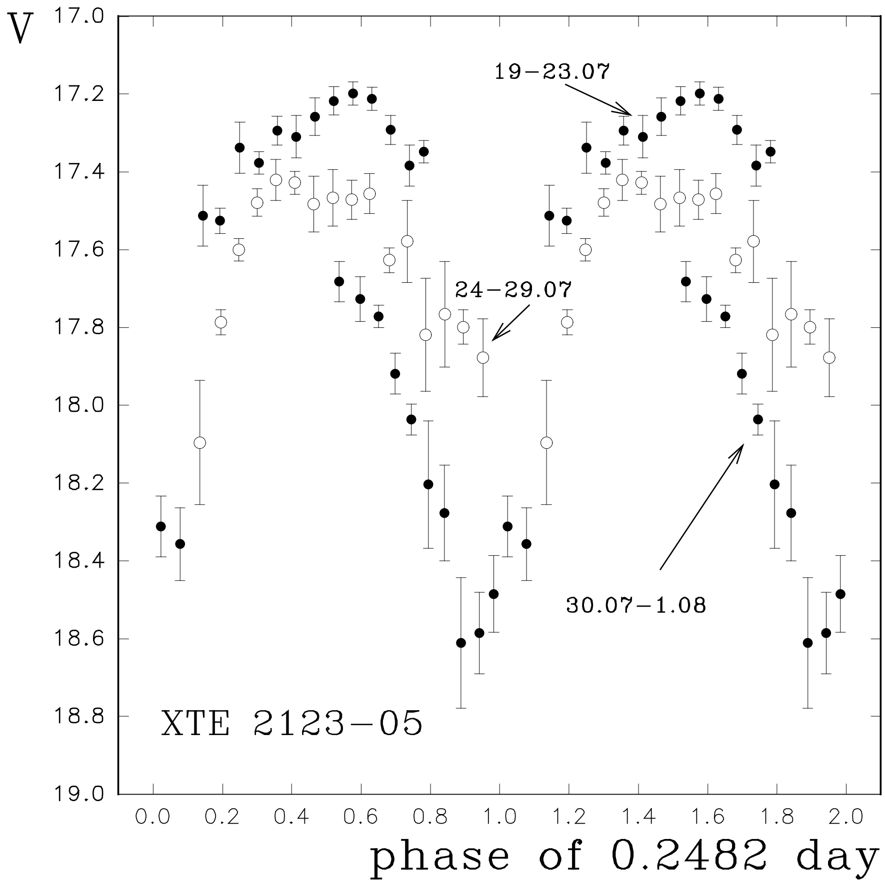

Figure 1: Fast evolution of the orbital lightcurves of XTE J2123-058 during 10 days of the outburst. The mean lightcurves that are averaged within three data sets are shown by arrows

The X-ray nova J2123-058 was discovered in 1998 by the Rossi X-Ray Time Explorer (RXTE) satellite [22]. The optical counterpart was identified with a star of $R = 17^m_.2$ by Tomsick *et al.* [23]. The optical observations of this nova have been carried out at IAC80 and 1-m Optical Ground Station (OGS) in the Observatorio del Teide (Tenerife); at 0.5-m amd 0.38-m telescopes in the Crimean Astrophysical Observatory; at 1.25-m telescope in the Crimean laboratory of Sternberg Astronomical Institute; at the 1-m telescope Mount Canopus in Tasmania and at the 1.2-m telescope at the Kryonerion Astronomical station of the National Observatory of Athens at Kryonerio of Korinthina.

The dense runs of observations allowed us to study the evolution of light modulation during the various stages of the outburst. It was shown that at the first stages the nightly partially eclipsed lightcurves were modulated on the $5^{h}_{.}95$ orbital period that exhibited growth of amplitude with time (up to $1^{m}_{.}4$). The evolution of the orbital light curves during one month are shown in Fig. 1. They are constructed for the data obtained at the TV complex of 0.5-m telescope. This variability was explained by a strong X-ray heating of a secondary component and accretion disk surrounding a primary one. The change of the lightcurves shape and amplitude was consistent with shrinkage of disk during the course of outburst [24]. One of the most significant result of our campaign was the detection of the rapid switching-off the X-ray heating. At least in 10 days the observed high-amplitude light modulation was disappeared and replaced on the typical two-humped ellipsoidal light curves with amplitude of $0^{m}_{.}4$. It happened just when this system has reached the quiet state.

XTE J2123-058 is believed to have a neutron star rather than a black hole as a compact component [25, 26].

XTE J1859+226

In 1999 Wood *et al.* reported the discovery of another new X-ray nova [27] XTE J1859+226 by RXTE. They found that the energy spectrum and its characteristics are reminiscent of a galactic black hole candidate. Garnavich and Stanek [28] detected of an optical counterpart to this transient as the star of $R = 15^{m}_{.}1$. It was found also [29] that this source shows the relativistic radio jet ejections.

Together with Japanese colleagues from Kyoto University we have undertaken the photometric observations in order to study the outburst decay and to search for possible periodicity. We found the light modulation with 6.47 hours soon after the start of the outburst, see [30]. However, neither this period was confirmed, nor another periodicity was found later.

Together with colleagues from Spain and UK we continued a monitoring of this nova over all outburst decay. The results of this campaign are in preparation.

REFERENCES

[1] *van Paradijs J., and McClintock J. E.* // X-ray Binaries. Optical and ultraviolet observations of X-ray binaries / Eds W. H. G. Lewin, J. van Paradijs and E. P. J. van den Heuvel.–Cambridge University Press, 1995.–P. 58.

[2] *Abramenko A. N., Prokof'eva V. V., Bondar' N. I., et al.* // Izv. Krim. Astrofiz. Obs.–1988.–**78**.–P. 182–192. (in Russian).

[3] *Pavlenko E. P., Shugarov S. Yu, Katysheva N. A.* // Astrofizika.–2000.–In press (in Russian).

[4] *Tsunemi H., Kitamoto S., Okamura S., Roussel-Dupre D.* Discovery of a bright X-ray nova, GS2000+25 // Astrophys. J.–1989.–**337**.–P. L81.

[5] *Pavlenko E. P., Prokof'eva V. V., Dolgushin A. I.* // Pis'ma v A. Zh.–1989.–**15**.–P. 611–616 (in Russian)

[6] *Charles P. A., Kidger M. R., Pavlenko E. P., et al.* The soft X-ray transient GS2000+25 -I.An 8.3-hr modulation during outburst // Mon. Notic. Roy. Astron. Soc.–1991.–**249**.–P. 567–572.

[7] *O'Donoghue D. and Charles P. A.* Have superhumps been seen in black hole soft X-ray transients? // Mon. Notic. Roy. Astron. Soc.–1996.–**282**.–P. 191–205.

[8] *Casares J., Charles P. A., Marsh T. R.* Dunamical evidence for a black hole in the X-ray transient QZ Vul (=GS2000+25) // Mon. Notic. Roy. Astron. Soc.–1995.–**277**.–P. L45.

[9] *Makino F. and the Ginga team* // IAU Circ.–1989.–N 4782.

[10] *Casares J., Charles P. A., Naylor T.* A 6.5-day periodicity in the recurrent nova V404 Cygni implying the presence of a black hole // Nature.–1992.–**355**.–P. 614–617.

[11] *Casares J., Charles P. A., Naylor T., Pavlenko E. P.* Optical studies of V404 Cyg, the X-ray transient GS 2023 + 338 -III. The secondary star and accretion disc // Mon. Notic. Roy. Astron. Soc.–1993.–**265**.–P. 834–852.

[12] *Pavlenko E. P., Martin A. C., Casares P. A., et al.* Orbital and quasi-periodic optical variations in the black hole X-ray binary V404 Cyg // Mon. Notic. Roy. Astron. Soc.–1996.–**281**.–P. 1094–1104.

[13] *Kuznetsova Yu. G., Pavlenko E. P., Sharipova L. M., et al.* Observations of typical, rare and unique phenomena in close binaries with extremal mass ratio // Odessa Astron. Publ.–in press.

[14] *Antokhina E. A., Cherepaschuk A. M., Shugarov S. Yu., Pavlenko E. P.* Orbital light curve and parameters of X-ray nova GS2023+338=V404 Cyg // IBVS.–1992.–**3777**.–P. 1–3.

[15] *Shahbaz T., Ringwald F. A., Bunn J. C., et al.* The mass of black hole in V404 Cygni // Mon. Notic. Roy. Astron. Soc.–1994.–**271**.–P. L10–L14.

[16] *Paciesas W. S., Briggs M. S., Harmon B. A., et al.* // IAU Circ.–1992.–N 5580.

[17] *Castro-Tirado A. J., Brandt S., Lund N.* // IAU Circ.–1992.–N 5587.

[18] *Castro-Tirado A. J., Pavlenko E. P., Shlyapnikov A. A., et al.* // IAU Circ.–1992.–N 5589.

[19] *Castro-Tirado A. J., Pavlenko E. P., Shlyapnikov A. A., et al.* Discovery of the optical counterpart of the soft X-ray transient GRO J0422+32 // Astron. and Astrophys.–1993.–**276**.–P. L37–L40.

[20] *Kato T., Mineshige S., Hirata R.* Discovery of orbital dips and superhumps in the optical counterpart of the x-ray transient GRO J0422+32 // Publs Astron. Soc. Jap.–1995.–**47**.–P. 31–39.

[21] *Casares J., Martin A. C., Charles P. A.* On the mass of the compact object in GRO J0422+32 // Mon. Notic. Roy. Astron. Soc.–1995.–**276**.–P. L35.

[22] *Levine A., Swank J., Smith E., et al.* // IAU Circ.–1998.–N 6955.

[23] *Tomsick J. A., Halpern J. P., Leighly K. M., et al.* // IAU Circ.–1998.–N 6957.

[24] *Zurita C., Casares J., Shahbaz T., et al.* Optical studies of the X-ray transient XTE 2123-058.-I.Photometry. // Mon. Notic. Roy. Astron. Soc.–2000.–**316**.–P. 137–145.

[25] *Takeshima T., Strohmayer T. E.* // IAU Circ.–1998.–N 6958.

[26] *Tomsick J. A., Kemp J., Halpern J. P., et al.* // IAU Circ.–1998.–N 6972.

[27] *Wood A., Smith D. A., Marshall F. E. et al.* // IAU Circ.–1999.–N 7274.

[28] *Garnavich Stanek* // IAU Circ.–1999.–N 7276.

[29] *Macwardt C.* RXTE observations of the new X-ray transient XTE J1859+226 // Proc. 3rd Microquasar Workshop, Granada, 2000.–in press.

[30] *Uemura M., Kato T., Pavlenko E., et al.* // IAU Circ.–1999.–N 7307.

NOVA–LIKE VARIABLE MV LYR: THE RESULTS OF A PHOTOMETRIC MULTILONGITUDE CAMPAIGN

N. A. Katysheva[1], E. P. Pavlenko[2], S. Yu. Shugarov[1], L. Cook[3], P. Abolmasov[1]

[1] *Sternberg State Astronomical Institute,*
13 Universitetskji pr., 119899 Moscow V-234, Russia
e-mails: nk@sai.msu.ru, shugarov@sai.msu.ru

[2] *Crimean Astrophysical Observatory, Ministry of Ukraine for Education and Science*
Naukove, 98409 Crimea, Ukraine
e-mail: pavlenko@crao.crimea.ua

[3] *Center for Backyard Astrophysics,*
1730 Helix Ct., Concord, CA 94518, USA
e-mail: lcoo@yahoo.com

The cataclysmic variable MV Lyr is nova-like variable, or "anti-dwarf nova". In 1979–1989 years this star similar to other "anti-dwarf novae" spent its time in a high brightness state ($B \simeq 12\overset{m}{.}5$) getting fainter by $2^m - 8^m$ sometimes and returning to the "on" stage. But later its behaviour became non-typical for these stars. The length of its first deep minimum was 10 years. The modern state is characterized by very strong outbursts and very frequent changes of the stages. The periods $0\overset{d}{.}128$ and $0\overset{d}{.}136$ were obtained for 1998 and 1999, respectively. We conclude about a possible relation between the photometric period and brightness.

INTRODUCTION

MV Lyr is one of the brightest cataclysmic variables in the northern sky. It was discovered by Parenago [1] in 1946 as a star with an irregular variability. However, many of its peculiarities had no explanation. It was classified as the nova-like subtype – a VY Scl-star, or "anti-dwarf nova". During the 1979–1989 years, MV Lyr – similar to other "anti-dwarf novae" – spent its time in a high brightness state ("on" stage, $B \simeq 12\overset{m}{.}5$), sometimes getting fainter by $2^m - 8^m$ ("off" stage, $B \simeq 18^m$) and returning to the "on" stage. But later its behaviour became non-typical for nova-like stars. The length of its first deep minimum was 10 years. In this state the outburst amplitude was $1^m - 4^m$. The main characteristics of its variability are the relatively stable intervals in the high and low states with a difference of about 5 magnitudes between states. The detailed description of the long-term photometric behaviour during 1951–1996 are presented in a review by Pavlenko & Shugarov [2] (see references in [2]) and some parameters of the system are in [3]. A longer-term light curve was compiled over 65 years by Kraicheva *et al.* [4]. The outburst in 1997 is described in [5].

The appearance of nova-like stars and, particularly, MV Lyr in the high brightness state is unpredictable: our experience has testified that the brightness of "ordinary" outbursts never reaches the brightness of the real "high" state in MV Lyr. Even the most powerful outbursts are fainter than the high state by 0.5 mag. Since 1994 MV Lyr changed its type of behaviour into a controversial type and we actively awaited a real "prolonged high" state. In 1998 when the brightness of MV Lyr jumped above the intermediate level which distinguishes an outburst from the "real" high state, we started a multilongitude photometric campaign. It was interesting to check: 1) how long such a high state would be lasting, 2) would the light variations be similar as those in the previous high state, or, furthermore, what other light variations could be observed?

OBSERVATIONS

Observations have been carried out using the Zeiss-600 and ZTE 1.25-m telescopes of the Crimean laboratory of the Sternberg astronomical institute, the 38-cm telescope of the Crimean Astrophysical Observatory, the Newtonian 30-cm telescope of the SAI student Observatory (Moscow) and the 44-cm Newtonian telescope of the Center of Backyard Astrophysics (California). The light detectors were CCD-cameras: ST-7 (Moscow, Crimea) and an unfiltered Cookbook 245 camera (California) and the multiplier tube (Crimea). Observations were performed with time resolutions of 16 seconds (California), 1.5 – 2 minutes for other CCD observations (in R-band of Johnson system) and 10 sec for the multiplier tube. The dead times between exposures were of about 13 seconds for the ST-7 and 6 seconds for the Cookbook 245. In total we obtained several thousand measurements over 68 nights in Moscow and in Crimea (1998: JD24450921–1115; 1999: JD2451302–1445) and

18 nights in California (JD2451403–1453). The comparison stars were used from [6] for Crimean-Moscow and GSC 3132:01048 for California data. The Moscow-Crimea data were reduced by using a code by V. Goransky.

THE LONG–TERM LIGHT CURVE

The light curve of MV Lyr over the last 25 years is shown in Fig. 1. The part of the curve in B-band (from 1979 till 1998) has been taken from [5]. The light curve in 1998–99 is plotted (R-band) accordingly our data. Over the first "low" state (1979–98) MV Lyr showed a sequence of relatively short dwarf-like outbursts of various amplitudes and durations (see [6]), they are superimposed on the level of quiet state ($B \sim 17\overset{m}{.}5$). In 1989 this state was rapidly changed to the high one ($B \sim 12\overset{m}{.}5$) that lasted until 1995. Then MV Lyr entered into the state that is different from its previous states: it displays a sequence of strong outbursts of near equal amplitudes ($4^m - 5^m$) that are larger than the larger outbursts of the first low state. Over our campaign (1998–99) MV Lyr displayed two bright outbursts (or, alternatively, one two-humped outburst).

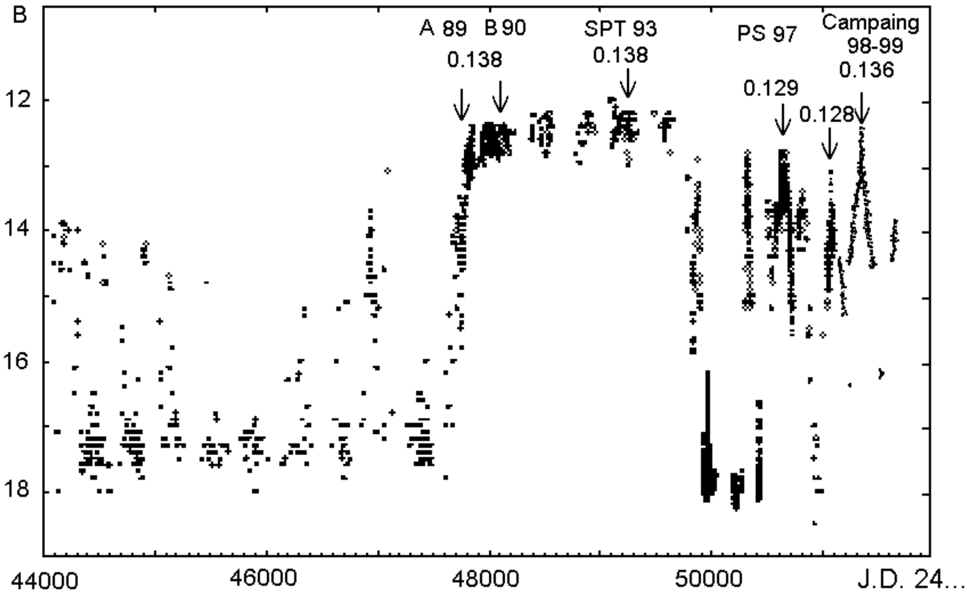

Figure 1: The overall light curve of MV Lyr during 1979–99. The magnitudes B (1979–97) and R (1998–99) are plotted versus Julian date. The arrows indicate the positions of intense observations: A89=[7], B90=[8], SPT93=[10], PS97=[5], 98–99=our campaign

THE SHORT–TERM VARIABILITY

The short-term variability (from minutes to hours) was observed every night. In Fig. 2 we present the several examples of the nightly light-curves for intermediate and a high level of brightness (photoelectric data by Shugarov and CCD data by Cook). The scale of x-axis is of about 4 hours, y-axis – 0.8 magnitudes.

The character of the periodic light variations in the vicinity of orbital period is still puzzling. The spectroscopic observations by Schneider *et al.* [9] and Skillman *et al.* [10] gave the $P_{orb} = 0\overset{d}{.}133$. The photometric behaviours have been studied by several authors, but they have no a final explanation. Borisov [8] found the period $0\overset{d}{.}1379$ observing this star at high level of the brightness and later Skillman *et al.* [10] confirmed the existence of this period for "on"-stage: $0\overset{d}{.}1377$. This value was somewhat longer than the spectroscopic period and was interpreted as possible positive superhumps. Pavlenko and Shugarov [5] found the most likely periods for light variations at $0\overset{d}{.}1294$ (or $0\overset{d}{.}1487$). The first one seemed to be preferable as it was close to that for known NEGATIVE superhumpers. The second period was less likely because of it is placed far above the known empirical relation between the fractional period excess ($P_{sh} - P_{orb}$), where P_{sh} and P_{orb} are the superhump and orbital periods, respectively [12]. In 1998 we observed the star during the less strong outburst and in 1999 during the brighter outburst. Being in the bright state, MV Lyr displayed mean light variations from night to night of up to 0.5 mag. We carefully subtracted this trend from our data in order to find the near-orbital ($3\overset{h}{.}2$) periodicity. More frequent photoelectric data were averaged within the CCD time resolution (1.5–2 min).

We constructed a power spectrum for the three sets of observations: 1) 1998 Crimean–Moscow CCD and photoelectric observations, 2) 1999 Crimean–Moscow CCD and photoelectric observations and 3) 1999 California CCD observations. Periodograms and data folded on these periods are shown in Fig. 3. The UPPER one corresponds to (1), the MIDDLE – to (2) and the LOWER periodogram – to (3). The most significant peak at

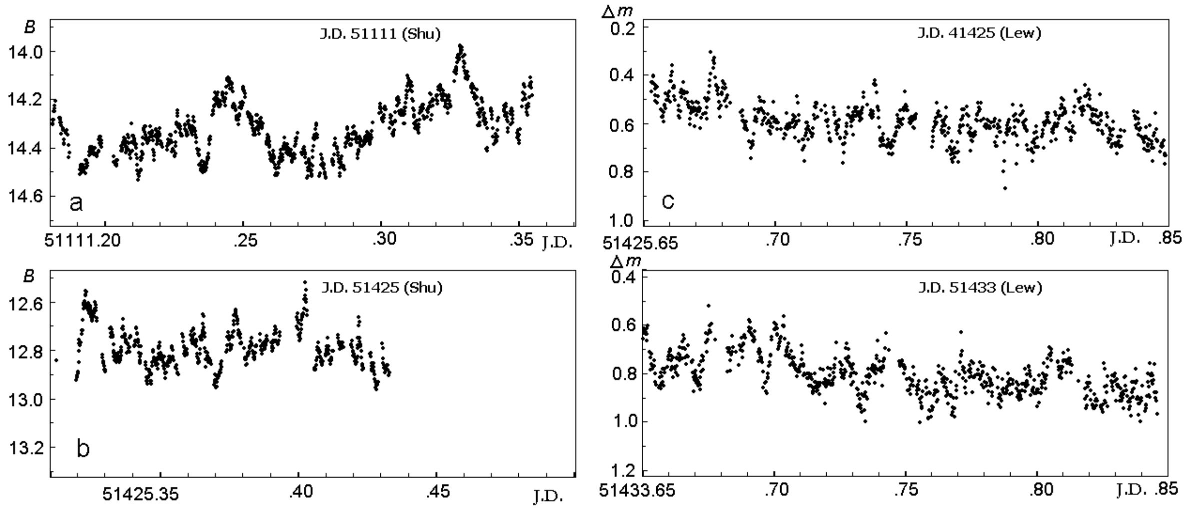

Figure 2: The examples of the short-term variability at the high level of brightness. Shu – photoelectric observations by Shugarov, Lew – CCD observations by Cook

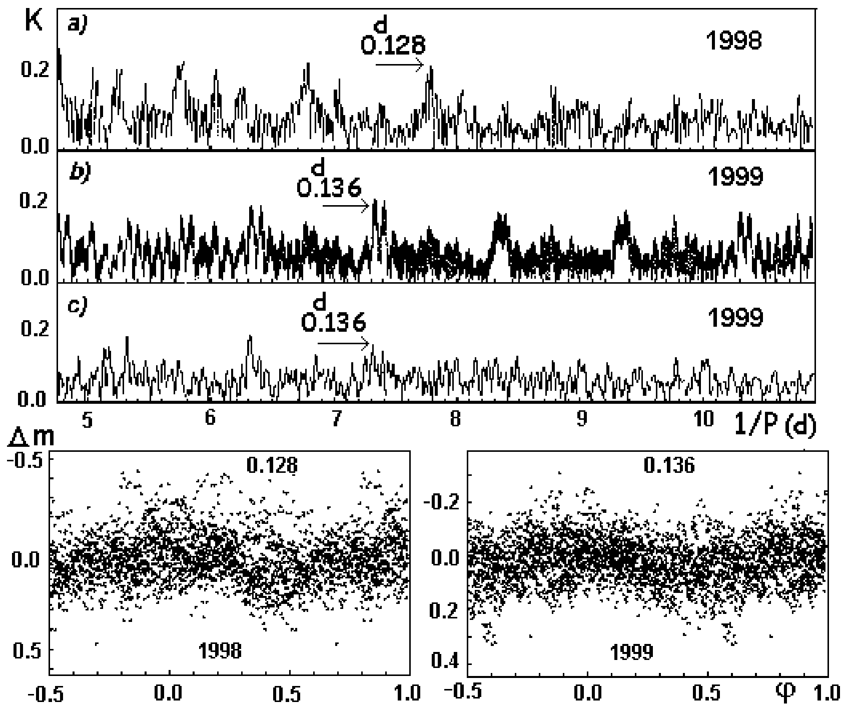

Figure 3: The power spectrum for MV Lyr for the intermediate and high level of brightness (above: a, b, c) and data folded on the best photometric period for 1998 and 1999 years, respectively (below)

the upper periodogram corresponds to the $0\overset{d}{.}1281$. For 1999 the most likely period was $0\overset{d}{.}1361$. The independent analysis of California data coincides with the Crimean–Moscow result, however, the one day alias harmonic $0\overset{d}{.}14$ yields a more significant peak. The data folded on the indicated periods are shown below. It is seen the larger scattering on the light curves are caused by a fast (minute) variability.

DISCUSSION

We gathered all the available data to find the near-orbital light variations [5, 8, 10] and plotted them against the brightness of MV Lyr. The result is given in Fig. 4. It is seen that the photometric period decreases when the brightness decreases. Obviously, it can't be caused by the known decreasing of the superhump period for the SU UMa stars over the course of the superoutburst: the scale of superhump period decrease is smaller. There must be something going on in the disk at larger radius when the system is brighter – and the periodic variation is longer than when the system is fainter.

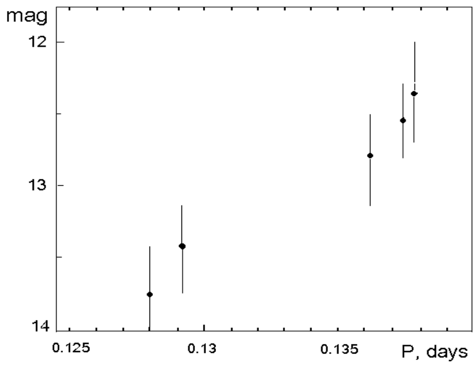

Figure 4: Magnitude versus the identified periods for quasi-periodic variations in MV Lyr. The bars signify the brightness range during intervals when each of the identified periodic variations was prominent

Future observations of this peculiar nova-like star are strongly recommended to study this relation. N. K., S. Sh. grateful for partial support of this work grants from RFBR (00–02–16471, 00–15–96553, 99–02–17589), Astronomy(1.4.2.2.) and Universities of Russia (991786).

REFERENCES

[1] *Parenago P. P.* Twenty seven variable stars // Perem. Zvezdy (Variable Stars).–1946.–**6**.–P. 25–30.

[2] *Pavlenko E. P., Shugarov S. Yu.* MV Lyrae – since Parenago to the present time // Astron. and Astrophys. Transaction.–1998.–**15**.–P. 89–100.

[3] *Cherepashchuk A. M., Katysheva N. A., Khruzina T. S., Shugarov S. Yu.* Highly Evolved Close Binary Stars. Catalog / Ed. A. M. Cherepashchuk.–Brussel: Gordon & Breach Sci. Publ., 1996.

[4] *Kraicheva A., Stanishev V., Spassovska I., Genkov V.* MV Lyr: accretion disk phenomena // Modern Problems of Stellar Evolution / Ed. D. S. Wiebe.–Moscow: Geos., 1998.–P. 222—225.

[5] *Pavlenko E. P., Shugarov S. Yu.* Photometric study of the nova-like variable MV Lyrae in 1997 // Astron. and Astrophys.–1999.–**343**.–P. 909–915.

[6] *Shugarov S. Yu., Pavlenko E. P.* MV Lyr in Low Brighness States: outbursts // Astron. Zh.–1998.–**75**.–P. 420–427.

[7] *Andronov I. L., Borodina I. G., Chinarova L. L., et al.* MV Lyrae: the cataclysmic variable // Soobsh. Spets. Astrof. Obs.–1992.–**69**.–P. 125–135.

[8] *Borisov G. V.* Detection of a photometric periodicity of novalike MV Lyr // Astron. and Astrophys.–1992.–**261**.–P. 154–156.

[9] *Schneider D. P., Young P., Shectman S. A.* MV Lyrae: a spectroscopic study of the low state // Astrophys. J.–1981.– **245**.–P. 644–649.

[10] *Skillman D. R., Patterson J., Thorstensen J. R.* Superhumps in Cataclysmic Binaries. IV. MV Lyrae // Publs Astron. Soc. Pacif.–1995.–**107**.–P. 545–550.

[11] *Pavlenko E. P.* MV Lyr in low brightness states: bursts and periods // Astron. Zh.–1998.–**75**.–P. 231–239.

[12] *Stolz B., Schoembs R.* The SU UMa star TU Mensae // Astron. and Astrophys.–1984.–**132**.–P. 187–194.

PHOTOGRAPHIC OBSERVATIONS OF THE DWARF NOVA V792 CYGNI

L. L. Chinarova, I. L. Andronov

Astronomical Observatory of Odesa National University
T. G. Shevchenko Park, 65014 Odesa–14, Ukraine
e-mail: il-a@mail.od.ua, astro@paco.odessa.ua, *WWW:* www.paco.odessa.ua/~il-a

The photographic observations of V 792 Cyg on the SAI archive plates have been analyzed. The seasonal outburst cycle length drastically changed from $25 - 29^d$ to $\approx 39^d$ between 1967 and 1973 years possibly indicating mass transfer variations at a time scale of few years.

According to the General Catalogue of Variable Stars (Kholopov *et al.*, 1985), V792 Cyg belongs to the UGSS subtype of dwarf novae with an outburst cycle length 26^d:. The star was measured on the archive plates of the Sternberg State Astronomical Institute (Moscow). The table of observations was published by Andronov *et al.* (1993). Then all the data except "fainter than", altogether 219 estimates (JD 2437118 – 46624) were analyzed. The parts of the curve which are most dense covered by observations are shown in Fig. 1.

For smoothing, we have used the method of "running parabolae" (Andronov, 1990). For the determination of the free parameter – the filter half-width Δt – the scalegram was computed, as proposed by Andronov (1997). The unbiased estimate of the standard deviation of the signal from the smoothing function σ_{O-C} as a function of the filter half–width Δt has a plateau at $\Delta t < 18^d$. After this value, the systematic deviations of observations from a smoothing curve drastically increase. The smoothing curve for $\Delta t = 18^d$ is shown in Fig. 1.

From a series of observations we have chosen the intervals with a duration of few cycles, similar to the algorithm of study of another dwarf nova EM Cyg (Andronov & Chinarova, 1996). Results of the periodogram analysis for 5 seasons obtained by a harmonic least squares fit (FOUR program, Andronov, 1994) are presented in the following table:

Table 1: Parameters of seasonal sine fits

Season	T_{start}	T_{end}	n	P	S	r	a
1	37118	37194	11	25.2±0.8	0.86	1.05±0.17	15.80±0.13
2	38876	39034	29	25.5±0.5	0.56	0.80±0.16	15.91±0.12
3	39262	39406	19	29.5±0.7	0.49	0.71±0.19	15.48±0.16
4	41801	41932	24	39.7±2.1	0.41	0.83±0.22	16.11±0.19
5	42507	42684	26	38.6±1.0	0.47	0.56±0.13	15.94±0.09

One may note significant season–to–season variability not only of the effective period P (mean cycle length), but also of the semiamplitude r and phase–averaged mean value a. Besides the periodogram analysis using equal weights of observations, we have applied the wavelet analysis of the data in these seasons. The mean wavelet periodogram was computed by using the algorithm proposed by Andronov (1998). The mean periods obtained by the wavelet analysis in the seasons 4 and 5 (most densely covered by the data) coincide with that of the periodogram analysis, within ~ 0.1 day.

The error estimate listed in Table 1 is overestimated, as the light curve is not harmonic, and an essential contribution to residuals is owed to systematic deviations of the true curve from a sinusoid. This is confirmed also by rather small values of the test – function S. Unfortunately, the small number of seasons does not allow to check up a presence of correlations between the characteristics of seasonal fits similarly to EM Cyg (Andronov and Chinarova, 1996).

A very interesting result is that in two last seasons the cycle duration of 39^d is much larger than in previous seasons. Such drastic changes of the cycle length are usually explained by variations of the accretion rate caused by, *e.g.*, magnetic activity of the red dwarf (Bianchini, 1990; Andronov and Shakun, 1990). It would be desirable to make a more detailed study of this system.

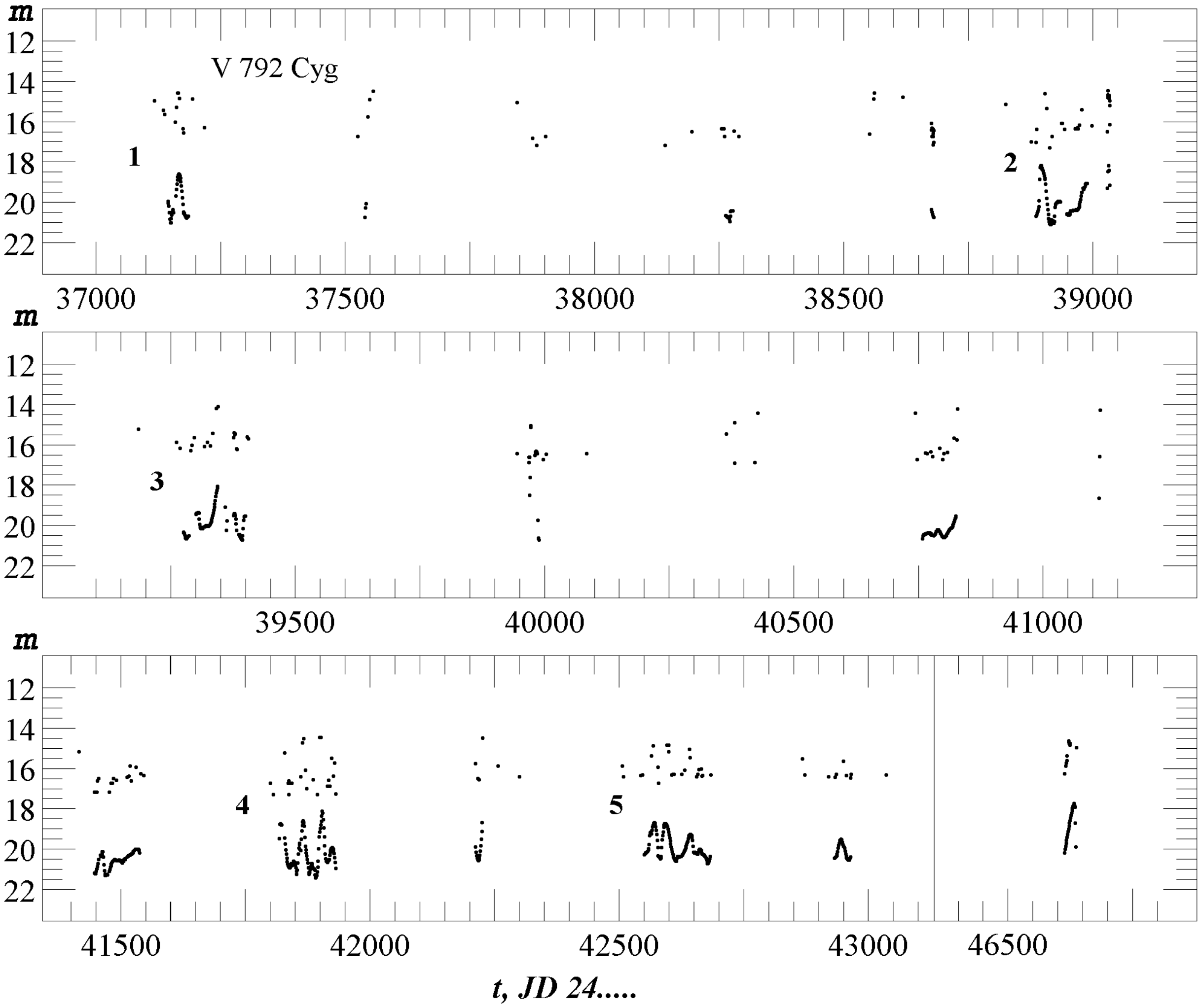

Figure 1: The light curve of V 792 Cyg and its approximation by "running parabolae" with a filter half–width $\Delta t = 18^d$ (shifted by 4^m). The numbers mark the seasons used for the periodogram analysis

REFERENCES

[1] *Andronov I. L.* Smoothing of Experimental Data by using the method of "Running Parabolae" // Kinematics and Physics of Celestial Bodies.–1990.–**6**, N 6.–P. 87–96.

[2] *Andronov I. L.* (Multi-)frequency variations of stars. Some methods and results // Odessa Astron. Publ.–1994.–**7**.–P. 49–54.

[3] *Andronov I. L.* Method of running parabolae: spectral and statistical properties of the smoothing function // Astron. and Astrophys. Suppl. Ser.–1997.–**125**, N 1.–P. 207–217.

[4] *Andronov I. L.* Wavelet analysis of time series by using the method of least squares with supplementary weights // Kinematics and Physics of Celestial Bodies.–1998.–**14**, N 6.–P. 490–511.

[5] *Andronov I. L., Chinarova L. L.* Outburst cycle length variations in the dwarf nova EM Cygni // Odessa Astron. Publ.–1996.–**9**.–P. 9–13.

[6] *Andronov I. L., Shakun L. I.* Alternating Cycle Durations in Dwarf Novae // Astrophys. and Space Sci.–1990.–**169**.–P. 237–240.

[7] *Andronov I. L., Sidorova I. A., Chinarova L. L.* Photographic observations of the dwarf nova stars HN, V792 Cygni, FS Aurigae // Preprint Ukr. Inst. Sci. Tech. Econ. Inform.–1993.–**379-Uk93**.–P. 1–12.

[8] *Bianchini A.* Solar-type cycles in close binary systems // Astron. J.–1990.–**99**, N 6.–P. 1941–1952.

[9] *Kholopov P. N., Samus' N. N., Frolov M. S., et al.* General Catalogue of Variable Stars.–Moscow: Nauka, 1985.–360 p.

MORPHOLOGY OF CIRCUMSTELLAR ENVIRONMENT AND SOME CHARACTERISTICS OF CIRCUMSTELLAR SHELLS OF STARS WITH THE R CORONAE BOREALIS VARIABILITY

A. E. Rosenbush

Main Astronomical Observatory, NAS of Ukraine
27 Akademika Zabolotnoho, 03680 Kyiv, Ukraine
e-mail: `mijush@mao.kiev.ua`

The well-known light minima of stars with the R Coronae Borealis variability are caused by the formation of an additional circumstellar dust shell, the screening shell, inside the permanent shell. Under the assumption of uniform distribution of matter in the circumstellar environment we estimated the optical thickness of the permanent gas–and–dust shell at 0.2–0.7, and its geometrical thickness is no less than 0.4 of its own radius. The wavelength dependence of extinction is close to neutral.
From spectral observations of R CrB itself in the 1985 minimum we traced the transformation of the stellar linear and molecular absorption spectrum to the emission spectrum and established that the fast variation of the U–B colour index by –0.6 in the light decline was caused purely by a change of the spectrum type. The spectrum transformation causes an increase of star brightness in the U, B, and V bands of about 1.4, 0.75, and 0.75 mags, correspondingly.
It is suggested that a high–velocity (>200 km/s) matter stream through the circumstellar environment is the cause of the excitation of the emissions observed during light minima when the photospheric flux is weakening.

INTRODUCTION

The set of unique characteristics of the stars with the R Coronae Borealis (RCB) type variability keeps constantly the high interest to them from observers and theorists. For all this, side by side with the progress in observations, negligibility in the theory is noted.

The principal variability – deep light declines up to 8 mag which last hundreds of days and are caused by dust condensation on the line of sight – remains the phenomenon with many questions, including even the lack of a simple geometric model of the phenomenon [1, 2, 3, 4].

The basis of the modern model is the cloud structure of the circumstellar permanent dust shell [2, 3] when one of the dust clouds in this shell forms on the line of sight, and, as a result, a visual light minimum is observed. This explains the lack of anticorrelation between variations of visual and infrared brightness during a minimum [5]. The lack of clear influence of the permanent shell, in which up to 40 percent of the bolometric luminosity of star is transformed, on apparent characteristics of the star at a light maximum supports the idea of its cloud structure. The difficulties of this model in simulating light minima were well known [3, 4].

As the result of our studies, we concluded that it is necessary to investigate not variables of the R Coronae Borealis type but the R Coronae Borealis phenomenon observed in various objects, for instance, in novae. It is need the high mass loss rate and the enhanced abundance of carbon. The hydrogen is necessary for the phenomenon. Hydrogen deficiency is a consequence of the phenomenon, and its full exhaustion means the cessation of the variability. This view helps us to understand many sides of the phenomenon. At a time we concluded that the 1972 rejection of the model of a spherical dust shell for the interpretation of the R Coronae Borealis phenomenon [5] was not sufficiently justified: not all sides of the phenomenon were known and were taken into consideration. Below we consider some principal consequences from the assumption of the uniform distribution of a matter in the circumstellar environs.

STRUCTURE OF CIRCUMSTELLAR ENVIRONS

Three spherical shells can exist in the environs of a star: two constant shells, the permanent and the fossil (the latter is not connected directly with current light minima), and a temporal, screening one. Both shells are formed in the outflow of mass with a high loss rate estimated at about 10^{-6} mass of the Sun per year.

The radius of permanent shell was estimated at 26 radii of the star or 2340 radii of the Sun [1]. The formation of this shell can occur in the framework of the homogeneous dust nucleation theory by Fadeyev [6], which gives the dust condensation zone radius close to this value. The mass of the shell is of 10^{-6} mass of the Sun.

Sometimes conditions can arise for dust condensation very close to the star, *i.e.*, a screening shell with a radius of 4–10 radii of star is formed [1]. We estimated the full mass of this shell at about 10^{-7} mass of the Sun. The screening shell has its own infrared excess which compensates the weakening of the permanent shell luminosity. The effective temperature of screening shell during its maximum optical thickness drops down to 700–900 K, which is equal to the permanent shell temperature.

OPTICAL THICKNESS OF PERMANENT SHELL

It is known that the permanent shell re–radiates up to 42 percent of the bolometric luminosity of the star itself [5]. If we assume that the shell only re–radiates, we have an indirect estimate of optical thickness of this shell at about 0.7.

FG Sge allows a more direct estimation. Since 1992 it shows the RCB type variability that allows us to compare stellar parameters before and after 1992. Since 1992 FG Sge was at the state of maximal brightness, *i.e.*, it had only the permanent shell, in the end of 1997 – the beginning of 1998, in 1999 and 2000. The difference of average brightness in these periods from the level before 1992 may be due to the extinction in the permanent shell. Our estimate for this is of $0\overset{m}{.}26$. It means that the permanent shell absorbs nearly 20 percent of the bolometric luminosity of the star itself. From published data we estimated that the bolometric luminosity of shell is nearly 25 percent of the bolometric luminosity of the star itself.

SIZE OF DUST PARTICLES

RY Sgr has a number of observations in the UV, where dust particles primarily show an evidence of their existence after condensation.

From the graphic and tabulated data of [7], in addition to the author's results, we can obtain the following data.

Firstly, the light minima were not seen in the UV. The decline of the 240 nm flux during a minimum occurs probably only up to the weakening of visual brightness by nearly 2^m. The following rise of extinction in the visual is not accompainied by a rise of extinction in the UV. According to [8], this may occur by the change of a dust particle size from 0.01 micron to 0.3 micron. The particle density does not increase, otherwise the extinction should continue to increase. From this we can draw the unexpected and interesting conclusion that the light minimum may be considered only as a consequence of a change of the dust particle sizes but not their density, and the dust nuclei are constantly present in the stellar atmosphere.

Secondly, the amplitude of the UV brightness pulsations outside minima is a factor of 1.8 higher, on the average, than in the visual pulsations. The higher amplitude of the UV pulsations can be interpreted as the consequence of condensation of dust particles, their growth up to radii of 0.003 micron and disruption in every pulsation.

The dust particles move away from the star, dragging the gas of the stellar atmosphere.

OUTFLOW VELOCITY AND ORIGIN OF EMISSION LINES

The kinetic energy of helium atoms which are the main gas component of the stellar atmosphere is as high as 800 eV and more at a 200 km/s velocity. This energy is sufficient to excite emission by the interaction with low–velocity atoms. It is known that emissions of C IV] 155.0 nm, C II 133.5 nm, *etc.* are observed beyond minima, *i.e.*, we have a clear indication on their origin in the permanent shell. If there is no dust, there are no UV emissions mentioned above. This is observed in XX Cam and HD 182040.

This transformation of energy occurs on the inner boundary of permanent shell on a level of 10–26 star radii at a density of about 10^{-14}–10^{-15} g/cm or a helium density of about 10^9 cm^{-3}.

Thus, we can identify the region of the origin of sharp emission lines or the "chromosphere" of the star with the zone of dust condensation or with the permanent and screening dust shells.

During light minima the absorption spectrum disappears and the emission spectrum appears. Such transformation determines almost completely the behaviour of U–B and B–V indices observed during a visual minimum.

VARIATIONS OF COLOUR INDICES AND SPECTRUM IN A LIGHT MINIMUM

Based on the R CrB minimum in 1985, for which our extensive spectral observations are available and a detailed photometry is published, we studied the effect of the disappearance of absorption lines and appearance of emission lines on the colour indices of the broad–band photometric U, B, and V system.

We obtained that the key points of spectral changes are three levels of brightness weakening.

I – $1^m_{\cdot}4 - 1^m_{\cdot}6$ – no considerable changes;

II – $2^m_{\cdot}9 - 3^m_{\cdot}4$ – the disappearance of absorptions and the appearance of emissions;

III – $4^m_{\cdot}3$ – the maximum of emission intensity and its following sharp drop.

It is necessary to compare these levels with the light and colour curves. After the light fading to the first level a sharp decrease of U–B began. At the second level, a sharp increase of B–V occurred. At the third level, the brightness is minimal, it is the reverse point of the light curve and a sharp extremum of U–B; the B–V behaviour did not change.

Thus, we make the opposite conclusion that the colour change is due mainly to the change from the absorption spectrum to the emission, and all variations in U–B from $+0^m_{\cdot}3$ to $-0^m_{\cdot}3$ in 1985 were related to this cause only. The B–V variation did not exceed $-0^m_{\cdot}1$. The estimation of spectral transformation on our spectrograms for the 1985 minimum in the B band gives a value of line contribution of about $0^m_{\cdot}75$. Thus, one can say that the lines contribute of about $0^m_{\cdot}75$ in the B band, and their contribution in the V band was slightly smaller. The contribution in the U band was well above, and it reached $1^m_{\cdot}4$. The light minima are distinguished by the intensity of emission lines. Therefore, the colour variations were dissimilar but the cause of variations is the same.

This moves away one of the principal objections against the uniform distribution of a dust in the circumstellar shells.

The well–known loops of a star on the "colour–brightness" diagram during its light minimum should be interpreted with this circumstance taken into consideration.

CONCLUSION

As an addition to the above, we present a possible version of the development of the RCB type variability in FG Sge as a consequence of formation of an uniform circumstellar dust shell.

Years before 1992 FG Sge had a small infrared excess appropriate to of a low dust mass of 4×10^{-10} mass of the Sun. The IR excess was constantly rising, and at some stage of its increase the first RCB minimum occurred. This behaviour is very similar to the RCB phenomenon in the DQ Her novae [1], when the IR excess appeared well before the beginning of the RCB–like visual decline at the transition stage of a nova outburst. *I.e.*, in FG Sge the first RCB minimum was also connected with the formation of a screening shell. At the same time there was no permanent gas–and–dust shell, as no characteristic emissions were observed during the first minimum, but only the blue-shifted circumstellar absorption D Na I lines. It is unlikely that the first dust cloud as a cause of a light fading is formed at once on the line of sight. If there had been so, the "chromospheric" emissions might have been observed in the 1992 minimum as they were observed in the following ones. This supports our assumption about the origin of emissions in the permanent shell.

Since 1972 we have again all grounds to use the dust shell model to interpret the R Coronae Borealis phenomenon. The lack of obvious progress in the theory is caused by the one–sided approach to this "unique" variability. It is a widespread phenomenon, and it is more correct to study the RCB phenomenon, observing various objects, including novae at the transition stage of outburst.

The full text will be published as two papers in the "Astrofizika/Astrophysics" journal in 2000 and 2001.

REFERENCES

[1] *Rosenbush A. E.* R Coronae Borealis type variables: review of observations // Astrophysics.–1996.–**39**, N 1.–P. 78–102.

[2] *Feast M. W.* Introduction review: Some general problems concerning RCB stars // Astron. Soc. Pacif. Conf. Ser.–1996.–**96**.–P. 3–11.

[3] *Clayton G. C.* The R Coronae Borealis stars // Publs Astron. Soc. Pacif.–1996.–**108**.–P. 225–241.

[4] *Rosenbush A. E.* What causes the R Coronae Borealis type minimum: dust cloud or dust shell? // Astron. Soc. Pacif. Conf. Ser.–1996.–**96**.–P. 91–94.

[5] *Forrest W. J., Gillett F. C., Stein W. A.* Infrared measurements of R Coronae Borealis through its 1972 March-June minimum // Astrophys. J.–1972.–**178**, N 3.–P. L129–L132.

[6] *Fadeyev Yu. A.* Carbon dust formation in the R Coronae Borealis stars // Mon. Notic. Roy. Astron. Soc.–1988.–**233**, N 1.–P. 65–78.

[7] *Clayton G. C., Whitney B. A., Stanford S. A., et al.* Observations of R Coronae Borealis stars in declines: empirical arguments for dust formation near the stellar surface // Astrophys. J.–1992.–**397**, N 2.–P. 652-663.

[8] *Draine B. T., Lee H. M.* Optical properties of interstellar graphite and silicate grains // Astrophys. J.–1984.–**285**, N 1.–P. 89–108.

OUTBURST ACTIVITY IN MAGNETIC CATACLYSMIC VARIABLES BY CAM AND QQ VUL

A. V. Halevin[1], **N. M. Shakhovskoy**[2], **I. L. Andronov**[1], **and S. V. Kolesnikov**[1]

[1]*Department of Astronomy and Astronomical Observatory, Odesa National University*
T. G. Shevchenko Park, 65014 Odesa, Ukraine
e-mail: avh@tm.odessa.ua, il-a@mail.od.ua, astro@paco.odessa.ua

[2]*Crimean Astrophysical Observatory, Ministry of Ukraine for Education and Science*
Naukove, 98409 Crimea, Ukraine
e-mail: shakh@crao.crimea.ua

Flare properties in magnetic cataclysmic variables BY Cam and QQ Vul are determined based on the observations obtained at AZT-11 and the Shain mirror telescope of the Crimean Astrophysical Observatory. The UBVRI AZT-11 photometry demonstrates a wide range of color properties of these events. There are significant differences between the flare amplitudes in BY Cam and QQ Vul. The correlation coefficient between the flare amplitude and smoothed brightness variations of QQ Vul is of about 0.83. Similar dependence for the flares of BY Cam is not detected. Some values of the cross-correlation "brightness-polarization" are as large as 0.7. There are no significant differences between the colors of observed flares, as for instance, one could expect for possible "accretion" and "red dwarf" flares.

INTRODUCTION

Magnetic cataclysmic variables are the close binary systems, which consist of a red dwarf filling its Roche lobe, and of a strongly magnetized white dwarf with a surface field of about tens to hundreds MGs (Meggitt, Wickramasinghe, 1984). In the AM Her objects, or "polars", the magnetic field of the white dwarf is sufficiently strong to prevent formation of the accretion disk which is present in non-magnetic or weakly-magnetic cataclysmic variables. In these systems, the gas motion is determined by the balance between the magnetic pressure and ram plus thermal pressure (Mukai, 1988). When the magnetic pressure becomes larger than the ram one, the matter of the ballistic stream starts to be coupled by magnetic field to fall along the field lines to the white dwarf's surface. The extension of the standard model of polars and its observational consequences have been discussed by Andronov (1987a). If we suggest a dipole geometry of the magnetic field, then the active regions on the white dwarf surface lies near magnetic poles. In the ballistic stream, a matter is fragmented by Rayleigh–Taylor instability on to the large diamagnetic blobs with sizes of about 10^9 cm (Hameury, King, Lasota, 1986; Beardmore, Osborne, 1997; Shakhovskoy *et al.*, 1999). Accretion of most massive blobs can produce the outbursts in such systems. The types of instability of accretion structure have been discussed by Andronov (1987b).

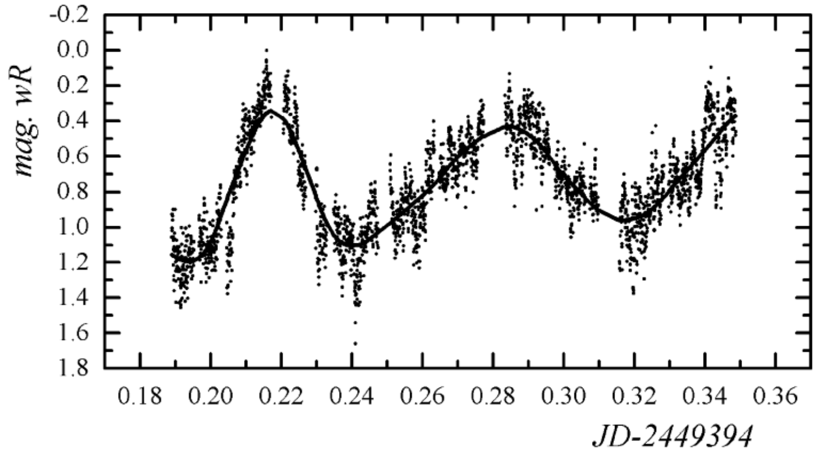

Figure 1: Smoothing by the "running parabolae method" of the orbital variability of BY Cam

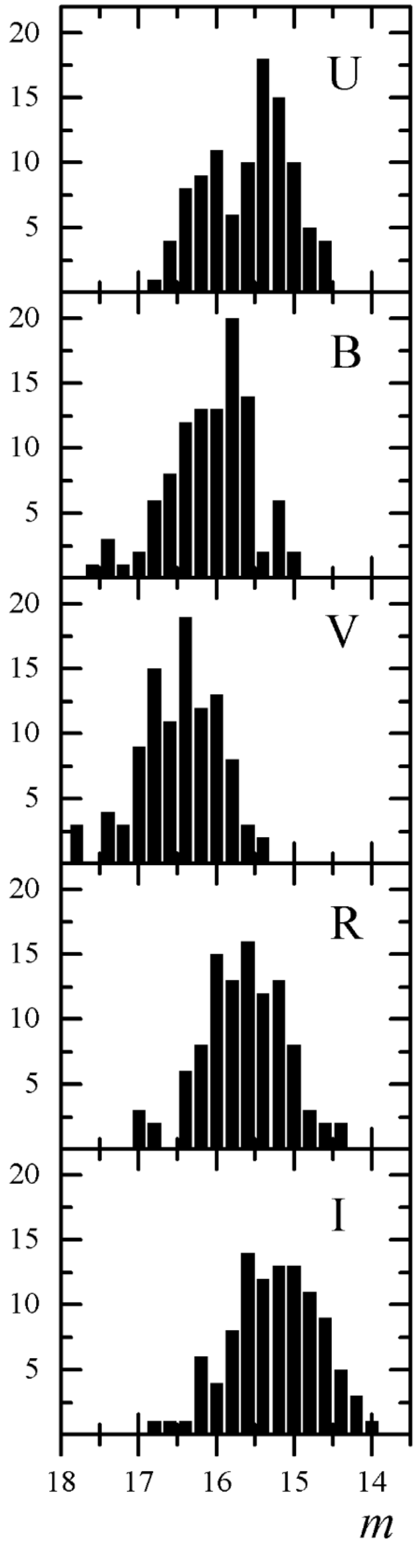

Figure 2: Distribution of the magnitudes of outbursts in UBVRI colours

OUTBURST ACTIVITY OF POLARS

On the photometric curves of polars, one can observe many outbursts, which have relative amplitudes of about $0.^{m}1-0.^{m}5$. They are explained as a product of an accretion of the massive and dense blobs in the gaseous stream onto the white dwarf's surface. Such structures will easier penetrate through magnitosphere and a significant part of the blobs do not fall with generating the accretion shock. These blobs fall directly onto the white dwarf's surface and, if the optical width exceeds ≈ 1, they can produce soft X-ray radiation with a nearly blackbody spectrum (Frank, King, Lasota, 1988). Secondary star in polars (red dwarf) also can be a source of blue outbursts likewise in the UV Ceti – type stars. Blobs, which are accreted with generating an accretion column near magnetic poles, are the sources of an infrared cyclotron radiation, hard X-ray bremsstrahlung radiation and a soft X-ray blackbody radiation re–radiated from the white dwarf's surface (Lamb, Masters, 1979).

So, one can observe 3 different types of outbursts:

1) Blobs accreting through shock wave with blue reflected component and infrared cyclotron spectra;

2) Blue outbursts from blobs, which are accreted directly into the white dwarf's photosphere;

3) Blue UV Ceti type outbursts from the red dwarf.

The first type can be surely distinguished among other types. But the distinction of the accretion and red dwarf's outbursts is much more difficult. In this latter case, only the Doppler tomography can resolve this problem. But some red dwarf's outbursts have a power which is much higher than that of the accretion outbursts. As an example, there is the unprecedented red dwarf's outburst in AM Her, which was observed by Shakhovskoy *et al.* (1993). This blue outburst had an amplitude of about 2^m and a duration of about 50 minutes. So, using multicolor observations, one can resolve only cyclotron outbursts and most powerful red dwarf's ones.

OBSERVATIONS

To study the outburst activity of polars, we have used high time resolution observations of two objects BY Cam and QQ Vul in the wide R filter (0.5–0.75 micron) obtained at the 2.6-m Shain mirror telescope and UBVRI observations obtained at the 1.25-m AZT-11 telescope (Shakhovskoy *et al.*, 1998).

Before measuring the outbursts amplitudes, we had removed orbital variability by using the method of "running parabolae" (Andronov, 1997). This method was applied to study separate outbursts clearly seen at the light curve. The statistical study of characteristics of the "shot" noise produced by overlapping outbursts for these objects was done by Shakhovskoy *et al.* (1999). It was based on the method (Andronov, 1994) using the autocorrelation functions biased by a trend removal and by a finite length.

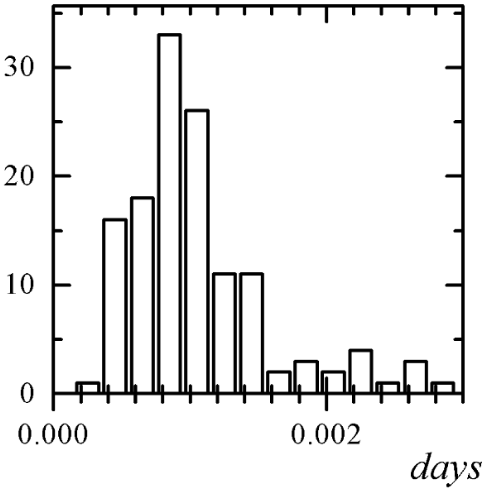

Figure 3: Distribution of the duration of the outbursts

We have determined the values of duration and true magnitudes of 239 outbursts for BY Cam and 56 ones for QQ Vul. Their durations lie in diapason 35 and 120 sec (see Fig. 1). These values correspond to a characteristic blob lengths of about 4–12 R_{wd}, despite the width of such "spaghetti" (Panek, 1980) is of about 1–2 km. There are no significant correlations between the brightness of system during outburst and the state of activity and circular polarization for BY Cam and QQ Vul. Hence, such accretion rate fluctuations can not provide significant polarization variability. This indicates that the accretion region's structure in these systems is complicated and the accretion may take place onto more than one magnetic poles.

Using the multicolour photometry, we had found that the majority of outbursts have two-component spectra with infrared and ultraviolet components (see Fig. 2). Red and infrared emission are explained by a cyclotron radiation of blobs, which penetrate through the shock wave and are cooling in strong magnetic fields above the white dwarf's surface. The ultraviolet component is probably explained by a blackbody re–emitted radiation from the white dwarf's surface, because the bremsstrahlung radiation at these wavelengths is very weak one.

DISCUSSION

The majority of outbursts observed in polars may be explained by accretion processes. As it was shown by Shakhovskoy *et al.* (1993), sometimes blue outbursts are observed in polars, which can be explained by a red dwarf's activity likewise in the UV Ceti–type stars. The resolving of the red dwarf outbursts can be possible, if the amplitude and duration of outburst exceed significantly the values which are typical for accretion events. But, as it is noted by Bonnet-Bidaud *et al.* (2000), possibly one may observe many low–amplitude outbursts of the red dwarf, which characteristics are very similar to the accretion ones, making their identification to be difficult. The energy distribution in the outburst's spectra does not give us a sure answer about their nature, because the most dense blobs, which can be accreted directly onto the white dwarf's surface, also produce blue outbursts. In the future we plan to apply a Doppler tomography of polars for resolving the outburst's locations.

REFERENCES

[1] *Andronov I. L.* "Swinging Dipoles" in Magnetic Close Binary Systems // Astrophys. and Space Sci.–1987a.–**131**.–P. 557–570.

[2] *Andronov I. L.* On the mechanism of the "Noisar" Phenomenon in Magnetic Close Binary Systems // Astron. Nachr.–1987b.–**308**.–P. 229–234.

[3] *Andronov I. L.* Autocorrelation function bias due to a limited number of de-trended observations. Applications to autoregressive models with noise // Astron. Nachr.–1994.–**315**.–P. 353–370.

[4] *Andronov I. L.* Method of running parabolae: spectral and statistical properties of the smoothing function // Astron. and Asrtophys. Suppl. Ser.–1997.–**125**.–P. 207–213.

[5] *Beardmore A. P., Osborne J. P.* Simultaneous rapid hard X-ray and optical variability in AM Herculis: measurement of blob parameters // Mon. Notic. Roy. Astron. Soc.–1997.–**290**.–P. 145–159.

[6] *Bonnet-Bidaud J. M., Mouchet M., Shakhovskoy N. M., et al.* Magnetic field and unstable accretion during AM Herculis low states // Astron. and Astrophys.–2000.–**354**–P. 1003–1010.

[7] *Frank J., King A. R., Lasota J.-P.* The soft X-ray excess in accreting magnetic white dwarfs // Astron. and Astrophys.–1988.–**193**–P. 113–118.

[8] *Hameury J. M., King A. R., Lasota J.-P.* Accretion flows in the non-synchronous magnetic cataclysmic variables // Mon. Notic. Roy. Astron. Soc.–1986.–**218**.–P. 695–710.

[9] *Meggitt S. M. A., Wickramasinghe D. T.* An interpretation of the polarization of AM Herculis type systems // Mon. Notic. Roy. Astron. Soc.–1984.–**207**.–P. 1–8.

[10] *Mukai K.* Accretion streams in AM Her type systems // Mon. Notic. Roy. Astron. Soc.–1988.–**232**.–P. 175–197.

[11] *Lamb D. Q., Masters A. R.* X and UV radiation from accreting magnetic degenerate dwarfs // Astrophys. J. Lett.–1979.–**234**.–P. L117–L122.

[12] *Panek R. J.* On the rapid variability of AM Herculis // Astrophys. J.–1980.–**241**.–P. 1077–1081.

[13] *Shakhovskoy N. M., Alexeev I. Yu., Andronov I. L., Kolesnikov S. V.* Unprecedented flare at red secondary component of AM Her // Cataclysmic variables and related Physics.–Bristol: Inst. Phys. Publ., 1993.–P.237–240.

[14] *Shakhovskoy N. M., Andronov I. L., Kolesnikov S. V., Halevin A. V.* Methodic of measurements of circular polarization by using one-channel photopolarimeter // Kinematics and Physics of Celestial Bodies.–1998.–**14**.–P. 468–472.

[15] *Shakhovskoy N. M., Andronov I. L., Kolesnikov S. V., Halevin A. V.* Blob parameters of accretion streams in magnetic cataclysmic variables // Odessa Astron. Publ.–1999.–**12**.–P. 242–244.

IS VW ARIETIS AN ELLIPSOIDAL BINARY?

T. N. Dorokhova

Astronomical Observatory, Odesa National University
T. G. Shevchenko Park, 65014 Odesa, Ukraine
e-mail: tnd@pulse.tenet.odessa.ua

The well-known δ Scuti type star VW Arietis, a primary component of the binary system BDS 1269, can be an ellipsoidal binary in its turn. This suggestion follows from the ratio of principal frequencies and is supported by the observed spectral features of the star.

The problem of the visual binary system BDS 1269, in which the primary component HD 15165 has the strong metal-deficient chemical composition whereas the secondary component HD 15164 is a quite normal F type star, is discoursed in the literature repeatedly. Although an angular separation between the components, 74 arcsec, is rather large, it was proved that BDS 1269 is a physical association. A long time the opinion prevailed that two stars of different ages were united in a system. It was considered even the suggestion [9] of the capture an old Population II star by a Population I object. This enigmatic primary component is a well-known δ Scuti star, VW Ari.

We obtained the dual-channel photometry of VW Ari at the Mt. Dushak-Erekdag station of Odesa Astronomical Observatory in Oct. 1993 [2]. The star has been observed on the same season in the Xinglong Observatory (China) and Observatorio del Teide (Spain) in the fifth campaign of STEPHI network [7]. I combined three data sets and proposed five-frequency solution: 6.23 c/d, 6.52 c/d, 9.34 c/d, 10.81 c/d, 12.85 c/d [3].

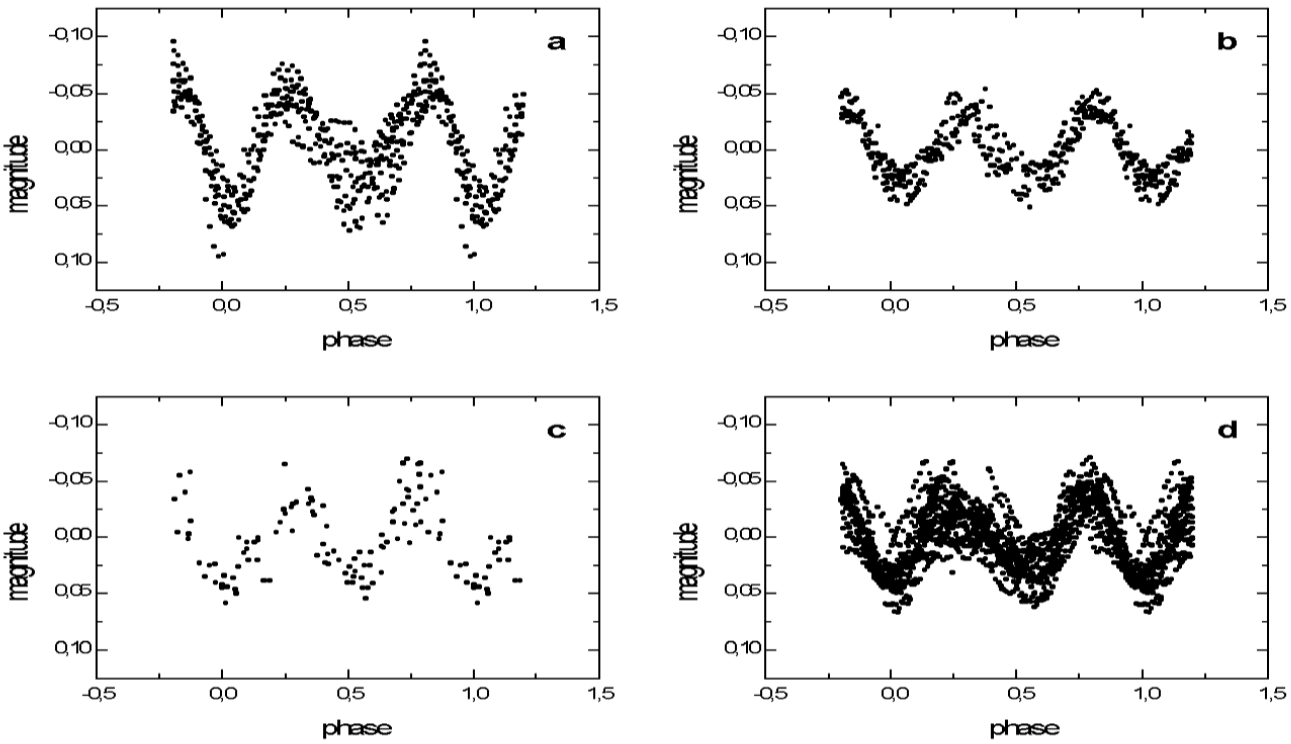

Figure 1: Phase diagrams for different data sets: a - data 1982, McNamara & Horan [8]; b - data 1987, Li & Jiang [6]; c - data 1990–1992, Hipparcos [5]; d - data 1993, STEPHI & Mt. Dushak-Erekdag [3]

Then we collected the previously obtained photometric data of VW Ari and re-analyzed the light curves. We noted that the frequency 9.34 c/d is more pronounced in the data series with the long time spanning (*e.g.*, [8], or [7]), whereas the frequencies close to 10.81 c/d are better seen in the short data runs (*e.g.*, [6]). On the other hand the frequencies 6.23 c/d and 9.34 c/d can be the second and third harmonics of the fundamental frequency 3.11 c/d from the exact relation *3.11 : 6.23 : 9.34=1:2:3*.

One can suppose that we deal with the light curve of a binary with an orbital period approximately $0^d_.321$. We fold the data with this period to see the phase diagram. In Fig. 1 the phase diagrams of the period of $0^d_.321$ are presented for the data from 1982 to 1993. All the double-wave curves have one special feature: one wave has less amplitude and more scatter than another wave, which is more regular. The phase diagrams are very similar to the diagrams of ellipsoidal binaries, for example, V2082 Cyg or DG Dra (see [5]).

By its spectral features VW Ari could be related to λ Bootis stars [1]. It is interesting that Farraggiana and Bonifacio [4] in their detailed review of the peculiar features of λ Bootis stars noticed that such features can arise in composite spectra of close binaries.

This way it is possible that the primary component of the binary system BDS 1269 consists of two normal stars and the previous problem of chemical peculiarity is solved. However, at present we can state, the problem of VW Ari is rather complicate and not solved yet, taking into account that, apparently, one of its components pulsates. Therefore, the measurements of radial velocities can resolve the problem.

REFERENCES

[1] *Chernyshova I. V., Andrievsky S. M., Kovtyukh V. V., et al.* The unusual A-star VW Ari: chemical composition revisited // Proceedings of the 26th Meeting and Workshop of the European Working Group on CP stars / Eds P. North, A. Schnell, J. Ziznovsky.–Tatranska Lomnica, 1998.–P. 332–334.

[2] *Dorokhova T. N., Dorokhov N. I., Mkrtichian D. E.* Photometry of low amplitudes δ Scuti type star VW Ari // Odessa Astron. Publ.–1997.–**10**.–P. 104–108.

[3] *Dorokhova T. N.* Unification of VW Arietis observations obtained in multisite campaign // Kinematics and Physics of Celestial Bodies.–1999.–**15**.–P. 160–170.

[4] *Farraggiana R., Bonifacio P.* Haw many λ Boo stars are binaries? // Astron. and Astrophys. Suppl. Ser.–1999.–**349**, N 2.–P. 521–534.

[5] Hipparcos and Ticho Catalogues: 1997, ESA SP-1200.

[6] *Li Z., Jiang S.* Multiple frequencies pulsation of the δ Scuti variable BDS 1269A // Acta Astrophysica Sinica.–1993.–**13**, N 5.–P. 233–244.

[7] *Liu Y. Y., Jiang S. Y., Michel E., et al.* On the multiperiodicity of the δ Scuti star BDS 1269A (VW Arietis) // Astron. and Astrophys. Suppl. Ser.–1996.–**120**, N 1.–P. 179–186.

[8] *McNamara B. J., Horan S. J.* The remarkable multiple mode δ Scuti star BDS 1269A // Astrophys. J.–1984.–**282**, N 3.–P. 741–747.

[9] *Rucinsky S. M.* The unique visual binary BDS 1269 // Acta Astronomica.–1978.–**28**, N 4.–P. 545–554.

SOME GROUPS OF THE REGULARITIES IN THE CYCLE–TO–CYCLE CHANGES IN THE MIRA–LIKE VARIABLES

V. I. Marsakova, I. L. Andronov

Odesa National University, Department of Astronomy
T. G. Shevchenko Park, 65014 Odesa, Ukraine
e-mail: vlada@mail.od.ua, il-a@mail.ru

The analysis of different light curve variations based on the characteristics of large number of individual pulsational cycles of 53 LPVs was done. Six groups of regularities are described: 1) cyclic period and amplitude variations; 2) variations of light curves (period, amplitude and slopes) of stars at the stage of helium-shell flash; 3) variations of light curves of stars of C and S spectral classes (main result is the mean brightness variations); 4) various behaviour of objects which are transient between Miras and semiregular variables; 5) secular increase or decrease of amplitude; 6) variations of the hump at ascending branch.

DATA PROCESSING

Long period variables (LPVs) are the pulsating stars which characterized by significant changes of the light curves from one pulsating cycle to another. The research of long-term changes of period and light curves of the LPVs leads to the important information on their pulsation and evolution and can give new criteria of their classification. In our research, the characteristics of large quantity of individual pulsational cycles were obtained for 53 LPVs and the analysis of different light curve variations was done.

To study cycle-to-cycle changes in the Mira variables, the dense series of data during long time interval (about several dozens or hundreds of periods) are necessary. To study changes from one cycle to another in Mira variables and some Mira-like semiregular variables we used the data in the long interval of time (80 years) from the AFOEV and VSOLJ databases.

The "asymptotic parabola" (Marsakova & Andronov, 1996) and "running parabola" and (Andronov, 1990; Andronov, 1997) fits were applied to determine the characteristics of extrema. Thus, the "asymptotic parabola" method was applied for majority of the stars, but the "running parabola" method was applied in a case of strong irregularities or hump at the ascending branch.

We have obtained the following characteristics of individual cycles: moments and magnitudes of extrema, and differences between them – individual periods, amplitudes, *etc.* The asymmetry, magnitude of the hump on ascending branch, slopes of the ascending and descending branch, mean brightness of the branches were also calculated. Analysis of variations of these characteristics with time and correlation analysis of them have been done. Analysis is analogous to one described by (Andronov & Marsakova, 1996).

RESULTS

As the result of our research, several groups of the typical light curve variations of 53 LPVs were distinguished and their characteristic long-term behaviour is thoroughly analyzed:

1) Cyclic secondary variations of the period, amplitude and other characteristics.

Variations of a period and amplitude, which are cyclic ones in the observational interval were found in some stars. But there are some difficulties: characteristic times of this cyclisity is of about 15000–23000 days, so we can't study more than 2–3 long cycles. In the T Cep star these variations of period, amplitude and characteristics of the hump in ascending branch were the most prominent ones. The cross-correlation analysis for these characteristics was done. Correlation coefficient between period and amplitude changes is equal to 0.93 and shift is equal to 3 pulsational cycles. Correlation coefficient between changes of amplitude and magnitude of hump is equal to 0.85 without shift (Marsakova & Andronov, 2000).

2) Stars with progressive period changes

Two types of light curve transformation were pointed out (Marsakova, 2000): in R Aql and R Hya a period decrease is followed by very strong amplitude decreasing, in T UMi a fast period decreasing is followed by significant changes of curve sharpness. It is suggested (Wood & Zarro, 1980; Gal & Szatmary, 1995) that T UMi is in the beginning of helium shall flash, but R Aql and R Hya are in the more later stages of it.

3) Light curve changes of C- and S-Miras

As the result of our research (Marsakova & Andronov, 1999) we note the following:

— Strong chaotic cycle-to cycle changes of all parameters of the light curves;
— Absence of significant systematic changes of period or small abrupt changes of period ($< 0.5^P$) which is typical for other Miras;
— Absence of significant amplitude variations which leads to the following:

  — Correlation between magnitude of different points of the curves (especially typical for C-stars).
  — Light curves of C-stars are very noisy during one cycle;
  — For the some stars a correlation between period and amplitude was obtained;

— A correlation between time between maxima and corresponding magnitude differences was obtained for the some stars;
— A correlations between period and magnitude in maximum was obtained for 5 from 10 S-stars;
— Strong variations of mean brightness:

  — cyclic: S Cep, U Cyg, V CrB, probably some other stars,
  — decreasing: V CrB, W Cas and probably T Cam, S Cas and V Cnc.
  Cyclic variations are more clear in C-stars. Trends appear in both groups (C and S) of stars and they also are observed in two stars of M-type: R LMi, R Dra.

— There are some moments in some stars when the photometric behaviour changes abruptly. Y Per: at J.D. 2447700 the variability changes from the Mira to the semiregular with double maxima but with keeping the value of the mean period. S UMa: abrupt change of O-C behaviour was appeared near J.D. 2430000 (change of the mean period and its stability) and, simultaneously, the double maxima in the light curve was appeared.
— Low amplitudes of C-Miras and high amplitudes of S-Miras are the well known facts;

Characteristics times of mean brightness changes are close to ones obtained in models (Winters *et al.*, 1994) taking into account the influence of dust-shell on light curves of LPVs.

4) Mira-like SRa variables

There are some variables (10 stars were studied, 9 SRa and Mira Y Per – classification of GCVS (Kholopov *et al.*, 1985)) which are transient between Miras and SRa. They have relatively small amplitudes and their amplitudes are significantly being changed with time. Most of these stars show the light curve variations which are close to ones detected in C-Miras (mean brightness variations, small amplitudes of Mira-like variability less than 2^m) and keep the constant mean period during the observed interval. So, Miras and some SRa variables of the C spectral type may be distinguished in one close group. There are semiregular variables in this group which are different from Miras only by small (about 2^m) amplitudes. And there is a subgroup of stars for which Mira-type and semiregular variability changes in the different time intervals (Y Per also belongs to this group).

5) Stars with secular amplitude changes

Also we have found 7 stars with amplitude increasing or decreasing (except the stars with progressive period changes). Among them are only 2 stars with amplitude decreasing, they are sure classified as semiregular variables: V Boo and RU Cyg. The SS Vir star was classified as semiregular in GCVS, but amplitude of its pulsation had to be increased with time and become more than 2^m in recent time, so this star can be reclassified into Miras.

6) Stars with humps at ascending branch

It was found that hump in some variables is more correlated with magnitude of minimum, but in other stars – of maximum. Correlations between mean hump duration and asymmetry of mean light curves as well as anticorrelation between mean hump duration and amplitude of mean light curves have been found.

Some regularities in the cycle-to-cycle variations were found such as follows:

- period-amplitude relations,
- correlation between period and difference in maximal magnitudes,
- correlation between magnitudes and various points of curve,
- correlation between slope of the descending branch and magnitude of minimum, *etc.*

Some papers are available at *http://ila.webjump.com* .

Acknowledgements. The authors are thankful to the observers contributing to the AFOEV and VSOLJ databases for their active monitoring of LPVs. These data were used for the current analysis.

REFERENCES

[1] *Andronov I. L.* Smoothing the experimental data by the method of "running parabolae" // Kinematics and Physics of Celestial Bodies.–1990.–**6**, N 6.–P. 87–90.

[2] *Andronov I. L.* Method of running parabolae: spectral and statistical properties of the smoothing function // Astron. and Asrtophys. Suppl. Ser.–1997.–**125**.–P. 207–213.

[3] *Andronov I. L., Marsakova V. I.* Phase curve changes and humps in Mira-type star U Her // Astrophys. and Space Sci.–1998.–**257**.–P. 49–61.

[4] *Gal J., Szatmary K.* T Ursae Miroris: Mira star with rapidly decreasing period // Astrophys. J.–1995.–**297**.–P. 461–464.

[5] *Khopolov P. N., Samus N. N., Frolov M. S., et al.* General Catalogue of Variable Stars, 4-th ed.–**2**.–1985.–360 p.

[6] *Marsakova V. I.* Variations of light curve parameters in Miras with progressive period changes // Astron. Soc. Pacif. Conf. Ser.–2000.–**203**.–P. 130.

[7] *Marsakova V. I., Andronov I. L.* Fitting the astronomical signals with asymptotic branches // Odessa Astron. Publ.–1996.–**9**.–P. 127–130.

[8] *Marsakova V. I., Andronov I. L.* Strong changes in photometrical behaviour of Carbon Miras // Odessa Astron. Publ.–1999.–**12**.–P. 205–209.

[9] *Marsakova V. I., Andronov I. L.* Unusual secondary variations in the Mira star T Cep // Astron. Soc. Pacif. Conf. Ser.–2000.–**203**.–P. 131–132.

[10] *Winters J. M., Fleischer A. J., Gauger A., Sedlmayr E.* Circumstellar dust shells around long-period variables. II. Theoretical lightcurves of C-stars // Astron. and Astrophys.–1994.–**290**.–P. 623–633.

[11] *Wood P. R., Zarro D. M.* Hellium-shell flashing in low-mass stars and period changes in Mira variables // Astrophys. J.–1981.–**247**.–P. 247–256.

IS THE SMALL–AMPLITUDE CEPHEID SZ TAU A POSSIBLE OVERTONE PULSATOR?

I. A. Usenko[1], V. V. Kovtyukh[1], S. M. Andrievsky[1], N. I. Gorlova[1], V. G. Klochkova[2], V. E. Panchuk[2]

[1] *Astronomical Observatory of Odesa National University*
T. G. Shevchenko Park, 65014 Odesa, Ukraine
e-mail: igus@deneb.odessa.ua

[2] *Special Astrophysical Observatory, Russian Academy of Sciences*
369167 Nizhny Arkhyz, Karachai-Cherkess Republic, Russia

On the base of 8 high-resolution CCD spectra, obtained by the 6-m telescope of SAO RAS (Russia) and 4-m telescope of KPNO (USA), we have determined the mean values of atmospheric parameters for small-amplitude Cepheid SZ Tau. Since SZ Tau is a member of NGC 1647 open cluster and calibrating object for "period – luminosity" relation, it is very important to specify the former [6] supposition that this Cepheid is an overtone pulsator, thereas [5] *HIPPARCOS* data provides fundamental tone for it. The mean T_{eff} and $\log g$ values determined spectroscopically can confirm this fact, in case that if the Turner's distance value for SZ Tau is true. Nevertheless, the chemical composition analysis shows that SZ Tau is the Cepheid in post red supergiant stage. The evolutionary stage of this object is discussed.

INTRODUCTION

The $3^{d}\!.15$ small-amplitude Cepheid (DCEPS) SZ Tau belongs to the galactic NGC 1647 open cluster. A connection between the distance to open cluster and absolute magnitude value for SZ Tau, – 542 ± 4 pc and $-3^{m}\!.09 \pm 0^{m}\!.04$ is considered in [6]. Combination of these data with the different SZ Tau radius values from 34.2 $R_{\odot}$ to 40.42 $R_{\odot}$ [6] has suspected it as overtone pulsator. According to period-luminosity relation for Cepheids open clusters $M_V = -1.15 - 2.94 \log P_0$, derived in [6], this DCEPS is a pulsator in *first* overtone. But for determination of luminosity and distance values, Turner [6] has used photoelectric UBV photometry data. Since the interstellar reddening is very irregular in the cluster area and SZ Tau is a marginal object, Turner's $E_{B-V} = 0^{m}\!.29 \pm 0^{m}\!.01$ value may be mistaken. And this fact, for in turn, has an influence on interpretation of SZ Tau pulsation tone. Nevertheless, [5] using *HIPPARCOS* trigonometric parallax value, estimated the distance to SZ Tau near 321 pc with corresponding values $M_V = -1^{m}\!.94$ and $E_{B-V} = 0^{m}\!.294$, respectively.

Therefore, we have set the following tasks for SZ Tau investigations:

• Using high-resolution spectrograms of this object, to determine its atmosphere parameters. The most interesting are the mean T_{eff} and $\log g$ values.

• To compare these data with those ones, obtained by other authors. To determine the luminosity value and to interpret the pulsation tone.

• To make the analysis of metallicity and CNO–elements abundance, as the key indicators of yellow supergiants evolution.

OBSERVATIONS AND RESULTS

In this work we have used high-resolution spectra of SZ Tau (echelle-spectrometer LYNX, 6-m telescope of SAO RAS; resolving power 24000, $S/N \approx 70 - 100$; and 4-m telescope KPNO; resolving power 80000, $S/N \approx 110$, respectively). The CCD spectra have been reduced using the DECH20 code. In our analysis, we did not use lines with equivalent widths greater than 150 mÅ. The internal accuracy of the equivalent widths is of the order of 5–10%. This estimate is based on the comparison of values derived from the lines present in two overlapping spectral orders.

A modified method of the spectroscopic analysis has been applied for SZ Tau. This method is described in detail by [1]. The principal difference between modified approach and standard technique of the spectroscopic analysis consists in the usage of Fe II lines for microturbulent velocity and gravity determination, instead of Fe I lines that are usually applied for this aim, but more affected by non-LTE effects. The use of Fe II lines, which seems to be free from significal influence of non-LTE effects, allows one to avoid some problems of standard spectroscopic analysis giving physically more acceptable results. Specially developed method of the T_{eff} determination based on the use of different spectroscopic criteria ([2] for yellow supergiants has been used in present study to derive this important atmosphere parameter for SZ Tau. WIDTH 9 code ([4] and Kurucz's grid of atmosphere models were employed to calculate the relative iron and CNO–elements content for this Cepheid. The results of calculations are presented in Table 1.

Table 1: Atmosphere parameters, Fe and CNO content for SZ Tau

Spectrum, No.	Phase (*)	T_{eff}	$\log g$	V_t	[Fe/H]	[C/H]	[N/H]	[O/H]
s15907 (SAO)	0.812	6075	2.20	4.70	+0.05	–0.19	+0.59	–0.19
s15908 (SAO)	0.820	6075	2.20	4.70	+0.05			
1 (KPNO)	0.963	6207	2.10	3.60	–0.01	–0.25	+0.51	–0.29
2 (KPNO)	0.279	5994	2.30	3.70	+0.03	–0.25	+0.43	+0.02
3 (KPNO)	0.593	5839	2.00	3.60	+0.04	–0.26	+0.47	–0.05
4 (KPNO)	0.924	6170	2.30	4.30	–0.01	–0.17	+0.42	–0.03
5 (KPNO)	0.237	6037	2.10	3.50	–0.03			
6 (KPNO)	0.549	5811	2.00	4.00	+0.03	–0.29	+0.43	+0.07
Mean		6042	2.15	4.00				

Reference: * – Phases values from [3]

DISCUSSION

Thus, we can conclude that:

1) Using the 8 high-resolution spectra, obtained on the different points of SZ Tau phase curve, we have obtained the mean value of $T_{eff} = 6042$ K. This result has a good agreement with [6] one (6062 K), determined by multicolour photoelectric photometry.

2) Luminosity values, derived from different radius estimates, show that SZ Tau position on the P – L diagram is very vague. If [6] data are true ($M_V = -3^m_.09 \pm 0^m_.04$), then they really corresponded to pulsation in the $first$ overtone. On the contrary, in case of [5] distance value ($M_V = -1^m_.94$), SZ Tau pulsates in $fundamental$ tone. The same conclusion we can make, estimating the mean $\log g$ value.

3) Abundance analysis shows that SZ Tau has solar metallicity, but CNO–elements content is testified to fact that the DCEPS is the post red giant star and it crossed Cepheids instability strip not for the first time.

4) SZ Tau evolutionary mass values lie in range from 3.7 to 5 $M_\odot$. Comparison with evolutionary tracks for a such mass value with $Z = 0.02$ testifies that the best fit for the cause of second crossing of Cepheids instability strip corresponds to mean radius values 38.6 $R_\odot$ for 5 $M_\odot$ and 27.8 $R_\odot$ for 4 $M_\odot$.

REFERENCES

[1] *Kovtyukh V. V., Andrievsky S. M.* // Astron. and Astrophys.–1999.–**351**.–P. 597.

[2] *Kovtyukh V. V., Gorlova N. I., Klochkova V. G.* // Sov. Astron. Lett.–1998.–**24**.–P. 372. (in Russian).

[3] *Kiss L. L.* // Mon. Notic. Roy. Astron. Soc.–1999.–**297**.–P. 825.

[4] *Kurucz R. L.* // The Stellar Populations of Galaxies: IAU Symp. 149 / Eds B. Barbuy, A. Renzini.–1992.–P. 225.

[5] *Szabados L.* // HIPPARCOS-Venice"97": Proc. ESA Symp., Venice, Italy, ESA SP-402, 1997.–P. 657.

[6] *Turner D. G.* // Astron. J.–1992.–**104**.–P. 1865.

Session 5. Some Aspects of a Stellar Evolution

Convener: Dr. Yakiv Pavlenko (MAO NASU, Ukraine)

THE SINGULAR SOURCE OF ENERGY OF STARS

B. E. Zhilyaev

Main Astronomical Observatory, NAS of Ukraine
27 Akademika Zabolotnoho St., 03680 Kyiv, Ukraine
e-mail: zhilyaev@mao.kiev.ua

INTRODUCTION

A fundamental suggestion of this work is that the luminosity of stars accounts for, not by the orthodox thermonuclear scenario alone, but the coupled system of the nuclear source and the black hole in their center. In general terms, the black hole (BH) works as a gravitational heat engine, so that the rate of accretion sets the pace for heat release. Such a BH reactor of $M = 10^{-5} M_{\odot}$ may be competitive in power with the nuclear burning for the Sun over the course of billion years. Apparent deficit of the solar neutrino flux count in favor of the coupled source of energy.

METHODS AND RESULTS

Let us suppose that the small BH exists in the center of a star and explore the consequences stemmed from this hypothesis. We may assume that small relict BH created in the early Universe [2] was captured by star from space or occurred for some another reason. The advanced theoretical treatment of both thermo- and gas-dynamical structure of BH in dense thermostat is that to be still studied in detail. Now, we are interested in the overall picture of the problem.

In the ambient BH atmosphere the radiation pressure is considered to balance the gravity in the equilibrium state. The radiation pressure arises because of the accretion of gas onto the BH when some part α of the original mass-energy of the particles is radiated away. So, in treating the problem the Eddington solution [3] is appropriate to use with a sufficient degree of accuracy. For hydrogen plasma with the Thomson scattering the BH luminosity should be no more than Eddington's limit

$$L_c = \frac{4\pi G m_p c M}{\sigma_T} = 3 \times 10^4 L_{\odot} \frac{M}{M_{\odot}}, \tag{1}$$

where G is the gravitational constant, m_p is the proton mass, c is the speed of light, σ_T is the Thomson cross-section and M is the BH mass. If the accretion rate sets the pace for energy release at a level of Eddington's limit, the BH mass growth rate is given by Equation [5]

$$-\varphi(R)\frac{dM}{dt} = \frac{GM}{R}\frac{dM}{dt} = L_c\,, \tag{2}$$

where $-\varphi(R) = \alpha c^2$ is the effective gravitational potential. For a Schwarzschild and a Kerr black hole α is of about 6% and 42%, respectively [4]. The BH mass growth rate may be written as

$$\frac{1}{M}\frac{dM}{dt} = \frac{4\pi G m_p}{\alpha c \sigma_T} = 7 \times 10^{-17} \alpha^{-1} \sec^{-1} = (0.5\,\alpha\, Gyr)^{-1}. \tag{3}$$

Surprisingly that in the equilibrium state a BH growth is a long lived process with e-folding rise time of billion years.

As expected, specific boundary conditions have to stabilize the neighborhood of the BH. The stability arises because the gravitational reactor is immersed into huge reservoir of dense heat-retaining matter, of the kind of "prison stability". The behavior of an unstable mode can be investigated if it is viewed as oscillator. Strong restoring forces are supplied by the radiation pressure with increasing the accretion rate and by the gravity and the outer pressure with its decreasing.

It is pertinent to cite one illustrative example. The contribution of the BH of $M = 10^{-5} M_{\odot}$ to the total solar luminosity is estimated to be 30% according to (1). The BH size is of about 1 cm, its effective temperature $T_{\rm eff} \sim 10^8$ K, the mass growth rate $\sim 10^{10}$ g/s. Adopting the central density and temperature $\rho = 160$ g/cm^3, $T = 1.5 \times 10^7$ K, as given by Allen [1], we get for the speed of accretion a value of about 10^8 cm/s. The speed of sound at the center of a solar model is equal to 4×10^7 cm/s. Its value increases to 1.1×10^8 cm/s if the more realistic central temperature $T = T_{\rm eff}$ has been adopted, as mentioned above. Hence, it seems likely that the subsonic accretion would result in the vicinity of the BH.

Of great importance that such a low mass BH is capable to initiate the essential rearrangement of solar structure. The striking central temperature peak may produce the convective core.

Within the self-consistent solar model based on the coupled source of energy the thermonuclear burning has decreased in importance with the trend towards smaller thermal and, in particular, neutrino fluxes. This latter presents the most challenging question of contemporary solar physics.

The availability of coupled source of energy may have an immense action on stellar evolution. For above cited example it is easy to see that growth of the BH mass up to 10^{-4} $M_{\odot}$ tends to increase the solar luminosity by several times in comparison with its present value on a time scale of $\sim 10^9$ years. In all appearance, the truthful stellar evolutionary tracks may differ significantly from those described by the present-day theory based on the orthodox thermonuclear scenario.

The question now arises of whence it follows that black holes can exist in stellar interior? There are not any explanations for this. All we can do is point at the Earth's life paradigm. Whence came life on the surface of the Earth? No one knows this. However, we live and explore life.

REFERENCES

[1] *Allen C. W.* Astrophysical Quantities.–University of London: The Athlone Press, 1973.

[2] *Carr B. J. and Hawking S. W.* // Mon. Notic. Roy. Astron. Soc.–1975.–**168**.–P. 399.

[3] *Eddington A. S.* The Internal Constitution of the Star.–Cambridge, 1926.

[4] *Petropoulos B. and Mavrogiannis M.* // Proc. 2nd Hellenic Astron. Conf., Thessaloniki.–1995.–P. 490.

[5] *Zeldovich Ya. B. and Novikov I. D.* Theory of Gravitation and Stellar Evolution.–Moscow: Nauka, 1971. (in Russian).

NEW PHYSICS OF THE BROWN DWARF AND L–DWARF ATMOSPHERES

Ya. Pavlenko

Main Astronomical Observatory, NAS of Ukraine
27 Akademika Zabolotnoho, 03680 Kyiv, Ukraine
e-mail: yp@mao.kiev.ua

Our main attention is paid for the formation of the spectra of the so-called objects of the Bottom of the Main Sequence. Substellar objects and brown dwarfs lie beyond the lower right end of the Main Sequence. Masses of the very red objects with the low-luminosity are too low for possible nuclear burning of the light elements (hydrogen, lithium or even deuterium) to stop their contraction.

INTRODUCTION

Spectral energy distributions of the recently discovered L-dwarfs are different from the conventional M-dwarfs. Ti and V atoms in atmospheres of M-dwarfs form oxygen molecules, which are the main absorbers governed the shapes of their SED's. Some atoms in atmospheres of L-dwarfs are significantly depleted into grain particles due to the low temperatures and high pressures regime. The differences in the observed SED's have prompted the use of a new spectral class for the coolest dwarfs [1, 2], first from the times of implementing classical MK classification. L-dwarfs are the low-mass objects, which occupy the part of the HR diagram with $1200 < T_{\rm eff} < 2200$ K.

INITIAL MASS FUNCTION

The observed mass distribution of LMS for Pleiades shows a slow positive slope toward lower masses [11]. The sample of the low-mass objects is the most populated in the Galaxy. Still, their contribution to the total barionic mass of the Galaxy is rather small ($< 5 - 10\%$). Moreover, recent observations of σ Ori open cluster provides new sample of the low-mass objects with $M < 15 M_J$, where M_J is the mass of Jupiter ($M_J = 0.001 M_\odot$) [12].

L– AND M–DWARFS: OPTICAL SPECTRA

Speaking strictly, only M-dwarfs are the *conventional* objects yet. Their spectra are governed by the molecular bands of TiO and VO of the huge strengths (Fig. 1, see also [13, 14]). The spectral energy distribution in the spectrum of young Teide1 brown dwarf [15] – member of the Pleiades open cluster, is shown in Fig. 1. Rebolo *et al.* [16] observed strong Li I 6708 Å line in the Teide1 spectrum. This is evidence that the lithium has been preserved in the atmosphere of the brown dwarf, although more massive M-dwarfs burnt their lithium.

L-dwarf spectra show quite different picture (Fig. 2):
– TiO and VO molecular bands are weak or even absent there.
– A strong head of (O-O) band of CrH appears at 8600 Å [21].
– We see very strong alkali resonance doublets: Cs, Rb, Na, Li.
– The strongest features in L-dwarf spectra are formed by the lines of K I + Na I resonance doublets [5, 6].
– Perhaps, BRI0021-024 presents an intermediate (L — M) case.

ALGORITHM OF FORMATION OF L–DWARFS SPECTRA

The photospheres of L-dwarfs are moved toward high pressure regions due to the very low temperatures and low opacities (Fig. 4). Some specific physical conditions are realized there:
– Depletion of atoms into molecular species (Pavlenko *et al.*, 1995).
– Formation of the dust particles (see Tsuji *et al.* [19] and [6] for more details).
– The "dusty" opacities due to the absorption and/or scattering processes.

Invited paper.

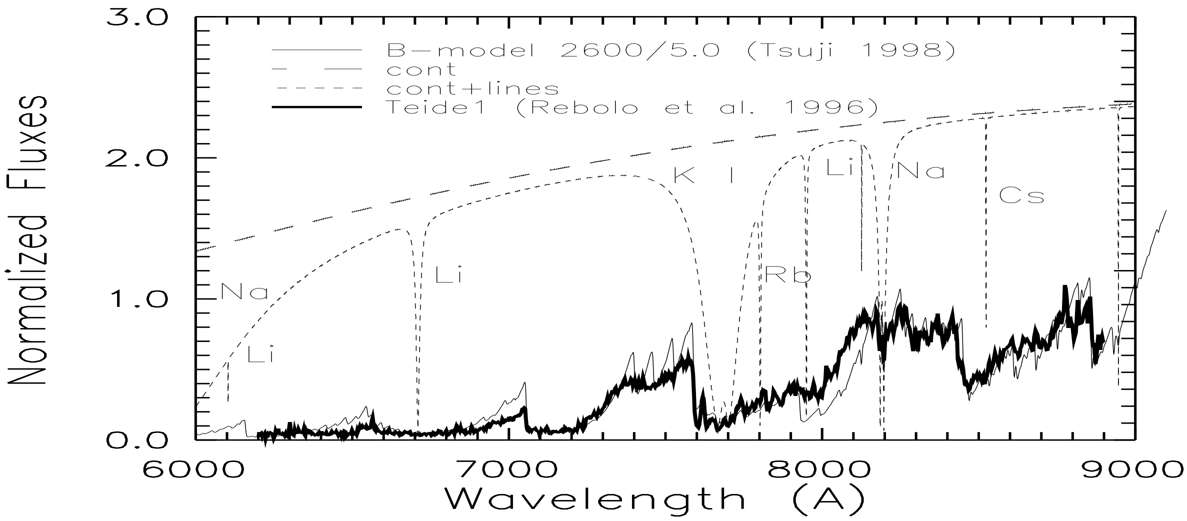

Figure 1: Comparison of the observed spectrum of Teide1 with theoretical spectra computed with use of the C-model atmosphere ($T_{\rm eff}$ = 2600 K, $\log g = 5.0$) by Tsuji [18]. Positions of the strongest atomic features which can be observed in M- and L- spectra are shown. The spectrum of Teide1 is clearly dominated by TiO and VO molecular bands whose abundances have been determined by chemical equilibrium. We have only considered the standard sources of opacities in these computations

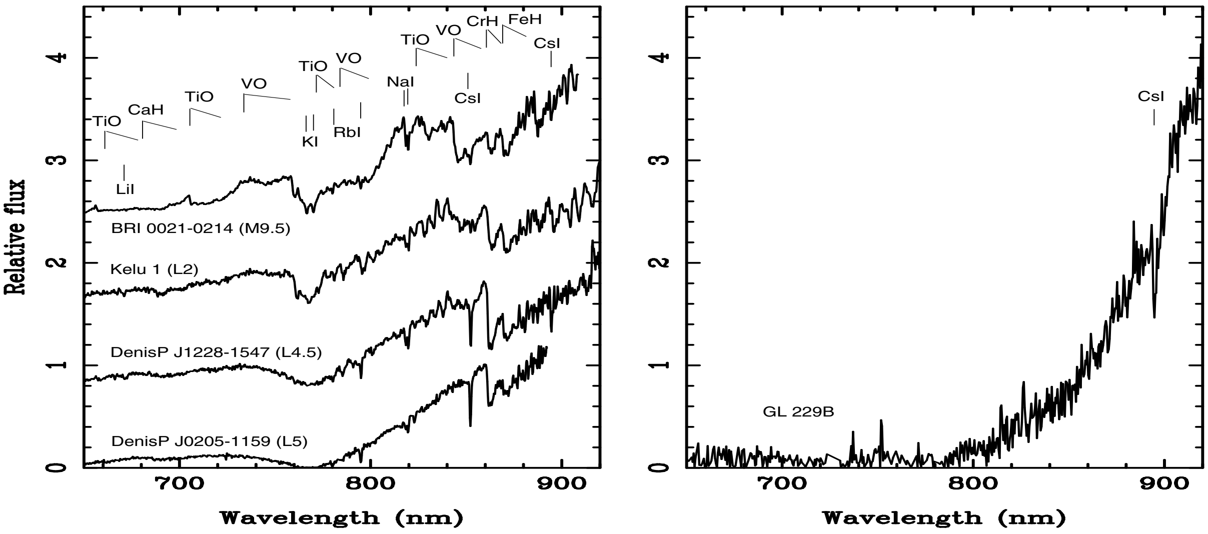

Figure 2: Far-red optical spectra for our sample. The observations are those of Kelu 1, DenisP J1228–1547 and DenisP J0205–1159 (KeckII spectrum). Data for BRI 0021-0214 and Gl 229B have been collected from Martín *et al.* [22] and from Schultz *et al.* [23], respectively. Spectral types for the L-dwarfs follow the classification by Martín *et al.* [1]. Spectra in the left panel have been shifted by 0.8 units for clarity. Identification of some atomic and molecular features is provided in the top of the figure (from PZR2000)

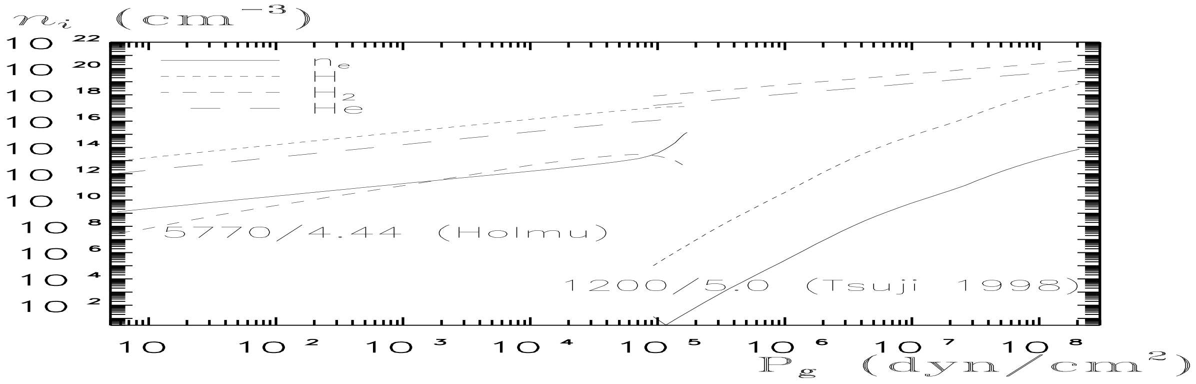

Figure 3: A comparison of the HOLMU solar model atmosphere [17] and 1400/5.0 C-type model atmosphere of L-dwarf [18]

DUST, MODEL ATMOSPHERES & SPECTRA

In the case of L-dwarfs we find a complicate case of the formation of the spectral energy distribution. Obviously, we have a temperature sequence of L-dwarf spectra [8]. Furthermore, following Tsuji (1998) we may suppose different cases of the impact of dusty opacities on model atmospheres: A-models are computed for the dusty-free media, physical conditions in B and C-models correspond to the dynamical equilibrium "dust-gas" phase transition, and the segregation of the dust and gas, respectively.

Equivalent widths of the resonance K I and Na I doublet lines are huge due to the broadening by atoms and molecules of hydrogen. Damping constants are of about $0.1-10.0$ instead of $0.005-0.1$ in the solar atmosphere. Residual fluxes of the lines of K I and Na I resonance doublets computed for the 1200/5.0 C-model by Tsuji [18] are shown in the Fig. 4. Formally, the computed equivalent widths of the doublets exceed 3 and 6 kÅ, respectively!

The comparison of the computed and observed spectra seems to be more interesting. In Fig. 5 we show the fit of the computed SED for a 1200/5.0 C-model atmosphere by Tsuji[18] to the observed spectrum of DenisP J0205-1159. We used a few additional suggestions to fit L-dwarf spectra [8]:

– there are some superdepletions of the molecular species in the atmospheres of L-dwarfs.

– there are some additional opacity (AdO) sources due to the additional absorption or scattering.

LITHIUM TEST

"Lithium test" was proposed by Rebolo *et al.* [24] to tell brown dwarfs from a sample of low luminosity dwarfs. Pavlenko *et al.* [25] shown that we could observe Li lines in spectra of young brown dwarfs which are "de-facto" the late-type M-dwarfs. Observations completed later confirmed the results [16, 26], see also [27].

"Lithium test" can be applied in the case of L-dwarfs. In that case, however, the main problem is not the molecular bands, but the huge wings of K I and Na I doublets and the "dusty" opacities. Furthermore, in some cases we can see the substellar meteorology effects – Li lines may by affects by the variable opacities provided by the dust clouds. Nevertheless, lithium lines should be detectable in the spectra of L-dwarfs or even T-dwarfs for $\log N(Li) \sim 3.0$ (*i.e.*, "cosmic value", see [8] for more details).

DEUTERIUM TEST

The "deuterium test" was proposed recently to tell brown dwarfs from a sample of low luminosity dwarfs. The problem here seems to be much more severe, than in the case of the "Lithium test". We may expect the appearance of the heavy water (HDO) bands in the IR part of cool dwarfs. However, there are strong bands of the "normal" water, *i.e.*, H_2O. Molecular bands of HDO and H_2O computed for Partrige & Schwenke line lists (*http://george.arc.nasa.gov/˜dschwenke*) and 1200/5.0 C-model by Tsuji (1998) are shown in Fig. 6. *In that case,* the bands of HDO for the normal "cosmic" deuterium abundance (D/H $\sim 10^{-5}$) should disappear under the bands of the more abundant H_2O.

SUMMARY (NEW PHYSICS)

New class of astrophysical objects discovered recently provides new challenges for the modern astrophysics. In fact, ultracool dwarf's family consists of various population, where substellar objects/brown dwarfs, low-mass

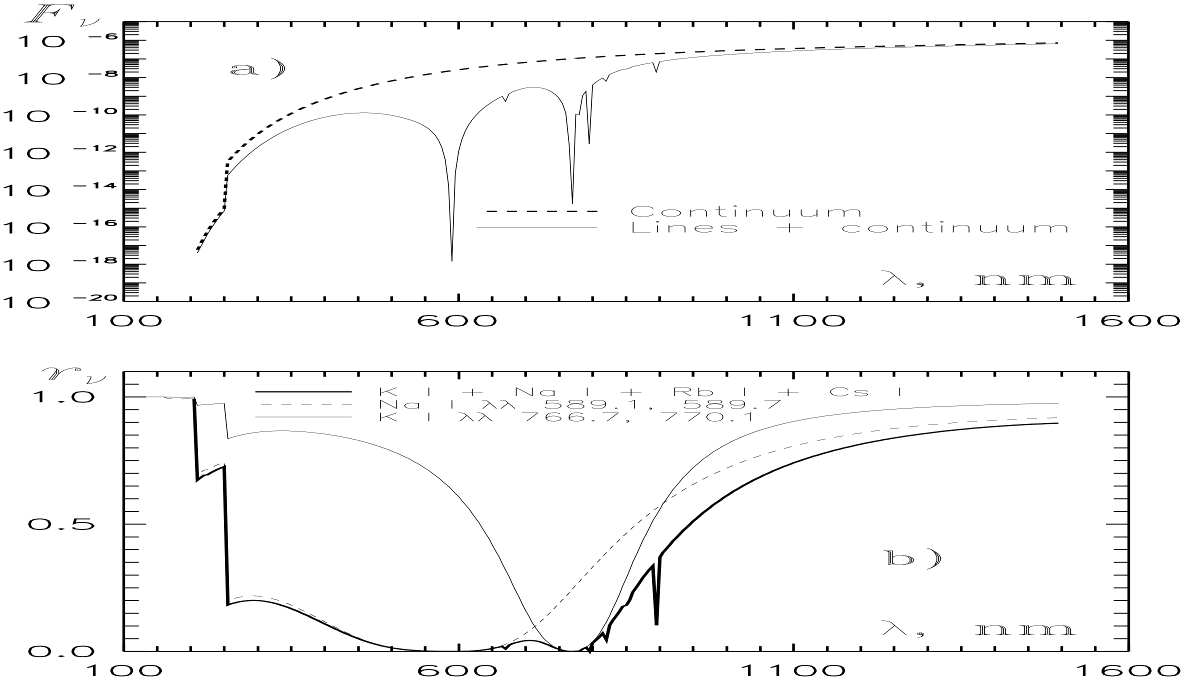

Figure 4: Theoretical fluxes and profiles of K I and Na I resonance doublet lines computed for the 1200/5.0 C-model atmosphere by Tsuji [18]

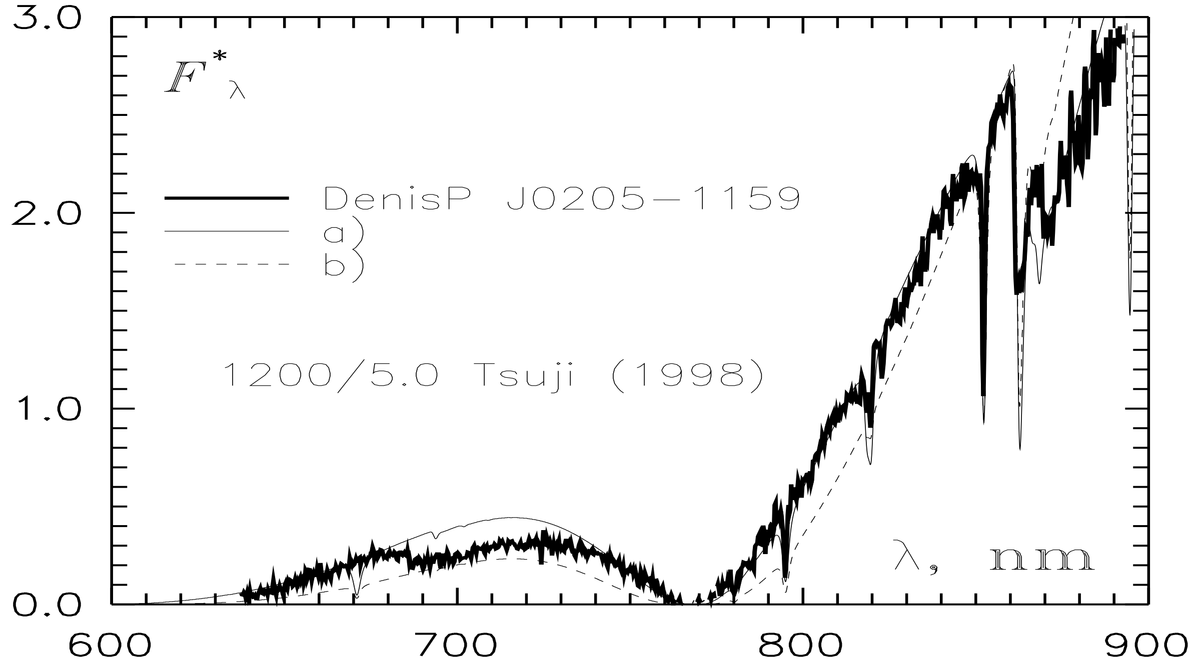

Figure 5: Fit to DenisP J0205-1159 spectra

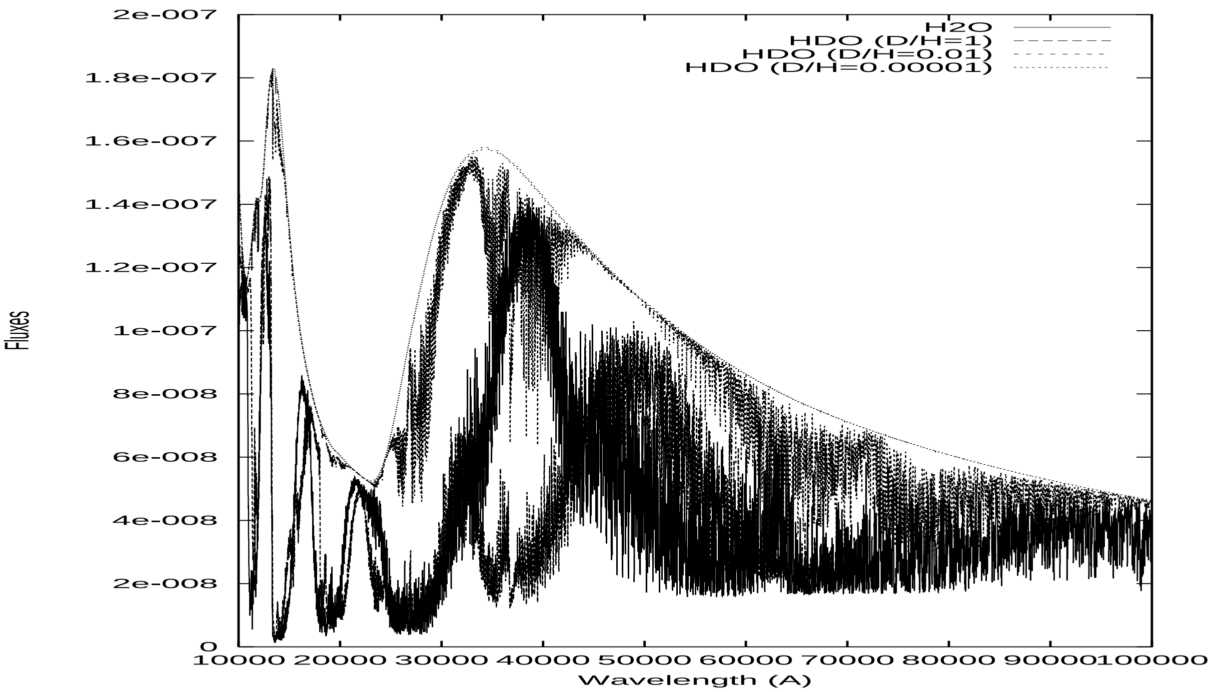

Figure 6: Bands of H_2O and HDO computed for 1200/5.0 C-model by Tsuji (1998)

dwarfs/stars and big (superbig?) planets can be found. Being the M-dwarfs at the beginning of their evolution, these objects then move to the L-dwarfs region. Time scale of the evolution depends on some parameters – masses, initial abundances, rotation, binarity, *etc.*

The situation with their emitted radiation regions (photospheres) is very specific. Indeed, we work in the boundary region between classical stellar astrophysics and canonical planetary science. Plasma of the atmospheres of the ultracool dwarfs exists in the low temperatures as well high pressures regime. Our knowledge about the physical process in the cool dense plasma is far from being perfect. Optical spectra of the coolest dwarfs are governed by the wings of K I and Na I doublets. Their profiles are pressure broadened. Moreover, to describe their shape we should use non-conventional methods for calculating the parameters of their broadening. In this case the micro and macro physics meet in L-dwarfs atmospheres.

Bands of TiO and VO spectra are weak or even disappear in L-dwarfs spectra. Obviously, Ti and V atoms should be depleted into dust particles, still the mechanisms of the dust formation cannot be modeled in detail. Then, dusty particles may provide original opacity.

No doubts, these effects should affect the temperature structure of atmospheres of L-dwarfs.

Acknowledgements. I am grateful to SOC and LOC Members of the Conference who have been kind enough to invite me to present these views. The study has been carried out in tight collaboration with my colleagues. Financial support of the project was provided by the Small Research Grant of the American Astronomical Society.

REFERENCES

[1] *Martin E. L., Delfosse X., Basri G., Goldman B., Forveille T., Zapatero Osorio M. R.* Spectroscopic Classification of Late-M and L Field Dwarfs // Astron. J.–1999.–**118**.–P. 2466–2480.

[2] *Kirkpatrick J. D., Reid I. N., Liebert J., et al.* Dwarfs cooler than "M": the definition of spectral type "L" using discoveries from the 2 Nicron All-Sky Survey (2MASS) // Astrophys. J.–1999.–**519**.–P. 802–833.

[3] *Allard F., Hauschildt P. H.* Model atmospheres for M(sub)dwarf stars. I. The base model grid // Astrophys. J.–1995.–**445**.–P. 433–453

[4] *Pavlenko Ya. V.* Analysis of the spectra of two Pleiades brown dwarfs: Teide1 and Calar3 // Astrophys. and Space Sci.–1997.–**253**.–P. 43–53.

[5] *Pavlenko Y. V.* Depletion of TiO and spectra of the coolest brown dwarfs // Odessa Astron. Publ.–1997a.–**10**.–P. 76–77.

[6] *Pavlenko Ya. V.* The lithium test and the spectra of late M-dwarfs and brown dwarfs: condensation effects // Astron. Rep.–1998.–**42**.–P. 787–792.

[7] *Tinney C. G., Delfosse X., Forveille T., Allard F.* Optical spectroscopy of DENIS mini-survey brown dwarf candidates // Astron. and Astrophys.–1998.–**338**.–P. 1066–1072

[8] *Pavlenko Y., Zapatero Osorio M. R., Rebolo R.* On the interpretation of the optical spectra of L-type dwarfs // Astron. and Astrophys.–2000.–**355**.–P. 245–255.

[9] *Strauss M. A., Fan X., Gunn J. E., et al.* The discovery of a field metane dwarf from Sloan Digital Sky Survey commissioning data // Astrophys. J. Lett.–1999.–**522**.–P. L61–L64.

[10] *Burgasser A. J., Kirkpatrick J. D., Brown M. E., et al.* Discovery of four field methane (T-type) dwarfs with the two Micron all-sky survey // Astrophys. J. Lett.–1999.–**522**.–P. L65–L68.

[11] *Zapatero Osorio M. R., Rebolo R., Martin E. L., et al.* Brown dwarfs in the PLeiades Cluster // ASP Conf. Ser. 154. The Tenth Cambrige Workshop on cool stars, stellar systems and the Sun / Eds R. A. Donahue, J. A. Bookbinder.–1998.–P. 1912.

[12] *Mundt R., Bailer-Jones C. A. L., Zapatero Osorio M. R., et al.* Discovery of very young free-floating giant planets in the Sigma Orionis Cluster // Astronomishe Gesellshaft Abstract Series.–1998.–**17**.–P. 11.

[13] *Kirkpatrick J. D., Henry J. T., McCarthy D. W. Jr.* A standard stellar spectral sequence in the red/near-infrared: classes K5 to M9 // Astrophys. J. Suppl. Ser.–1991.–**77**.–P. 417–440.

[14] *Pavlenko Ya. V.* Analysis of the spectra of two Pleiades brown dwarfs: Teide1 and Calar3 // Astrophys. and Space Sci.–1997.–**253**.–P. 43–53.

[15] *Rebolo R., Zapatero Osorio M. R., Martin E. L.* Discovery of a brown dwarf in the PLeiades star cluster // Nature.–1995.–**129**.–P. 129.

[16] *Rebolo R., Martin E. L., Basri G. W., Zapatero Osorio M. R.* Brown dwarfs in the Pleiades cluster confirmed by the lithium test // Astrophys. J. Lett.–1996.–**469**.–P. L53–L56.

[17] *Holweger H., Muller E. A.* The photospheric barium spectrum: solar abundances and collision of Ba II lines with hydrogen // Solar Phys.–1974.–**39**.–P. 19–27.

[18] *Tsuji T.* Dust in very cool dwarfs // Low-Mass Stars and Brown Dwarfs in Stellar Clusters and Associations / Eds R. Rebolo, E. Martin, M. R. Zapatero Osorio.–La Palma.–1998.–P. 43.

[19] *Tsuji T.* Dust formation is stellar photospheres: a case of very low mass stars and a possible resolution on the effective temperature scale of M dwarfs // Astron. and Astrophys.–1996.–**305**.–P. L1–L4.

[20] *Gurvitch L. V., Veitz I. V., Medvedev V. A., et al.* Thermodynamic properties of the individual materials.–Moscow: Nauka, 1979.–551 p.

[21] *Pavlenko Ya. V.* CrH Molecular bands in the spectra of late-type dwarfs // Astron. Rep.–1999.–**43**.–P. 847–752.

[22] *Martin E. L., Rebolo R., Zapatero-Osorio M. R.* Spectroscopy of New Substellar Candidates in the Pleiades: Toward a Spectral Sequence for Young Brown Dwarfs // Astrophys. J.–1996.–**469**.–P. 706–714.

[23] *Schultz A. B., Allard F., Champin M., et al.* First results from the Space Telescope imaging spectrograph: optical spectra of Gliese 229B // Astrophys. J. Lett.–1998.–**492**.–P. L181–L184.

[24] *Rebolo R., Martín E. L., Magazzu A.* Spectroscopy of a brown dwarf candidate in the alpha Persei open cluster // Astrophys. J. Lett.–1992.–**389**.–P. L83–L86.

[25] *Pavlenko Y. V., Rebolo R., Martin E. L., Garcia Lopez R. J.* Formation of lithium lines in very cool dwarfs // Astron. and Astrophys.–1995.–**303**.–P. 807–818.

[26] *Martin E. L., Basri G., Zapatero Osorio M. R.* The Lithium Test in Young Brown Dwarf Candidates // Astron. J.–1999.–**118**.–P. 1005–1015.

[27] *Pavlenko Y. V.* A Lithium Test and Modeling of Lithium Lines in Late-Type M Dwarfs: Teide1 // Astrophys. Rep.–1997a.–**41**.–P. 537–542.

ELECTRODYNAMICS OF THE MAGNETOSPHERES OF COLLAPSING STARS

V. Kryvdyk

Department of Astronomy, Taras Shevchenko National University
6 Glushkova, 03022 Kyiv, Ukraine
e-mail: kryvdyk@mail.univ.kiev.ua

The particles acceleration and its non-thermal emission in the magnetospheres of collapsing stars are considered. The magnetic field in magnetosphere increases considerably, when the star is compressed under the collapse. The charged particles will be accelerated in this field. These particles will generate radiation when moving in the magnetic field. The effect can be observed by means of modern instruments [7]. The radiation flux grows during a stellar collapse in millions times and can be observed in the form of radiation pulse with duration equal to the stellar collapse time. This flux depends on the distance to the star, its magnetic field, and the particle spectrum in the magnetosphere. In this paper the radiation fluxes are calculated for various collapsing stars with the initial dipole magnetic fields and the initial power-series, relativistic Maxwell, and Boltzmann particles energy distributions in the magnetosphere.

INTRODUCTION

Collapse begins when the mass of stellar core exceeds the Chandrasekhar bound, and the star become dynamically unstable. The star will compress and its radius will decrease. After that, the star can evolve by several ways. The first way is that a star explodes and loses its mass. The collapse of a massive star ($M_\odot \leq 3 \div 6M_\odot$) may results in the formation of a neutron star or a black hole. The neutron star formation can accompany by the explosion and loss of mass. This phenomenon is observed as a supernova star. The star with smaller mass collapses to a white dwarf [10, 11], the process may be accompanied by the formation of a planetary nebula. The second way is realized when a star collapses without the loss of mass. In this case it is very difficult to observe the collapse and hitherto there are no strong astronomical data conforming the evidence of this stage.

A star emits the electromagnetic radiation under the collapse. In this paper the non-thermal radiation from the collapsing stars with the initial dipole magnetic field at the non-relativistic stage is studied and the method for the observation of collapse using the data on this radiation is proposed.

MAGNETOSPHERES OF COLLAPSING STARS

The external electromagnetic field of a collapsing star is given by [2, 7]

$$B(r,\theta,t) = (1/2)F_0 R r^{-3}\left(1 + 3\cos^2\theta\right)^{1/2} \tag{1}$$

Here $F_0 = B_0 R_0^2$ is the initial magnetic flux of star with the radius R having the initial radius R_0 and the initial magnetic field B_0.

The field structure and particles dynamics in the magnetosphere are influenced by three factors: particles pressure, collisions, and star rotation. As follows with the detail analysis [7], these effects can be neglected during the collapse.

The initial concentrations of charged particles in the magnetosphere have been chosen as the power-series, relativistic Maxwell, and Boltzmann distributions which can be described, respectively, by the formulas

$$N_1(E) = K_C E^{-\gamma}; \tag{2}$$

$$N_2(E) = K_M E^2 \exp(-E/kT); \tag{3}$$

$$N_3(E) = K_B \exp(-E/kT). \tag{4}$$

Here K_C, K_M, K_B are the spectral coefficients; k is the Boltzmann constant; E is the particles energy and T is the temperature in the magnetosphere; γ is the power spectrum.

PARTICLE DYNAMICS AND SPECTRUM CHANGE IN THE MAGNETOSPHERE

The particles dynamics and their acceleration during the collapse are considered by means of the method of adiabatic invariant so as magnetosphere plasmas is frozen in magnetic field and is a collision-free. The particles energy change in this case as the results of two mechanisms. The first mechanism is a betatron acceleration of particles in the variable magnetic field, the second one is a bremsstrahlung energy loss in this field. For the resulting rate of particle energy change in the magnetosphere we get [7]:

$$\frac{dE}{dR} = \left(\frac{dE}{dR}\right)_a + \left(\frac{dE}{dR}\right)_s = a_1 \left(\frac{2GM}{R_*}\right)^{\frac{1}{2}} \left(\frac{R_*-1}{R^3}\right)^{\frac{1}{2}} E - a_2 F_0^2 R^2 E^2 r^{-6}, \tag{5}$$

Here $a_1 = (5k_1/3)(3\cos^4\theta + 1.2\cos^2\theta - 1)(1+3\cos^2\theta)^{-2}$; $a_2 = (e^4/6m^4c^7)(1+3\cos^2\theta)\sin^2\theta$; k_1=2 and k_1 =1 for relativistic and non-relativistic particles, respectively; $R_* = R_0/R$; G is the gravitational constant, M is the mass of collapsing star.

The particle dynamics and their spectrum changing in the magnetosphere in form of the equation for particle transitions in the regular magnetic field are considered as [7]

$$\frac{\partial N}{\partial R} = f_1(E,R)\frac{\partial N}{\partial E} + f_2(E,R)N = 0. \tag{6}$$

Here $f_1(E,R) = ER^{-1}[a_1 - a_2F_0^2[R^7R_*/2GM(R_*-1)]^{1/2}Er^{-6}$; $f_2(E,R) = R^{-1}\{a_1 - 2[\,R^7(R_*-1)]^{\,1/2}E\}$.

In paper [7] Eq. (6) has solved for the two special cases. In the first case it is assumed that energy losses do not influence the particles spectrum in the magnetosphere. Then the second term in the right part of Eq. (5) can neglected and the solution of Eq. (6) for the initials distribution (2)–(4) are as follows:

$$N_1^{'}(E,R) = K_p E^{-\gamma} R_*^{-\beta_1}; \tag{7}$$

$$N_2^{'}(E,R) = K_M E^2 R_*^{-\beta_2} \exp(-E/kT); \tag{8}$$

$$N_3^{'}(E,R) = K_B R_*^{-\beta_3} \exp(-E/kT), \tag{9}$$

Here $\beta_1 = a_1(\gamma - 1)$; $\beta_2 = a_1(E/kT\ln E - 3)$; $\beta_3 = a_1(E/kT\ln E - 1)$.

Eqs. (7)–(9) determine the particle spectrum in the magnetosphere and its evolution during collapse for the first case when the energy losses can be neglected. This case is typical for the initial stage of the collapse and we will consider it in this paper. The second case is realized in the final stage of the collapse, when the magnetic field attains the extremely value and the energy losses influence considerably on the particle spectrum. We will consider this case in later on but not in this paper.

NON–THERMAL RADIATION FROM COLLAPSING STARS

For the power-series, relativistic Maxwell, and Boltzmann distributions (7)–(9) the ratio between the radiation flux from collapsing stars and its initial radiation flux, respectively, [7] are following:

$$I_{\nu P}/I_{\nu P0} = (\nu/\nu_0)^{(1-\gamma)/2} R_*^{\gamma-2} \int (R_*)^{-a_1(\gamma-2)} \sin\theta d\theta, \tag{10}$$

$$I_{\nu M}/I_{\nu M0} = R_*^{-3}(\nu/\nu_0)(1/kT) \int R_*^{-\beta_2} \exp(-E/kT) \sin\theta dE d\theta, \tag{11}$$

$$I_{\nu B}/I_{\nu B0} = R_*^{-3}(kT)(\nu/\nu_0) \int R_*^{-\beta_3} E^{-2} \exp(-E/kT) \sin\theta dE d\theta \tag{12}$$

Using Eqs. (10)–(12) the radiation flux from collapsing stars can be calculated. The ratio between the radiation flux from collapsing stars and its initial flux for different radius R_* and temperature $1\,eV \leq kT \leq 9\,eV$ by $\nu/\nu_0 = 1$ are given in Tables 1–2. This value is obtained by the numerical integration of Eqs. (10)–(12) in the range $2\ eV \leq E \leq 1000\ eV$, $0 \leq \theta \leq \pi/2$ for different radius R_*, temperature kT and index γ.

Table 1: The value $I_{\nu P}/I_{\nu P0}$ for various R_* and γ by $\nu/\nu_0 = 1$

γ	2.4	2.6	2.8	3.0	3.2	3.4	3.6	3.8	4.0
R_*					$I_{\nu P}/I_{\nu P0}$				
10	4.75	12	32.6	93.7	281	864	2710	8600	27600
40	14.6	76.1	443	2740	17500	$1.15e5$	$7.60e5$	$5.09e6$	$3.43e7$
80	26.7	203	1740	15700	$1.46e5$	$1.38e5$	$1.33e7$	$1.29e8$	$1.26e9$
100	32.6	281	2710	27600	$2.89e5$	$3.09e6$	$3.35e7$	$3.67e8$	$4.04e9$
200	61.2	774	10900	$1.61e5$	$2.46e6$	$3.81e7$	$5.98e8$	$9.47e9$	$1.51e11$
400	117	2170	44400	$9.56e5$	$2.11e7$	$4.74e8$	$1.08e10$	$2.47e11$	$5.71e12$
600	172	3980	$1.02e5^*$	$2.72e6$	$7.45e7$	$2.08e8$	$5.87e10$	$1.67e12$	$4.80e13$
800	226	6140	$1.83e5$	$5.71e6$	$1.83e8$	$5.94e8$	$1.96e11$	$6.50e12$	$2.17e14$
1000	281	8600	$2.89e5$	$1.02e7$	$3.67e8$	$1.34e10$	$4.98e11$	$1.86e13$	$7.03e14$

$^*1.02e5 = 1.02 \times 10^5$

Table 2: The value $J_{\nu M}/J_{\nu M0}$ and $J_{\nu B}/J_{\nu B0}$ for various R_* by $\nu/\nu_0 = 1$, $1eV \leq kT \leq 9eV$

	kT=1 eV			kT=5 eV			kT=9 eV	
R_*	$J_{\nu M}/J_{\nu M0}$	$J_{\nu B}/J_{\nu B0}$	R_*	$J_{\nu M}/J_{\nu M0}$	$J_{\nu B}/J_{\nu B0}$	R_*	$J_{\nu M}/J_{\nu M0}$	$J_{\nu B}/J_{\nu B0}$
37	6.04	204	145	1	405	300	1	54.3
38	14.5	491	150	2.8	1500	350	1	1360
39	35.2	1210	155	9.25	5420	400	1	22800
40	87.5	3019	160	29.7	19000	450	4.89	$2.76e5$
41	221	7660	165	93	65000	500	32.5	$2.59e6$
42	568	19800	170	283	$2.16e5$	550	181	$1.98e7$
43	1480	52200	175	838	$6.96e5$	600	872	$1.27e8$
44	3940	$1.40e5$	180	2420	$2.19e6$	650	3720	$7.04e8$
45	10600	$3.79e5$	185	6810	$6.69e6$	700	14300	$3.45e9$
46	29100	$1.05e6$	190	18700	$1.99e7$	750	49900	$1.51e10$
47	80900	$2.93e6$	195	50200	$5.80e7$	800	$1.61e5$	$6.06e10$
48	$2.28e5$	$8.35e6$	200	$1.32e5$	$1.65e8$	850	$4.86e5$	$2.23e11$

CONCLUSIONS

We can see from Tables 1–2 that the radiation flux grows during the collapse very rapidly (in millions times and especially in comparison with the initial flux). The radiation flux grows the most rapidly for collapsing stars with the cool magnetospheres ($kT \leq 1\ eV$). For these stars the flux increases in million times, when the stellar radius decreases in ten times (Table 2). For the magnetospheres with middle temperature ($1\ eV \leq kT \leq 3\ eV$) the flux grows at the later stage of a collapse. By the collapse of stars with the high-temperature magnetospheres the radiation flux grows at the still latest stage collapse, when the stellar radius decreases in hundreds times. The radiation flux from stars with Boltzmann distributions grows more rapidly in comparison with the stars having relativistic Maxwell distribution.

The general conclusions from the obtained results are the following. The stellar magnetic field will be increased considerable during the collapse. The charged particles can be accelerated in this magnetic field, which will emitted the electromagnetic waves in the wide frequency range from radio waves to gamma rays. The radiation flux grows during collapse and reaches the maximum at the final stage of a collapse. We can observe this radiation as the radiation impulses in the wide frequency range. The pulse duration completes with the collapse time determining the initial mass and initial radius of collapsing star. The intensity of these pulses are very strong, and the radiation flux from collapsing stars at the final stage of a collapse exceeds the initial flux in millions times. We can see (Table 1–2) that the radiation fluxes for stars with the initial fluxes in range [1]–[6], [8, 9] $10^{-22}\,\mathrm{erg/cm^2\,s\,Hz} \leq I_{\nu_0} \leq 10^{-30}\,\mathrm{erg/cm^2\ s\ Hz}$ can increase to $10^{-16}\,\mathrm{erg/cm^2\,s\,Hz} \leq I_{\nu_0} \leq 10^{-24}\,\mathrm{erg/cm^2\,s\,Hz}$ and more.

Thus, collapsing stars can be the powerful sources of the non-thermal radiation impulse. Where this impulse can be observed? First of all, in the middle of powerful gamma bursts and X bursts, which are not periodical and can be connected with the precollapse stars and the stars being at the stages of evolution those precede the neutron star formation and supernova explosion. The impulse non-thermal radiation can be observed also before explosion of nova and from the white dwarfs in double systems at the stage of accretion induced collapse. Periodical impulse of the non-thermal radiation can be generated by the pulsation of the stars with magnetic field as since in this case the charged particles can be accelerated and they can emitted the radiation.

REFERENCES

[1] *Beresinsky V. S., Bulanov S. V., Ginzburg V. L., Dogiel V. A., Ptuskin V. S.* Asrophysics of cosmic rays.–Moscow: Nauka, 1984.–380 p.

[2] *Ginzburg V. L., Ozernoy L. M.* About gravitational collapse of magnetic star // J. Exper. and Theor. Phys.–1964.–**47**.–P. 1030–1040.

[3] *Ginzburg V. L., Syrovatskii S. I.* Origin of cosmic rays.–Moscow: Izd. AN USSR, 1963.–384 p.

[4] *Gudel M., Benz A. O.* Radio spectra of dMe and dKe stars // Astron. Soc. Pacif. Conf. Ser.–1996.–**93**.–P. 303–305.

[5] *Gudel M., Benz A. O., Guiman E. F., Sthmitt J. H. M. M.* Nonthermal microvawe emission from F dwarfs: 71Tau, a For, and open cluster moving group membership // Astron. Soc. Pacif. Conf. Ser.–1996.–**93**.–P. 306–308.

[6] *Linsky J. L.* Steady radio emission from stars // Astron. Soc. Pacif. Conf. Ser.–1996.–**93**.–P. 436–446.

[7] *Kryvdyk V.* Collapsing stars as sources of electromagnetic radiation // Kinematics and Physics of Celestial Bodies.–1998.–**14**, N 6.–P. 475–489.

[8] *Utana G., Trigilio C., Catalano S.* Radio emission from Algol-type binaries. I. Results of 1992-1993 VLA Survey // Astron. and Astrophys.–1998.–**329**, N 3.–P. 1010–1018.

[9] *Van den Oort G. M. J.* Non-thermal emission mechanism in stellar coronae // Astron. Soc. Pacif. Conf. Ser.–1996.–**93**.–P. 263–272.

[10] *Shapiro S. L., Teukolsky S. A.* Black Holes, White Dwarfs, and Neutron Stars.–Moscow: Mir, 1985.–665 p.

[11] *Zeldovich J. B., Novikov I. D.* Theory of gravity and stellar evolution.–Moscow: Nauka, 1977.–494 p.

MAGNETIC ROTATOR AND ITS EVIDENCE IN β LYRAE SYSTEM

M. Yu. Skulsky

Lviv Polytechnic National University, Lviv, Ukraine
e-mail: mysky@polynet.lviv.ua

A main attention is paid to the evidence that the losing star of β Lyrae interacting binary system should be considered as the magnetic rotator with magnetosphere formed around it. Fragment of analyzing the observed secondary periods is presented, which has led to interconsistent magneto-hydrodynamical system of periodicities and resonances. In particular, new periods are discovered with the duration of $10^d.93$, $13^d.23$ and $564^d.85$. The latter period is fundamental one, and the longest observed period of $282^d.425$ is its harmonics and the period of running tidal wave. The reasons of the different values of this long-term period duration, obtained by different groups of observers are presented.

We make a conclusion on the base of long-term observations and studies of the spectrum of β Lyrae interacting binary system that unordinary approaches to its studies and search for new phenomena are necessary in order to understand the nature of this unique object. In 1980-1998 we have carried out measurements of Zeeman splitting of atmospheric lines of the bright component, which resulted in the discovery of the variable effective magnetic field with the orbital phase (Skulsky, 1982, 1985). Having solved this quasisinusoidal curve, we obtained that the mean field value is equal to $H_e = (-1198 \pm 32)$ G with the amplitude of $A = (475 \pm 51)$ G, and the field maximum and minimum corresponding to phases of $0.355P$ and $0.855P$ (Skulsky, 1990; Burnashev and Skulsky, 1991). Magnetic field is discovered for the first time on the surface of the component (hereafter, loser), which continues losing its mass very actively at the stage of finishing the first mass transfer in the binary system. That is why we have performed another research. CCD-observations of the two emission-absorption lines SiII6347, 6371 completed in the early nineties at the 2.6-m telescope, confirmed the magnetic field existence, but they showed a considerably less mean field value and rather different shape of its amplitude change (Skulsky and Plachynda, 1993). With the use of our absolute spectrophotometrical data, we have found out (Burnashev and Skulsky, 1986), that the variations of the equivalent width of depression at the λ 5200 Å in the β Lyrae spectrum correlate with the magnetic field variations (the relationship takes place between the photometrical indexes which are sensitive to the depression value, and the magnetic field strength values). The changes of absolute flux in the H_α-emissions are also synchronous with the effective magnetic field variations of the loser (Burnashev and Skulsky, 1991). The results of high spectral resolution CCD-observations of the H, HeI, SiII emission lines, in particular these of H_α and HeI7065 ones (their strong emission profiles are comparatively less distorted by absorption) have shown an evident correlation of Doppler shifts of emission line centers with the phase variations of effective magnetic field strength (Skulsky and Mal'kov, 1992; Skulsky, 1992a; Skulsky, 1993b). We have also detected another facts arguing that having the magnetosphere formed around the loser, the magnetic field influences upon the mass transfer between the components and the gaseous structure formation in the β Lyrae interacting binary system (see also Skulsky, 1992b, 1992a, 1993c).

Magnetic field behavior in the β Lyrae system is very ambiguous one, the field changes differently in the different lines, also short- and long-term variations take place there. That is why we expected independent studies of the magnetic field to be performed by other observers. However, having the publications reviewed in this field, we have found out that such investigations were not performed till the present time, and the magnetic field does not used mostly when studying this system. Therefore, we would like to stress the fact firstly, that the loser is magnetic rotator, and especially that photometrical and polarimetrical investigation data as well as spectral ones published in different periods by many observers, correlate well with the curve of magnetic field strength variation. Let us look at some of these papers. First of all it concerns radial velocities of strong emission lines in the visible range (for example, see Fig. 8 and 9 in the paper by Harmanec *et al.*, 1996; hereafter, HMB96), as well as many lines of the far ultraviolet, in particular high excitation lines CIII1175, SiIV1402 (for example, see Fig. 2–6 in the paper by Hack *et al.*, 1977). The extremes for all of these dependencies coincide with the magnetic field extremes. Let us remind that "β Lyr is not an eclipsing binary at wavelengths shortward of 1200 Å" (Polidan, 1989). Really, light curve of the β Lyrae at λ 955 Å presented in Fig. 6 of those paper, does not look like an eclipsing curve of one component by another at all, but its minimum coincides with the magnetic field maximum in the $0.355P$ phase, and variable maxima of this light curve are located within the range of second extremum of magnetic field strength curve, *i.e.*, both curves are intercorrelated. Some groups of researchers, in particular HMB96 and Hoffman *et al.*, 1998, find arguments to introduce terms "extended jets" or "a bipolar flow of gas oriented perpendicular to the orbital plane of the binary" in order to explain the phenomena related to the mass transfer between the components and mass loss outside the binary system. However, such jets or bipolar flows become quite natural when they are directed along the magnetic field dipole axis of the loser, all the more so that the deviation angle of this axis is rather high with respect to the orbital plane (Skulsky, 1985).

Secondly, we present here the information about some results of our analysis of periodicities and oscillations being observed within the last 20 years. As it was found out by us, this phenomenon is related directly to the magnetic field of the loser. Description of this phenomenon could be started from the detection of real variations of physical parameters with the secondary system period of 1.85 days. This period is surprisingly close to the seventh part of the orbital period, and as a rule it appeared well at the convolution of observed data with this period within one-two years of observations. We have firstly detected such periodicity on the variation curve with the orbital period phase of the absolute radiative flux in the strong emission line H_α (Burnashev and Skulsky, 1980). Variation curve of magnetic field of the loser with the orbital period phase showed the noticeable oscillations with this period as well (Skulsky, 1990). The work by Hoffman *et al.*, 1998 on β Lyrae spectropolarimetry is also important for us. Having their observation data convoluted with the $1\overset{d}{.}85$ period we received yet another confirmation of existence of this period with high variation amplitude.

The reliable data were published recently concerning the detection of another two periods, but these ones are featured by a considerably less variation amplitude. One of these periods, which exceeds much the orbital one, is also discussed for over 20 years (Alduseva and Kovalenko, 1976; Guinan, 1989). It was calculated recently in the range of $(283 \pm 1)^d$ on the base of independent light curves by two groups of observers. Van Hamme *et al.*, 1995 (hereafter, HWG95) obtained its averaged value with the duration of $(283.39 \pm 0.26)^d$ by means of the light curves within more than 150 years of observations. Having the most accurate observations of the last 36 years reduced into the single V-band intensity orbital light curve, the HMB96 group has calculated this period (by means of deviations from the averaged light curve) also with higher accuracy $(282.425 \pm 0.070)^d$ at the variable amplitude of $A = 0\overset{m}{.}0236 \pm 0\overset{m}{.}0008$. There was no physical explanation presented to the evident difference by $0\overset{d}{.}965$ almost between the results of identical determinations of this period, which exceeds much the 3σ value, as well as for the physical reasons of arising this period.

The second period with the duration of 4.7479 is less than orbital one, and it is calculated by means of solving curves of radial velocities of strong emission lines by HMB96 group. They have noticed that this period is in "causal relationship" with the long-term and orbital periods (for the season of 1994 with $P = 12\overset{d}{.}9385$):

$$3 \times \{(12\overset{d}{.}9385)^{-1} - 2 \times (282\overset{d}{.}425)^{-1}\} = (4\overset{d}{.}7479)^{-1}$$

The evidence of three secondary periods in different observations enforced us to analyze them. It is appeared that all the three periods are in resonance relationship, which is to be considered as the new phenomenon. However, let us present the fragment of this study concerning the two last periods detected by means of the light curves and the radial velocity curve. This will allow us to be sure in their relationship with magnetic field, to understand the nature of the long-term period and difference in its duration calculated by two groups of researchers.

Let us write the obtained equation in analytic form, having denoted long-term and short-term periods as T and T_1, respectively:

$$T_1^{-1} = 3(P^{-1} - 2T^{-1}). \tag{1}$$

Let us notice firstly, that the T_1 period is defined from the radial velocity curves of emission lines and they correlate with the magnetic field strength curve (Skulsky, 1992a, 1993b). Secondly, $T_1 = 0.367P$, *i.e.*, it is close to $0.355P$ phase of the loser magnetic field maximum (Burnashev and Skulsky, 1991). Also this period gives the information about the orientation of the axis of the surface magnetic field in relation to gravitational axis-line of both component centers. That is why the T_1 period could be considered as the specific oscillation in the phase space of the orbital period, connected with the proper phase angle of the first extremum of the magnetic field. This allowed to make the following assumption: there exists also physically similar period of $T_2 \cong T_1 + P/2$ (*i.e.*, it should define the second extremum of the magnetic field of the loser) which is conjugated with T_1 in such way that their overlapping gives the long-term period T as their beating period (at the simultaneous interaction of these three secondary periods with the orbital one). Expected period T_2 has appeared to be close to $0.855P$ phase of the magnetic field minimum, so we have found the second "causal relationship":

$$(12^d.9385)^{-1} + 4 \times (282^d.425)^{-1} = (10^d.93494)^{-1}$$

where $T_2 = 10^d.93494 = 0.845P$, and the orbital period value corresponds to 1994 as it was in Equation (1). Having written this equation in the analytical form as well:

$$T_2^{-1} = P^{-1} + 4T^{-1}, \tag{2}$$

we found the causal relationships for orbital and long-term periods from the system of Equations (1) and (2):

$$P = \frac{9T_1T_2}{3T_1 + 2T_2} \quad \text{and} \quad T = \frac{18T_1T_2}{3T_1 - T_2}. \tag{3}$$

Having substituted T_1 and T_2, we found a numeric value of $T = 282^d.439$, which agrees well with the value of $T = 282^d.425$ determined by HMB96 group. Therefore, the assumption of resonance relationship between T_1, T_2 and T is correct.

Relationships (3) look like classical formulas of superposition of oscillations with close periods. Having applied these formulas, we receive the resulting period

$$T_{rez} = \frac{2T_1T_2}{T_1 + T_2} = 6^d.62099, \tag{4}$$

which is close to the half-orbital one and their interaction should give the beating period:

$$T_{bt} = \frac{T_{rez}P}{2(T_{rez} - P/2)} = 282^d.269. \tag{5}$$

This value also agrees well with the T value of HMB96 group.

However, these are noticeable differences and our analysis showed that the HMB96 group did not take the orbital period variations into account (β Lyrae system has constant increase of the orbital period dP/dt = 18.9 s per year (Mandushev, 1988; Harmanec and Scholz, 1993; Wilson and Van Hamme, 1999)). That is why we made the necessary corrections to (1) and (2) Equations and reduced all their periods to the one effective season of the light curve averaged over 36 years of observations. It was 1980, and the set of corresponding periods is given below.

Now we can easily explain also the differences in period durations $T = (283.39 \pm 0.26)^d$ and $T = (282.425 \pm 0.070)^d$ obtained by two groups of researchers HWG95 and HMB96, respectively. Taking into consideration that HWG95 determined the period $T = 283^d.39$ as the averaged value over the 150 years of observations, and using the (1) – (5) system of equations, we have obtained the value of $T_{bt} = 283^d.3904$ for the light curve centered in the season of 1920. The corresponding set of periods for 1920 is given in the table as well:

1980	1920
$P = 12^d.9355$	$P = 12^d.9224$
$T = 282^d.42524$	$T = 283^d.3904$
$T_1 = 4^d.746634$	$T_1 = 4^d.739723$
$T_2 = 10^d.932617$	$T_2 = 10^d.928985$
$T_{rez} = 6^d.619338$	$T_{rez} = 6^d.611950$

Therefore, difference $\Delta T = 0^d.965$ between T values obtained by HWG95 and HMB96 groups of authors, is explained by the sample of observations forming these light curves. Time difference between effective forming of these light curves equals to 60 years which gives the orbital period increase by $\Delta P = 0^d.0131$. This has led to the changes of related periods T_1, T_2 and T.

Physical nature of the long-term period T could be also easily understood now by means of substituting the value of full orbital period and doubled value of T_{rez} into Equation (5) (it means, assuming that magnetic and rotation period values of the loser are equal and $P_{mag} = P_{rot} = 2T_{rez}$ since axial rotation period of the loser is observed to be a little longer than the orbital one (Kosovichev and Skulsky, 1990; Harmanec and Scholz, 1993)). In this case their beating period in 1980 was equal to:

$$P_{bt} = \frac{P_{orb}P_{rot}}{P_{rot} - P_{orb}} = 564^d.85158 = 2T.$$

Thus, $P_{bt} = 564\overset{d}{.}85$ is the fundamental period in β Lyrae system, and the period $T = 282\overset{d}{.}425$ means its first harmonics and (on the base of the theory of tidal waves in a binary systems (Kato, 1974; Kosovichev and Skulsky, 1990)) simultaneously is the period of running tidal wave at the loser surface. Really, this wave appears because of asynchronism of orbital and rotational periods:

$$P_{run} = \frac{P_{rot}P_{orb}}{2(P_{rot} - P_{orb})} = T = 282\overset{d}{.}42579.$$

Let us make a conclusion:
long-term period T is the period of running tidal wave at the loser surface and at the same time it is in resonance relationship with the short-term periods T_1 and T_2, which determination is strongly connected with the magnetic field structure and geometry; all periods, fundamental one as well as short-term ones, form the interconsistent magnetohydrodynamical system of the periodicities which is being changed gradually together with the orbital period change during completion of the quick final stage of the primary mass transfer between β Lyrae interacting system components.

REFERENCES

[1] *Alduseva V. Ya. and Kovalenko V. M.* Close binary systems and their evolution.–Publ. Moscow Univ, 1976.–P. 195.

[2] *Burnashev V. I. and Skulsky M. Yu.* // Pis'ma in Astron. Zh.–1980.–**6**.–P. 587. (in Russian).

[3] *Burnashev V. I. and Skulsky M. Yu.* // Pis'ma in Astron. Zh.–1986.–**12**.–P. 535. (in Russian).

[4] *Burnashev V. I. and Skulsky M. Yu.* // Bull. Crimean Astrophys. Obs.–1991.–**83**.–P. 108.

[5] *Guinan E. F.* // Space Sci. Rev.–1989.–**50**.–P. 35.

[6] *Hack M., et al.* // Astrophys. J. Suppl. Ser.–1977.–**34**.–P. 565.

[7] *Harmanec P. and Scholz G.* // Astron. and Astrophys.–1993.–**279**.–P. 131.

[8] *Harmanec P., et al.* // Astron. and Astrophys.–1996.–**312**.–P. 879 (HMB96).

[9] *Hofman J. L., Nordsieck K. H. and Fox G. K.* // Astron. J.–1998.–**115**.–P. 1576.

[10] *Kato S.* // Publs Astron. Soc. Jap.–1974.–**26**.–P. 341.

[11] *Kosovichev A. G. and Skulsky M. Yu.* // Pis'ma in Astron. Zh.–1990.–**16**.–P. 240. (in Russian).

[12] *Mandushev G .I.* // Astron. Tsirc.–1988.–**1533**.–P. 15. (in Russian).

[13] *Polidan R. S.* // Space Sci. Rev.–1989.–**50**.–P. 89.

[14] *Skulsky M. Yu.* // Pis'ma in Astron. Zh.–1982.–**8**.–P. 238. (in Russian).

[15] *Skulsky M. Yu.* // Pis'ma in Astron. Zh.–1985.–**11**.–P. 51. (in Russian).

[16] *Skulsky M. Yu.* // Mittelungen KSO Tautenberg.–1990.–**125**.–P. 146.

[17] *Skulsky M. Yu.* Stellar magnetism.–Saint-Petersburg: Nauka, 1992a.–P. 127. (in Russian).

[18] *Skulsky M. Yu.* // Pis'ma in Astron. Zh.–1992b.–**18**.–P. 711. (in Russian).

[19] *Skulsky M. Yu.* // Pis'ma in Astron. Zh.–1993a.–**19**.–P. 45. (in Russian).

[20] *Skulsky M. Yu.* // Pis'ma in Astron. Zh.–1993b.–**19**.–P. 116. (in Russian).

[21] *Skulsky M. Yu.* // Pis'ma in Astron. Zh.–1993c.–**19**.–P. 417. (in Russian).

[22] *Skulsky M. Yu. and Malkov Yu. F.* // Astron. Zh.–1992.–**69**.–P. 291. (in Russian).

[23] *Skulsky M. Yu. and Plachinda S. I.* // Pis'ma in Astron. Zh.–1993.–**19**.–P. 517. (in Russian).

[24] *Van Hamme W., Wilson R. E. and Guinan E. F.* // Astron. J.–1995.–**110**.–P. 1350 (HWG95).

[25] *Wilson R. E. and Van Hamme W.* // Mon. Notic. Roy. Astron. Soc.–1999.–**303**.–P. 736.